



## Durham E-Theses

---

### *Estimations of $Q$ from seismic Rayleigh waves*

Burton, Paul W.

#### How to cite:

---

Burton, Paul W. (1973) *Estimations of  $Q$  from seismic Rayleigh waves*, Durham theses, Durham University. Available at Durham E-Theses Online: <http://etheses.dur.ac.uk/9218/>

#### Use policy

---

The full-text may be used and/or reproduced, and given to third parties in any format or medium, without prior permission or charge, for personal research or study, educational, or not-for-profit purposes provided that:

- a full bibliographic reference is made to the original source
- a [link](#) is made to the metadata record in Durham E-Theses
- the full-text is not changed in any way

The full-text must not be sold in any format or medium without the formal permission of the copyright holders.

Please consult the [full Durham E-Theses policy](#) for further details.

Estimations of Q from Seismic Rayleigh Waves

Paul W Burton B.A. (Cantab)

January 1973



This thesis is submitted for the degree of Ph.D.  
at the University of Durham and to the best of my  
knowledge no part of it has previously been  
submitted to this or any other university.

*Paul W. Burton.*

Paul W Burton  
The Graduate Society  
University of Durham

January 1973

## ABSTRACT

The specific attenuation factor,  $Q_Y^{-1}$ , has been estimated from seismic Rayleigh waves in the frequency range 0.015-0.11 Hz. The 95% confidence limits determine a narrow region around all estimates.

The observational data consists of digitised Rayleigh wave traces from film chips of the long period vertical component instruments of the WWSSN stations. Events used are nuclear explosions in Novaya Zemlya, the Lop Nor region of China (Southern Sinkiang Province) and the Aleutian Islands.

The group velocity and spectral amplitudes are obtained for each seismogram using an improved "multiple filter technique".  $Q_Y^{-1}$  is estimated by a least squares regression fit to the subsequent amplitude-distance plots.

Values of  $Q_Y^{-1}$  are generally larger when determined from Novaya Zemlya (.004) than for the Lop Nor test site (.003). The largest values of  $Q_Y^{-1}$  (.009) are found at low frequencies (0.02 Hz), implying a zone of high dissipation in the upper mantle sampled by these frequencies alone.

The observed values of  $Q_Y^{-1}$  are directly inverted using an extended Monte-Carlo technique - "Hedgehog". This successfully inverted the data from Novaya Zemlya revealing a region of high dissipation coincident with the low velocity zone, although low velocity is not assumed. The inversion model shows  $Q_\alpha^{-1} = .002$ ,  $Q_\beta^{-1} = .0045$  for the uppermost 120 km and  $Q_\alpha^{-1} = .007$ ,  $Q_\beta^{-1} = .015$  ( $Q_\alpha = 140$ ,  $Q_\beta = 65$ ) in the absorption zone below 120 km.

### ACKNOWLEDGEMENTS

Dr H I S Thirlaway and Professor M H P Bott have established a close liaison between the UKAEA Seismology Unit at Blacknest and the Department of Geology at the University of Durham. This liaison has allowed me to pursue these studies and write this thesis, and has given me the rare opportunity to see one objective from two viewpoints. I am very grateful to Dr H I S Thirlaway and Professor M H P Bott for giving me these opportunities.

Dr R E Long and Dr H I S Thirlaway supervised me for the three years. I am sincerely grateful to all the people who have helped me in many ways during this period, in particular I thank: Mr C Blamey, Mr A Douglas, Miss P K Eves, Mr E G Ford, Mr B L N Kennett and Mr J B Young.

My especial thanks are due to Mr P D Marshall who has tolerated all my questions and encouraged me with the answers and help at all times.

CONTENTS

Page

ABSTRACT

ACKNOWLEDGEMENTS

INTRODUCTION

I.1	"Q".	1
I.2	Q Determinations in the Laboratory.	2
I.3	Q Mechanisms.	3
I.4	Q Determinations from the Real Earth.	5

CHAPTER 1

1.1	The Amplitude of Rayleigh Waves.	7
1.2	The Time or Frequency Domain?	8
1.3	Amplitudes in the Frequency Domain.	10
1.4	Factors Necessary to Estimate $Q^{-1}$ .	12

CHAPTER 2

2.1	The Data.	14
2.2	Data Analysis.	17
2.2.1	Spectral Amplitudes.	
2.2.2	Group Velocity.	
2.3	Reduction of Errors.	20
2.3.1	Spectral Amplitude Measurements.	
2.3.2	The Frequencies of Spectral Amplitudes and Group Velocities.	
2.3.3	Group Velocity Errors.	
2.3.4	Redetermination of the End of the Signal.	
2.4	Amplitude-Distance Plots and Estimations of Q.	32
2.5	The Best Line.	33
2.5.1	Average $Q^{-1}$ .	
2.5.2	Assumptions for Linear Regression.	
2.6	Summary.	35

CHAPTER 3

3.1	The Estimations of $Q_Y^{-1}(f)$ .	36
3.2	The Influence of Noise.	37
3.2.1	Low Frequency Noise.	
3.2.2	High Frequency Noise.	
	3.2.2.1 Spectral Phase and the Highest Signal Frequency.	
	3.2.2.2 Spectral Amplitude and the Highest Signal Frequency.	
	3.2.2.3 Group Velocity and the Highest Signal Frequency.	
3.3	Statistical Comparison of the $Q_Y^{-1}(f)$ values.	41
3.3.1	$Q_Y^{-1}$ as a function of Frequency.	
3.3.2	$Q_Y^{-1}(f)$ Compared between Events.	
3.4	Average $Q_Y^{-1}(f)$ Values.	45
3.4.1	$Q_Y^{-1}$ at Low Frequencies.	
3.4.2	$Q_Y^{-1}$ at High Frequencies.	
3.5	Summary.	46

	<u>Page</u>
CHAPTER 4	
4.1	A Theoretical Formulation for the Dissipation and Dispersion of Rayleigh Waves. 47
4.2	The Attenuation of Rayleigh Waves on a Half Space. 53
4.3	Partial Derivatives for Inversion Purposes. 54
4.4	Simple Qualitative Inversion of the $Q^{-1}(f)$ Data. 56
4.5	Model Inversion of the $Q^{-1}(f)$ Data. 57
4.6	Conclusions. 58
CHAPTER 5	
5.1	'Hedgehog' - Direct Inversion. 60
5.1.1	Introduction.
5.1.2	'Hedgehog'.
5.2	Inversion. 62
5.2.1	The General Model.
5.2.2	Inversion of 3NZA.
5.2.3	Inversion of 2CA and 5A.
5.3	Interpretation. 67
CHAPTER 6	
	Concluding Comments. 70
APPENDIX A	The WWSSN Recording Stations Used for Each Event. 74
APPENDIX B	The Estimations of $Q_Y^{-1}$ from Seismic Rayleigh Waves. 78
APPENDIX C	The Instrument Response. 79
APPENDIX D	Least Squares Fitting of "the best" Straight Line. 82
APPENDIX E	The Comparison of Two Regression Lines. 87
	The Average Gradient for Several Regression Lines.
APPENDIX F	Two Proofs. 91
APPENDIX G	Computer Program Listings. 94
REFERENCES	97
ENCLOSURES	
1	Marshall and Burton. The Source-Layering Function of Underground Explosions and Earthquakes - An Application of a "Common Path" Method. (1971).
2	Burton and Kennett. Upper Mantle Zone of Low Q. (1972).
3	Burton and Blamey. A Computer Program to Determine the Spectrum and a Dispersion Characteristic of a Transient Signal. (1972).

Too well I know these godlike ones.  
They will that men believe on them,  
and that doubt be held sin.

Friedrich Wilhelm Neitzche



## INTRODUCTION

### I.1 "Q"

The importance of  $Q$  is demonstrated by Knopoff's (1964) statement "Were it not for the intrinsic attenuation of sound in the earth's interior, the energy of earthquakes of the past would still reverberate through the interior of the earth today".

It is obvious that after an event has taken place the energy from it is gradually absorbed by the earth and converted into heat - this is a normal consequence of the non-elastic phenomenon of dissipative wave propagation. However the means and amounts of this dissipation are generally not known. The geophysicist is interested in knowing if certain areas of the earth are better or worse dissipators of seismic energy than others. Such information may throw light on the interior of the earth in terms of the chemistry and physics of materials and mechanisms at depth.

Any seismic wave is composed of a set of harmonics or a continuous range of frequencies ( $f$ ). To quantify the amount of attenuation (dissipation) suffered by each harmonic we use the attenuation factor  $Q(f)$ , or more sensibly we use the specific attenuation factor,  $Q^{-1}$ , because this is directly proportional to the amount of attenuation.

For a propagating monochromatic wave its attenuation may be described by an exponential function of the form:

$$D = \exp\left(\frac{-\omega}{2} \int_{t_1}^{t_2} \frac{dt}{Q}\right)$$

$\omega$  = angular frequency (radians/s)

$t$  = travel time.

In terms of frequency,  $f$ , and assuming a phase velocity  $c$  we have

$$\begin{aligned} D &= \exp\left(-\pi f \int_{x_1}^{x_2} \frac{dx}{cQ}\right) \\ &= \exp\left(\frac{-\pi f X}{cQ}\right) \end{aligned}$$

where  $X$  is the distance travelled.



In terms of a spatial attenuation coefficient,  $\gamma$ , we have the function  $\exp(\gamma x)$  and so

$$\gamma = \frac{-\pi f}{cQ} \text{ km}^{-1}$$

If we were dealing with standing waves we would measure their amplitude at a point as it varies in time, essentially a damping factor of the form  $\exp(\gamma t)$  is determined. The  $Q$ s for the two possible types of experiment,  $Q_T$  for travelling or  $Q_S$  for standing waves, are not the same and Knopoff, Aki et al. (1964) have rigorously shown that

$$UQ_S = c Q_T$$

where  $U$  is the group velocity. In this work, unless specifically stated,  $Q_T$  is to be assumed.

From these equations it is clear that  $Q$  is dimensionless and a measure of the loss or attenuation per cycle of a wave, rather than a measure of loss with absolute distance as is the case for the attenuation coefficient  $\gamma$ . This is simply shown by expressing  $\gamma$  in terms of wavelength  $\lambda$

$$\gamma = -Q^{-1} \frac{\pi}{\lambda} \text{ km}^{-1}$$

## I.2 Q DETERMINATIONS IN THE LABORATORY

Observational data on  $Q$  usually falls into one of three categories:

- 1 Laboratory experiments on non earth materials
- 2 Laboratory experiments on earth materials
- 3 Experiments on the real earth

with the errors involved increasing from category to category.

For liquids  $Q^{-1}$  is found to be proportional to the frequency. Pinkerton (1947) plots  $\frac{\gamma}{f^2}$  against frequency and the straight lines of zero slope which he obtains illustrate the result very well.

The attenuation coefficient,  $\gamma$ , for solids is usually found to be proportional to the frequency and hence values of  $Q^{-1}$  are frequency independent. This implies the theory of constancy of  $Q$  over all frequencies.

For example Peselnick and Zietz (1959) measured the  $Q$  of Solenhofen Limestone using compressional pulses in the frequency range 3-15 Mc/s and found it to be 110. More recent measurements by Mason and Kuo (1971) for Pennsylvania Slate over the frequency range .01-20 megahertz gave an approximately constant value.

The concept of constant  $Q$  is important because if it is accepted for the real earth then any deviation from "normal"  $Q$  will imply a change in substance, physical or chemical. But a distinction must be made between the  $Q$  of body waves and surface waves. Yamakawa and Sato (1964) state that body wave  $Q$  is a physical constant for a medium whereas surface wave  $Q$  depends on the physical properties and the structure of the medium. The  $Q$  of surface waves, like the velocity, may have an "apparent" frequency dependence simply due to the geometry of a layered structure.

Other people have investigated the joint problem of liquid and solid; Born (1941), has investigated sandstone with varying water contents. His pleasing results are that  $Q^{-1}$  becomes more frequency dependent as the water content increases.  $Q^{-1}$  is constant for the dry rock case, Figure I.1 is taken from Born's work.

The disadvantage of these experiments is that they are conducted at non-geophysical frequencies. We are really interested in the range .001 to 10 Hz.

### I.3 Q MECHANISMS

Several mechanisms have been put forward to describe microscopic  $Q$ , and a good review paper is that of Jackson and Anderson (1970).

Some of the less successful mechanisms involve atomic diffusion and dislocation mechanisms. The better mechanisms seem to involve

- 1 partial melting
- 2 grain boundary relaxations and
- 3 a mechanism of "high temperature, internal friction background" (i.e. vacancy creation and diffusion) which obeys

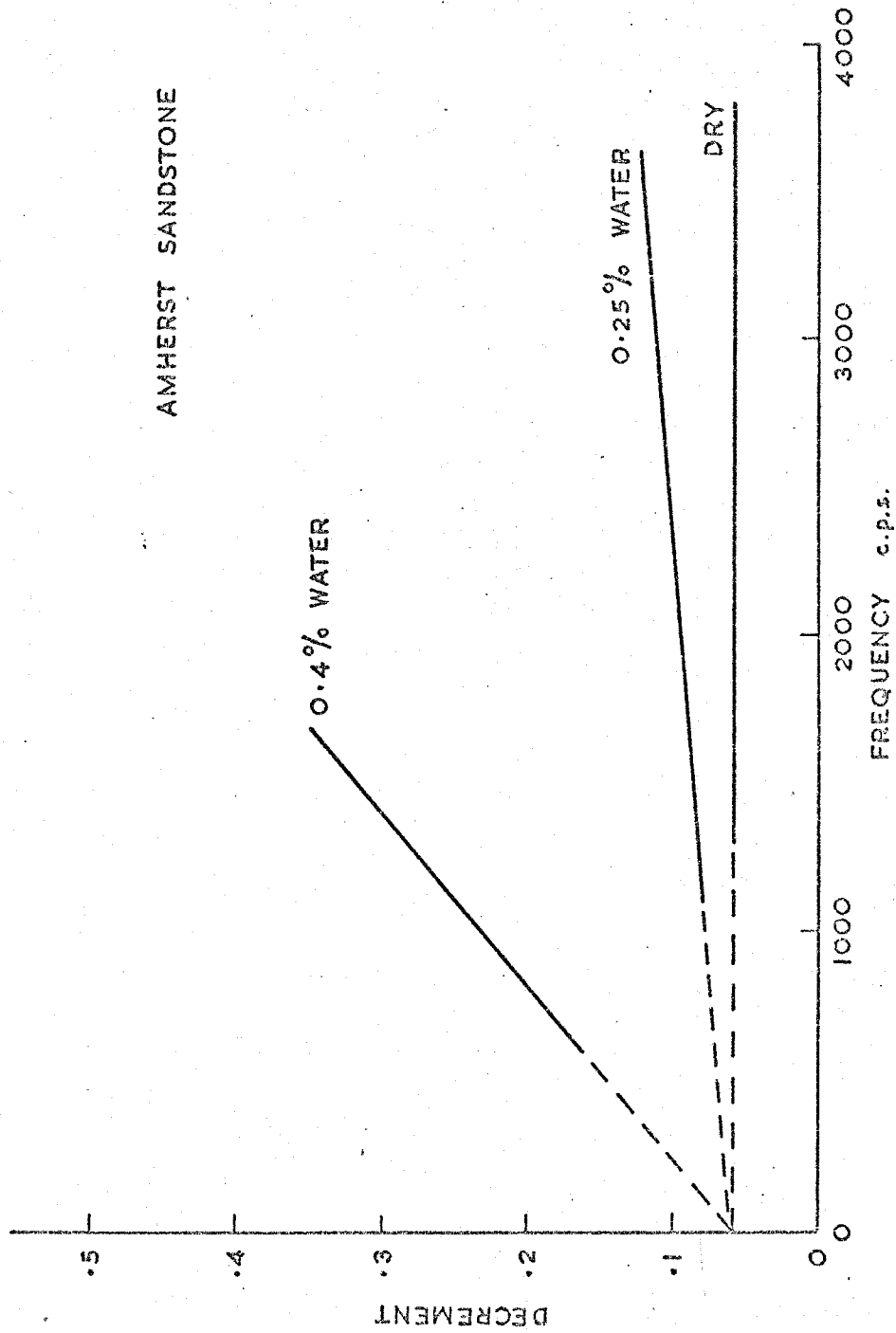


FIGURE I.1 SANDSTONE WITH VARYING AMOUNTS OF INTERSTITIAL WATER (BORN)  
 (LOG DECREMENT  $\propto Q^{-1}$ )

$$Q^{-1} = \frac{A}{f} \exp(-H/RT)$$

where H is the appropriate energy required for initiation and T is the absolute temperature. Note that for this mechanism  $Q^{-1} \propto f^{-1}$ .

Processes such as diffusion of dislocations and crystal point defects, fluid flow in pores and phase changes will act to relieve an applied stress - these are relaxation mechanisms. Energy is absorbed and then released during consecutive halves of a cycle and this energy transfer takes a finite relaxation time.

Zener (1948) has shown that if the rate of stress relief is proportional to stress for constant strain then each of the above processes creates an internal friction  $Q^{-1}$  of the form

$$Q^{-1} = \frac{M_u - M_R}{M_u} \frac{f/f_p}{1 + (f/f_p)^2}$$

$M_u$ : "unrelaxed" elastic modulus

$M_R$ : relaxed elastic modulus

$f_p$ : constant of proportionality between stress and rate of stress relaxation.

If the mechanism is thermally activated then the relaxation times are pressure and temperature dependent. We would therefore expect the internal friction to vary with depth. Allowing for the effect of temperature on relaxation times alters the above expression for  $Q^{-1}$  to

$$Q^{-1} = \frac{M_u - M_R}{M_u} \frac{\frac{f}{f_p} \exp\left(\frac{-H}{RT}\right)}{1 + \left(\frac{f}{f_p} \exp\left(\frac{-H}{RT}\right)\right)^2}$$

However, it is not possible to state that one particular mechanism is entirely responsible for attenuation effects.

Also, a particular attenuation mechanism may be quite strongly frequency dependent - but if we consider a wide range of chemical and physical properties (for example grain and pore size within the earth) and a multi component, multi phase system then we may obtain a  $Q^{-1}$  which is only weakly frequency dependent. The earth's heterogeneity may average a Q mechanism to produce a predominantly frequency independent result.

Experimental measurements of  $Q$  for the real earth differ in their degree of directness and in the number of secondary effects which have to be considered e.g. reflection coefficients.

Body wave determinations of  $Q$  usually rely on the spectral ratios of two distinct seismic wave phases. If we take the spectral ratios for the phases (from the same event)  $P$  and the surface reflection  $pP$  for recordings at the same station then we have a  $Q_\alpha$  dependent quantity. The difference between the two phases is caused mainly by the epicentre-hypocentre structure at the source and the loss of energy at the surface reflection. The surface reflection is an unwanted secondary effect which when taken into consideration is a source of error. Niazi (1971) used the technique to determine  $Q_\alpha$  values for the upper mantle; his results have been criticised by Buchbinder (1972).

The phases  $PcP$  and  $P$  have been used to determine  $Q_\alpha$  in the mantle. Ibrahim (1971) obtains the ratio  $PcP/P$  and chooses as the best  $Q$  values those which reduce the scatter in his data; the technique seems to be effective.

The work of Kovach and Anderson (1964) produced values for  $Q_\beta$  using  $S$  waves reflected at the core mantle boundary;  $ScS$ ,  $sScS$ ,  $ScS_2$ ,  $sScS_2$  were observed and  $Q_\beta$  determined. The surface reflected waves allow distinct  $Q_s$  to be determined for the upper and lower regions of the mantle, giving values of 200 and 2200 respectively.

Both of these last two methods assume coefficients of reflection and obtain  $Q$  indirectly by the comparison of two or more different phases of seismic energy. To determine the degree of attenuation directly it is necessary to observe the same wave at more than one point.

The surface waves from a large earthquake will travel round the earth several times before they are attenuated down to the noise level - hence they may be recorded more than once at the same station. The amplitude attenuation can then be easily measured from the two consecutive time series.

A disadvantage of this technique is the values of  $Q$  being determined for one very specific path. Kanamori (1970) made measurements for both Love and Rayleigh waves and found that  $Q$  differed considerably for differing great circle paths. His values for Rayleigh wave  $Q_R$  are  $180 \pm 80$  and for Love waves  $110 \pm 40$ , using Kurile Island earthquakes. A further disadvantage is that the period range is approximately 150-350 seconds, a range very much restricted to these large earthquakes. Such long periods are required for the method because shorter periods are attenuated rapidly with distance.

A different approach to the problem is given in the work of Carpenter and Marshall (1970). A nuclear explosion is used as the source of surface waves and assuming a circular radiation pattern the great circle technique need not be used. Instead, there are several recording stations around the event, but at different distances and a simple plot of amplitude against distance is obtained, which simply determines  $Q$ . This is discussed in more detail later.

A final important technique is the observation of the normal modes of oscillation of the earth. These are of long period and therefore contain information about the earth at depth. However such observations are made at two points in time, not space, and  $Q_S$  is determined for these standing waves.

All of these techniques have their particular difficulties. Body wave techniques involve the determination of reflection coefficients while surface wave measurements must necessarily lead to an inversion problem when a depth dependence for  $Q$  is required.

## CHAPTER 1

### 1.1 The Amplitude of Rayleigh Waves

A general expression for the amplitude  $A(f)$  of a seismic Rayleigh wave (vertical component) in a layered medium is

$$A(f,r) = K.L(f,d).I(f).S(f).D(f,r).G(f,r) \quad 1.1$$

- f = frequency Hz
- K = a constant
- r = distance from source
- L = amplitude response of layered medium (depth d)
- I = instrument transfer function
- S = source spectral function
- D = absorption term
- G = geometrical spreading correction.

This Rayleigh wave amplitude  $A(f)$  is expressed in the frequency domain (Toksoz, Ben-Menahem and Harkrider 1964); the amplitude  $A(t)$  observed on the seismogram is similar to the above expression except the terms are convolved and not multiplied.

Carpenter and Marshall considered the time domain problem for an expanding pressure pulse as source. Their work shows that for measurements of period,  $T$ , made directly from the seismogram that

$$A(T) = K' U(dU/dT)^{-1/2} (\Delta^{-1/2} \sin^{-1/2} \Delta) \exp\left(\frac{-\pi E \Delta}{QUT}\right) \quad 1.2$$

where  $E$  is the radius of the earth and  $\Delta$  the angular distance of travel.

This may be rewritten as

$$A(T) = K'' \left[ (E \sin \Delta)^{-1/2} \right] \left[ U(E \Delta \frac{dU}{dT})^{-1/2} \right] \exp\left(\frac{-\pi E \Delta}{QUT}\right) \quad 1.3$$

where the term in  $(E \sin \Delta)^{-1/2}$  takes account of geometrical spreading, and not  $\Delta^{-1/2} \sin^{-1/2} \Delta$  implied by equation 1.2. The term  $U(E \Delta \frac{dU}{dT})^{-1/2}$  arises because the stationary phase approximation has been used to determine the far field Rayleigh wave shape in the time domain from a frequency domain formulation. Their measurements were confined to the apparent period (the time between



successive peaks) and the amplitude for that period, these are strictly time domain measurements.

## 1.2 The Time or Frequency Domain?

The question of relative merit of data representation in the time or frequency domain appears trivial (because both forms are just different representations of the same data), but it is important. There are definite advantages to be gained by working in the frequency domain.

We have to consider the effect of instrumentation. The instrumental response is inherently a frequency domain description. We may consider an input in the time domain to an instrumental "black box" filter and observe its output, but to appreciate the change in waveform, and correct for it, we require a set of magnifications at the different frequencies and the corresponding phase delays. Correction with these values is simple division, the alternative is a lengthy time domain deconvolution process.

Also, the apparent periods measured in the time domain are forced upon us by the individual record, and more likely than not, they are not directly comparable between one record and the next. Worse than this, when an apparent period is measured and a value assigned, say 15s, we are not certain how many periods are compounding to that waveform. A nominal value of 15s may easily cover the true range 12-19s. To correct for this partial dispersion it is necessary to apply the stationary phase correction, and to accept that the earth is not a perfect Fourier filter.

The stationary phase approximation generates a term for correcting amplitudes measured from a time series which is of the form

$$U.R^{-1/2} \left(\frac{dU}{dT}\right)^{-1/2} T^{-1} \quad 1.4$$

where R is the distance travelled and equal to  $E\Delta$ . For a particular type of explosion, underground or atmospheric, this term is further modified

in its T dependence and becomes in both cases

$$U.R^{-1/2} \left(\frac{dU}{dT}\right)^{-1/2} T^{-3/2} \quad 1.5$$

As expected the correction is determined by the group velocity and period we are considering and the rate of change in that group velocity. Further, there is a distance term,  $R^{-1/2}$ , implying that the longer the path on the earth's surface then the greater will be the reduction in time domain amplitudes due to smearing by dispersion.

The meaning of term 1.5 is usually hidden and confused by introducing the geometrical spreading term,  $(E \sin \Delta)^{-1/2}$  (for surface waves) at an earlier stage, and splitting the term into a geometrical and dispersive term

$$\begin{aligned} & \left[ U.R^{-1/2} \left(\frac{dU}{dT}\right)^{-1/2} T^{-3/2} \right] \left[ (E \sin \Delta)^{-1/2} \right] \\ & \equiv \left[ E^{-1} \Delta^{-1/2} \sin^{-1/2} \Delta \right] \left[ U.T^{-3/2} \left(\frac{dU}{dT}\right)^{-1/2} \right] \end{aligned} \quad 1.6$$

However, for the stationary phase correction to hold a condition to be fulfilled is (where k is wavenumber)

$$\frac{t \frac{d^3 w}{dk^3}}{\left(t \frac{d^2 w}{dk^2}\right)^{3/2}} < \epsilon \quad 1.7$$

and if this quantity does not converge to such a limit then the method is invalid (Bath, "Mathematical Aspects of Seismology", p.43). Such convergence is certainly in question near turning points of the dispersion curve, when

$\frac{dU}{dk} = \frac{d^2 w}{dk^2} = 0$ . Examination of the averaged group velocity curves published by Oliver (1962), show three turning point regions for which

$\frac{d^3 w}{dk^3}$  is certainly non zero, the one of importance creating the Airy phase for periods around 18s. Thus, condition 1.7 need not hold and the Airy phase approximation (Pekeris (1948) considers 3rd order phase terms)

may be more appropriate than the simple second order stationary phase approximation. The Airy phase has been shown to propagate with a different dependence on distance than the remainder of the Rayleigh wave (Ewing, Jardetzky and Press (1957), Pekeris (1948)), and has occasionally been regarded as a separate phase,  $R_g$ , although it is only part of the fundamental Rayleigh mode. The non-Airy phase Rayleigh mode has distance dependence  $R^{-1}$ , the Airy phase depends on  $R^{-5/6}$ . Increasing distance makes the Airy phase stand out from the rest of the mode, hence its mistaken identity on the seismogram as a unique phase  $R_g$ .

Even if the Airy phase is avoided (although it often contains most of the energy!) a set of values at different "apparent" periods for the dispersive term in 1.6 is still inadequate to correct amplitudes measured from the time series. At a particular apparent period the dispersive expression is a function of the type of path traversed by the wave train. Continental, mixed and oceanic paths assign widely different values to this expression because of the different dispersion characteristics. Application of the stationary phase approximation as a "path type" correction has been applied by some researchers, notably Marshall and Basham (1972) to redetermine  $M_s$  values. It is apparent that systematic errors will still remain because the individual epicentre-station path correction was replaced by an average, for example, all continental paths were averaged as one group type correction. It would be extremely laborious to determine this correction term for all paths and periods.

However, such path corrections are an unfortunate artifact of amplitude measurements made directly from the partially dispersed time-series representation of the data. A great advantage of working in the frequency domain is that dispersion expressions of the type in 1.6 simply disappear: this alternative is now considered.

### 1.3 Amplitudes in the Frequency Domain

Rayleigh waves which have propagated a large distance are of the

form

$$f(t) = \int_{-\infty}^{\infty} S(\omega) f(k_{\gamma}) \exp [i(\omega t - k_{\gamma} R - \phi)] d\omega \quad 1.8$$

where  $f(t)$  is an observed seismogram (ignoring the transducing and distorting instrument effects),  $S(\omega)$  the spectrum of the generating force and  $k_{\gamma}$  the Rayleigh wave number. This integral could be approximated by the stationary phase approximation to give the direct observables  $A(T)$ ; the difficulties of this method are explained above. Alternatively the seismogram  $f(t)$  is Fourier analysed to give

$$A(f) = \int_{-\infty}^{\infty} f(t) \exp [-i2\pi ft] dt \quad 1.9$$

This approach has only been possible since the advent of algorithms to simplify Fourier transform calculations, and large computers to carry out the calculations; the lack of these forced the use of previous techniques.

We have now returned to the simple form of equation 1.1

$$A(f,r) = K L(f,d).I(f).S(f).D(f,r).G(f,r)$$

with  $G(f,r) = (E \sin \Delta)^{-1/2}$

$$D(f) = \exp(-\pi f E \Delta / c Q)$$

The assumption will be made that the amplitude response of the layered medium  $L(f,d)$  does not introduce a non circular radiation pattern. Also  $A(f,r)$  will be taken as instrument corrected, that is  $A(f,r)/I(f)$ .

Therefore, the distance dependence of spectral amplitudes is

$$A(f,r) = K'(E \sin \Delta)^{-1/2} \exp(-\pi f E \Delta / c Q) \quad 1.10$$

Brune (1962) has shown for surface waves that the group velocity  $U$  rather than phase velocity  $c$  ought to be used in the attenuation expression.

Taking logs gives

$$\log_{10} [A(f,r)] + 0.5 \log_{10} (E \sin \Delta) = -(Q^{-1})(\pi f E \Delta / U) + \log_{10} K'' \quad 1.11$$

This is the amplitude-distance dependence expressed as a straight line with the general form " $y = Q^{-1} x + b$ ". The amplitudes are corrected for geometrical spreading and the "distance" term,  $\pi f E \Delta / U$ , condenses the true

distance, frequency and group velocity dependence into one term. The slope of the line should give estimates of  $Q^{-1}$ , and the scatter of points an estimate of the errors involved.

It is worth noting that the dimensions of the Fourier spectra  $A(f,r)$  are length x time e.g. microns seconds, but measurements made directly from the seismogram have the dimensions of length. This is because the Fourier amplitudes apply to a continuous function and are really spectral densities. If one Fourier spectral amplitude  $A$  (dimension  $LT$ ) is assumed to cover the frequency interval  $\Delta f$  (dimension  $T^{-1}$ ) then the product  $A \times \Delta f$  may be related to the amplitudes as measured on the seismogram.

Also, the validity of the Fourier expansion should be verified for propagation on the surface of a globe. Brune et al. (1961) have carried out some work with this purpose in mind. The correct functions to be used in a series expansion for a spherical system are the Legendre polynomials. Brune et al. (1961) have shown that a Fourier expansion and a Legendre expansion are almost identical, except at the antipode, where there is a rapid phase advance of  $\pi/2$  between the two systems. This implies Hilbert transformation of a waveform as it goes through an antipode: Brune et al. (1961) observed such a change in a model experiment they conducted. However, at other regions of the global surface the Fourier expansion is an excellent match to the Legendre. Since none of the surface waves used in this work were observed for propagation paths of greater length than  $\pi$  these antipodal considerations need not concern us.

#### 1.4 Factors Necessary to Estimate $Q^{-1}$

From the discussion of equation 1.11 it is apparent that to estimate  $Q^{-1}$  it is necessary to measure the following

- $A(f,r)$ : the Fourier spectral amplitudes for a range of distances.
- $\Delta$ : epicentre-station distance
- $f$ : frequency
- $U$ : group velocity

and an instrument correction for the spectral amplitudes.

The data used and the measurements taken are discussed in the next chapter.

## CHAPTER 2

### 2.1 The Data

The records of some large nuclear explosions were chosen for analysis, these events are listed in Table 2.1 and Figure 2.1. The emphasis was on atmospheric explosions for the following reasons:

1. Atmospheric explosions have been of significantly greater yield than underground explosions and so a better signal-to-noise ratio will be expected for the available records.
2. Larger events, atmospheric explosions, are more efficient generators of low frequencies than are smaller events. A large event will therefore sample a greater depth of the earth.

One earthquake was examined for comparison purposes, this also appears in Table 2.1 and Figure 2.1. Earthquakes in general were not used, and explosions preferred, because:

1. Depth and Origin Time: for explosions the epicentre is usually constrained to zero depth thereby removing a source of error from the origin time. The origin time is vital for the determination of the wave train group velocities and usually it is more accurately known for explosions than for earthquakes.
2. Radiation patterns: for the method to be used it is important that equal or known quanta of radiation energy are emitted from the source in all directions. It is well known that earthquakes show various radiation patterns, determined by the phase concerned; and hence the energy emitted from an earthquake is a function of azimuth.

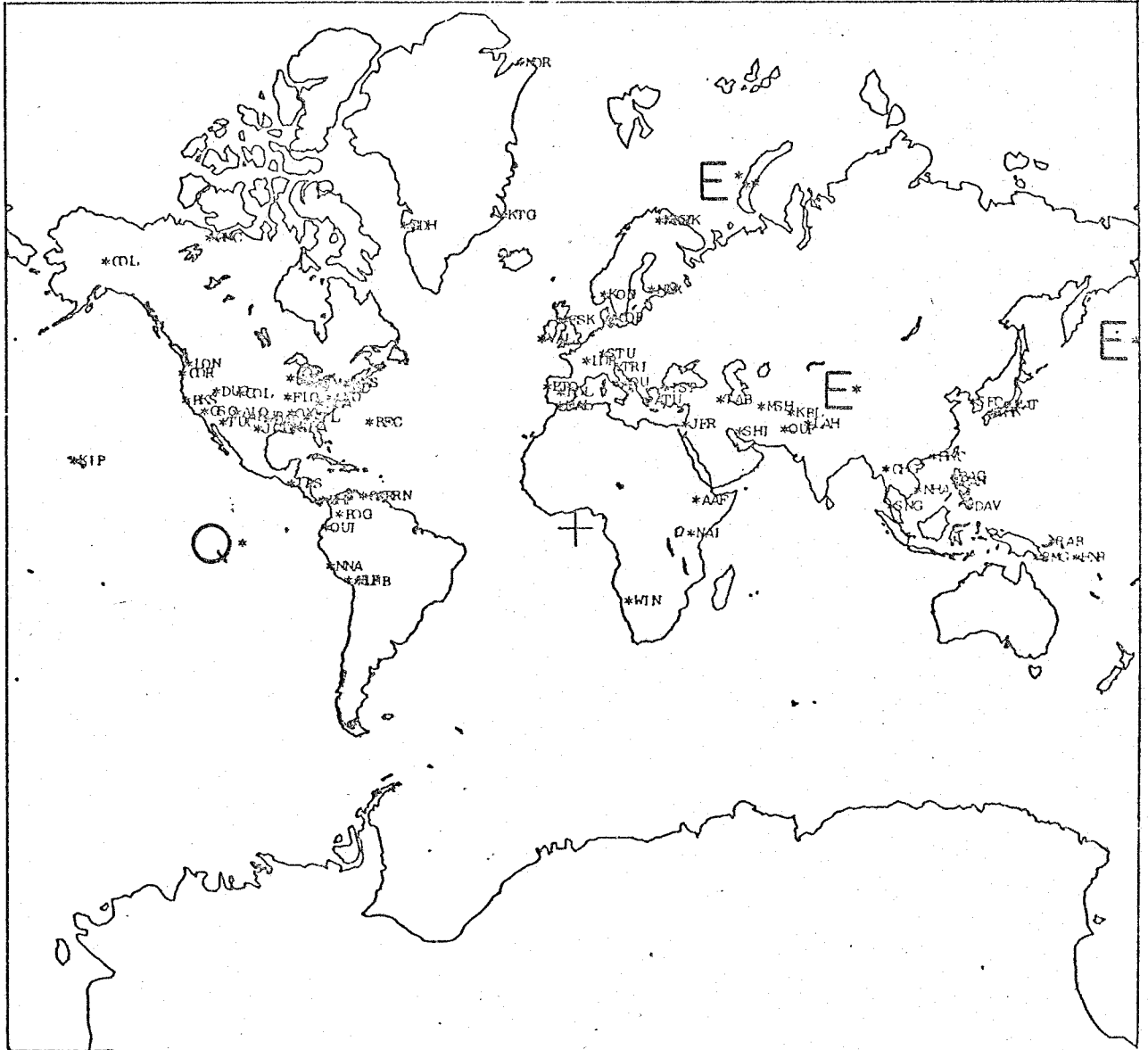
It is here considered that such a radiation pattern is not sufficiently well known to be removed from the measurements, in the sense that geometrical spreading may be corrected for and removed. An explosion intrinsically radiates equal quanta

Region	Event Type	Date	Time GMT	Latitude	Longitude	Body Wave Magnitude $m_b$	Source of Information
Novaya Zemlya	Atmospheric	27. 9.62	08 03 16.4	74.3° N	52.4° E	5¼-5½ (Pal)	PDE No 76-62
Novaya Zemlya	Atmospheric	22.10.62	09 06 10.1	73.4° N	54.9° E	5-5¼(Pal)	PDE No 84-62
Novaya Zemlya	Atmospheric	24.12.62	11 11 42.0	73.6° N	57.5° E	Similar to 27.9.62	PDE No 103-62
Aleutian Islands (Longshot)	Underground	29.10.65	21 00 00.1	51.433° N	179.183° E	5.97	Marshall et al. 0-67/66
Lop Nor (China)	Atmospheric	17. 6.67	00 19 07.9	40.73° N	89.56° E	4.6(CGS)	PDE No 47-67
Novaya Zemlya	Underground	7.11.68	10 02 05.3	73.4° N	54.9° E	6.0(CGS)	PDE No 87-68
Lop Nor (China)	Atmospheric	29. 9.69	08 40 31.0	40.7° N	89.6° E	4.7	LASA Bulletin
Northern Easter Island	Earthquake	17. 6.67	00 56 29.4	4.5° S	104.73° W	4.8(CGS)	PDE No 41-67

Table 2.1 Event Time, Epicentre and Origin Time



EVENT EPICENTRES AND THE W-SSN STATIONS USED



MERCATOR PROJECTION

ALL BEARINGS CORRECT AND ORTHOMORPHIC

FIGURE 2.1

in all azimuthal directions, that is if we ignore the lateral variations in geological structure and the specific attenuation factor  $Q^{-1}$ . Further, it would be impossible to distinguish between anomalous source effects and anomalous lateral variations of  $Q^{-1}$ .

3. Spectral content: Carpenter and Marshall (1970) have published the source spectrum for atmospheric explosions. It is approximately a constant, as expected, because intuitively it is the Fourier transform of an impulse in the time domain. In determining  $Q^{-1}$  as a function of frequency all frequencies are of equal interest, therefore it is pleasing to have all frequencies equally represented in the source spectrum.

A spectral source-layering term for underground explosions,  $S_u(f) \cdot L_u(f,d)$ , has been published (Marshall and Burton 1971) and this represents the product of the source spectrum with the amplitude response of the layered medium at the epicentre. This function can be seen to be monotonically decreasing for underground explosions, whereas the similar function for an earthquake has a minimum turning point (Marshall and Burton 1971 Figures 2 and 4), commonly referred to as a spectral hole. The hole in an earthquake spectrum is associated with the depth of the source interacting with the source mechanism (Douglas, Hudson and Khembhavi 1971) and therefore no explosion will exhibit such a phenomenon, for this reason, because they are near surface events. This smoothness of the underground spectral frequency content means that no particular group of frequencies in the spectrum will be particularly difficult to investigate because of suppression at the source.

It should be possible to determine the underground explosion source function, rather than the source-layering term, by applying the "Common Path" method to a large explosion and the subsequent cavity collapse.

The cavity collapse records from the large Cannikin event are of sufficient signal-to-noise ratio to encourage such an investigation.

With the events chosen because of the above reasons the available WWSSN film chip recordings for the long period, vertical component system were examined. The WWSSN gives good world coverage with standard instrumentation.

The records which were digitised are listed in Appendix 1.

In all several hundred records were examined and about 200 of these were digitised. Many of the records examined were not digitised because of their poor quality, extremely poor signal-to-noise, "knitting" records, coincident events or simply because the relevant event was not found. Much of the data obtained from the WWSSN records are of excellent quality, especially the earlier data recorded with a fast drum speed.

The digitised records were sampled every 1.6s, determining a Nyquist frequency of 0.3125 Hz. The digitising was performed on an AGI film assessor which was especially suitable for WWSSN film chips. This machine steps along the time axis at equal increments, and the digitised amplitude coordinate was obtained by matching crosswires to the top side of the seismogram. Digitising started at a minute marker or at a known number of sample intervals before a prominent record feature and continued until the end of the record. Care was taken to omit any lateral refractions, or reflections of seismic energy and to avoid digitising the minute markers.

Measurements were taken from the individual record calibration pulses and instrument parameters noted, in accordance with the work of Espinosa, Sutton and Miller (1965). Appendix C describes the calculation of  $I(f)$  from these measurements.

To complete the initial data it is necessary to know the epicentral coordinates and the origin times for events. These are obtained from the PDE cards published by the USCGS. Also the coordinates

of the WWSSN stations are required, these are published in the WWSSN handbook (1965).

## 2.2 Data Analysis

The data analysis falls into two main parts; the determination of the spectral Fourier amplitudes and the group velocities, followed by the estimations of  $Q^{-1}$  using a least squares technique.

Initial information was obtained using the program GEDESS (Young and Gibbs 1968). This program calculates the epicentre-station separation  $\Delta^{\circ}$  and allows for the ellipticity of the earth. The program also calculates the estimated time of arrival of the Rayleigh 40s period wave (assuming a velocity of 3.97 km/s) from an epicentre to any recording station. This helped to find the correct event when other events occurred on the same record.

Spectral amplitudes and group velocities were obtained using the "Time Series Analysis Program" (TSAP) described in the attached report (Burton and Blamey 1972). This program was written in its present form especially for this work, its structure will be summarised briefly here and its advantages described later.

### 2.2.1 Spectral Amplitudes

The spectrum  $x(f)$  of a continuous time series  $x(t)$  is usually given as the Fourier Transform integral

$$x(f) = \int_{-\infty}^{\infty} x(t) \exp(-i2\pi ft) dt \quad 2.1$$

Experimentally sampled data  $X(t)$  differs from  $x(t)$  in several respects. Because it is sampled data it is a discrete valued function rather than continuous, and so the transform integral is replaced by a summation and the values of  $f$  and  $t$  become discrete. Further, the range of integration cannot possibly be infinite. We obtain a function of the form

$$Z(f_j) = \sum_{n=0}^{N-1} X(t_n) \exp\left(\frac{-i2\pi jn}{N}\right) \quad |j| \leq \frac{N}{2} \quad 2.2$$

when there are  $N$  points in the time series. The increment  $dt$  is omitted because it is now only of use as a scaling factor. But it is important to include the scaling factor, which is the sampling interval, when converting to absolute values (Enochson and Otnes 1968).

If the value  $N$  is increased so that the new  $N = 2^L$  (integer  $L$ ) then expression 2.2 may be rapidly calculated using the Cooley-Tukey algorithm. It is the combined simplification caused by these algorithms and the availability of fast computers which make possible the treatment of data in the frequency domain.

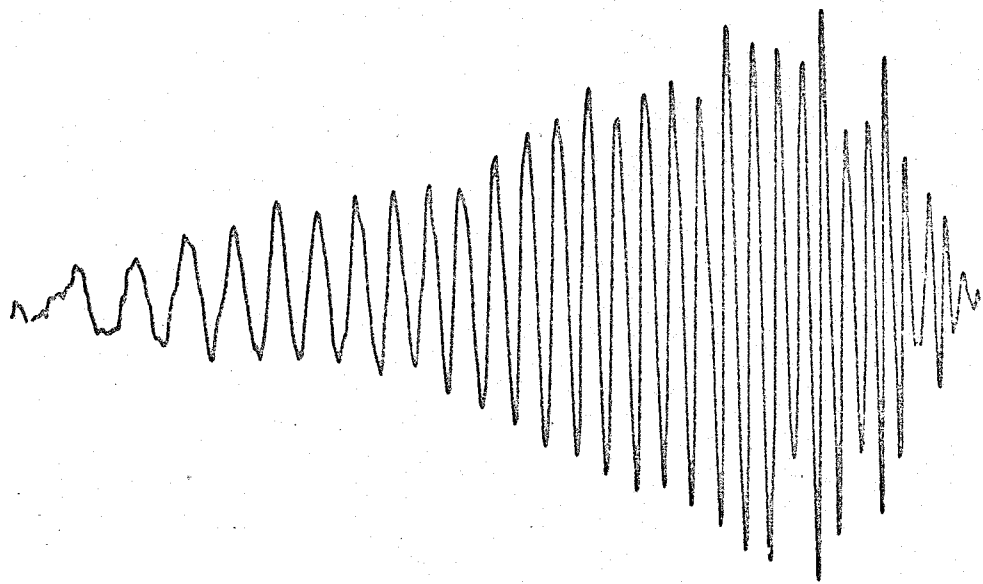
The function  $Z(f_j)$  in 2.2 is complex; it contains information about both amplitude and phase for the spectrum. This is discussed in detail by Burton and Blamey (1972).

The real and imaginary parts of the instrument transfer function,  $I(f)$ , may easily be allowed for by complex division in the frequency domain.

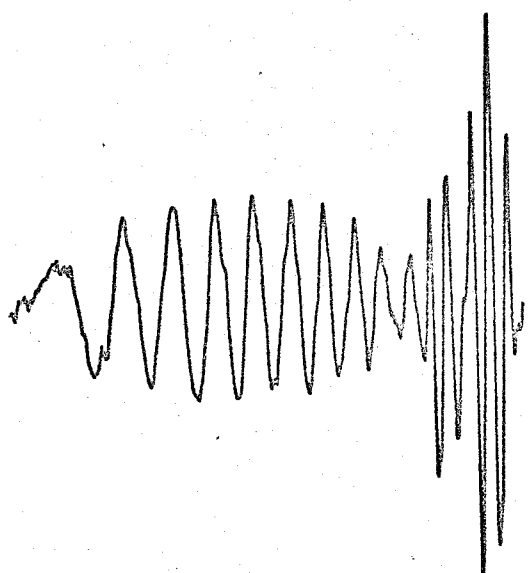
The spectra obtained after allowing for instrumental distortions are filtered to remove very low frequencies, that is the fundamental and a few higher harmonics. Also the spectra are smoothed, simply averaging eight consecutive values to give a smoothed value, but moving along in steps of four values at a time.

Three seismograms illustrating the "raw" data are shown in Figure 2.2. The records at Malaga and Kongsberg have good signal-to-noise; the one for Kap Tobin is very noisy. The amplitude spectra for these seismograms after correcting for the instrument transfer function, removal of low frequencies and smoothing are shown in Figures 2.3-2.5. The Malaga spectrum is excellent data. The spectra for the Kongsberg and Kap Tobin records show some of the possible sources or elimination of errors.

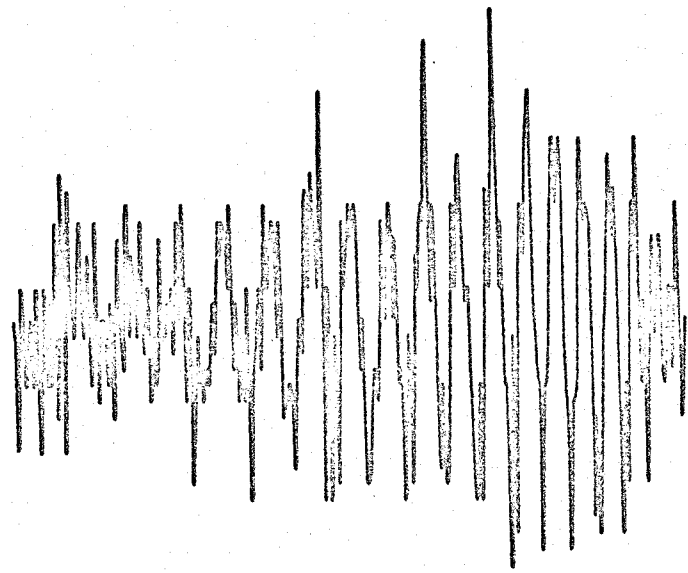
The spectral values for Kongsberg have two distinct holes at frequencies 0.05 and 0.075 Hz. Such spectral holes are not a common occurrence but will obviously influence the  $Q^{-1}$  values and broaden the confidence limits around these frequencies. These holes probably result



Malaga, Spain  
NZA 24.12.62  
 $\Delta = 47.3^\circ$



Kongsberg, Norway  
NZA 27.9.62  
 $\Delta = 21.5^\circ$



Kap Tobin,  
Greenland  
CA 29.9.69  
 $\Delta = 58.85^\circ$



FIGURE 2.2 Three Typical Seismograms

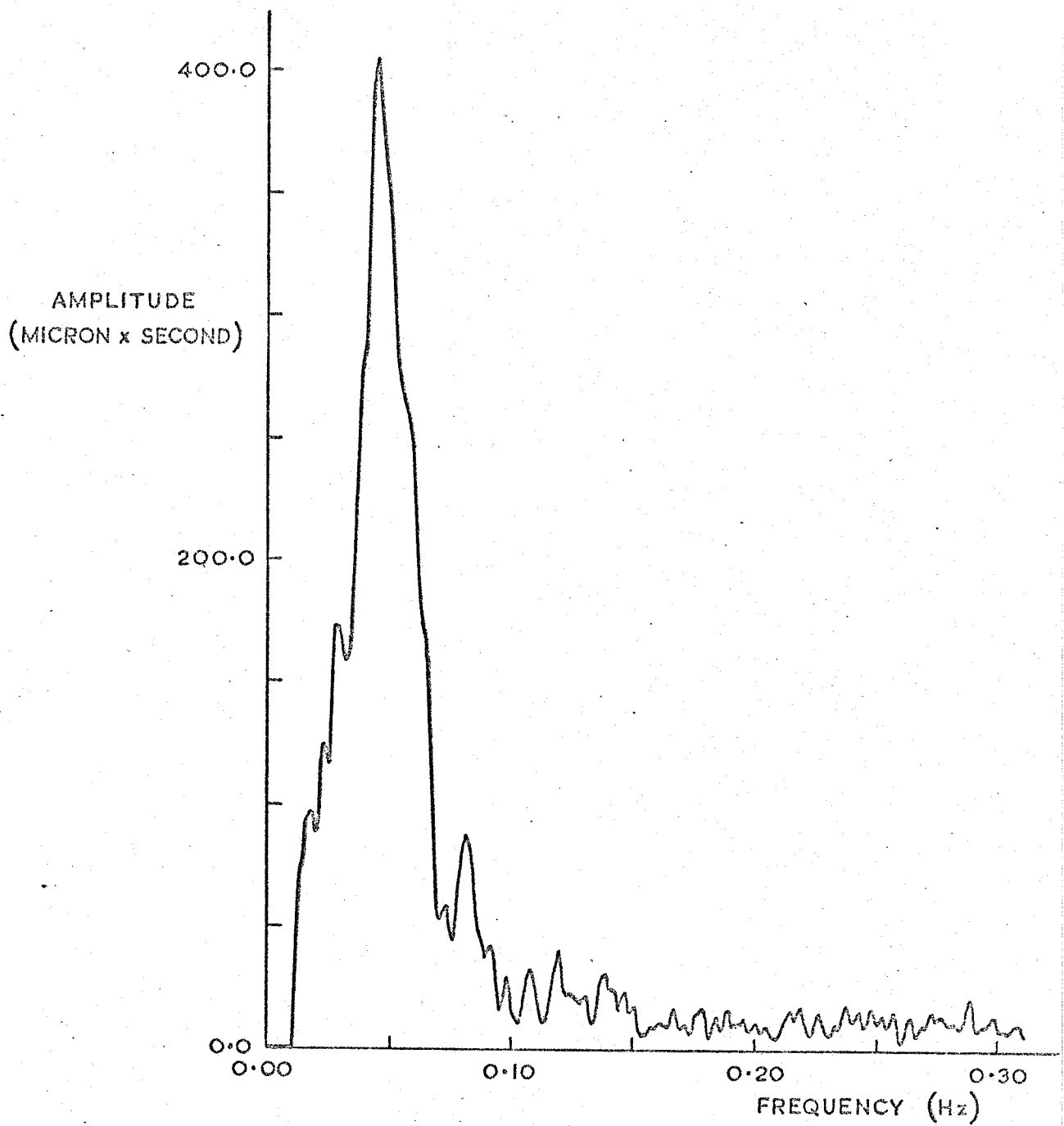


FIGURE 2.3 SPECTRAL AMPLITUDES FROM MALAGA SEISMOGRAM  
(EVENT: ATMOSPHERIC EXPLOSION,  
NOVAYA ZEMLYA, 24th DECEMBER 1962,  
DISTANCE = 5260 km)

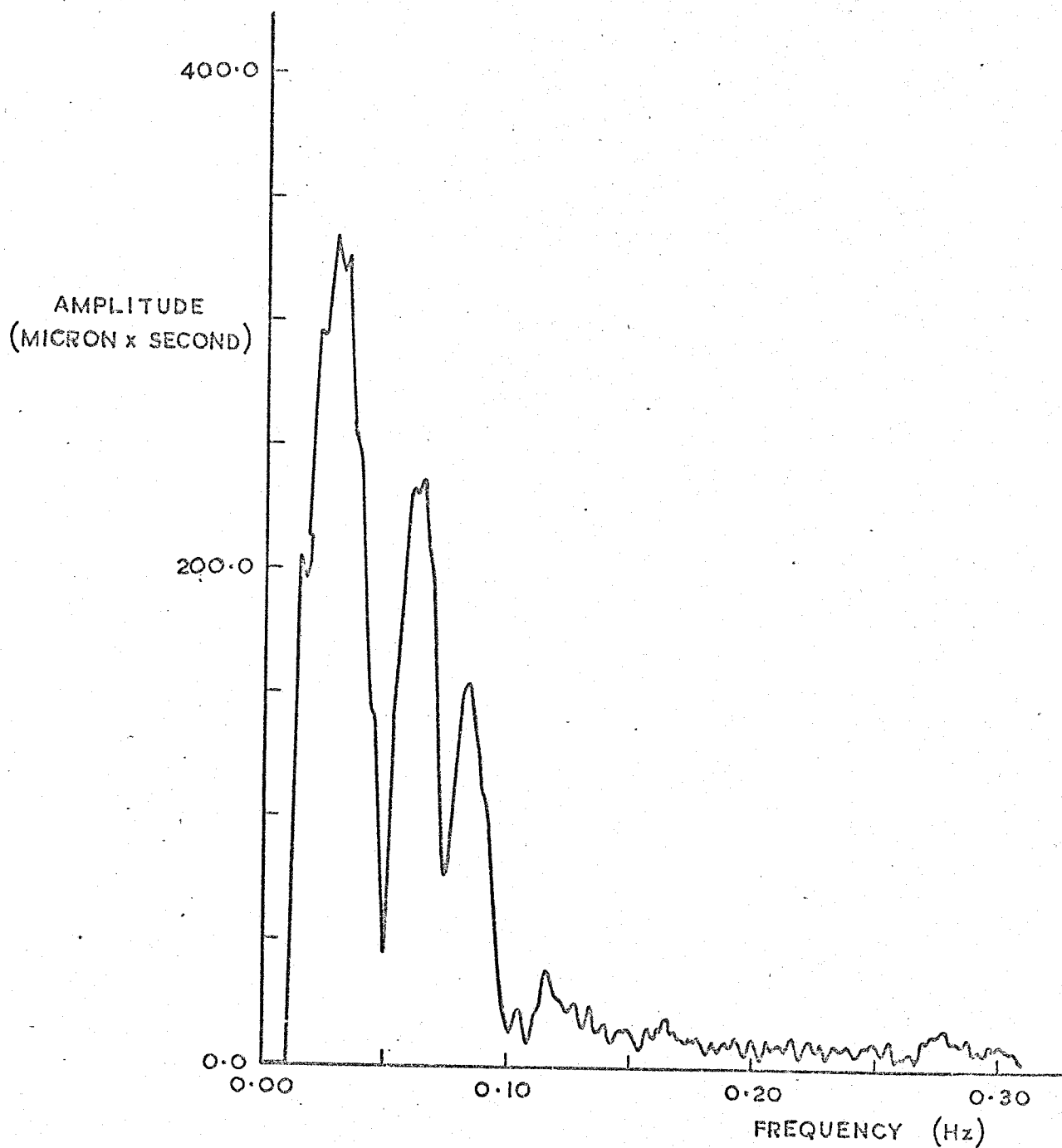


FIGURE 2.4 SPECTRAL AMPLITUDES FROM KONGSBERG SEISMOGRAM  
(EVENT: ATMOSPHERIC EXPLOSION,  
NOVAYA ZEMLYA, 27th SEPTEMBER 1962,  
DISTANCE = 2391 km)



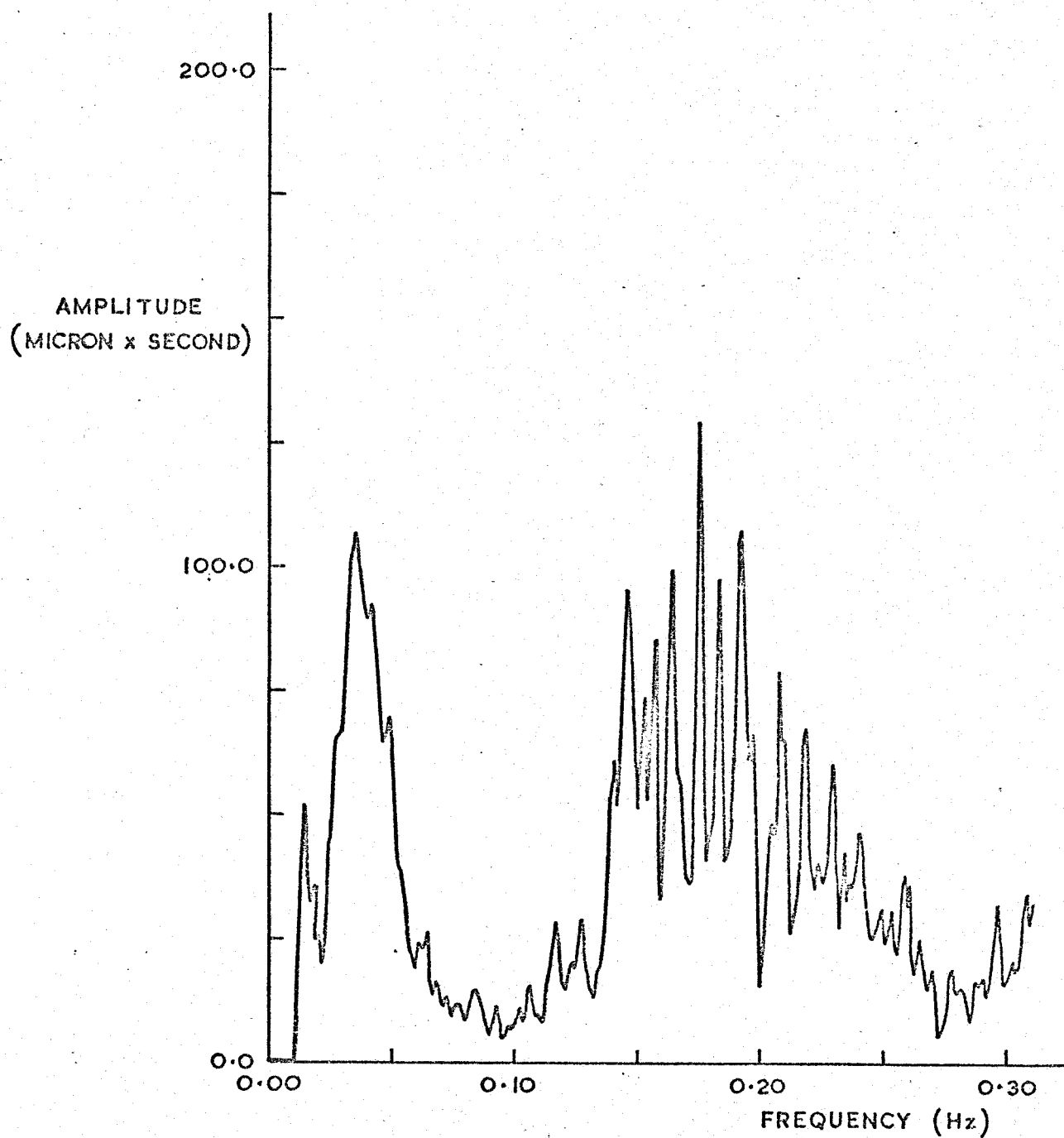


FIGURE 2.5 SPECTRAL AMPLITUDES FROM KAP TOBIN SEISMOGRAM  
(EVENT: ATMOSPHERIC EXPLOSION,  
S. SINKIANG PROV., CHINA, 29th SEPTEMBER 1969,  
DISTANCE = 6544 km)

from multipathing between Novaya Zemlya and Kongsberg, causing destructive wave interference at these particular frequencies.

The spectrum of the very noisy Kap Tobin record is surprisingly good for the frequency range of interest, up to 0.1 Hz. The signal spectrum has obviously been separated from the noise, there is a pronounced microseism peak in the range 0.15-0.25 Hz. It is quite apparent that poor signal-to-noise in the time domain does not necessarily imply poor signal-to-noise in the frequency domain. The Kap Tobin record also shows evidence of low frequency barometric noise around 0.017 Hz, but this is described later.

These three seismograms illustrate the data ideal along with factors which will subsequently contribute to the experimental errors.

### 2.2.2 Group Velocity

The group velocities for the frequencies required were determined for each record using the multiple filtering technique of Dziewonski, Block and Landisman (1969). The technique used differs from that of Dziewonski et al. in one important respect, for this work the group velocities were determined at exact Fourier harmonics to eliminate frequency errors. The method and the reasons for doing this are described later.

Dziewonski's method uses the formulation of Goodman (1960) who investigated the determination of instantaneous amplitude and phase for a dispersed time series. It is not sufficient to filter a seismogram for a set of specific frequencies because the filter output will also be an oscillating signal and its maximum point will therefore be difficult to determine. Goodman (1960) assigned a non-oscillating instantaneous amplitude and phase,  $R(t)$  and  $\phi(t)$ , to a signal  $A(t)$  by using the analytic signal definition

$$R(t) e^{i\phi(t)} = A(t) - iH(t) \quad 2.3$$

where ideally  $H(t)$  is the Hilbert transform of  $A(t)$  and

$$R(t) = [A^2(t) + H^2(t)]^{1/2} \quad 2.4$$

If the frequency domain filter response to a seismogram is  $a(f)$  then also required is the quadrature filter response  $h(f)$ . The quadrature filtering is simply the Hilbert transform (H) of the filter response  $a(f)$ , this simply means that the filter response  $a(f)$  is advanced by  $\pi/2$  giving  $h(f)$ .

The spectrum of 2.3 may be approximated by the form

$$\begin{bmatrix} 1 & g(f) \\ -g(f) & |g(f)|^2 \end{bmatrix} a(f) \quad 2.5$$

which improves in efficiency as  $g(f) \rightarrow i$  (Goodman 1960). However since the work of Goodman modern fast Fourier transform (F) techniques make such approximation negligible and the Hilbert transform may easily be found because

$$F H (A(t)) = i \text{ sign } (f) F(A(t)) \quad 2.6$$

Equation 2.4 gives a non-oscillating signal waveform from which the discrete instantaneous amplitudes  $R(t)$  may be determined. Figure 2.6 illustrates group velocity determination at the filter frequency 0.033 Hz for an atmospheric explosion at Novaya Zemlya (NZA 24.12.62) recorded at Kongsberg. The relation between the instantaneous amplitudes  $R(t)$  and the group velocity or group arrival time is easily seen. The figures 6, 7 and 8 of Burton and Blamey (1972) show that the process may be extended to determine group arrival times and the consequent group velocities for a range of frequencies.

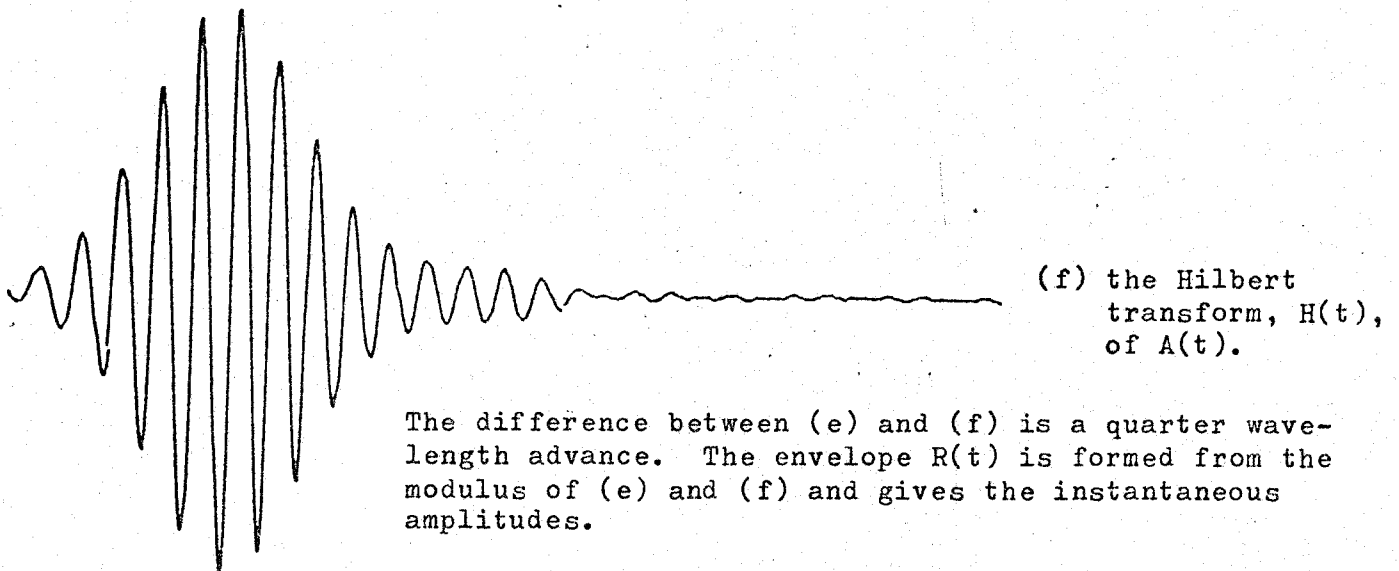
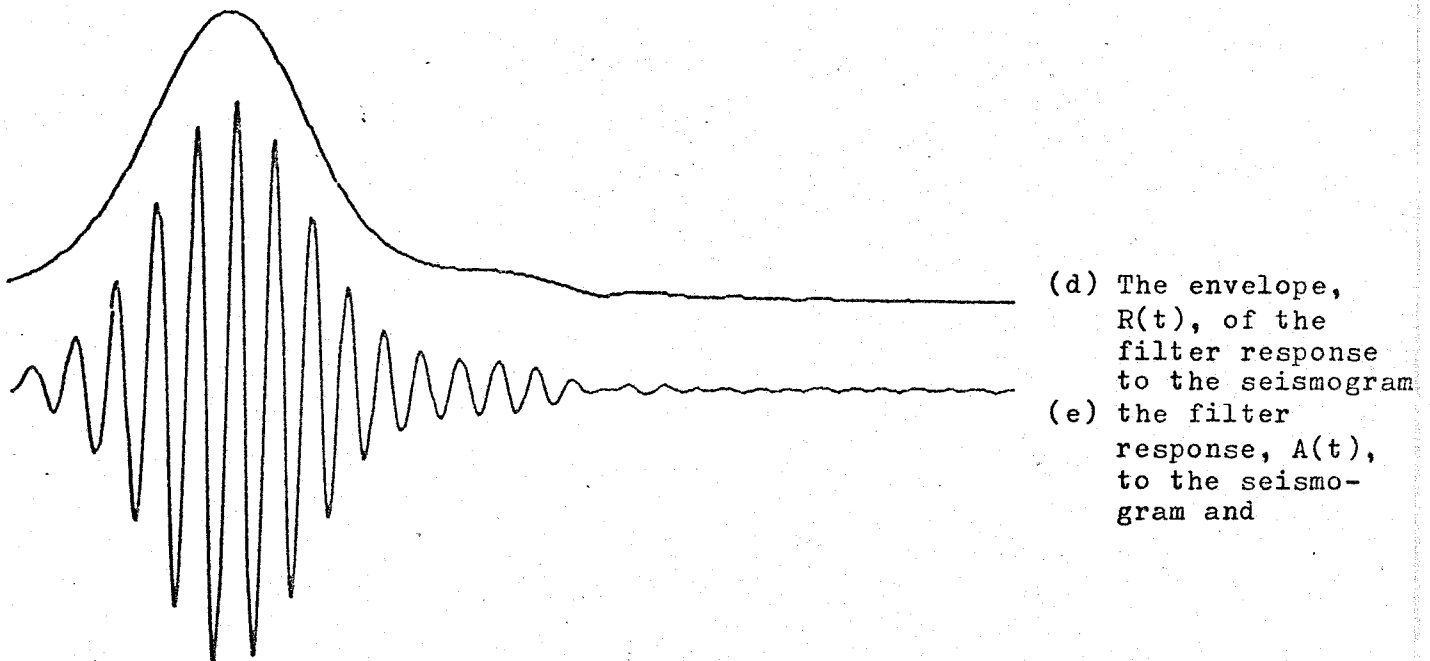
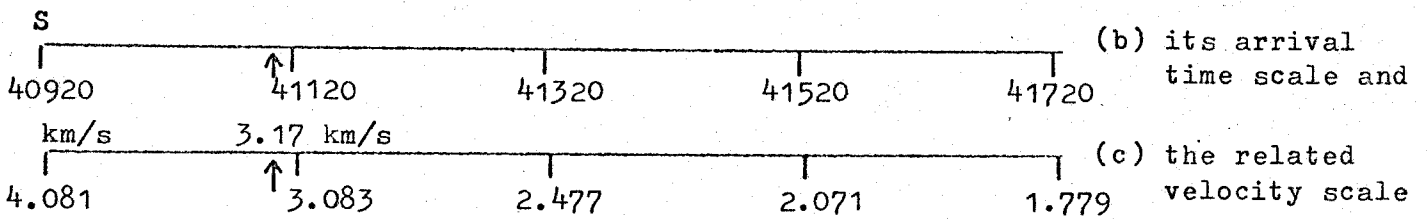
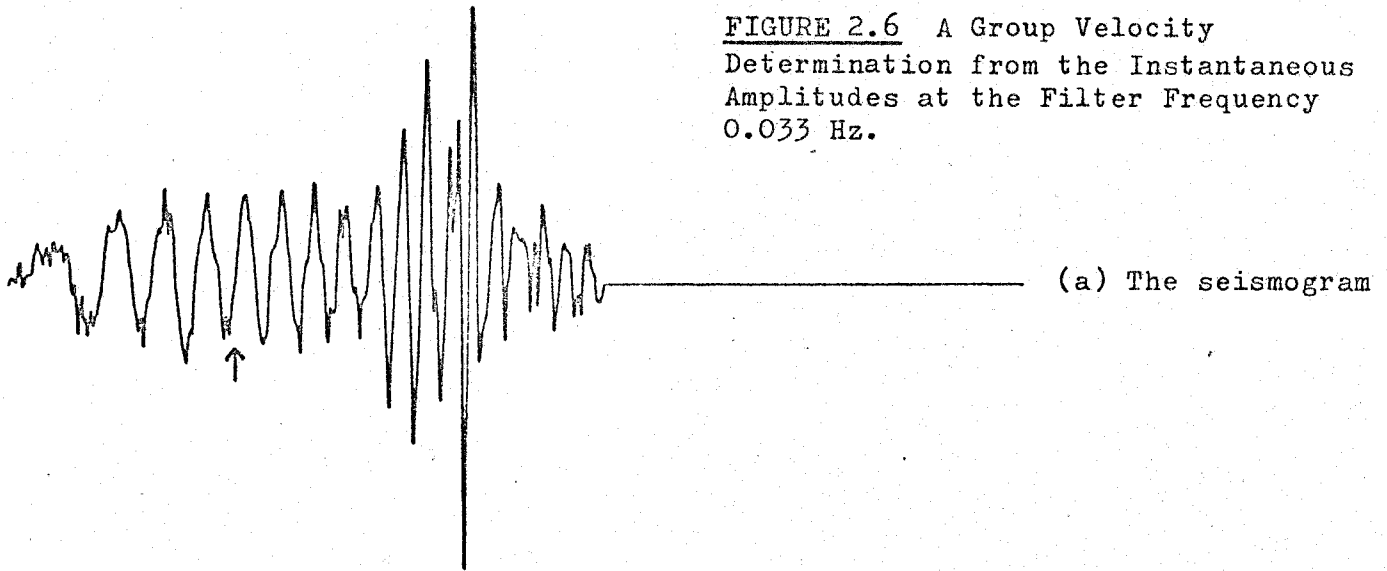
### 2.3 Reduction of Errors

Of the many possible sources of error in the analysis of the time series several could be reduced, whilst others had to be accepted.

#### 2.3.1 Spectral Amplitude Measurements

It was first decided that all spectral amplitudes would be determined for the same frequency values for the Fourier Harmonics, irrespective of the record length. Since all records were increased in length to satisfy the relation  $N=2^L$  this was simply a matter of choosing a consistent value for  $L$  ( $L=11$  was chosen) and so all records were increased to 2048 points and the Fourier Harmonics are therefore

**FIGURE 2.6** A Group Velocity  
 Determination from the Instantaneous  
 Amplitudes at the Filter Frequency  
 0.033 Hz.



The difference between (e) and (f) is a quarter wave-length advance. The envelope  $R(t)$  is formed from the modulus of (e) and (f) and gives the instantaneous amplitudes.

$$f_j = \frac{f_{NYQ} \times j}{N/2} \quad 2.7$$

The sampling interval used is 1.6s and so the Nyquist frequency is

$$\begin{aligned} f_{NYQ} &= \frac{1}{3.2} \text{ Hz} \\ &= 0.31250 \text{ Hz} \end{aligned}$$

the fundamental Fourier Harmonic is

$$\begin{aligned} \Delta f &= \frac{f_{NYQ}}{N/2} \\ &\sim 0.00305 \text{ Hz} \end{aligned}$$

and the Fourier Harmonic series is

$$f_j = j \times \Delta f \quad (0 < j \leq N/2) \quad 2.8$$

Amplitude measurements at these frequencies may be in error

because of

- 1 Digitising errors
- 2 Digitising excess record
- 3 The instrument correction
- 4 Noise
- 5 Higher modes
- 6 Fourier analysis preferred to Legendre polynomial.

#### 1 Digitising Errors

The first type of digitising error is caused simply by the machine resolution. The machine used, an AGI Film Assessor, displayed the x and y coordinates to four significant figures. The last figure (one assessor unit) resolved  $10^{-5}$  m on the film chip. The factor between a film chip and the original seismogram is an eight fold reduction and so

$$1 \text{ assessor unit} = 8.10^{-5} \text{ m of original seismogram (a.u.)}$$

Any y coordinate was usually repeatable to better than  $\pm 4$  a.u. or  $3.10^{-4}$  m of original seismogram. An absolute random digitising error of  $\pm 0.3 \cdot 10^{-5}$  m for the original sized seismogram is good and no attempt was made to improve this resolution.

However, an attempt was made to minimise the introduction of high frequencies caused by motion of the digitiser between digits during hand digitising. The introduction of these high frequencies is demonstrated in a paper by Bogert et al. (1962). The crosswires were always traced along the top side of the seismogram line, this arbitrary decision prevents the digitising trace oscillating within the thickness of the seismogram line.

The first digit was always set to read 5000 a.u. so that the digitised trace was on a pedestal. Whenever possible the seismogram was orientated so that the last digit would be the same as the first, to eliminate a step effect at the end of the record. During the program processing the digitised time series was depedestalled by removing the mean. Also the series was cosine tapered at each end to ensure a smooth junction between the trace and baseline and avoid spurious high frequency content.

Occasionally a mispunch would occur during digitising and the most significant figure would be omitted. If such a trace was Fourier analysed then the "spike" caused in this way would dominate the spectral content. So all traces were graphed out before processing by TSAP, and these glitches removed.

## 2 Digitising Excess Record

Any excess of digitised record is only obvious in the time domain display (with an exception to be discussed later) and can be dealt with when the digitised trace is first graphed out. Any excess record will alter the Fourier harmonic amplitudes at the frequencies it contains, this is normally the higher frequencies because they occur at the end of the dispersed record. Lateral refractions may be identified by matching the separation between crossovers for a later part of the time trace with an earlier section. Such lateral refractions must be removed because they have not travelled by the direct path from epicentre to receiver.

### 3 The Instrument Correction (Described in Appendix C)

The instrument corrections used assigned a small, but finite, value for magnification at the low frequencies (less than .01 Hz) whereas the peak magnification might be several hundred times larger. A nuclear explosion does not usually produce such low frequencies. But for the uncompensated WWSSN seismometer the barometric noise amplitude is proportional to the square of the period. It was found that these small amplitudes at low frequencies, when divided by a very small magnification as instrument correction, dominated the event itself. On reverse transforming to the time domain, all that could be seen was a large amplitude low frequency component with a tiny seismogram superimposed onto it! So all frequencies lower than 0.0125 Hz were filtered out.

### 4 Noise

The enhancement of low frequency noise, and its removal, has been described above. The frequency range of interest is about 0.014-0.1 Hz and any higher frequencies are omitted. An explosion does not produce energy which propagates for large distances with frequencies much greater than 0.1 Hz, so the seismic noise peak at about 0.12 Hz is omitted. Fourier analysis of the trace does separate out the signal from this noise peak as is shown by Figure 2.2 and Figure 2.5 (seismogram and spectrum). The frequencies of interest stand out as a separate peak and are clearly distinguished from the noise peak, thus eliminating this systematic source of noise.

Random noise in the useful frequency range cannot be distinguished, but a useful frequency range for a particular signal spectrum may be obtained by considering signal-to-noise in the entire range. For example in Figure 2.5 it is apparent that .015 to .09 Hz is good. A particularly noisy station may show a noise spectrum generating ground motion of the order of microns, this may fluctuate down to  $m\mu$  in a short time (Brune and Oliver 1959).

## 5 Higher Modes

It is assumed in this analysis that only the fundamental Rayleigh mode is analysed, no reason was found to doubt this. If higher modes were present they would disturb the spectral values at high frequencies. No coherent high frequency energy was ever found superimposed onto the seismograms, and no high frequency dispersion branches were found in the group velocity determinations. The assumption that Fourier analysis was analysis of the fundamental mode always appears to be valid.

## 6 Fourier Analysis Preferred to Legendre Polynomials

This has already been described. Because none of the Rayleigh waves used pass through an antipode the Fourier representation is excellent. If the waves did pass through an antipode only the phase properties would be incorrect, and this has no bearing on the present analysis.

At this stage of the processing, when the time series has been depedestalled, cosine tapered, increased to  $2^L$  points and Fourier analysed, it is possible to improve the spectrum by smoothing. Smoothing is especially valid because the spectrum is greatly overdetermined. A typical record of length 500 points (about 13 minutes) has been increased to 2048 points. The spectrum therefore has four times as many frequency points or harmonics than are required to uniquely determine it. (Assuming that the time series does not contain any frequencies greater than the Nyquist.) A reasonable smoothing would decrease the number of harmonics by a factor of four. The smoothing chosen compounds eight values at a time, but steps along the frequency harmonics four at a time. The smoothed spectrum is now less erratic for noisy signals. The smoothing operation is also designed so that the new frequency values generated still correspond to the old exact Fourier harmonics, with a step of  $4 \times \Delta f$  between each smoothed value.



The number of harmonics filtered out at low frequencies is 41 (due to the long period noise and instrument response previously mentioned) and so the available frequency harmonics which are non-zero are  $42\Delta f$  up to the Nyquist. However all the frequency harmonics, from the zero DC component onwards are smoothed as described above. The harmonics available after smoothing are

$$4\Delta f, 8\Delta f - - - - - \text{Nyquist.}$$

But spectral values up to  $41\Delta f$  have been set to zero and so the first smoothed harmonic which is not contaminated by this filtering is  $48\Delta f$ ; the smoothed, uncontaminated harmonics now available are

$$48\Delta f, 52\Delta f - - - - - \text{Nyquist}$$

and those selected to be punched out from the computer processing are  $48\Delta f - 360\Delta f$ . There are 79 values in this frequency range 0.015-0.110 Hz. It later appears that this choice of upper frequency content is perhaps over optimistic; and is often seriously contaminated by noise.

### 2.3.2 The Frequencies of Spectral Amplitudes and Group Velocities

In this section a modification to the technique of Dziewonski et al. is described, which was thought to be desirable in general, and necessary in this particular study.

The paper by Dziewonski, Bloch and Landisman (1969) describes their "multiple filter technique". The points of interest here are

- 1 The seismogram  $x(t)$  is Fourier transformed producing
- 2 the complex array  $Z(\omega)$  at
- 3 the Fourier harmonics  $\omega_j$ .
- 4 Centre frequencies for group velocity determination are selected according to a rule of the type

$$\frac{\omega_{c,n-1}}{\omega_{c,n}} = k \quad 2.9$$

- 5 A range of group arrival times,  $\tau_m$ , is selected

$$\tau_m = \frac{\text{DISTANCE}}{V_m}$$

6. Filters of constant  $Q$  (ratio of peak frequency to bandwidth) are formed, the filter or frequency window centred at  $\omega_n$  is

$$W_n(\omega) = \exp\left[-\alpha\left(\frac{\omega - \omega_{c,n}}{\omega_{c,n}}\right)^2\right]$$

where the constant  $\alpha$  determines roll-off.

There are two separate frequency arrays. The values of the Fourier harmonics are directly determined by the number of points in the time series and the sample interval, as before

$$\omega_j = j \times \Delta\omega \quad 0 < j < N/2$$

with

$$\Delta\omega = \frac{\omega_{NYQ}}{N/2}$$

and  $\omega$  is angular frequency.

Centre frequencies are chosen according to  $\omega_{c,n-1}/\omega_{c,n} = k$ ; and so it is unlikely for these centre frequencies to correspond to an exact harmonic. For the Dzierwonski technique the harmonic nearest to a given  $\omega_{c,n}$  is chosen to replace  $\omega_{c,n}$  in all computation. Dzierwonski et al. (1969) stated that "the maximum deviation of the harmonics from the array frequencies was always less than 1.5 per cent".

The rule for selection of centre frequencies makes the interval between these frequencies a function of frequency since

$$\Delta\omega_{c,n} = \omega_{c,n} - \omega_{c,n-1}$$

$$\Delta\omega_{c,n} = \omega_{c,n} (1-k)$$

and the smallest interval occurs at the lowest frequency.

To ensure that two centre frequencies for group velocity determination are replaced by different Fourier harmonics (if this is not done then the same group velocity will be assigned) we must have

$$\Delta\omega_{c,n} > \Delta\omega$$

$$\therefore \omega_{c,n} (1-k) > \frac{\omega_{NYQ}}{N/2}$$

Assuming the values:

$$\omega_{c,n} = 2\pi \times 0.01 \text{ rad s}^{-1}$$

$$k = 0.95$$

$$\omega_{NYQ} = 2\pi \times 0.5 \text{ rad s}^{-1}$$

gives  $N > 2000$

To ensure that the low centre frequencies, and therefore group velocities, are distinct we have a necessary lower limit on the record length.

Further, we may wish to improve the condition that the error introduced by replacing a centre frequency by a harmonic is less than 1%.

$$\frac{\omega_{c,n} - \omega_j}{\omega_{c,n}} < 0.01$$

The greatest possible error in the offset from a filter centre frequency to a harmonic is  $\frac{1}{2}\Delta\omega$ , the best it can be is right; averaging out at  $\frac{1}{4}\Delta\omega$ . So on average  $\omega_{c,n} - \omega_j = \frac{1}{4}\Delta\omega$  and we have

$$\frac{\frac{1}{4}\Delta\omega}{\omega_{c,n}} < 0.01$$

$$\frac{\omega_{NYQ}}{2N\omega_{c,n}} < 0.01$$

$$N > \frac{50\omega_{NYQ}}{\omega_{c,n}}$$

and using the previous values for  $\omega_{NYQ}$  and  $\omega_{c,n}$

$$N > \frac{50 \cdot 2\pi \cdot 0.5}{2\pi \cdot 0.01}$$

$$\therefore N > 2500$$

Even applying these conditions to the above values we find the ratio of the average error in a filter frequency to the gap between filter frequencies is

$$\text{ratio} = \frac{\Delta\omega}{4\Delta\omega_{c,n}}$$

$$\therefore \text{ratio} = 1/5$$

and so this resolution is not too good.

This discrepancy between the harmonic frequencies at which spectral amplitudes are determined, and the filter frequencies for determining group velocities, may influence any investigation of  $Q^{-1}$  as a function of frequency because  $Q^{-1}$  is determined using amplitudes and velocities presumed determined at the same frequency. This situation may be altered quite easily.

First, it is apparent that angular frequency may be replaced by frequency in all the above calculations so that  $\omega_j$  becomes  $f_j$ , which is a more familiar quantity.

If the selection equation 2.9 is changed to

$$f_{c,n} - f_{c,n-1} = k'$$

then by careful choice of  $f_{c,1}$  and  $k'$  it is possible to match all the centre frequencies to exact Fourier harmonics. Then, the above limitations are removed, and there is no discrepancy between spectral and group velocity frequencies. We have a frequency selection rule of the form

$$f_{j,n} - f_{j,n-1} = k'' \Delta f$$

where  $\Delta f$  is the fundamental. The equation finally used was

$$f_{j,n} - f_{j,n-1} = 8 \Delta f$$

and the value selected for  $f_{j,1}$  was  $48 \Delta f$  because this exactly corresponds to the first smoothed harmonic frequency of interest (see before).

Selecting  $8 \Delta f$  as the interval ensured that a group velocity was determined at every other frequency for which a spectral amplitude had been calculated, giving 40 values in the required frequency range. Because the interval chosen is an even number of  $\Delta f$ s simple linear interpolation exactly half way between two adjacent group velocity values generates the other 39 values required.

This process gives exactly matching smoothed spectral amplitudes and group velocities, without any frequency errors, by careful choice of the smoothing operation and selection of the filter centre frequencies as exact harmonics.

### 2.3.3 Group Velocity Errors

Errors in simple velocity determination are of the form

$$\frac{\delta U}{U} = \frac{\delta \Delta}{\Delta} - \frac{\delta t}{t}$$

The angular distance,  $\Delta$ , is accurately known (Young and Gibbs, GEDESS, 1968) and errors are confined to measurements of the group arrival time. Values of the group arrival time must be within the time span of the digitised seismogram, however, times assigned to individual samples may be in error for two reasons:

- 1 It has been assumed that the digitising machine increment between samples remains constant and
- 2 the reduction of seismograms to film chips (x8) is exact and no photographic "shrinkage" takes place.

The first assumption was checked for systematic variations.

There are two time scales in use on film chips, they are  $3.10^{-3}m$  representing 48s and  $3.10^{-3}m$  representing 96s. Because 1 assessor unit represents  $10^{-5}m$  of film the digitising increments used were 10 a.u. and 5 a.u., both representing a 1.6s sample interval. A typical 10 minute record is therefore about 3750 a.u. or 1875 a.u. long. After digitising such a record and returning to the starting point the starting point reading was never found to differ by more than 3 a.u. from its original value, showing remarkable consistency in the long term average sample interval. Any random variations in the sample length were not evident when the digitised series was graphed out and so are ignored.

Photographic reduction proves not to be exact. When the digitising of a record started exactly on the leading edge of a minute marker then

the number of samples in the first three minutes was noted. Assuming the sample interval is 1.6s (it has been shown to be at least constant above) then about 112.5 samples would be expected. The number of samples required would occasionally differ by 2 from this figure. Because the mechanical sample interval is certainly constant this implies that the time scales differ because of inexact reduction, by about 1%.

It is possible to exactly determine the time sample interval by digitising between two minute markers, counting the number of samples, and hence deducing the interval (DELA). This would lead to an independent value of DELA for each seismogram, the accuracy being that of the mechanical sample interval. This was not done because the value of DELA determines the subsequent Fourier harmonics for a record and it was desirable to have matching harmonics for all records. To simplify the analysis this error of about 1% was tolerated, rather than eliminated as was possible.

Consequently, errors in the group arrival time increase with record length and this <sup>a</sup> effects high frequencies more than low frequencies (because low frequencies usually arrive first). Considering a wave with travel time 30 minutes (about 60<sup>o</sup>) to the first sample, and of length 10 minutes, errors in the group velocity at the latter end of the record are

$$\frac{\delta U}{U} \sim \frac{6}{40.60} \times 100\% = 0.25\%$$

This effect is obviously very small and worth accepting to obtain the matching Fourier harmonics.

A much larger error may be introduced by bursts of noise. The seismic noise around 0.1 Hz is important in this respect. A dispersed Rayleigh signal may contain energy around 0.1 Hz, usually at the latter end of the signal, but noise energy at the same frequency may be superimposed randomly on the record. The noise energy may be greater than the modal

propagated energy and the program technique has no means of distinguishing the two. Because the program searches to find when the most energy (of a particular frequency) arrives, and then assigns a group arrival time to that peak (see Burton and Blamey 1972) the corresponding group velocities may be in considerable error.

Such errors are not serious because obviously if the local noise amplitude is greater than the propagated wave amplitude then the spectral Fourier amplitude can no longer be regarded as a Rayleigh fundamental mode amplitude. These values of amplitude can only be used to determine  $Q^{-1}$  if the noise may be corrected for at each recording station. When these errors occur the signal-to-noise ratio for the frequency domain must be worse than 1:1.

#### 2.3.4 Redetermination of the End of the Signal

It has already been stated that if the record is digitised beyond the end of the true signal then this excess signal will contribute erroneously to the signal spectral amplitudes, usually at the higher frequencies. Once a group velocity curve has been obtained then it is possible to redetermine the end of the signal. Essentially noise is removed which has an apparent velocity less than the slowest determined group velocity,  $U_s$  km/s. There are four velocities of interest here for a digitised signal. The velocity to the first sample is  $V_F$ , to the last sample  $V_L$  (noting that the number of samples has been increased to  $2^L$ ) and the velocity to the last true digit before increasing to  $2^L$  is  $V_{ED}$ . Their relative sizes are  $V_F > U_s > V_{ED} > V_L$ ; ideally  $U_s$  is close to  $V_{ED}$  so that little extra record is present to introduce spurious spectral content. The instantaneous amplitudes  $R(t)$  described in section 2.2.2 are stored in a matrix, the E matrix, as a function of both velocity and filter frequency. Instantaneous amplitudes for a particular frequency form one column of the E matrix, and subsequent columns store  $R(t)$  for further frequencies. The maximum of the entire matrix is set to 99 dB and all other values are

normalised relative to this maximum. The seismogram of Figure 2.7 recorded at Lahore (Pakistan) produces the E matrix, contoured at 5 dB intervals, shown in Figure 2.8. Velocities  $V_F$ ,  $U_S$ ,  $V_{ED}$  and  $V_L$  are easily identified on this figure. Everything represented on the contour plot, or in the E matrix, with velocity  $< 2.26$  km/s is meaningless in terms of real data and represents rounding error. Therefore in the region of 2.26 km/s the contour lines are closely packed and parallel to the x axis - because there is a discontinuity between genuine time domain content and very low level time domain content outside the observed length of the signal time range. The dB jump in the E matrix representation is about 30 dB.

The minimum value of group velocity is about 2.80 km/s. This particular value is chosen because it is slower than the velocity of the highest frequency analysed and this velocity is several dBs down from the ridge followed by the group velocity curve. The region between 2.80 and 2.26 km/s, for all frequencies, can only represent noise; it is non propagating energy or lateral refractions. Ideally this region should not exist, and so the arrival time corresponding to  $U_S = 2.80$  km/s is calculated and the digitised record truncated to this new length. Figure 2.7 shows the alteration in seismogram length and Figure 2.9 the contour plot for the new E matrix.

Where possible this process was applied to all seismograms, to improve the spectral amplitudes (by lowering their noise content). However this method cannot improve the seismogram for velocities within the true signal range, and only helps to isolate the pure signal.

#### 2.4 Amplitude-Distance Plots and Estimations of Q

For each event the data are now in the form of fundamental Rayleigh mode amplitudes (approximated to by Fourier amplitudes) and group velocities as functions of frequency for a set of stations at varying distances from the epicentre.

Every block of station data is essentially amplitude and group velocity as a function of frequency at fixed  $\Delta$ , this has to be manipulated



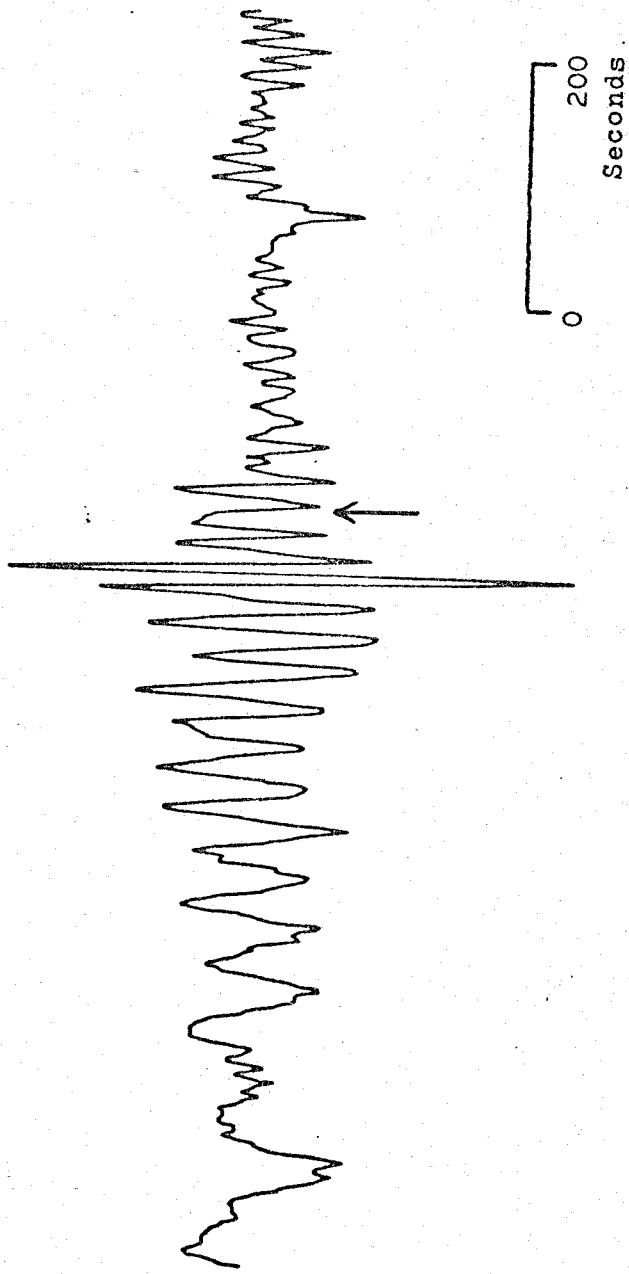
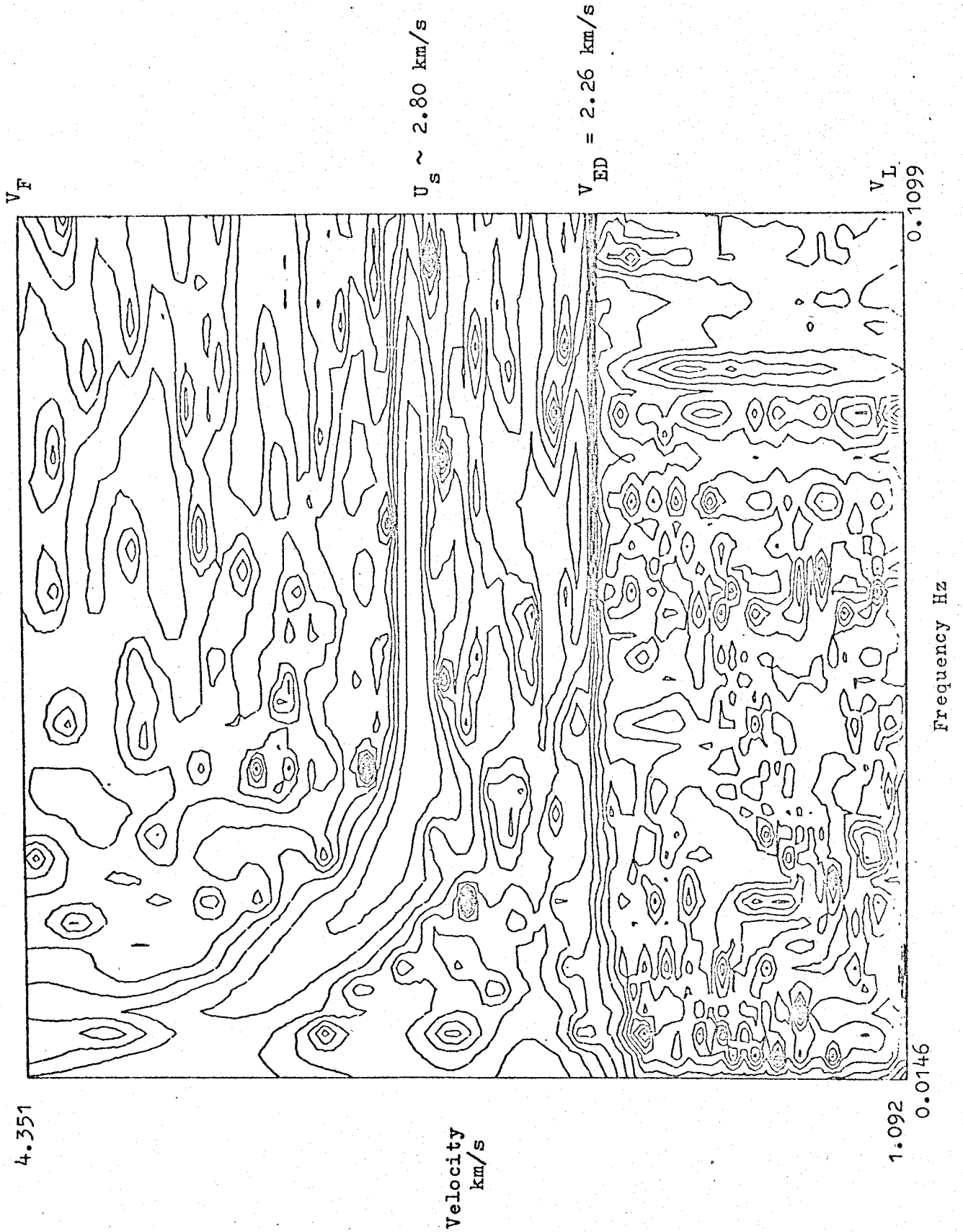


FIGURE 2.7 The Lahore Seismogram for the Atmospheric Explosion NZA 24/12/62 ( $\Delta = 43^\circ$ )  
The Redetermined Record End is Marked by the Arrow.



**FIGURE 2.8** The Contoured E Matrix for the Full Length Lahore Seismogram.

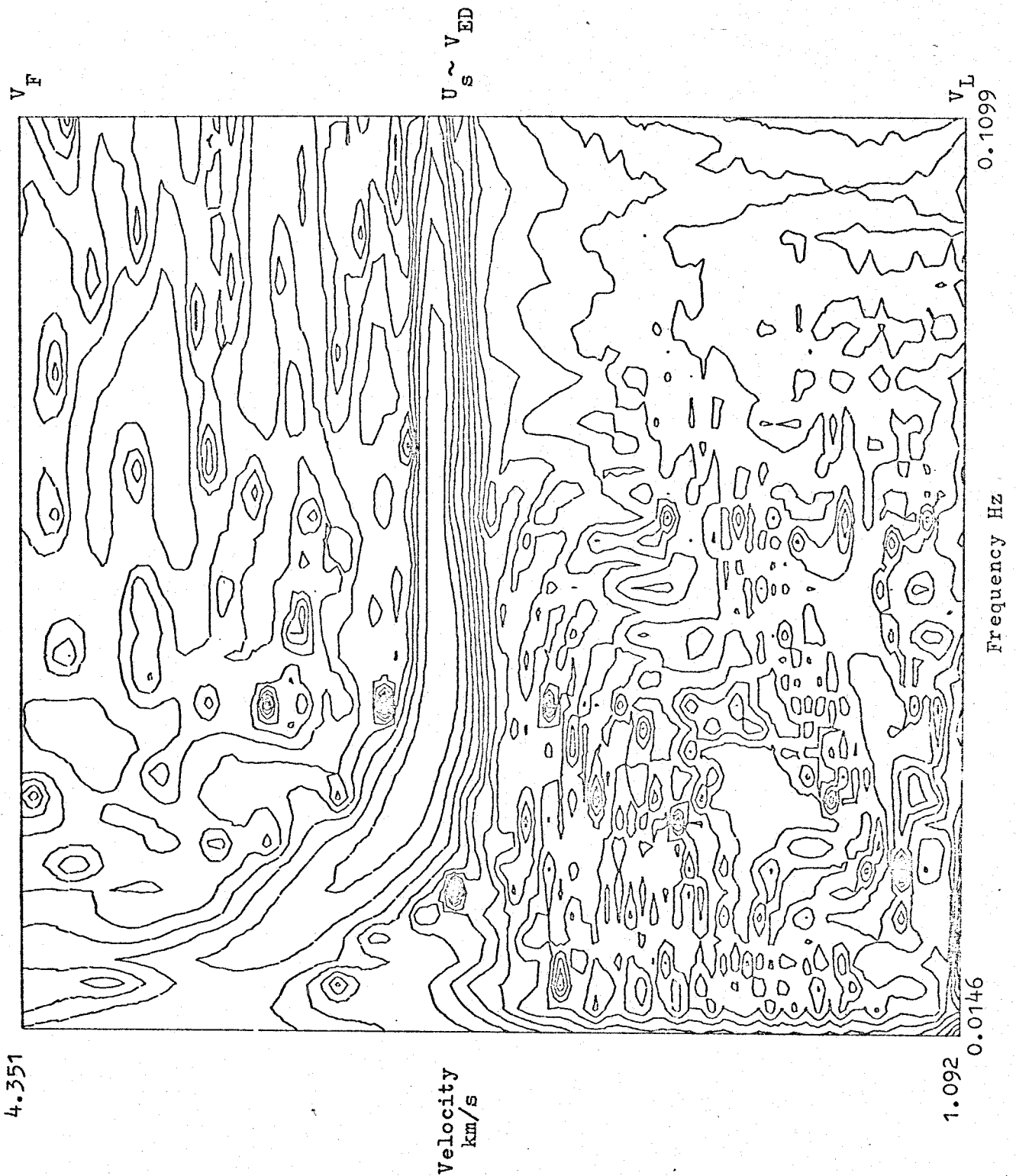


Figure 2.9 The Contoured E Matrix After Redetermining the End of the Lahore Seismogram.

into the form amplitude and group velocity as a function of  $\Delta$  at fixed frequency, so that spatial  $Q$  may be determined. The required plot is given by equation 1.11 as

$$\log_{10}(A(f,r)) + 0.5 \log_{10}(E \sin \Delta) = -(Q^{-1})(\pi f E \Delta / U(f,r)) + \text{const} \quad 2.10$$

where the left hand side is plotted as ordinate and  $\pi f E \Delta / U$  as abscissa. The slope of the best line through these points estimates  $Q^{-1}$ . Note that it is inverse  $Q$ , not  $Q$ , which is physically estimated; the more natural and useful quantity of  $Q^{-1}$  will be used.

Appendix G contains the program AVD which performs this data manipulation, geometrical spreading correction and estimation of  $Q^{-1}$ . From a measure of the scatter of the data points about the best line confidence limits for  $Q^{-1}$  are also determined.

## 2.5 The Best Line

### 2.5.1 Average $Q^{-1}$

Simple linear least squares regression was found to be a very close approach to the best line fit, and is thus used. The program AVD contains a subroutine which determines regression coefficients and hence  $Q^{-1}$  and the confidence limits.

The basic assumption for this regression is that the ordinate alone contains errors. The present data are a good approximation to this, the errors in amplitude measurements being far greater than for group velocity.

This is easily demonstrated by considering surface wave magnitudes. An underground explosion, MILROW, has average surface wave magnitude determined by the USCGS as  $M_s = 5.0$ . Using the formula

$$M_s = \log_{10} Y + 2.0 \quad 2.11$$

gives the yield  $Y$  kton as 1000 kton. The event is large and good signal-to-noise is generally to be expected.  $M_s$  values are calculated from formulae of the type

$$M_s = \log A(T) + B(\Delta) \quad 2.12$$

where  $B(\Delta)$  is a distance correction term. Ideally an event gives the same  $M_s$  value wherever it is recorded, with good signal-to-noise the scatter should be small and attributable to 10% errors in instrument magnification and hence in the amplitude  $A$ . The recording at Blacknest of MILROW gave  $M_s = 4.52$ , an apparent deviation from the mean magnitude of 10% (Marshall, Corbishley and Gibbs 1970). This would imply an error in  $A$  of 300%, obviously this is not so. In some way the path between MILROW and Blacknest is anomalous, the measured amplitude is in error by about 10% but is anomalous by a much greater margin.

But average  $Q^{-1}$  is being estimated. A reasonably accurate measurement of amplitude at a station may have a large anomaly margin from the expected value. For least squares fitting purposes such anomalous deviations must be regarded as "errors", and as shown above of the order of 10% errors. Also, because the average is sought, any extremely anomalous values must be subjectively rejected, this was done rarely. If many events at the same site had been used it would have been possible to isolate these anomaly margins as station path corrections.

Errors in the ordinate are possibly 10% whilst about 0.25% in the group velocity. The ratio of errors between the two axes is 40:1, this is possibly optimistic but an order of magnitude certainly prevails. Simple linear regression is therefore a good approximation to the best line. A more sophisticated regression fitting is described in Appendix D, and the errors in reducing this to the present case are discussed there.

It is worth noting that the abscissa term also contains the variables  $\Delta$  and  $f$ , errors in the abscissa will compound to form

$$\frac{\delta "x"}{"x"} = \frac{\delta \Delta}{\Delta} + \frac{\delta f}{f} - \frac{\delta U}{U}$$

Ignoring  $\delta \Delta$  leaves  $\delta f$  and  $\delta U$ , the importance of ensuring that group velocity and amplitude are measured at the same exact frequencies is again apparent.

A typical plot of amplitude/distance at frequency 0.0525 Hz

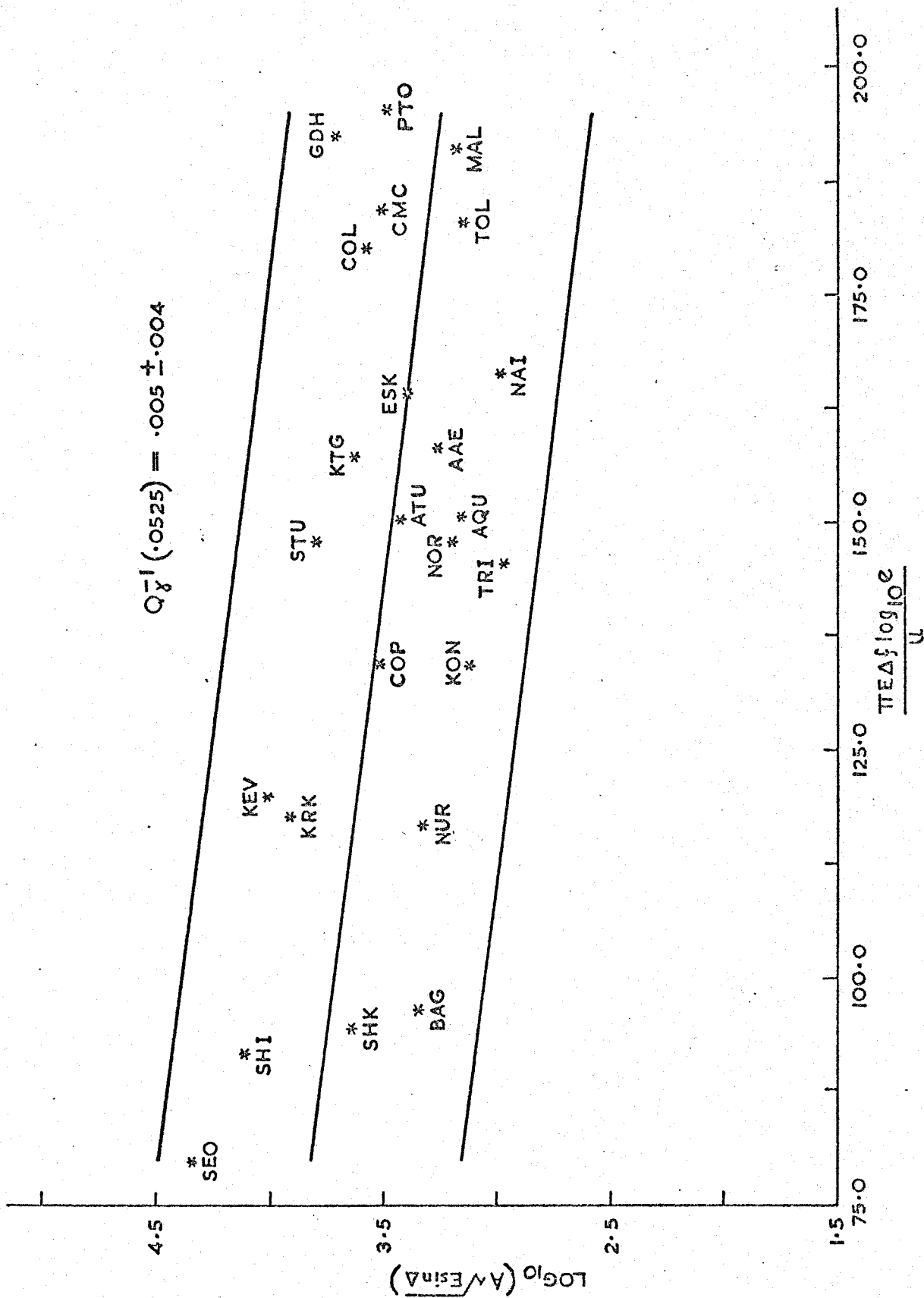


FIGURE 2.10 AN AMPLITUDE-DISTANCE PLOT FOR AN ATMOSPHERIC EXPLOSION AT S. SINKIANG PROV., CHINA  
 (1744 JUNE 1967. FREQUENCY = 0.0525 HZ. THE REGRESSION LINE AND 95% SCATTER ARE MARKED)

is shown in Figure 2.10, this gave a value of  $Q_Y^{-1} = .005 \pm .004$ , with 95% confidence limits. Student's t for this line is 2.62, significant at the 98% level, implying that there is good correlation between the ordinate and abscissa, this reasserts that a line is a good curve to fit to this data. (The correlation coefficient = -.49.)

Figure 2.10 also shows the deviation of the individual data points from the least squares line, these deviations are in agreement with the preceding argument concerning the variation of  $M_s$  values.

### 2.5.2 Assumptions for Linear Regression

Using linear regression with one independent variable assumes that the ordinate,  $y_{ij}$ , is a normal deviate distributed about a mean  $\mu_i$  which is of the form  $\alpha + \beta (x_i - x)$  with variance  $\sigma_i^2$ , and all variances are equal (Miller and Kahn 1962).

To test normality it would be necessary to have  $n_i$  values of the amplitude (for one frequency) at each station, this would require a series of similar explosions detonated at the same site. This cannot be tested when  $n_i$  is small as in this study, further, the explosions are all different and unrepeatable events. To test for equal variances it would be necessary to apply Bartlett's test, again impossible when  $n_i$  is small.

The assumption of linearity is adequately tested by calculation of the correlation coefficient and Student's t for each line.

### 2.6 Summary

This chapter has described the data used and its analysis to produce spectral amplitudes and group velocities for the fundamental Rayleigh mode, both for varying frequency and distance. The data was then manipulated to produce arrays of amplitude against distance at a frequency. The slope of the best line (chosen to be linear regression with one independent variable) through these data points is the required estimation of  $Q^{-1}$ .

## CHAPTER 3

### 3.1 The Estimations of $Q_Y^{-1}(f)$

The techniques described in the previous chapter were used to produce values of  $Q_Y^{-1}$  as a function of frequency. This was done for each of the nuclear explosions listed in Table 2.1 and one earthquake for comparison purposes. The 95% confidence limits around each  $Q_Y^{-1}(f)$  value were also calculated. Values of  $Q_Y^{-1}(f)$  and confidence limits are obtained from the best line fit to the amplitude/distance plot for a particular frequency, the program AVD performs this operation and it is described elsewhere. The results of this process are shown in the eight figures, 3.1-3.8, and listed in Appendix B.

Figure 3.8 shows the  $Q_Y^{-1}$  values obtained using eleven station recordings of an earthquake. As expected these results are very poor, and obviously this method is not applicable to an earthquake. The major reason for this is the radiation pattern which earthquakes usually possess. Also, earthquakes must necessarily occur in an anomalous environment; the local  $Q$  at source is probably laterally very inhomogeneous. Confidence limits are therefore very broad for the earthquake.

Nine recordings of the 80 kton "LONGSHOT" underground nuclear explosion (Marshall et al. 1966) were used to obtain Figure 3.7. Broad confidence limits are again apparent, especially at low frequencies, but these results are an improvement over the earthquake and use fewer stations. Broader confidence limits at the lower frequencies are to be expected because an underground explosion contributes more energy to the higher frequencies. However, in general these results are again poor probably because "LONGSHOT" occurred in another anomalous region - an island arc - where lateral inhomogeneities in  $Q$  are to be expected. The paper of Barazangi et al. (1972) well illustrates the unusual  $Q$  variations to be expected in such anomalous regions.



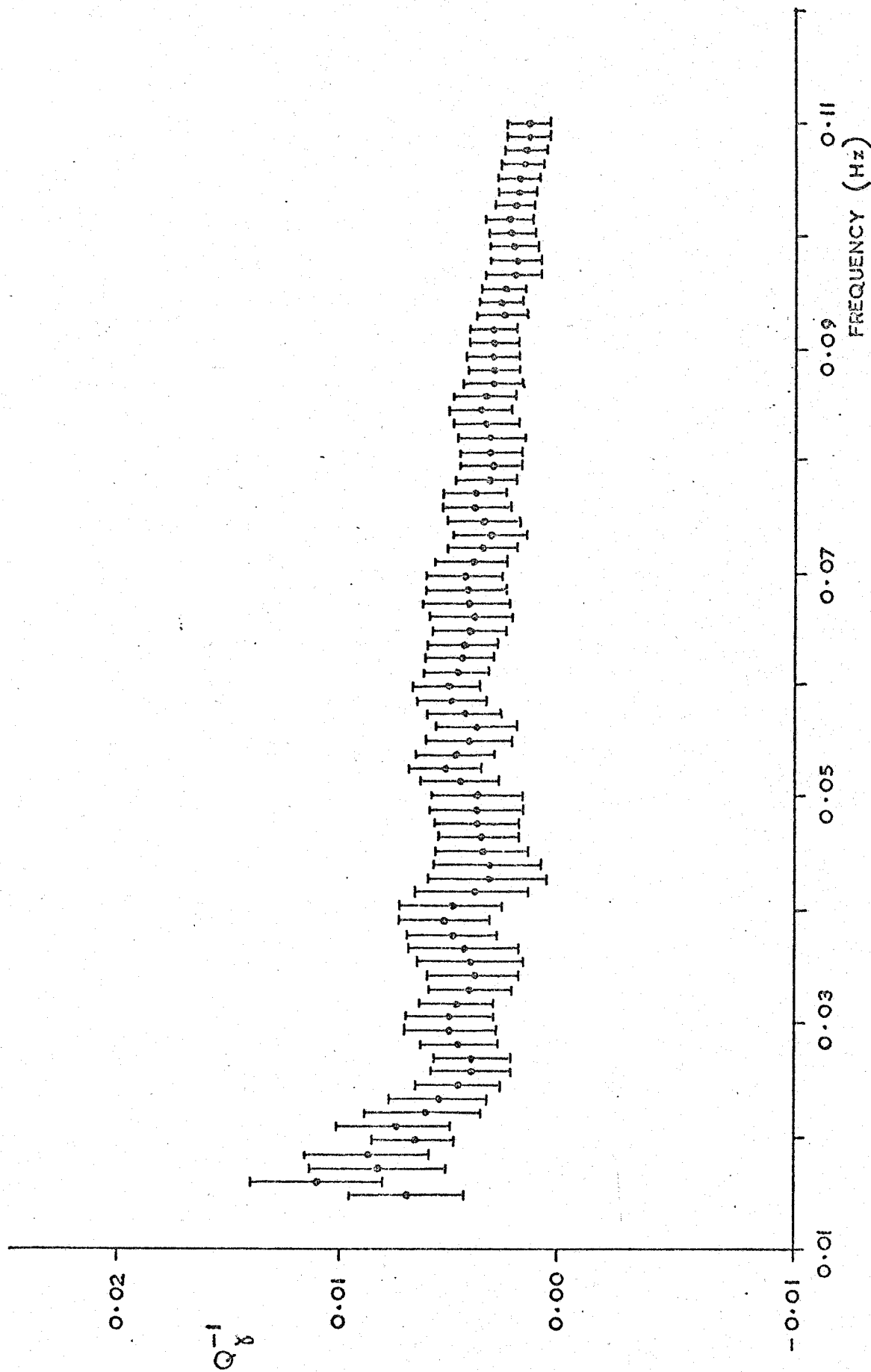


FIGURE 3.1  $Q_y^{-1}$  AND 95 P.C. CONFIDENCE LIMITS ESTIMATED USING 28 RECORDINGS OF THE ATMOSPHERIC EXPLOSION IN NOVAYA ZEMLYA, 27th SEPTEMBER 1962

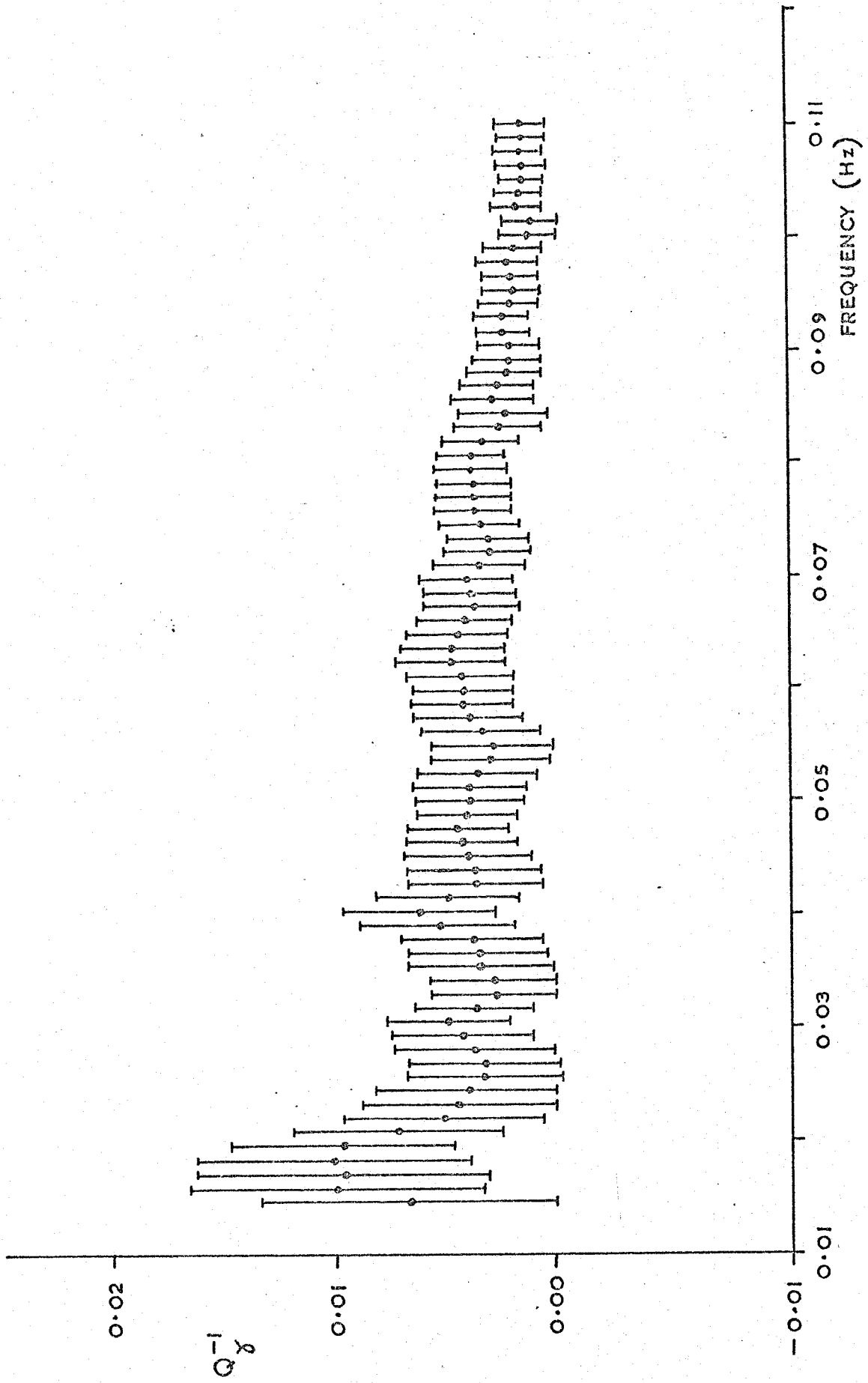


FIGURE 3.2  $Q_y^{-1}$  AND 95% C. CONFIDENCE LIMITS ESTIMATED USING 27 RECORDINGS OF THE ATMOSPHERIC EXPLOSION IN NOVAYA ZEMLYA, 22ND OCTOBER 1962

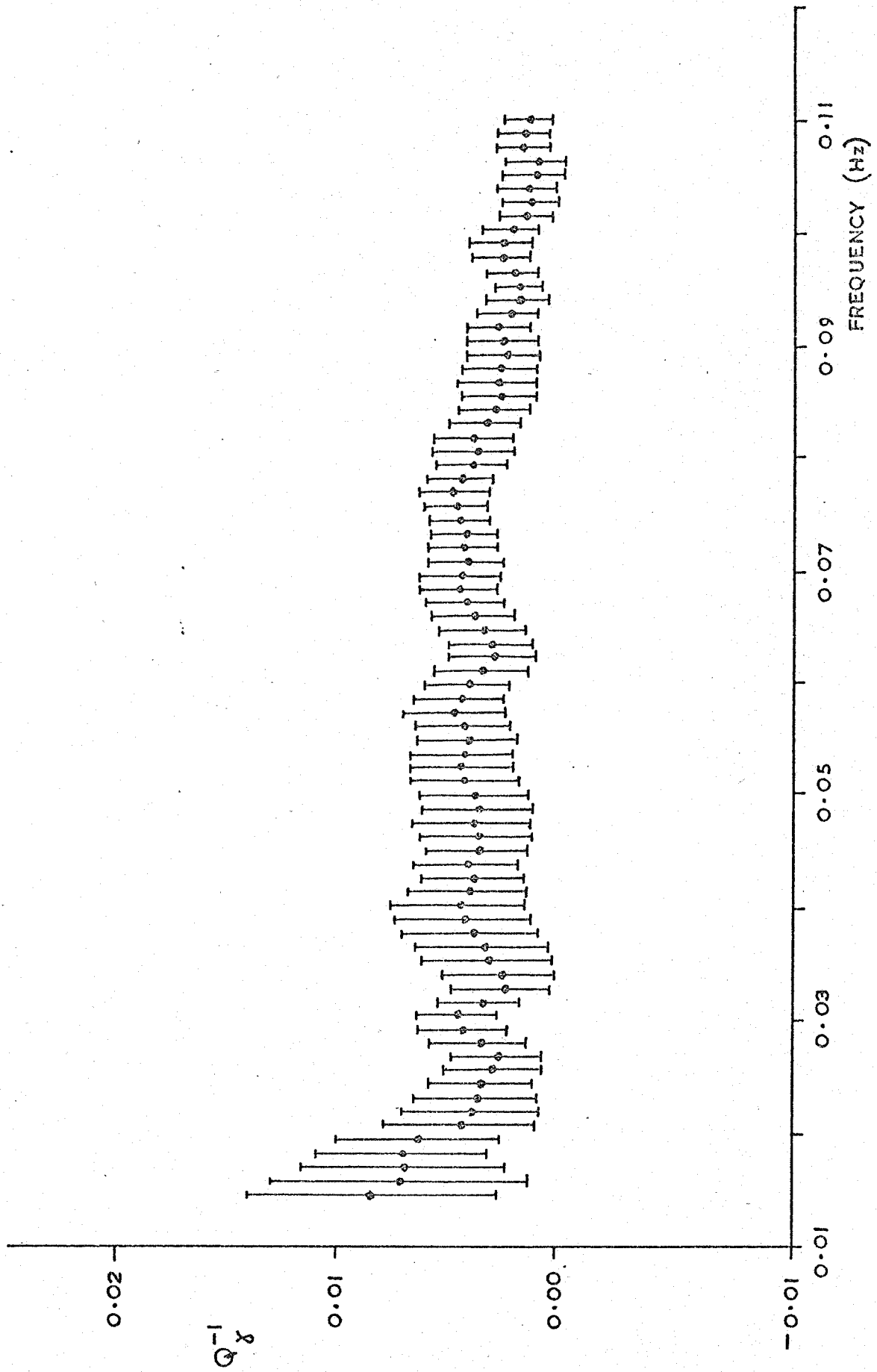


FIGURE 3.3  $Q_y^{-1}$  AND 95 P.C. CONFIDENCE LIMITS ESTIMATED USING 26 RECORDINGS OF THE ATMOSPHERIC EXPLOSION IN NOVAYA ZEMLYA, 24th DECEMBER 1962

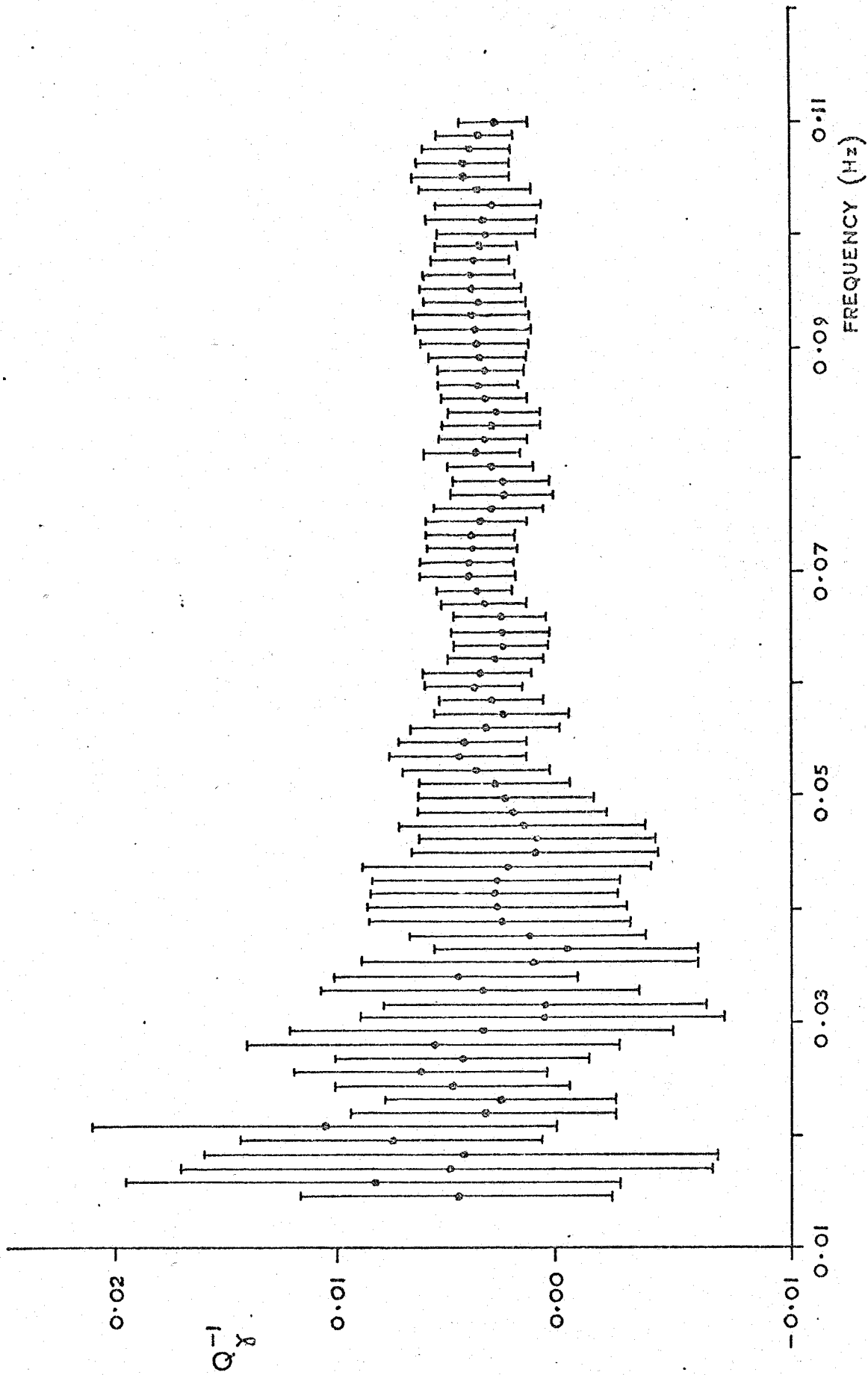


FIGURE 3.4  $Q_y^{-1}$  AND 95 P.C. CONFIDENCE LIMITS ESTIMATED USING 16 RECORDINGS OF THE UNDERGROUND EXPLOSION IN NOVAYA ZEMLYA, 7th NOVEMBER 1968

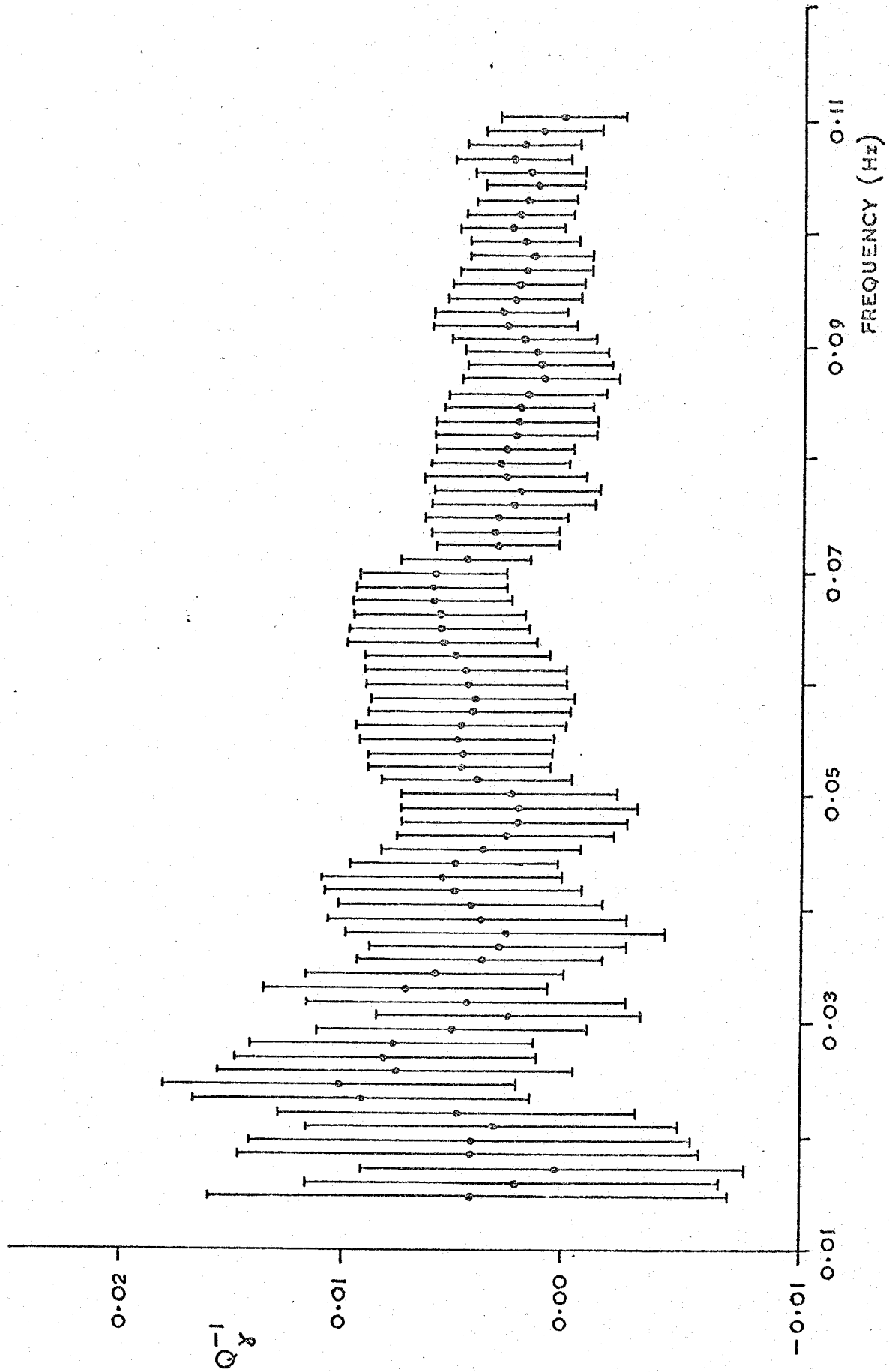


FIGURE 3.5  $Q_y^{-1}$  AND 95% CONFIDENCE LIMITS ESTIMATED USING 24 RECORDING OF THE ATMOSPHERIC EXPLOSION IN SOUTHERN SINKIANG PROV., CHINA, 17th JUNE 1967

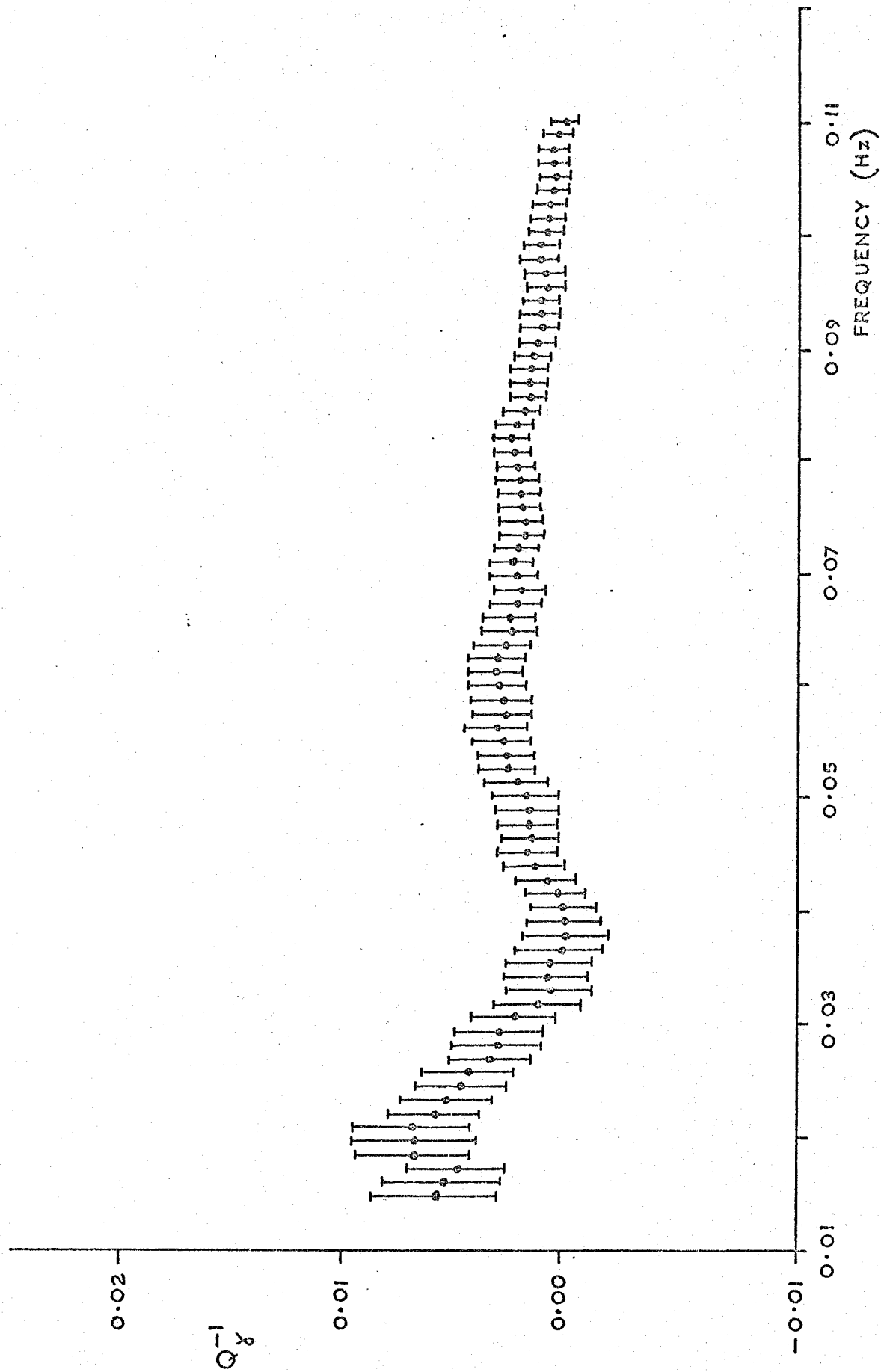


FIGURE 3.6  $Q_{.95}^{-1}$  AND 95 P.C. CONFIDENCE LIMITS ESTIMATED USING 39 RECORDINGS OF THE ATMOSPHERIC EXPLOSION IN SOUTHERN SINKIANG PROV., CHINA, 29th SEPTEMBER 1969

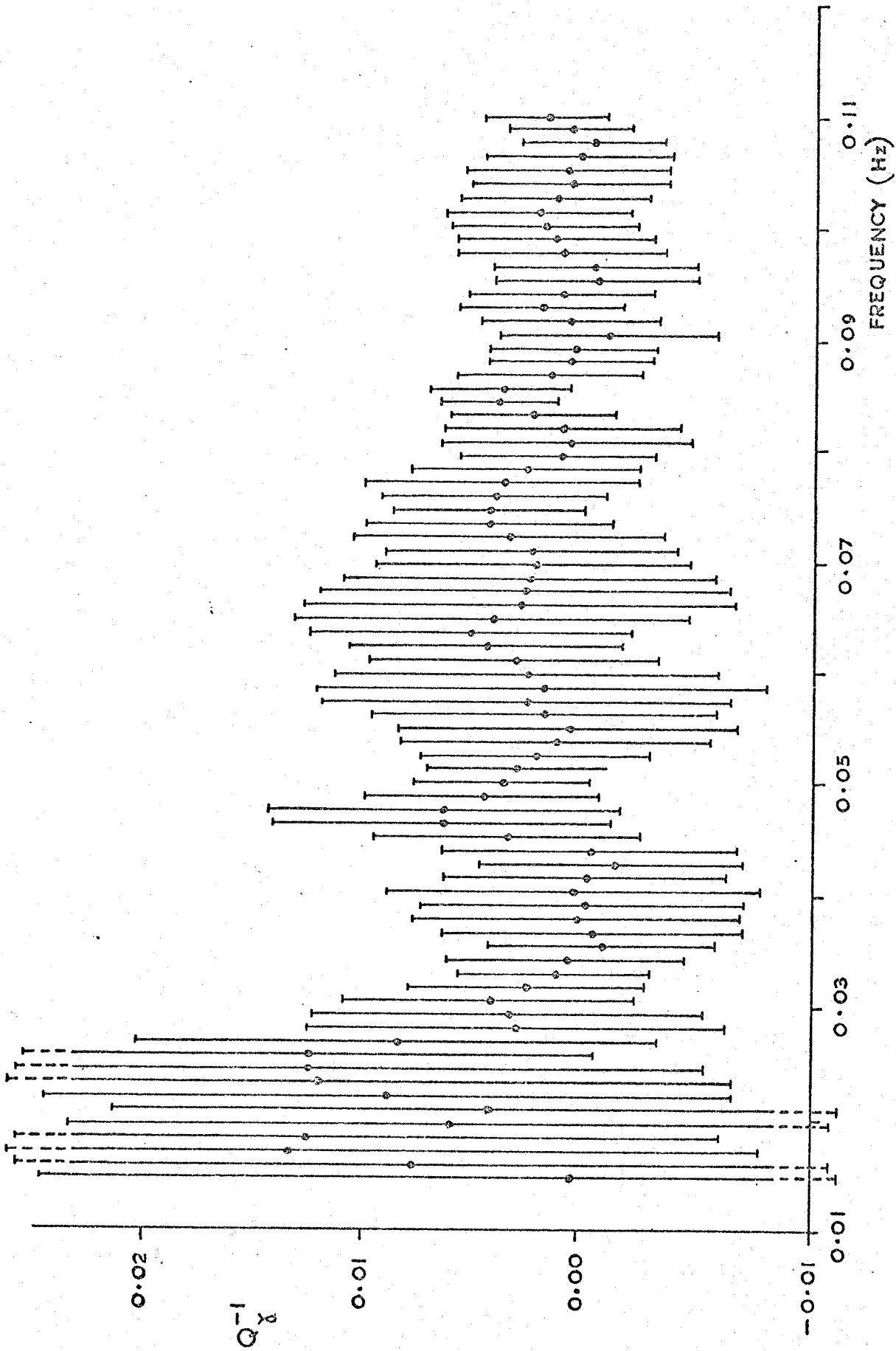


FIGURE 3.7  $Q_y^{-1}$  AND 95 P.C. CONFIDENCE LIMITS ESTIMATED USING 9 RECORDINGS OF THE UNDERGROUND EXPLOSION "LONGSHOT" ALEUTIAN ISLANDS, 29th OCTOBER 1965

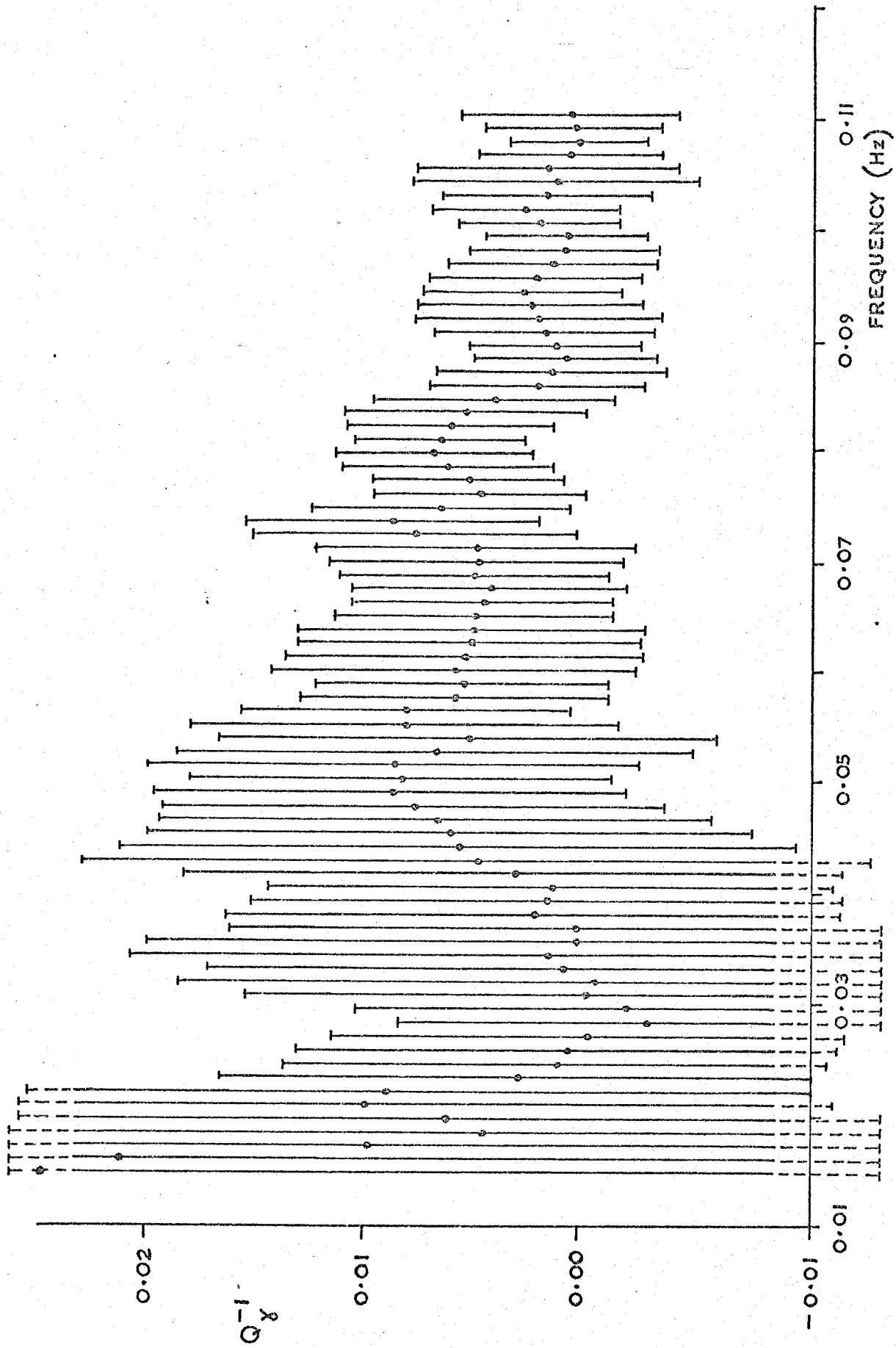


FIGURE 3.8 POOR RESULTS FOR  $Q_y^{-1}$  USING II RECORDINGS OF AN EARTHQUAKE



Figures 3.1-3.6 show well determined  $Q_{\gamma}^{-1}(f)$  values. These improvements have resulted for several reasons. Several station recordings of each event were used, the explosions occurred in "normal" regions and large explosions with good signal-to-noise were chosen.

It is worth noting that the stations SNG, CHG, JER and IST were omitted from the atmospheric explosion in China, 17/6/67, because they consistently plotted low on amplitude-distance plots, for example Figure 3.9. This implies anomalously highly attenuating paths to these stations, or incorrect instrument responses. All of these paths are influenced by the tectonically active Himalayas, presumably a region of particularly high  $Q_{\gamma}^{-1}$  has been traversed.

### 3.2 The Influence of Noise

#### 3.2.1 Low Frequency Noise

The underground explosion at Novaya Zemlya shows the expected broader confidence limits at low frequencies, which improve for higher frequencies. Signal-to-noise was generally poorer for this event than the others, because underground contained explosions are generally smaller than uncontained atmospheric explosions.

It is generally true for all the events that the confidence limits broaden at the low frequencies. There are two factors contributing to this. The spectrum predicted by Carpenter and Marshall (1970) for an atmospheric explosion is about 7 db down from its peak value at frequency 0.02 Hz; also this corresponds to the region of instrument response roll-off for the vertical component, LP system, of the WWSSN, and so little propagation energy will be recorded by the seismogram from the event. Further these WWSSN instruments are barometrically uncompensated for atmospheric variations, and barometric noise is proportional to the period squared.

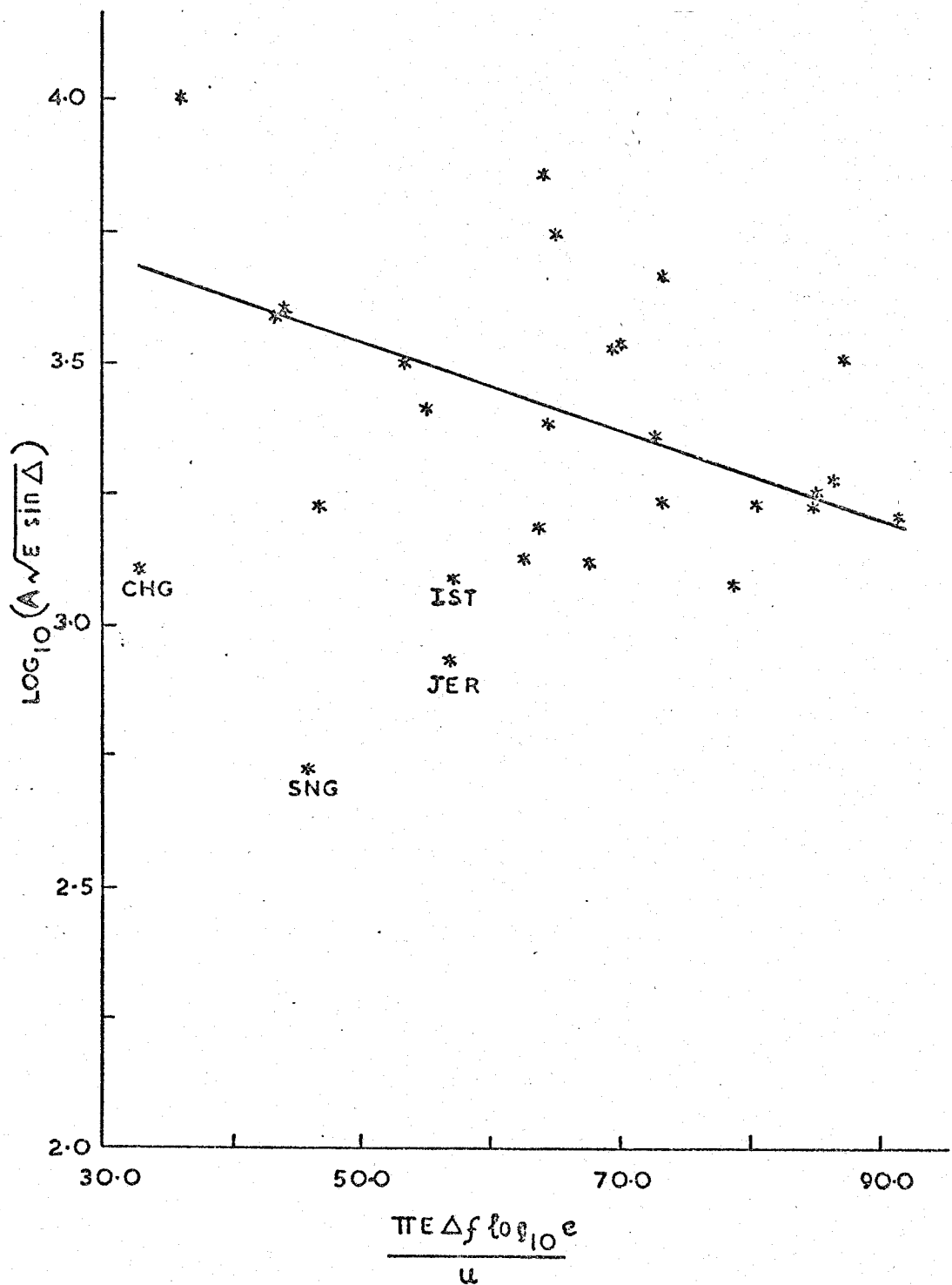


FIGURE 3.9 THE STATIONS CHG, SNG, IST, JER CONSISTENTLY PLOTTED LOW FOR THE EVENT CA 17/6/67 (FREQUENCY = .0281 HZ,  $Q_y^1 = .008 \pm .006$  FOR 24 STATIONS)

The net result is that long period energy propagated from an explosion is recorded at a low magnification and is contaminated by local barometric noise producing a broadening of the confidence limits at this end of the spectrum.

### 3.2.2 High Frequency Noise

For high frequencies the confidence limits narrow to a remarkable extent. Also, for the atmospheric explosions  $Q_{\gamma}^{-1}(f)$  tends to zero for these high frequencies. This seems to imply that included in the spectral estimates of the Rayleigh fundamental mode is a large amount of non-propagating energy, local station noise. Brune and Oliver (1959) have presented information demonstrating the existence of a long period noise peak around 8s period, and this noise peak will extend into and contaminate the high frequencies in this work. What has been plotted on the amplitude/distance graphs at high frequencies is the amplitude of the propagating fundamental Rayleigh mode plus local noise superimposed onto a geometrical spreading term (which generally increases with distance). The net result is a set of roughly similar values, decreasing very slowly with distance and implying little attenuation ( $Q_{\gamma}^{-1} \rightarrow 0$ ). This result for the atmospheric explosions is contradicted by the one underground explosion (Novaya Zemlya) of Figure 3.4 which shows reasonable attenuation at high frequencies,  $Q_{\gamma}^{-1} = 0.004$ . This is simply because the underground explosion does generate propagating energy of high frequencies, whereas the atmospheric explosions contain very little energy at high frequencies in comparison to the local non-propagating noise. This raises the problem how much real data is contained in the results for each event; up to what frequency may it be assumed that the energy recorded has been propagated from the event and a value of spatial  $Q_{\gamma}^{-1}$  may be assigned?

Three separate items of information were used to determine the highest useful frequency contained by each seismogram. For each seismogram the graphs of unwound spectral phase, spectral amplitudes and the group velocity curve were required. An example of a typical seismogram is shown in Figure 3.10, recorded at Kevo from the atmospheric explosion of September 29 1969 at S Sinkiang Province, China. This seismogram shows the low frequencies arriving first, but contaminated by the superposition of high frequency noise creating a typical signal-to-noise problem. Further along the record an Airy phase is seen with an obvious high frequency content. The Figures 3.11-3.13 show spectral phase, spectral amplitudes and the group velocity curve obtained from the Kevo seismogram. The highest useful frequency contained by the seismogram is now obtained as follows:

#### 3.2.2.1 Spectral Phase and the Highest Signal Frequency

Figure 3.11 shows unwound spectral phase, that is, the phase is not allowed to oscillate between  $-\pi$  and  $+\pi$  but is made continuous. The subroutine DRUM (Robinson 1966) given by Burton and Blamey (1972) performs this operation. This phase curve would be perfectly smooth for a pure, noiseless signal. Figure 3.11 is smooth up to frequency 0.125 Hz where a small perturbation may be seen, this is the threshold of noise onset in the frequency domain for this signal. The perturbation marks the onset of random energy.

#### 3.2.2.2 Spectral Amplitude and the Highest Signal Frequency

Spectral amplitudes are shown in Figure 3.12. This graph shows a distinct minimum at 0.125 Hz which divides the spectrum into the two expected regions of signal and noise. Obviously the choice of this particular point is more arbitrary than for the phase perturbation, but it does give a good estimate of the highest available frequency in the signal.

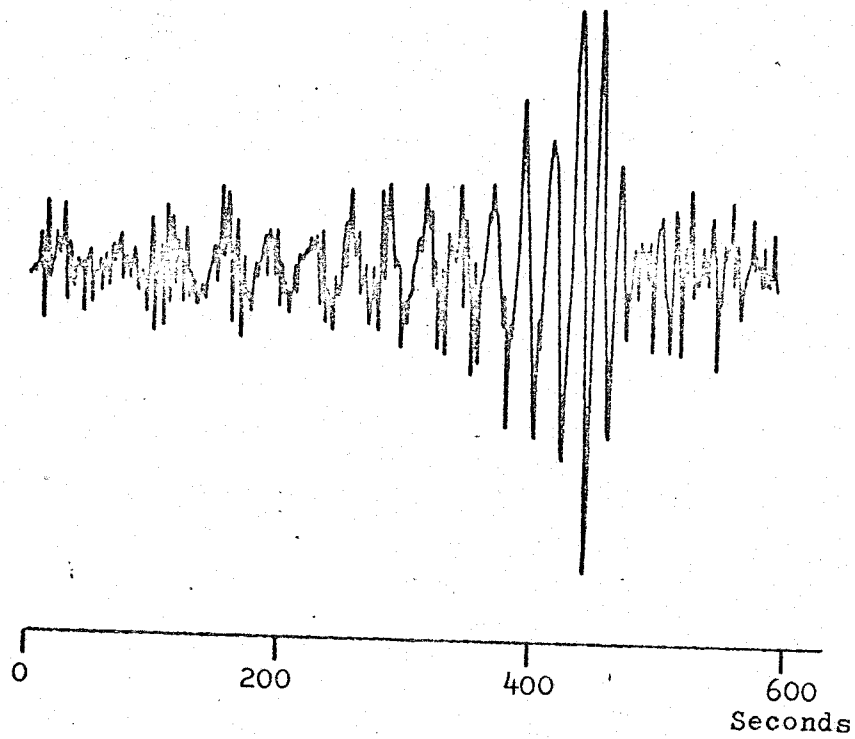


FIGURE 3.10

A Seismogram Recorded at Kevo, Finland (from an Atmospheric Explosion At S Sinkiang Prov, China, 29 September 1969. Distance = 4783 km).

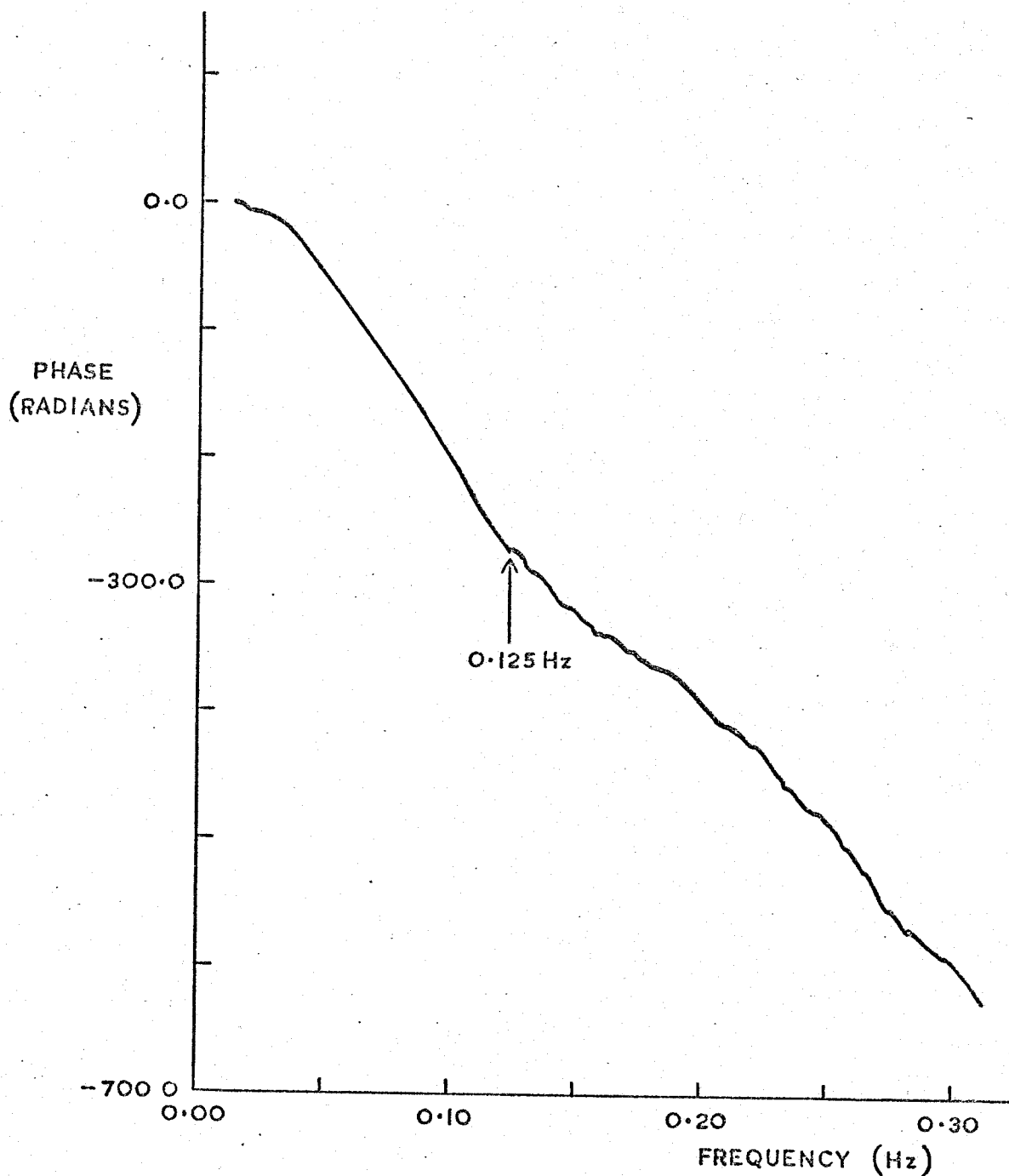


FIGURE 3.11 SPECTRAL PHASE ("UNWOUND PHASE") FOR THE KEVO SEISMOGRAM  
(NOTE THE PERTURBATION AT 0.125 Hz)

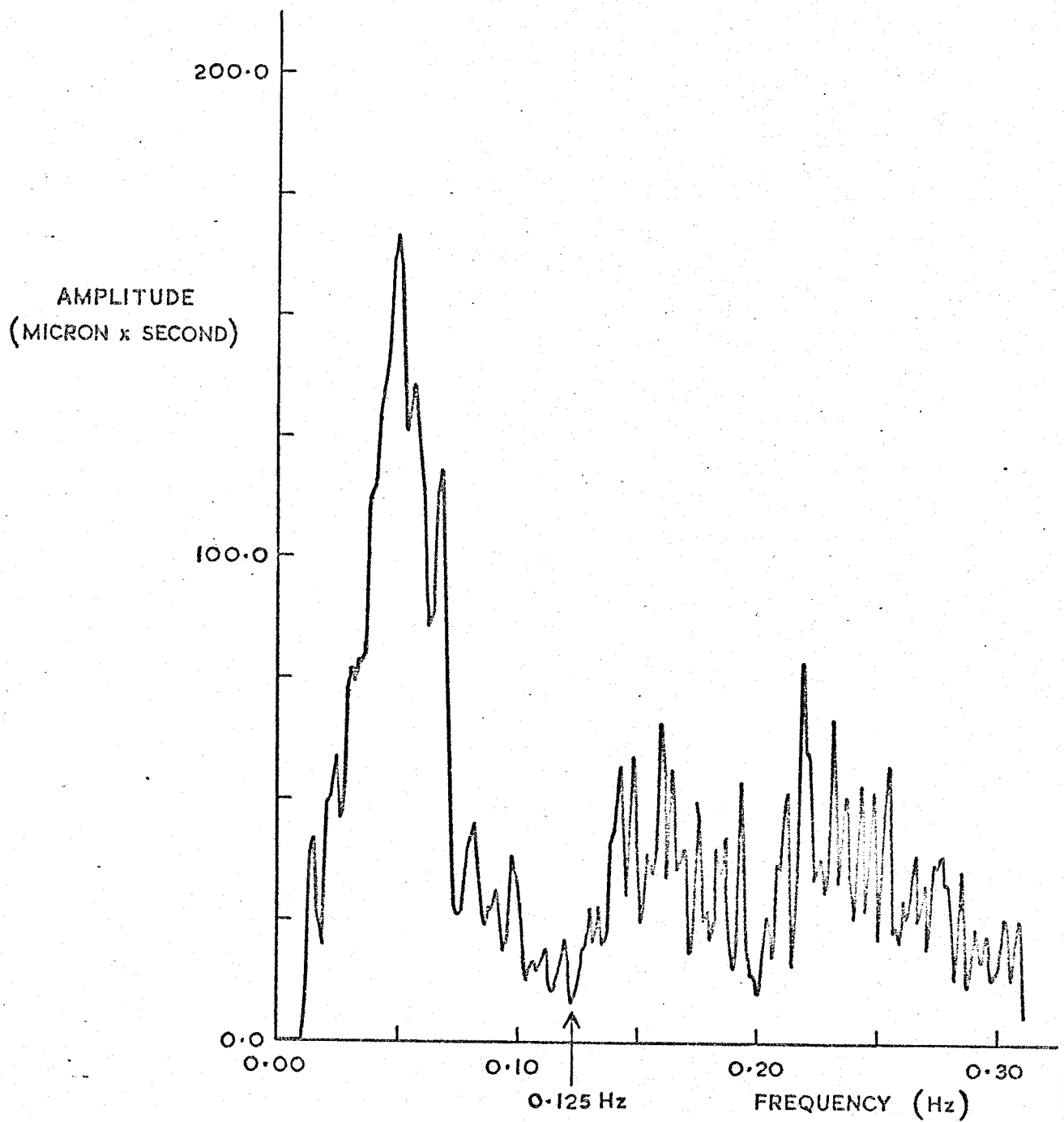


FIGURE 3.12 SPECTRAL AMPLITUDES FOR THE KEVO SEISMOGRAM  
(NOTE THE SIGNAL-NOISE SEPARATION AT 0.125 Hz)

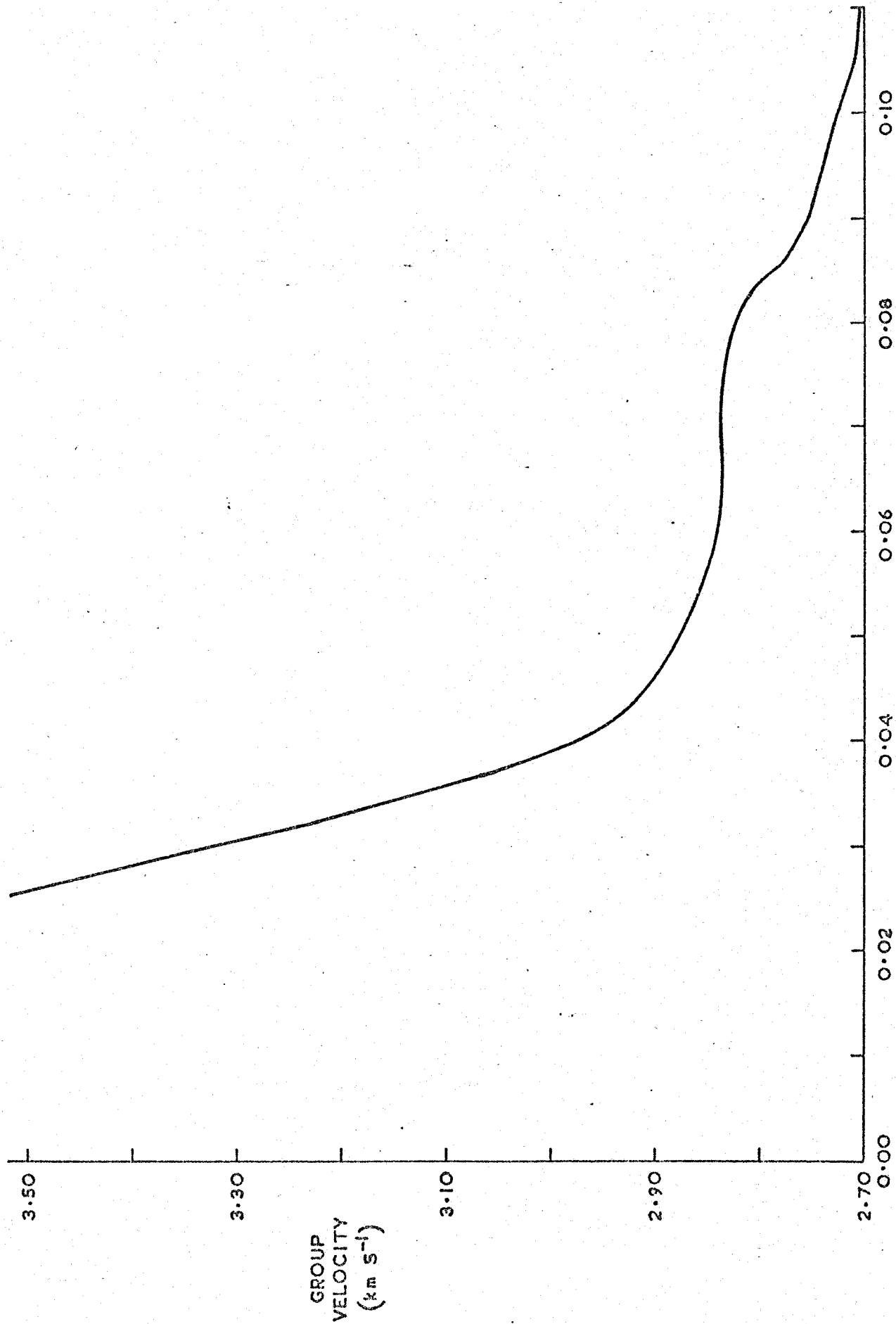


FIGURE 3.13 THE GROUP VELOCITY CURVE FOR THE KEVO SEISMOGRAM



### 3.2.2.3 Group Velocity and the Highest Signal Frequency

Figure 3.13 shows a perfectly good group velocity curve for the Kevo record. This is expected because the highest frequency has been demonstrated to be 0.125 Hz and so a representation which only goes to 0.11 Hz should be noise free. The frequency 0.11 Hz had been chosen as the highest frequency to be analysed and so this particular signal is good for processing in the entire frequency range of interest.

It has already been shown (section 2.3.3) that the group velocity curve will only contain spurious values at a particular frequency if the signal-to-noise ratio is worse than 1:1. This is a weak test to determine the highest frequency present in the signal, whereas the phase test will be shown to be far more restrictive.

These three measurements were made for all the seismograms. For the phase and amplitude curves a grid, drawn onto a transparent overlay, was used to give accurate measurements; this made the phase measurements especially accurate. A summary of the results obtained is in Table 3.1. If a higher frequency greater than 0.11 Hz was obtained from any measurement then it was subsequently set to 0.11 Hz to form the average for a particular event because this is the highest frequency to be used. The abbreviations A, U and Q mean atmospheric or underground explosion or earthquake, and NZ represents Novaya Zemlya, C, explosions in China etc. The term 3NZA is the average for the three atmospheric explosions at Novaya Zemlya.

Table 3.1 shows that the phase measurement is the most restrictive determination of the highest frequency, it always assigns a lower value than either of the other two methods.

Also note that as expected the underground explosion at Novaya Zemlya goes to higher frequencies than the atmospheric explosions at this site. Using the highest frequency obtained from phase measurements for the three atmospheric explosions, 3NZA, gives  $.0761 \pm .0217$  Hz and for the underground explosion, NZU,  $.0977 \pm .0145$  Hz. The validity of the average, 3NZA, is demonstrated later. If it is assumed that all events have the same highest frequency then these values are two samples from the same population, this hypothesis may be tested by calculating "Student's t" for the difference between the two means. The value of "t" obtained is 3.997 which for 95 degrees of freedom is significant at the 99.99% level. The comparable "t" values for the columns headed Amplitude, Group Velocity and Average Result are 5.489, 2.744, 4.147 and are significant at 99.99, 99.9, 99.99% levels respectively. The relatively high frequency content of the underground bomb is confirmed; the importance of this will be seen later.

### 3.3 Statistical Comparison of the $Q_Y^{-1}(f)$ values

Two types of comparison of the  $Q_Y^{-1}(f)$  data are required. The first comparison uses a single event and takes a  $Q_Y^{-1}$  value at a particular frequency and compares it to the  $Q_Y^{-1}$  values at all the other frequencies, the process cycles through all the frequencies in turn. This essentially tests to see if  $Q_Y^{-1}(f)$  is frequency dependent, albeit a pseudo dependence on frequency.

The second type of comparison is between two events. The  $Q_Y^{-1}$  are compared between the two events at corresponding frequencies, to determine if the values obtained are statistically different.

The values of  $Q_Y^{-1}$  have been determined using linear regression which assumed a line of the type

$$Y = Q_Y^{-1} X + b$$

3.1

Event	Number of Stations	1. Phase	2. Amplitude	3. Group Velocity	Average Result
NZA 27. 9.62	28	.0736±.0189	.0763±.0046	.0843±.0200	.0782±.0164
NZA 22. 10.62	27	.0794±.0188	.0841±.0190	.0867±.0180	.0828±.0190
NZA 24. 12.62	26	.0754±.0256	.0779±.0228	.0812±.0342	.0798±.0285
NZU 7. 11.68	18	.0977±.0145	.1032±.0109	.1018±.0157	.1029±.0142
CA 17. 6.67	24	.0846±.0211	.0956±.0151	.0942±.0173	.0910±.0184
CA 29. 9.69	39	.0797±.0186	.0831±.0178	.0830±.0158	.0818±.0177
3NZA Average	81	.0761±.0217	.0794±.0175	.0841±.0254	.0803±.0219
2CA Average	63	.0816±.0199	.0879±.0171	.0873±.0166	.0853±.0181
5A Average	144	.0785±.0209	.0831±.0173	.0855±.0220	.0825±.0202
LONGSHOT "L"	9	.0711±.0105	.0756±.0106	.0789±.0135	.0761±.0123
EARTHQUAKE "Q"	11	.0836±.0145	.0923±.0156	.0846±.0107	.0846±.0101

Table 3.1 The highest useful signal frequencies Hz determined using

- 1 Spectral phase,
- 2 Spectral amplitudes and
- 3 The group velocity curve.

where Y and X are amplitude and distance terms,  $Q_Y^{-1}$  and b the line gradient and intercept. A data set of n pairs of observables,  $(x_{1i}, y_{1i})$ , approximates to 3.1 but is scattered about it. The confidence limits on  $Q_Y^{-1}$  values are one instance of this scatter. A second data set,  $(x_{2i}, y_{2i})$ , will again be of the form 3.1. Whether the two data sets are from different events, but at the same frequency, or from the same event but at different frequencies does not matter - the problem is to compare two regression lines. The theory described by Brownlee (1965, p349---) has been incorporated into the programs CNL and C2L (Appendices E and G) to perform the comparisons in the two cases.

The first test performed is Fisher's F test on the ratio of the residual variances about the two regression lines. This test indicates if both lines are samples from the same parent population, and if this test is failed (Not from the same population) then no more tests are conducted. The second test takes the two values of gradient, that is  $Q_Y^{-1}|_1$  and  $Q_Y^{-1}|_2$ , assumes they are equal, and then calculates a statistic to check this hypothesis. All tests are performed at the 95% confidence level. In all cases failure of a test is indicated by 0, success by 1, and a 2 indicates that a test has not been performed.

### 3.3.1 $Q_Y^{-1}$ as a Function of Frequency

The tests on each event to investigate the regression coefficients as a function of frequency produce a 79 x 79 triangular matrix (79 frequencies were analysed). A typical result sheet for the F test is shown in Figure 3.14 and this was conducted on the event NZA 24/12/62.

The simple representation of Figure 3.14 quickly produces an important result. The data distinctly divides into two populations. There is a low frequency population for .0354 Hz and below, and a high frequency population beyond this point. Each population forms a distinct triangle, divided by a rectangular area for which no further tests may be performed because the variances of the two populations are unequal.

Frequency	TEST MATRIX
0.01465	2
0.01587	12
0.01709	112
0.01831	1112
0.01953	11112
0.02075	111112
0.02197	1011112
0.02319	10111112
0.02441	000111112
0.02563	0001111112
0.02686	00011111112
0.02808	00111111112
0.02930	000111111112
0.03052	0001111111112
0.03174	0011111111112
0.03296	11111111111112
0.03418	1111111000000012
0.03540	1110000000000012
0.03662	111000000000000112
0.03784	11000000000000112
0.03906	010000000000001112
0.04028	0100000000000001112
0.04150	11000000000000111112
0.04272	111000000000000111112
0.04395	1110000000000001111112
0.04517	11100000000000011111112
0.04639	01000000000000001111112
0.04761	00000000000000111111112
0.04883	0100000000000000111111112
0.05005	0000000000000001111111112
0.05127	00000000000000011111111112
0.05249	000000000000000111111111112
0.05371	0000000000000001111111111112
0.05493	00000000000000011111111111112
0.05615	000000000000000111111111111112
0.05737	0000000000000001111111111111112
0.05859	0100000000000001111111111111112
0.05981	01000000000000011111111111111112
0.06104	00000000000000011111111111111112
0.06226	000000000000000111111111111111112
0.06348	010000000000000111111111111111112
0.06470	010000000000000111111111111111112
0.06592	010000000000000111111111111111112
0.06714	010000000000000111111111111111112
0.06836	010000000000000111111111111111112
0.06958	010000000000000111111111111111112
0.07080	010000000000000111111111111111112
0.07202	110000000000000111111111111111112
0.07324	111000000000000111111111111111112
0.07446	111000000000000111111111111111112
0.07568	111000000000000111111111111111112
0.07690	010000000000000111111111111111112
0.07813	110000000000000111111111111111112
0.07935	010000000000000111111111111111112
0.08057	000000000000000111111111111111112
0.08179	000000000000000111111111111111112
0.08301	010000000000000111111111111111112
0.08423	010000000000000111111111111111112
0.08545	000000000000000111111111111111112
0.08667	000000000000000111111111111111112
0.08789	000000000000000111111111111111112
0.08911	000000000000000111111111111111112
0.09033	000000000000000111111111111111112
0.09155	010000000000000111111111111111112
0.09277	010000000000000111111111111111112
0.09399	010000000000000111111111111111112
0.09521	111000000000000111111111111111112
0.09644	111000000000000111111111111111112
0.09766	010000000000000111111111111111112
0.09888	000000000000000111111111111111112
0.10010	010000000000000111111111111111112
0.10132	010000000000000111111111111111112
0.10254	010000000000000111111111111111112
0.10376	000000000000000111111111111111112
0.10498	000000000000000111111111111111112
0.10620	000000000000000111111111111111112
0.10742	000000000000000111111111111111112
0.10864	000000000000000111111111111111112
0.10986	010000000000000111111111111111112

FIGURE 3.14

Results of Inter-Frequency "F" Tests for NZA 24/12/62 (0 Indicates Test Failed, 1 Test Passed, 2 Test not Conducted).

It is worth noting Scheffe's (1964) observations concerning the effects of non-normality on the variance ratio. If non-normality is present, specified by finite kurtosis, then confidence levels are affected. But inequality of variances has little effect on inferences about means if the degrees of freedom are equal for the two variances, although inferences about variances will be seriously affected. However, explanations other than non-normality seem more likely for the two apparent regions.

It will later be seen that a Rayleigh wave frequency, .0354 Hz, corresponds to an approximate depth of penetration, 110 kms. This corresponds to the expected geophysical change from lithosphere to asthenosphere, where lateral variations in  $Q_Y^{-1}$  may be widespread. Such variations would influence the variance of any estimate of  $Q_Y^{-1}$ . Also, a subsequent inversion of this  $Q_Y^{-1}(f)$  data shows the presence of a high  $Q^{-1}$  layer, which is only sampled by the low frequency population.

Instrumental roll-off and the lack of barometric compensation in the WWSSN seismometers also exacerbate the signal-to-noise problem at low frequencies, and must lead to increased variance for these  $Q_Y^{-1}$  estimates.

The second test, comparing the individual  $Q_Y^{-1}$  values or gradients, shows that the values in each population are comparable within that population, but where the F test had failed no comparisons were made.

For this event it therefore appears that two regions of  $Q_Y^{-1}$ , in terms of frequency, have been observed. From Figure 3.1 it is apparent that the low frequency population is of higher  $Q_Y^{-1}$ , and experiences greater attenuation.

A similar division was found for the other events of importance. The frequency at which the division occurred for each atmospheric explosion, the major events, is listed below.

Event	Highest Frequency of Low Frequency Population
NZA 24.12.62	.03418 Hz
NZA 27. 9.62	.03418 Hz
NZA 22.10.62	.03540 Hz
CA 17. 6.67	.03662 Hz
CA 29. 9.69	.03418 Hz

The mean frequency for this table indicates population division at 0.035 Hz.

### 3.3.2 $Q_{\gamma}^{-1}(f)$ Compared Between Events

It is necessary to compare the  $Q_{\gamma}^{-1}(f)$  data between separate events at corresponding frequencies, it may then be possible to pool the data from such events and improve the results. The program used to carry out this comparison is C2L, it follows the testing procedure already described. Comparison of the events NZA 24.12.62 and NZA 27.9.62 produces the results shown in Figure 3.15. Columns headed NFTEST, NATEST give the result of the F test and then the gradient comparison test. If the gradients are comparable, statistically equal, a pooled gradient and confidence limits are also formed (otherwise this column is set to zero). The number of frequencies within the valid range for which the F test failed when comparing two events is summarised for several events in Table 3.2.

The data was then pooled to form the following averages. The three atmospheric explosions at Novaya Zemlya were averaged forming 3NZA, the two explosions in China formed 2CA. Finally, all the atmospheric explosions were combined giving 5A. The figures 3.16 and 3.17 show the individual  $Q_{\gamma}^{-1}(f)$  values, without confidence limits, for the atmospheric explosions at Novaya Zemlya and in China. Trends for the three NZA events are very similar and are reflected in the average 3NZA (Figure 3.16). The two events in China differ considerably around .038 Hz, this is probably due to the poor signal-to-noise for CA 17.6.67, but the average 2CA (Figure 3.18) follows the general trends of CA 29.9.69 which has good signal-to-noise. (The combined

NOVAYA ZEMLYA 24/12/62 ATMOSPHERIC 26 STATIONS  
 NOVAYA ZEMLYA 27/9/62 ATMOSPHERIC 28 STATIONS

	FREQUENCY	A1	A2	NFTST	NATEST	NBTEST	NEW GRADIENT	A LIMITS
1	0.014650	-C.CC8798	-0.007155	1	1	0	-0.007526	0.002349
2	0.015870	-C.CC7606	-C.011179	0	2	2	0.0	0.0
3	0.017090	-C.CC7411	-C.CC8450	1	1	1	-0.008048	0.002496
4	0.018310	-C.CC7482	-C.CC8911	1	1	1	-0.008276	0.002200
5	0.019530	-C.CC6757	-C.CC6889	1	1	1	-0.006844	0.001735
6	0.020750	-C.CC6940	-C.CC7746	1	1	1	-0.006530	0.001976
7	0.021970	-C.CC4392	-C.CC6434	1	1	1	-0.005516	0.001889
8	0.023190	-C.CC4219	-C.CC5805	1	1	1	-0.005095	0.001653
9	0.024410	-C.CC3575	-C.CC4909	1	1	1	-0.004494	0.001403
10	0.025630	-C.CC3459	-C.CC4341	1	1	1	-0.003947	0.001330
11	0.026860	-0.CC3263	-C.CC4299	1	1	1	-0.003838	0.001267
12	0.028080	-C.CC4081	-C.CC4891	1	1	1	-0.004529	0.001303
13	0.029300	-C.CC4781	-C.CC5258	1	1	1	-0.005044	0.001370
14	0.030520	-C.CC5037	-C.CC5312	1	1	1	-0.005188	0.001247
15	0.031740	-C.CC4022	-C.CC4977	1	1	1	-0.004541	0.001172
16	0.032960	-C.CC3025	-C.CC4398	1	1	1	-0.003775	0.001370
17	0.034180	-C.CC3187	-C.CC4248	1	1	1	-0.003770	0.001536
18	0.035400	-C.CC3660	-C.CC4395	1	1	1	-0.004064	0.001776
19	0.036620	-C.CC3874	-C.CC4672	1	1	1	-0.004311	0.001829
20	0.037840	-0.CC4399	-0.005147	1	1	1	-0.004814	0.001684
21	0.039060	-0.CC4735	-C.CC5539	1	1	1	-0.005187	0.001692
22	0.040280	-C.CC4937	-C.CC5203	1	1	1	-0.005088	0.001765
23	0.041500	-0.CC4552	-C.CC4286	1	1	1	-0.004404	0.001740
24	0.042720	-C.CC4205	-C.CC3582	1	1	1	-0.003901	0.001697
25	0.043950	-C.CC4591	-C.CC3603	1	1	1	-0.004038	0.001606
26	0.045170	-C.CC4112	-C.CC3844	1	1	1	-0.003963	0.001462
27	0.046390	-C.CC4099	-C.CC3987	1	1	1	-0.004037	0.001435
28	0.047610	-C.CC4354	-C.CC4095	1	1	1	-0.004210	0.001530
29	0.048830	-C.CC4083	-C.CC4138	1	1	1	-0.004114	0.001543
30	0.050050	-C.CC4221	-C.CC4108	1	1	1	-0.004159	0.001511
31	0.051270	-C.CC4639	-C.CC4851	1	1	1	-0.004753	0.001402
32	0.052490	-0.CC4761	-C.CC5472	1	1	0	-0.005145	0.001321
33	0.053710	-0.CC4757	-C.CC5052	1	1	0	-0.004916	0.001357
34	0.054930	-0.CC4523	-C.CC4450	1	1	0	-0.004483	0.001390
35	0.056150	-C.CC4723	-C.CC4146	1	1	0	-0.004403	0.001330
36	0.057370	-C.CC5093	-C.CC4643	1	1	1	-0.004843	0.001318
37	0.058590	-C.CC4906	-C.CC5268	1	1	0	-0.005109	0.001193
38	0.059810	-C.CC4521	-C.CC5422	1	1	0	-0.005029	0.001129
39	0.061040	-C.CC3889	-C.CC5039	1	1	1	-0.004542	0.001166
40	0.062260	-C.CC3380	-C.CC4859	1	1	1	-C.004198	0.001176
41	0.063480	-C.CC3461	-C.CC4709	1	1	1	-0.004137	0.001168
42	0.064700	-C.CC3834	-C.CC4408	1	1	1	-0.004153	0.001184
43	0.065920	-0.CC4250	-C.CC4336	1	1	1	-0.004299	0.001257
44	0.067140	-C.CC4632	-C.CC4528	1	1	1	-0.004573	0.001267
45	0.068360	-C.CC4874	-C.CC4538	1	1	1	-0.004685	0.001209
46	0.069580	-C.CC4804	-C.CC4643	1	1	1	-0.004715	0.001183
47	0.070800	-C.CC4520	-C.CC4341	1	1	0	-0.004422	0.001134
48	0.072020	-0.CC4682	-C.CC3830	1	1	0	-0.004206	0.001060
49	0.073240	-C.CC4629	-C.CC3528	1	1	0	-0.004011	0.001080
50	0.074460	-C.CC4836	-C.CC3797	1	1	1	-0.004264	0.001020
51	0.075680	-C.CC4959	-C.CC4130	1	1	1	-0.004504	0.001017
52	0.076900	-C.CC5080	-C.CC4209	1	1	1	-0.004601	0.001016
53	0.078130	-0.CC4810	-C.CC3680	1	1	1	-0.004186	0.000954
54	0.079350	-C.CC4269	-C.CC3494	1	1	1	-0.003850	0.000984
55	0.080570	-0.CC4215	-0.003529	1	1	1	-0.003807	0.000984
56	0.081790	-C.CC4215	-C.CC3455	1	1	1	-0.003807	0.001110
57	0.083010	-C.CC3691	-C.CC3706	1	1	1	-0.003699	0.001032
58	0.084230	-C.CC3290	-C.CC3984	1	1	1	-0.003668	0.001000
59	0.085450	-C.CC3076	-C.CC3760	1	1	1	-0.003452	0.001044
60	0.086670	-0.CC3169	-C.CC3389	1	1	1	-0.003291	0.001030
61	0.087890	-C.CC3053	-C.CC3372	1	1	1	-0.003232	0.000967
62	0.089110	-C.CC2819	-C.CC3396	1	1	1	-0.003144	0.000949
63	0.090330	-C.CC2892	-C.CC3380	1	1	1	-0.003167	0.000902
64	0.091550	-C.CC3086	-C.CC3405	1	1	1	-C.003262	0.000835
65	0.092770	-C.CC2656	-C.CC3059	1	1	1	-0.002874	0.000827
66	0.093990	-C.CC2216	-C.CC3054	1	1	0	-0.002670	0.000790
67	0.095210	-0.CC2147	-C.CC2968	1	1	0	-0.002593	0.000711
68	0.096440	-C.CC2488	-C.CC2532	1	1	0	-0.002512	0.000794
69	0.097660	-0.CC2551	-C.CC2403	1	1	1	-0.002651	0.000827
70	0.098880	-C.CC2547	-C.CC2500	1	1	1	-0.002700	0.000837
71	0.100100	-0.CC2529	-C.CC2616	1	1	0	-0.002577	0.000779
72	0.101320	-C.CC1845	-C.CC2691	1	1	0	-0.002312	0.000755
73	0.102540	-C.CC1661	-C.CC2460	1	1	0	-0.002102	0.000720
74	0.103760	-0.CC1771	-C.CC2346	1	1	1	-0.002088	0.000737
75	0.104980	-C.CC1538	-C.CC2269	1	1	1	-0.001941	0.000798
76	0.106200	-C.CC1441	-C.CC2107	1	1	1	-0.001805	0.000789
77	0.107420	-C.CC1575	-C.CC1995	1	1	1	-0.001986	0.000718
78	0.108640	-C.CC1926	-C.CC1835	1	1	1	-0.001877	0.000716
79	0.109860	-C.CC1746	-C.CC1839	1	1	0	-0.001796	0.000696

FIGURE 3.15 Comparison of Regression Values for NZA 24/12/62 and NZA 27/9/62 at Each Frequency.



	NZA 24.12.62	NZA 27. 9.62	NZA 22.10.62	CA 17. 6.67	CA 29. 9.69	NZU 7.11.68
NZA 24.12.62	-					
NZA 27. 9.62	1	-				
NZA 22.10.62	6	11	-			
CA 17. 6.67	7	13	1	-		
CA 29. 9.69	8	16	1	1	-	
NZU 7.11.68	25	27	24	23	20	-

Table 3.2 The number of frequencies at which the F test fails for comparison of two events. The underground explosion NZU 7.11.68 differs from the atmospheric explosions.

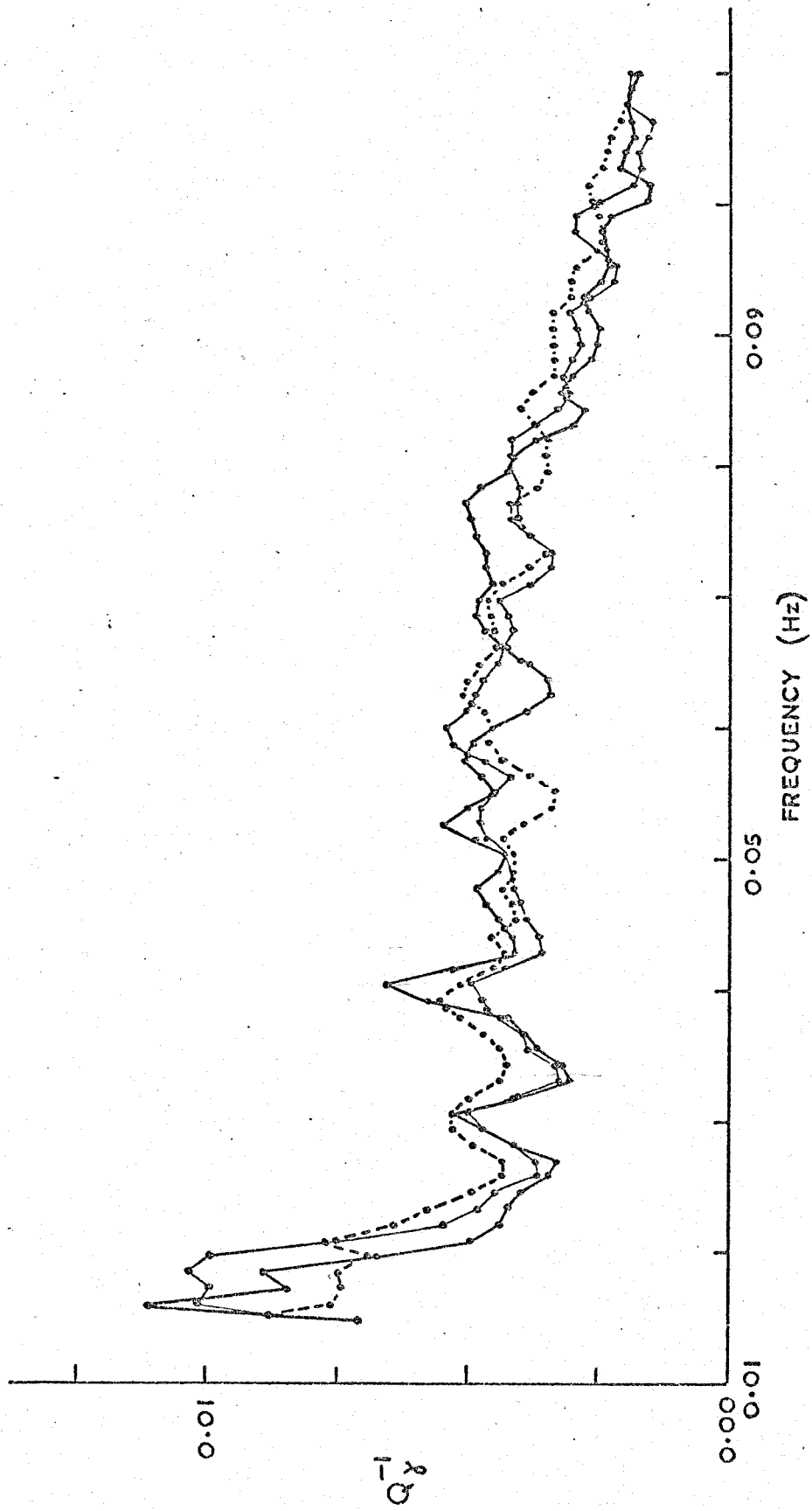


FIGURE 3.16 ESTIMATES OF  $Q_y^{-1}$  FOR THE THREE ATMOSPHERIC EXPLOSIONS AT NOVAYA ZEMLYA

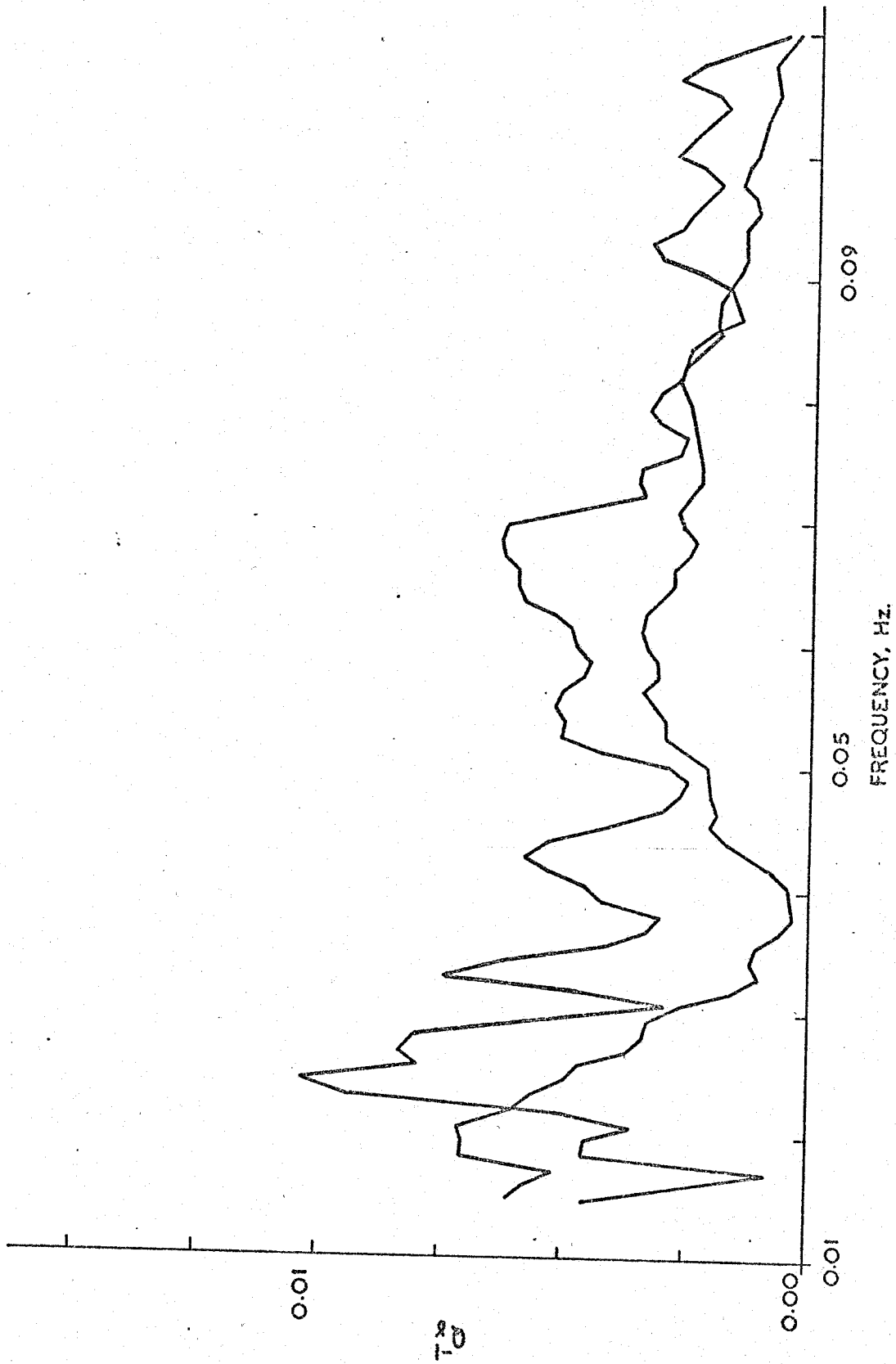


FIGURE 3.17 ESTIMATES OF  $Q_1^2$  FOR THE TWO ATMOSPHERIC EXPLOSIONS IN CHINA (S. SINKIANG PROV.)

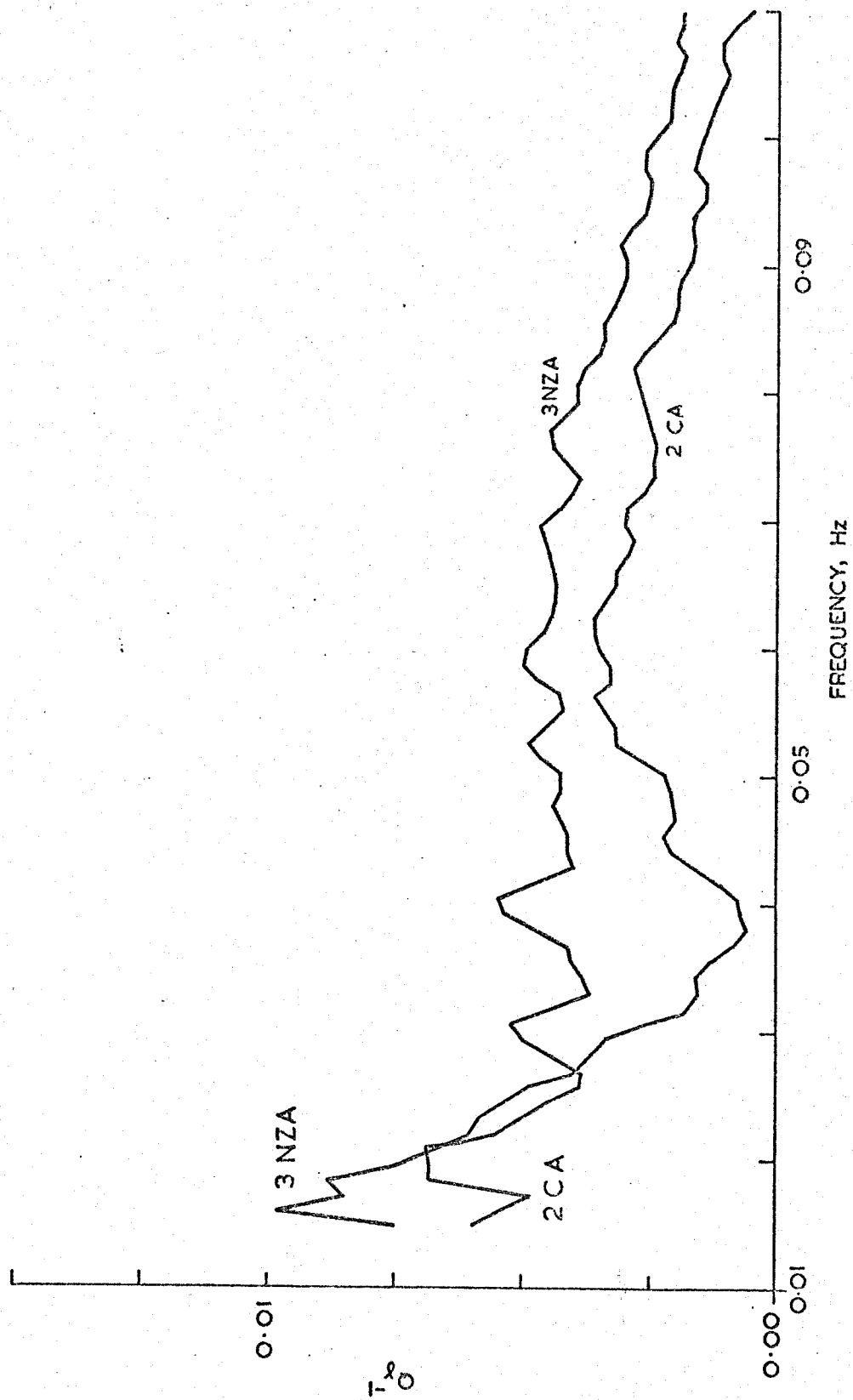


FIGURE 3.18 AVERAGE  $Q_y^{-1}$  ESTIMATES FOR TWO SETS OF ATMOSPHERIC EXPLOSIONS:  
 1) THREE IN NOVAYA ZEMLYA (3NZA) AND 2) TWO IN CHINA (2CA)

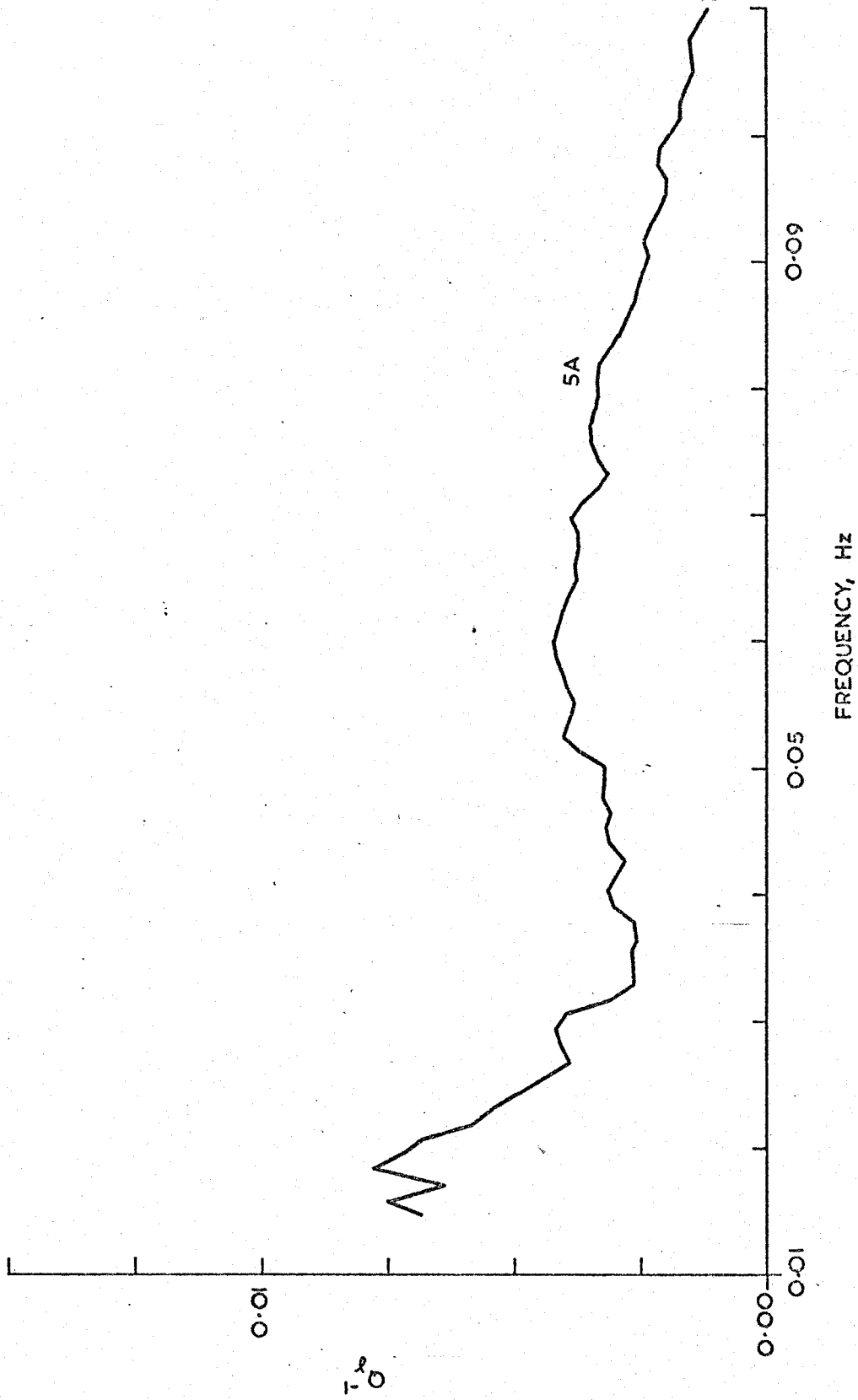


FIGURE 3.19 AVERAGE  $Q_y^{-1}$  ESTIMATED USING FIVE ATMOSPHERIC EXPLOSIONS, THREE IN NOVAYA ZEMLYA (3NZA) AND TWO IN CHINA (2CA)

average for the five atmospheric explosions shown in Figure 3.19.) The averages 3NZA, 2CA and 5A with their appropriate 95% confidence limits are shown in Figures 3.20-3.22.

### 3.4 Average $Q_Y^{-1}(f)$ Values

#### 3.4.1 $Q_Y^{-1}$ at Low Frequencies

The figures for 3NZA, 2CA and 5A still persist in showing high  $Q_Y^{-1}$  at low frequencies. This will later be interpreted as a layer of greater attenuation at depth.

Broader confidence limits are still apparent at low frequencies, but this does not necessarily mean that these results are poorer, instead it is informative. Two populations may have the same mean, but with different variances, one population is "broader" than the other. Samples from the broader population will contain a wider range of values and so the confidence limits on the calculated mean will be wider than for the other population. Low frequencies penetrate deeper into the earth than high frequencies, presumably sampling a wider range of  $Q_Y^{-1}$  values. Also the depth to which low frequencies penetrate may be expected to contain lateral inhomogeneities. Both effects broaden the confidence limits and simultaneously increase their interpretational use!

#### 3.4.2 $Q_Y^{-1}$ at High Frequencies

The tendency at high frequencies is for  $Q_Y^{-1}$  to trend towards zero. This has already been explained in terms of the propagational frequency content for each explosion. However, figure 3.23 shows an interesting comparison between the atmospheric average 3NZA and the underground explosion NZU 7/11/68. For NZU the erratic behaviour of the mean and the very broad confidence limits (Figure 3.4) at low frequencies indicates little low frequency energy content, but for high frequencies the situation has obviously improved. From Table 3.1 we expect NZU to contain useful propagating energy up to about 0.10 Hz, while 3NZA will contain energy up to 0.08 Hz. The curves for 3NZA and NZU start to diverge for frequencies around

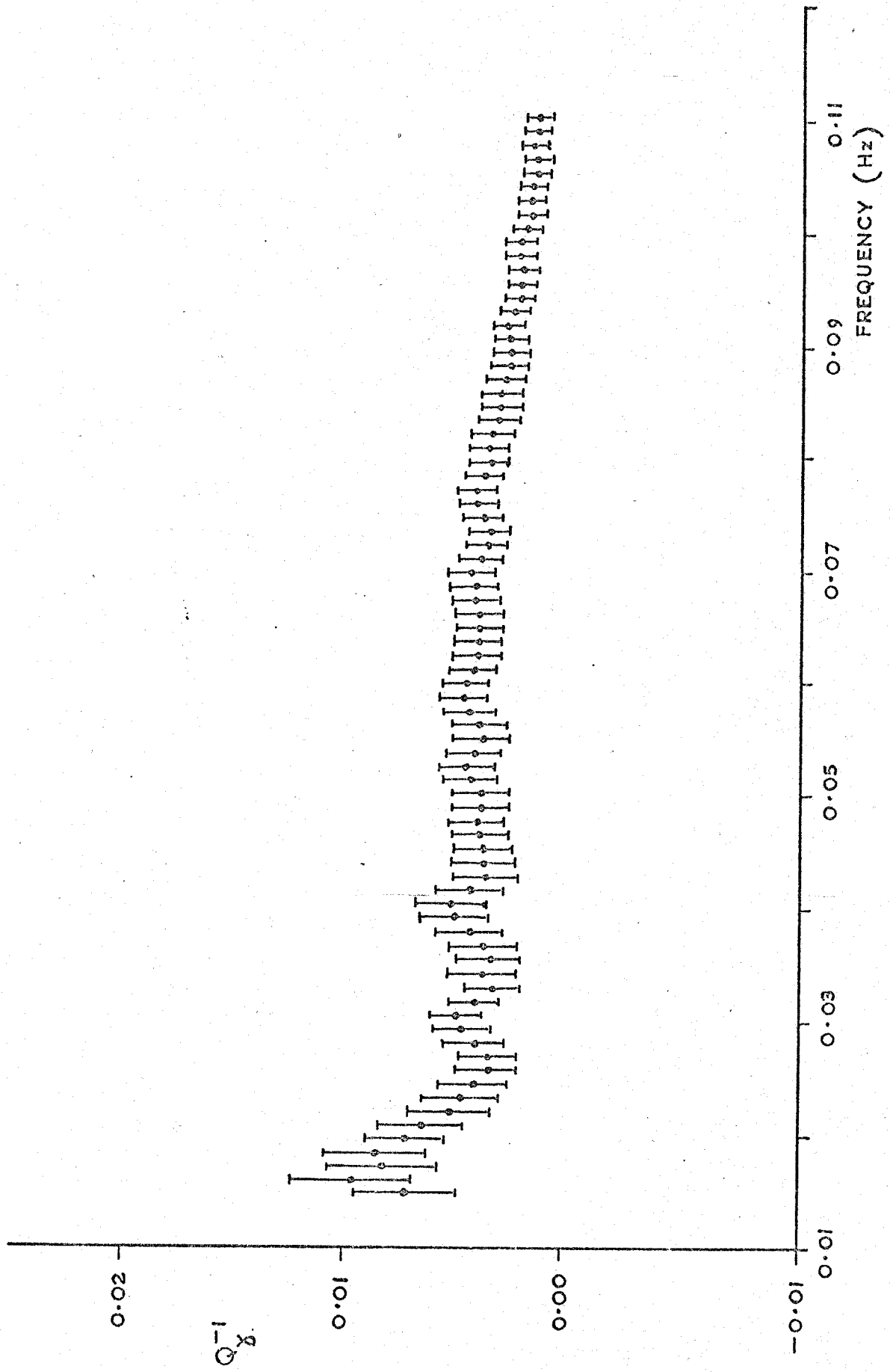


FIGURE 3.20  $Q_y^{-1}$  AND 95 P.C. CONFIDENCE LIMITS ESTIMATED USING THE 3 ATMOSPHERIC EXPLOSIONS IN NOVAYA ZEMLYA

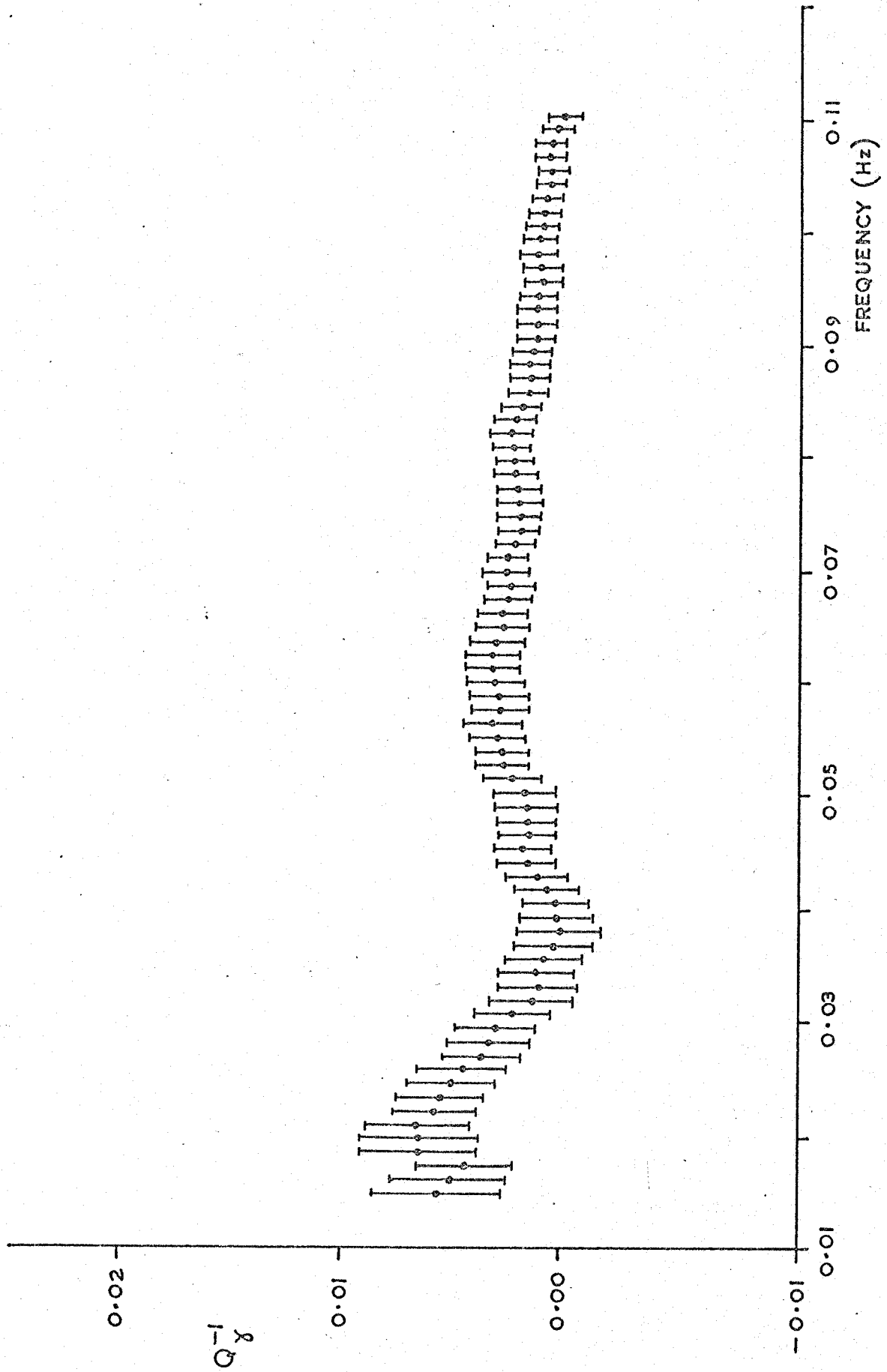


FIGURE 3.21  $Q_y^{-1}$  AND 95 P.C. CONFIDENCE LIMITS ESTIMATED USING THE 2 ATMOSPHERIC EXPLOSIONS IN SOUTHERN SINKIANG PROV., CHINA



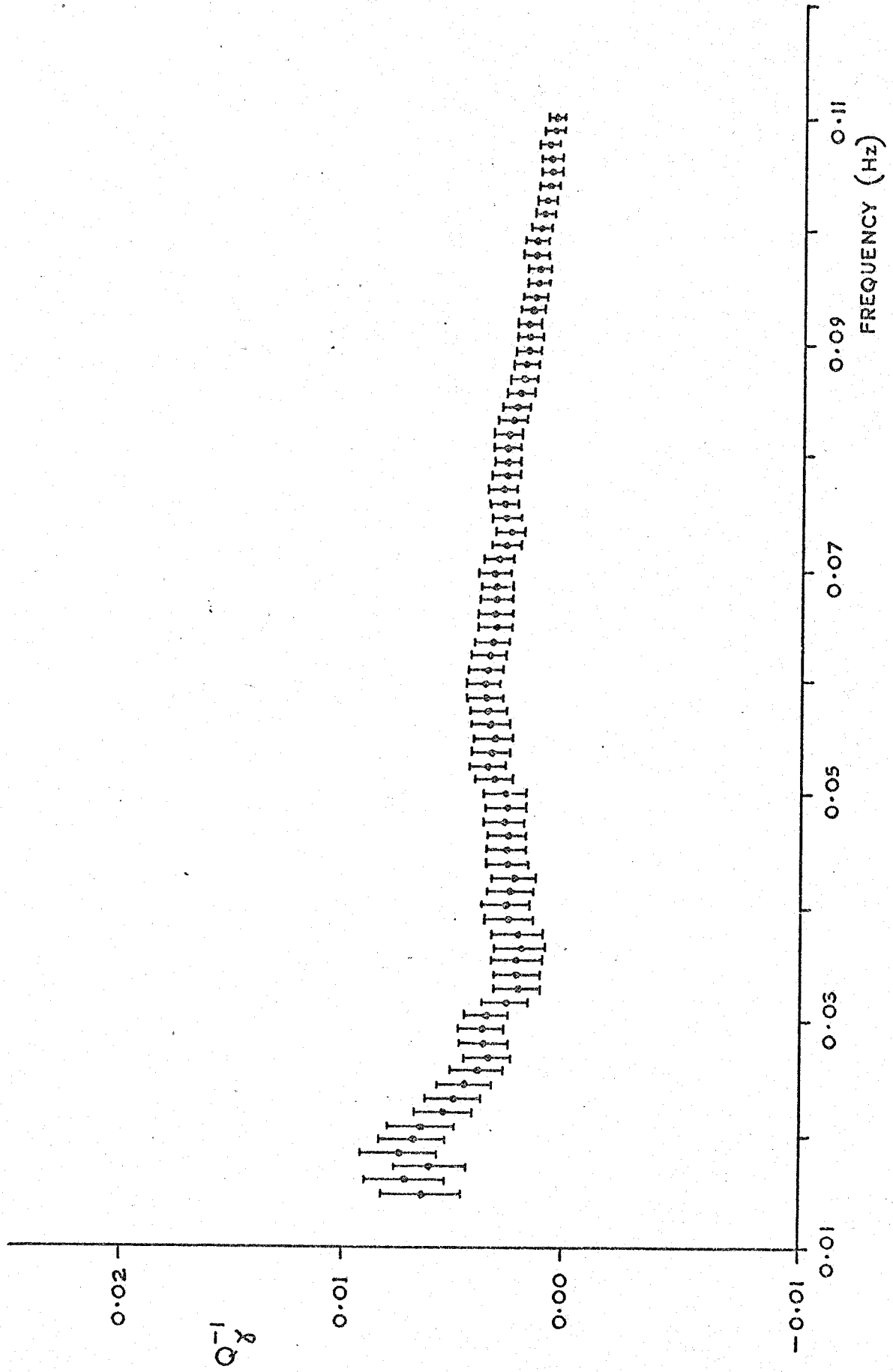


FIGURE 3.22  $Q_y^{-1}$  AND 95 P.C. CONFIDENCE LIMITS ESTIMATED USING THE 5 ATMOSPHERIC EXPLOSIONS, 3 IN NOVAYA ZEMLYA AND 2 IN CHINA

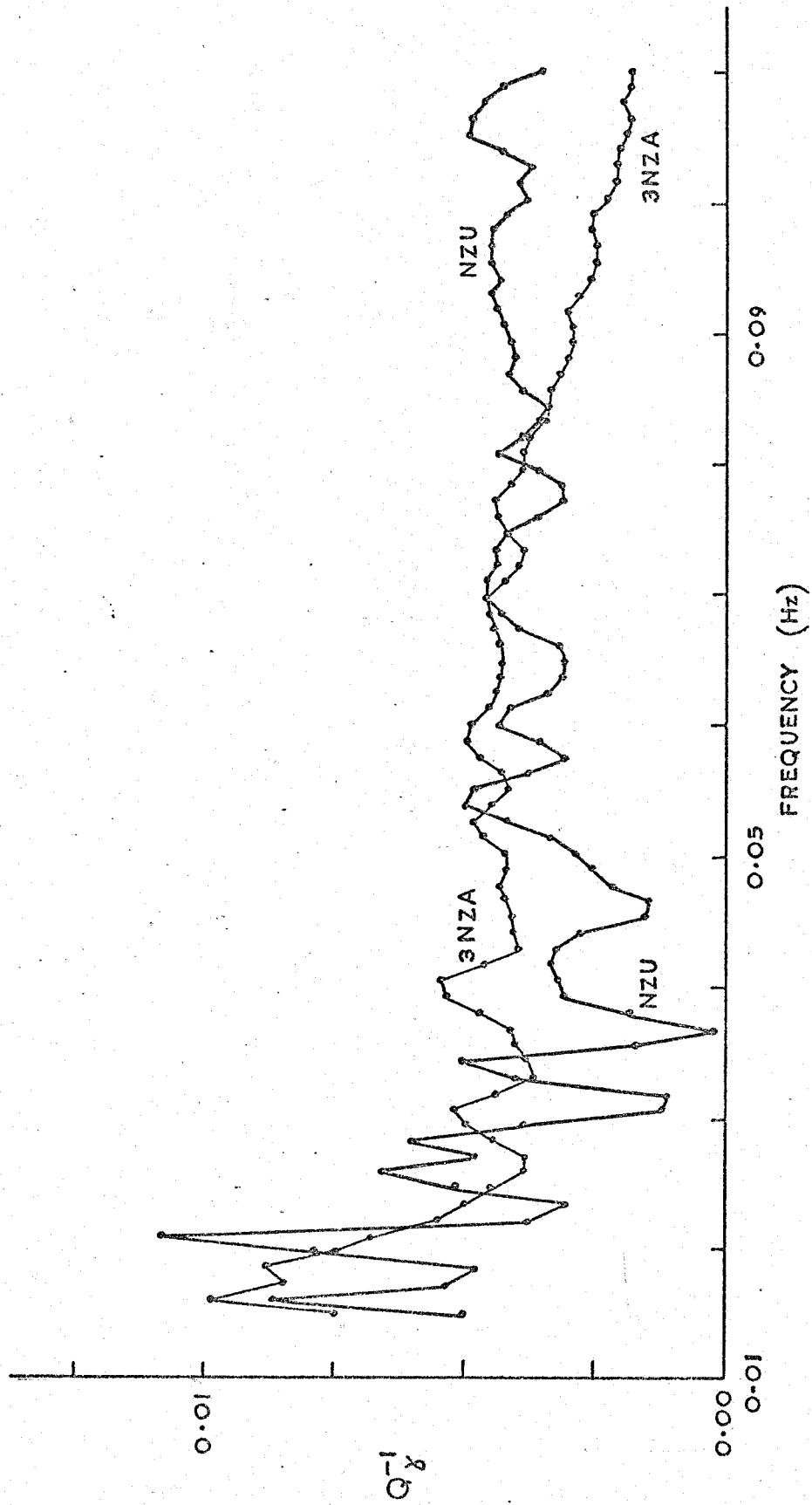


FIGURE 3.23 AVERAGE  $Q_y^{-1}$  FOR THE THREE ATMOSPHERIC EXPLOSIONS COMPARED TO  $Q_y^{-1}$  FOR THE UNDERGROUND EXPLOSION AT NOVAYA ZEMLYA

0.08 Hz, 3NZA trends towards zero while NZU gives a reasonable attenuation value,  $Q_{\gamma}^{-1} \sim 0.004$ . For frequencies greater than 0.08 Hz the underground explosion NZU is probably a better estimator of  $Q_{\gamma}^{-1}$  than 3NZA, simply because it does contain high frequency propagating energy.

### 3.5 Summary

The estimated values of  $Q_{\gamma}^{-1}(f)$  have been presented for each event analysed, along with 95% confidence limits. The data for the separate atmospheric explosions has been combined to form improved averages. In all cases the highest useful frequency of propagating energy has been determined.

In general the  $Q_{\gamma}^{-1}(f)$  values determined from Novaya Zemlya are greater than the equivalent values obtained from the explosions in China. In all cases the attenuation is greater at low frequencies, implying an attenuating layer at depth. It is now necessary to invert the  $Q_{\gamma}^{-1}(f)$  data from a function of frequency for surface waves into a variation with depth, determining  $Q_{\alpha}^{-1}$  and  $Q_{\beta}^{-1}$  for compressional and shear bodily waves.

## CHAPTER 4

### 4.1 A Theoretical Formulation for the Dissipation and Dispersion of Rayleigh Waves

For the future purpose of inverting the experimental  $Q_Y^{-1}$  data it is necessary to describe the evaluation of the dissipation parameter by theoretical means. This will also throw light on  $Q^{-1}$  as an important earth parameter.

Any expression for the amplitude of a surface wave at angular frequency  $\omega$  will contain the wave propagation term

$$\exp [i(\omega t - \underline{k} \cdot \underline{r}) ] \quad 4.1$$

where  $\underline{k}$  is the wave number vector and  $\underline{r}$  the distance. Assuming isotropy this becomes

$$\exp [i(\omega t - kr) ] \quad 4.2$$

If dissipation is present then  $k$  is complex, if dissipation is small amplitudes may be calculated, using complex  $k$ , as if dissipation was not present. The wave number  $k$  becomes\*

$$k(\omega) = k_0(\omega) + \delta k(\omega) \quad 4.3$$

where  $k_0$  is the wave number in the elastic case and is pure real, and  $\delta k(\omega)$  is complex.

---

\*This representation for the wave number was shown to me by J Hudson. This differs from the work of Anderson, Ben-Menahem and Archambeau (1965) who use  $k = k_1 + ik_2$ , viscoelasticity only introducing an imaginary term for dissipation. Allowing  $\delta k(\omega)$  to be complex leads to causally related information about dissipation and dispersion, the relation is obtained by Futterman's methods (1962).

The term  $\delta k(\omega)$  may be written

$$\delta k(\omega) = \phi(\omega) + i\gamma(\omega) \quad 4.4$$

and the term 4.2 becomes

$$\exp [i(\omega t - \phi(\omega)r)] \exp [\gamma(\omega)r] \quad 4.5$$

As expected  $\gamma(\omega)$  determines spatial attenuation, which we hope to prove negative, whilst  $\phi(\omega)$  is a phase term, and  $\gamma(\omega)$  may be rewritten as

$$\gamma(\omega) = -\omega/2Q_\gamma(\omega)U(\omega) \quad 4.6$$

Group velocity,  $U$ , is used for surface waves; the argument is given by Brune (1962) and Knopoff et al. (1964).

The wave number  $k_o(\omega)$  is obtained as solution to the surface wave equation which involves the earth parameters  $\alpha_o$  and  $\beta_o$  (compressional and shear velocities). For the elastic half space case this characteristic equation is

$$\left(2 - \frac{c_o^2}{\beta_o^2}\right) - 4\left(1 - \frac{c_o^2}{\alpha_o^2}\right)^{\frac{1}{2}} \left(1 - \frac{c_o^2}{\beta_o^2}\right)^{\frac{1}{2}} = 0 \quad (\text{Bullen 1965}) \quad 4.7$$

$c_o$  is the velocity of the surface waves, and this may be represented by

$$F_o(k_o, \omega, \alpha_o, \beta_o) = 0 \quad 4.8$$

because  $k_o(\omega) = \frac{\omega}{c_o}$ . When dissipation occurs the visco-elastic wave number  $k$  is the solution of

$$F(k, \omega, \alpha, \beta) = 0 \quad 4.9$$

where  $k, \alpha, \beta$  are all complex and  $\alpha, \beta$  are of the form

$$\alpha(\omega) = \alpha_o + \delta\alpha(\omega) \quad 4.10$$

If we now assume a plane  $N$  layered earth model where  $h_l$  denotes the thickness of the  $l$ th layer then identity 4.9 becomes

$$F(k, \omega, h_l, \alpha_l, \beta_l) = 0 \quad 4.11$$

and adapting a statement by Anderson, Ben-Menahem and Archambeau (1965),

$\delta k(\omega)$  is given by the partial derivative summation

$$\delta k(\omega) = \sum_{l=1}^N \left[ \frac{\partial k_o}{\partial \alpha_{ol}} \delta \alpha_{l1} + \frac{\partial k_o}{\partial \beta_{ol}} \delta \beta_{l1} \right] \quad 4.12$$

In the work of Anderson et al.  $\delta \alpha_{l1}$ ,  $\delta \beta_{l1}$  are pure imaginary, here they are complex.

The wave number  $k_o$  may be determined by applying equation 4.8 to a layered structure, that is solving

$$F_o(k_o, \omega, h_1, \alpha_{o1}, \beta_{o1}) = 0 \quad 4.13$$

The solution for  $k_o$  is obviously of the form  $k_o(\omega, h_1, \alpha_{o1}, \beta_{o1})$  and so the derivatives in 4.12 are of the form

$$\frac{\partial k_o(\omega, h_1, \alpha_{o1}, \beta_{o1})}{\partial \alpha_{o1}} \quad 4.14$$

The Thomson-Haskell matrix formulation (Thomson 1950, Haskell 1953, 1964) for surface waves on a layered structure will later be used to obtain solutions for  $k_o$  for a chosen layered model. The program, written by A Douglas, was adapted to produce the derivatives of equation 4.14 by solving equation 4.13 for  $k_{oj+}$  and  $k_{oj-}$  by using  $\alpha_{oj} + d\alpha_o$  followed by  $\alpha_{oj} - d\alpha_o$  and then perturbing the parameters of each layer in turn and re-solving

$$F_o(k_{oj\pm}, \omega, h_1, \alpha_{o1} \pm \delta_{lj} d\alpha_o, \beta_{o1}) = 0 \quad 4.15$$

The small increment  $d\alpha_o$  is added to  $\alpha_{oj}$  only (and  $j$  eventually runs from 1 to  $N$ , perturbing each layer in turn) and the new wave number  $k_{oj+}$  obtained.

The required derivative is then approximated by

$$\left. \frac{\partial k_o}{\partial \alpha_{ol}} \right|_{\omega} \Big|_{l=j} = \frac{k_{oj+} - k_{oj-}}{2d\alpha_o} \Big|_{\omega} \quad 4.16$$

Because  $k_o(\omega) = \frac{\omega}{\alpha_o(\omega)}$  a small positive change in  $\alpha_o(\omega)$  produces a small negative change in  $k_o(\omega)$ ; the derivatives are always negative.

The derivatives with respect to  $\beta$  are obtained in a similar manner, and they too are all negative.

Equation 4.12 may be written in full as

$$R(\delta k(\omega)) = \varnothing(\omega) = \sum_{l=1}^N \left[ \frac{\partial k_o}{\partial \alpha_{o1}} R(\delta \alpha_1) + \frac{\partial k_o}{\partial \beta_{o1}} R(\delta \beta_1) \right] \Bigg|_{\omega} \quad 4.17a$$

$$I(\delta k(\omega)) = \gamma(\omega) = \sum_{l=1}^N \left[ \frac{\partial k_o}{\partial \alpha_{o1}} I(\delta \alpha_1) + \frac{\partial k_o}{\partial \beta_{o1}} I(\delta \beta_1) \right] \Bigg|_{\omega} \quad 4.17b$$

By considering small changes in the body wave velocity  $\alpha_{o1}$  it may be shown that (Appendix F)

$$I(\delta \alpha_1) = \frac{Q_{\alpha 1}^{-1} \alpha_{o1}}{2} \quad 4.18a$$

$$I(\delta \beta_1) = \frac{Q_{\beta 1}^{-1} \beta_{o1}}{2} \quad 4.18b$$

here  $Q_{\alpha 1}^{-1}$ ,  $Q_{\beta 1}^{-1}$  are specific attenuation factors for bodily waves.

The equations 4.18 allow us to express the attenuation coefficient  $\gamma(\omega)$  of equation 4.17b in terms of physically obtainable quantities, which was our major objective.

Further, the R and I parts of  $\delta \alpha_1$ ,  $\delta \beta_1$  are causally related and the treatment described by Futterman (1962) may be applied. The dissipative effects ( $I(\delta \alpha_1)$ ) are related to the dispersive effects ( $R(\delta \alpha_1)$ ) and applying Futterman's results gives (See Appendix F)

$$R(\delta \alpha_1) = \frac{\alpha_{o1}}{\pi} Q_{\alpha 1}^{-1} \ln \psi_{\omega_o} = \frac{2}{\pi} I(\delta \alpha_1) \ln \frac{\omega}{\omega_o} \quad 4.19a$$

$$R(\delta \beta_1) = \frac{\beta_{o1}}{\pi} Q_{\beta 1}^{-1} \ln \psi_{\omega_o} = \frac{2}{\pi} I(\delta \beta_1) \ln \frac{\omega}{\omega_o} \quad 4.19b$$

where  $\omega_o$ , as Kolsky (1956) would have it, is a "disposable constant".

Therefore substituting in 4.17 we have

$$\varnothing(\omega) = \frac{2}{\pi} \ln \left( \frac{\omega}{\omega_o} \right) \gamma(\omega) \quad 4.20a$$

$$\gamma(\omega) = \sum_{l=1}^N \left[ \frac{\partial k_o}{\partial \alpha_{o1}} \frac{Q_{\alpha 1}^{-1}}{2} \alpha_{o1} + \frac{\partial k_o}{\partial \beta_{o1}} \frac{Q_{\beta 1}^{-1}}{2} \beta_{o1} \right] \quad 4.20b$$

$$\delta k(\omega) = \gamma(\omega) \left( \frac{2}{\pi} \ln \frac{\omega}{\omega_o} + i \right) \quad 4.21$$

Using knowledge of the specific attenuation factor (body waves), the velocity of body waves and the derivatives  $\frac{\partial k_o}{\partial \alpha_{o1}}$  the attenuation

coefficient  $\gamma(\omega)$  may be calculated for a layered structure. As expected the attenuation coefficient is negative, directly determined by the sign of the derivatives which are always negative. Further, if the group velocity for the model is known then  $Q_\gamma^{-1}$  may easily be calculated from  $\gamma(\omega)$ , by 4.6

$$Q_\gamma^{-1}(\omega) = \frac{-2U(\omega)\gamma(\omega)}{\omega} \quad 4.22$$

The Thomson-Haskell method determines the phase velocity dispersion for the model, the group velocity dispersion is easily obtained from this by using the usual equation

$$U(\omega) = \frac{d\omega}{dk} = C + k \frac{dc}{dk} \quad 4.23$$

We may take the argument further and calculate the change in the Rayleigh wave phase velocity caused by dispersion linked, as above, with the dissipation.

A change in the wavenumber of  $-\delta k$  is linked with a change  $+\delta c$  in the Rayleigh velocity  $C_0$

$$k_0 - \delta k(\omega) = \frac{\omega}{C_0 + \delta C(\omega)} \quad 4.24$$

and because

$$k_0 = \frac{\omega}{C_0}$$

$$\delta k(\omega) = \frac{\omega}{C_0} - \frac{\omega}{C_0 + \delta C(\omega)}$$

$$\therefore \delta k(\omega) \sim - \frac{\omega \delta C(\omega)}{C_0^2} \quad 4.25$$

Taking the real parts and rearranging gives

$$\delta C(\omega) = - \frac{C_0^2}{\omega} \phi(\omega)$$

$$\therefore \delta C(\omega) = - \frac{C_0}{\omega} \gamma(\omega) \frac{2}{\pi} \ln \frac{\omega}{\omega_0}$$

$$\therefore C(\omega) = C_0 \left( 1 - \frac{C_0}{\omega} \gamma(\omega) \frac{2}{\pi} \ln \frac{\omega}{\omega_0} \right)$$

$$\therefore C(\omega) = C_0 \left( 1 + \frac{Q_\gamma^{-1}}{\pi} \frac{C_0}{U(\omega)} \ln \frac{\omega}{\omega_0} \right) \quad 4.26$$



This equation is similar to a solution given by Kolsky (1956) for compressional waves in a rod

$$C(\omega) = C_0 \left( 1 + \frac{\tan \delta}{\pi} \ln \frac{\omega}{\omega_0} \right) \quad 4.27$$

where  $\tan \delta$  may be read as  $Q_a^{-1}$ . The group velocity appears in equation 4.26 because the energy of surface waves travels with this velocity rather than the phase velocity, and so is required in the attenuation expression 4.6. This second type of dispersion is a geometrical effect which occurs for surface waves because longer periods reach to greater depths within the earth than shorter periods, therefore sampling a different velocity structure. Because a different velocity structure is sampled a different Rayleigh wave velocity results for each frequency. This does not occur for body waves because all frequencies follow the same path, unless scattered in a frequency dependent manner. So for body waves the phase and group velocities (hence the energy velocity for these seismic frequencies) are almost identical, the difference is caused by dispersion linked to dissipation which is a small effect. If surface waves were not dispersed by geometrical means (as calculated by the Thomson-Haskell technique) then equation 4.26 would reduce to a form equivalent to 4.27.

It is usual to calculate Rayleigh wave geometrical dispersion using Thomson-Haskell matrices with frequency independent body wave velocities. If frequency dependent body wave velocities are used, and attenuation is allowed for, (essentially solving equation 4.11) the resulting Rayleigh wave dispersion curve has been shown to differ by 1% from the simpler model (Carpenter and Davies 1966). In this study derivatives of the  $\frac{\partial k_0}{\partial \alpha_0}$  type were obtained using the simple elastic Thomson-Haskell formulation and then the attenuation coefficient calculated from equation 4.20b. Obviously there are some feedback errors in this process because the derivative expressed in 4.14 should really include attenuation and be of the form

$$\frac{\partial k(\omega, h_1, \alpha_1, \beta_1, Q_{\alpha 1}^{-1})}{\partial \alpha_1}$$

4.27

Such considerations were ignored. Also the possibility that the attenuation frequency relation (equation 4.6) is not linear is ignored, that is relations of the form  $\gamma(\omega) \propto \omega^P$  (P not necessarily integer) which are considered advantageous by Strick (1967) are not considered, because the advantages gained are largely in the theoretical presentation of the attenuation mechanism.

#### 4.2 The Attenuation of Rayleigh Waves on a Half Space

Before any attempt is made to invert the observed  $Q_\gamma^{-1}$  data into an attenuation-depth model involving  $Q_\alpha^{-1}$ ,  $Q_\beta^{-1}$  by using equations 4.20b and 4.22 for  $\gamma(\omega)$  as a function of  $Q_\alpha^{-1}$ ,  $Q_\beta^{-1}$  and  $Q_\gamma^{-1}$  as a function of  $\gamma(\omega)$  respectively, it would be useful to obtain a simple, if approximate, relation of the form  $Q_\gamma^{-1} \sim f(Q_\alpha^{-1}, Q_\beta^{-1})$ . With such an approximate equation it would be possible to estimate the range of values for  $Q_\alpha^{-1}$ ,  $Q_\beta^{-1}$  which ought to be considered for inversion purposes.

Equation 4.7 gives the characteristic equation for a Rayleigh wave in a perfectly elastic half space, this equation has the physical solution

$$c_0 = 0.98 \beta_0 \quad 4.28$$

Obviously dispersion does not occur with such a model. For a homogeneous viscoelastic half space an expression was obtained by Press and Healy (1957) relating the Rayleigh wave attenuation to Poisson's ratio,  $Q_\alpha^{-1}$ ,  $Q_\beta^{-1}$  only. Press and Healy obtained their expression by allowing the velocities in the characteristic equation 4.7 to become complex, their expression is quite complicated but following Anderson et al. (1965) it may be written as

$$Q_\gamma^{-1} = m Q_\alpha^{-1} + (1-m) Q_\beta^{-1} \quad 4.29$$

where m is a complicated function of Poisson's ratio.

However, a much simpler equation may be obtained using the equation 4.20b for  $\gamma(\omega)$ . Rewriting equation 4.20b for a half-space

immediately gives

$$\gamma(\omega) = \frac{\partial k}{\partial \alpha} \frac{Q_{\alpha}^{-1}}{2} + \frac{\partial k}{\partial \beta} \frac{Q_{\beta}^{-1}}{2} \quad 4.30$$

and assuming a Poisson solid ( $\alpha = \sqrt{3}\beta$ )

$$\gamma(\omega) = \frac{\partial k}{\partial \beta} \frac{\beta}{2} (Q_{\alpha}^{-1} + Q_{\beta}^{-1}) \quad 4.31$$

Ignoring the dispersive effects of viscoelasticity implies equation 4.28

which will be written, for simplicity of manipulation, in the form

$$C_0 = n\beta \quad 4.32$$

$$\therefore k = \frac{\omega}{n\beta}$$

$$\therefore \frac{\partial k}{\partial \beta} = \frac{-\omega}{n\beta^2} + \frac{1}{n\beta} \frac{\partial \omega}{\partial \beta} \quad 4.33$$

Now assuming that  $\frac{\partial \omega}{\partial \beta} = 0$ , that is non dispersive body waves (which is experimentally true!) gives

$$\frac{\partial k}{\partial \beta} = \frac{-\omega}{n\beta^2} \quad 4.34$$

therefore

$$\gamma(\omega) = \frac{-\omega}{n\beta} \frac{1}{2} (Q_{\alpha}^{-1} + Q_{\beta}^{-1}) \quad 4.35$$

which leads to

$$Q_{\gamma}^{-1} = Q_{\alpha}^{-1} + Q_{\beta}^{-1} \quad 4.36$$

Before this equation is used it is worthwhile calculating the partial

derivatives  $\frac{\partial k_0}{\partial \alpha_{01}}$ ,  $\frac{\partial k_0}{\partial \beta_{01}}$  to show the limitations of this equation.

### 4.3 Partial Derivatives for Inversion Purposes

As has already been described the partial derivatives were obtained by using the Thomson-Haskell procedure to solve a layered structure for the wavenumber  $k_{oj+}$ , then perturbing the velocity  $\alpha_{oj}$  in the  $j$ th layer, and re-solving for  $k_{oj-}$ ; hence  $\left. \frac{\partial k_0}{\partial \alpha_{oj}} \right|_{\omega}$  and similarly  $\left. \frac{\partial k_0}{\partial \beta_{oj}} \right|_{\omega}$  may be calculated for a range of  $\omega$ . An alternative procedure would be to use the surface wave energy equation described by Jeffreys (1961) and this has been done by Takeuchi, Dorman and Sato (1969) to perform numerical

inversion of surface wave data.

The velocity depth model assumed from which the derivatives were calculated is listed in Table 4.1. This is a simple six layered continental type model, chosen because most of the propagation paths used in this work are largely of continental type. The model is also illustrated in Figure 4.1, and its characteristic group velocity curve in Figure 4.2.

The partial derivatives of the wavenumber,  $k_o$ , with respect to both body wave velocities for the six layers are shown in Figures 4.3 and 4.4, as functions of frequency. It is immediately apparent that for a given layer (value of  $l$ )  $\frac{\partial k_o}{\partial \beta_{ol}}$  is an order of magnitude larger than  $\frac{\partial k_o}{\partial \alpha_{ol}}$ .

This implies, referring to equation 4.20b for the attenuation coefficient  $\gamma(\omega)$ , attenuation of shear waves has a greater contribution to  $\gamma(\omega)$  for surface waves than does compressional wave attenuation. (Of course assuming  $Q_\alpha^{-1}, Q_\beta^{-1}$  are of the same order.) The further implication is

$$\frac{\partial Q_\gamma^{-1}}{\partial Q_\beta^{-1}} > \frac{\partial Q_\gamma^{-1}}{\partial Q_\alpha^{-1}} \quad 4.37$$

which is born out by the observations of Anderson et al. (1965).

Two more comments are worth noting about the way the derivatives change with frequency and as a function of layer depth. The derivatives show a pronounced negative minimum at a particular frequency, the deeper the layer the lower the frequency. This quality is retained even for the derivatives of deep layers with respect to compressional wave velocity, Figure 4.5 for  $\frac{\partial k_o}{\partial \alpha_{ol}}$  shows this well. This variation is again expected because Rayleigh waves of different frequencies spread their energy through the layers to different extents. High frequencies are concentrated in the upper layers and only influence the derivatives for the upper layers. Conversely the derivative values for high frequencies in the lower layers are zero; there is no high frequency energy in the lower layers. Kolsky has shown in "Stress waves in solids" (1953) that at a depth of one wave-

Thickness of Layer $h_1$ km	P-Wave Velocity $\alpha_1$ km s <sup>-1</sup>	S-Wave Velocity $\beta_1$ km s <sup>-1</sup>	$\frac{3}{4} \left( \frac{\alpha_1}{\beta_1} \right)^2$ ( $=Q_{\alpha_1}^{-1} / Q_{\beta_1}^{-1}$ )
14.0	6.10	3.50	2.29
22.0	6.50	3.72	2.29
22.0	8.06	4.40	2.51
10.0	8.08	4.46	2.51
55.0	8.121	4.45	2.51
$\infty$	8.50	4.96	2.19

Table 4.1 Assumed Velocity-Depth Model

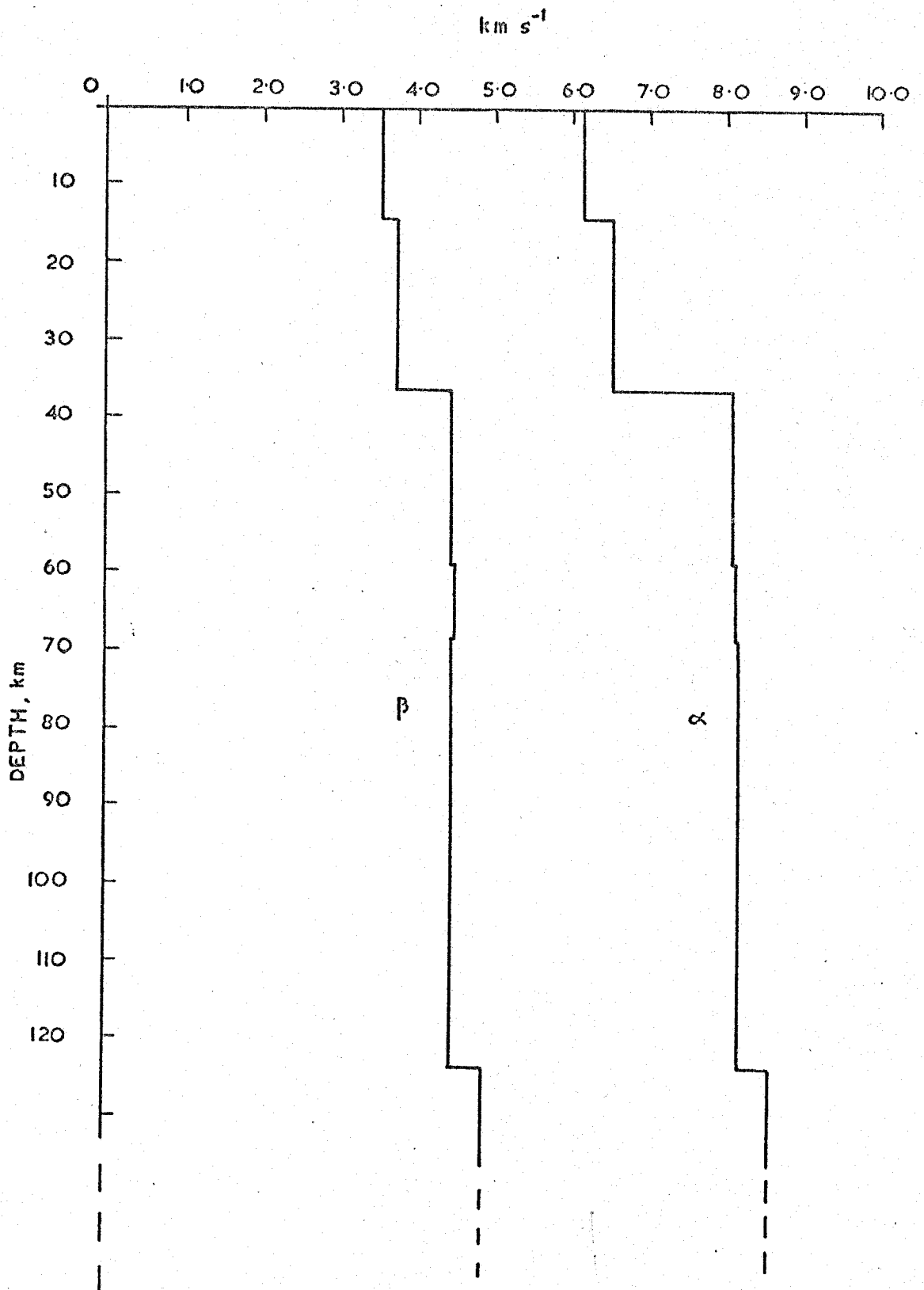


FIGURE 4.1 THE VELOCITY-DEPTH MODEL ASSUMED FOR  
INVERSION PURPOSES

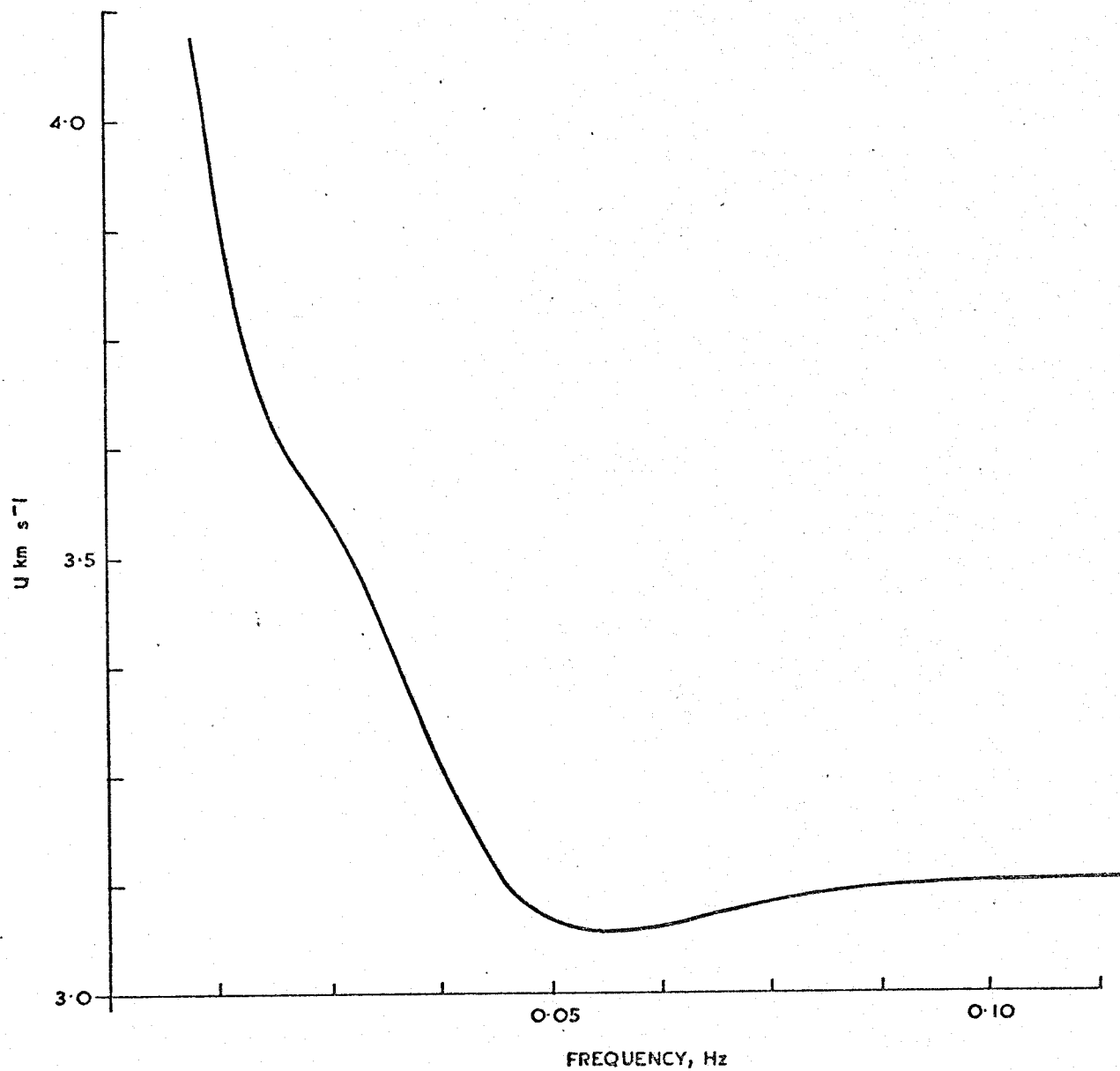


FIGURE 4.2 THE GROUP VELOCITY DISPERSION CURVE ( $U$ ) FOR THE ASSUMED VELOCITY-  
DEPTH MODEL

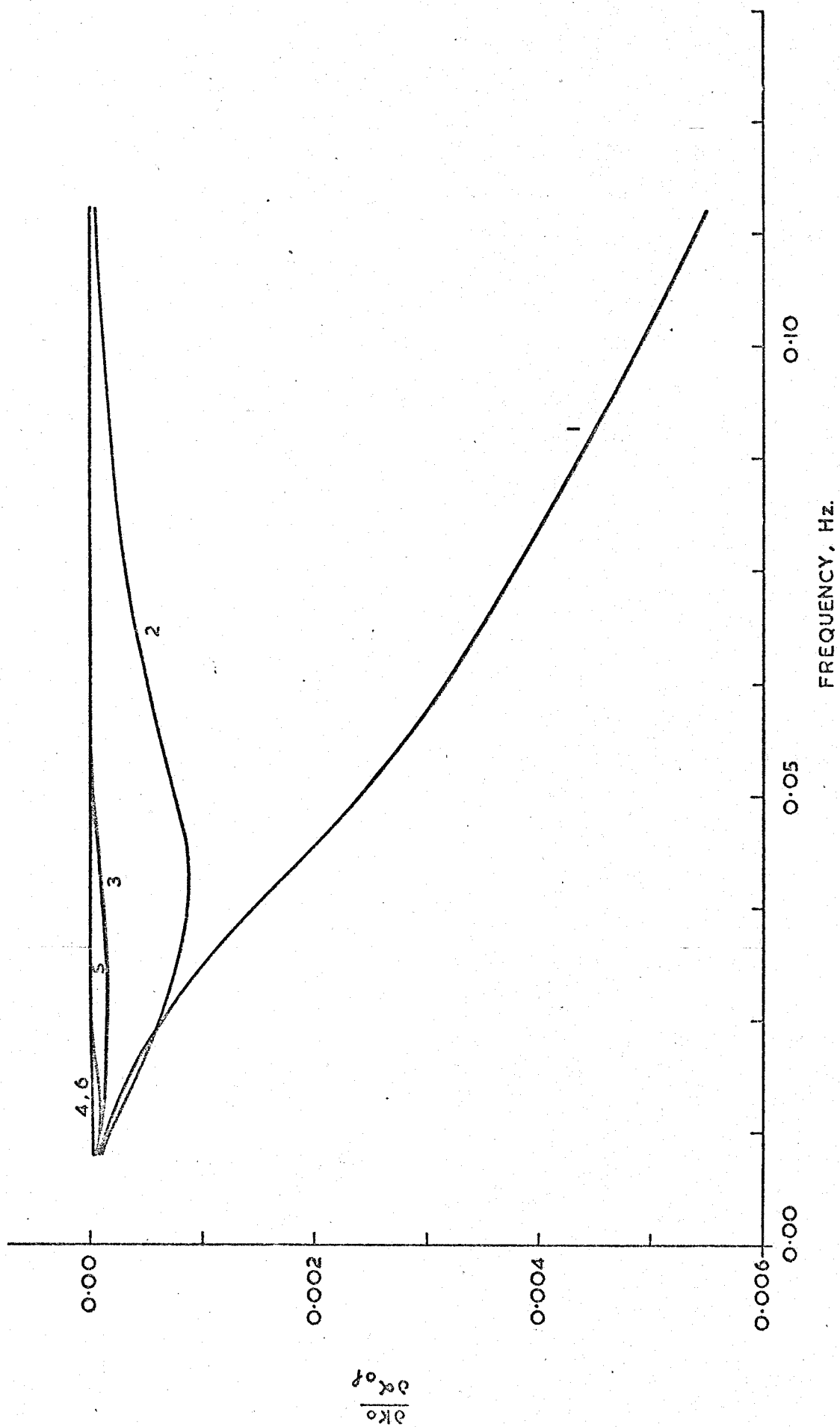


FIGURE 4.3 DERIVATIVES  $\frac{\partial k_0}{\partial \omega}$  FOR THE SIX LAYERED VELOCITY-DEPTH MODEL (LAYERS,  $\rho$ , MARKED 1 TO 6)



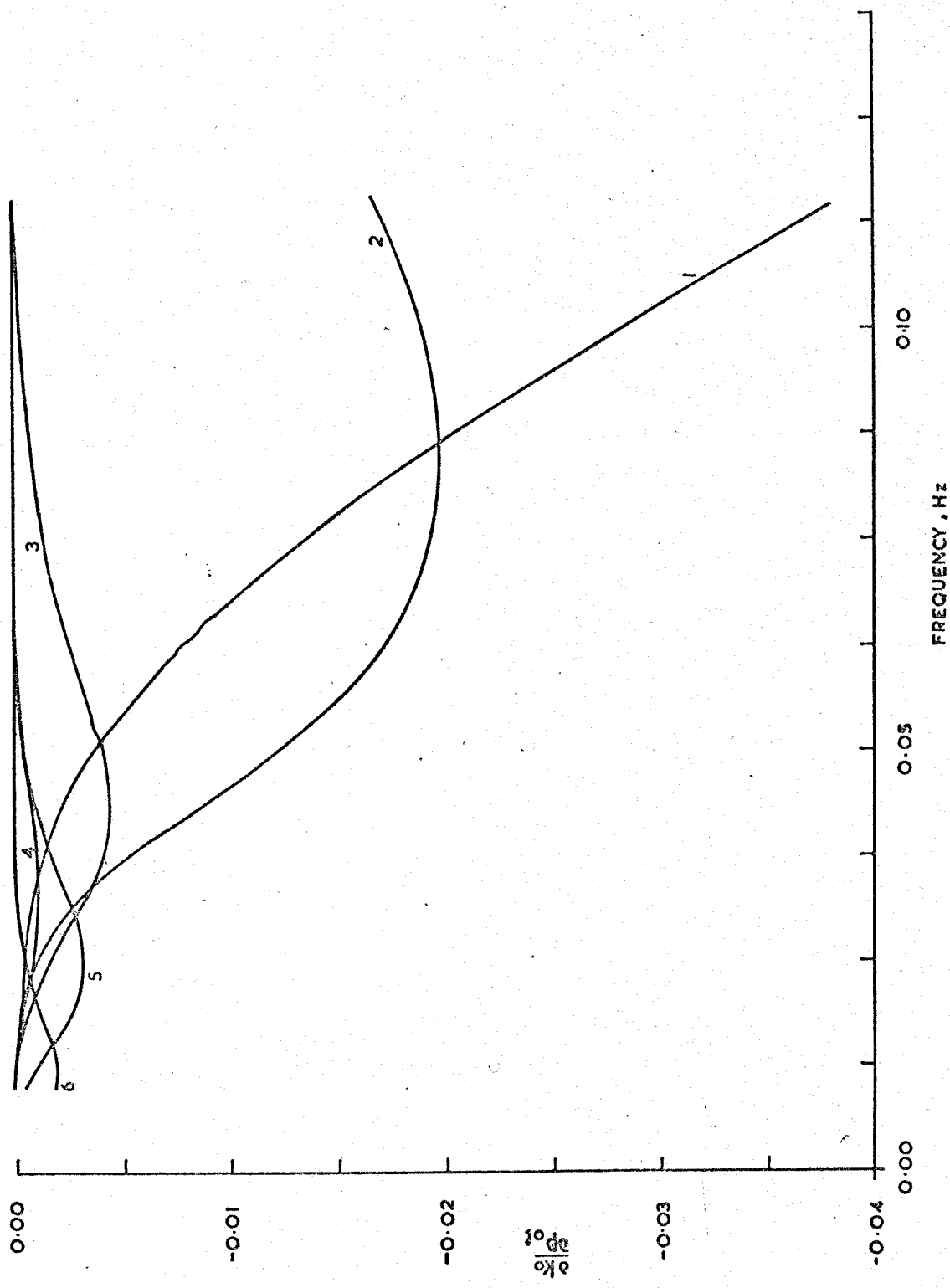


FIGURE 4.4 DERIVATIVES  $\frac{\partial k_0}{\partial \rho_0}$  FOR THE SIX LAYERED VELOCITY-DEPTH MODEL (LAYERS A, MARKED 1 TO 6)

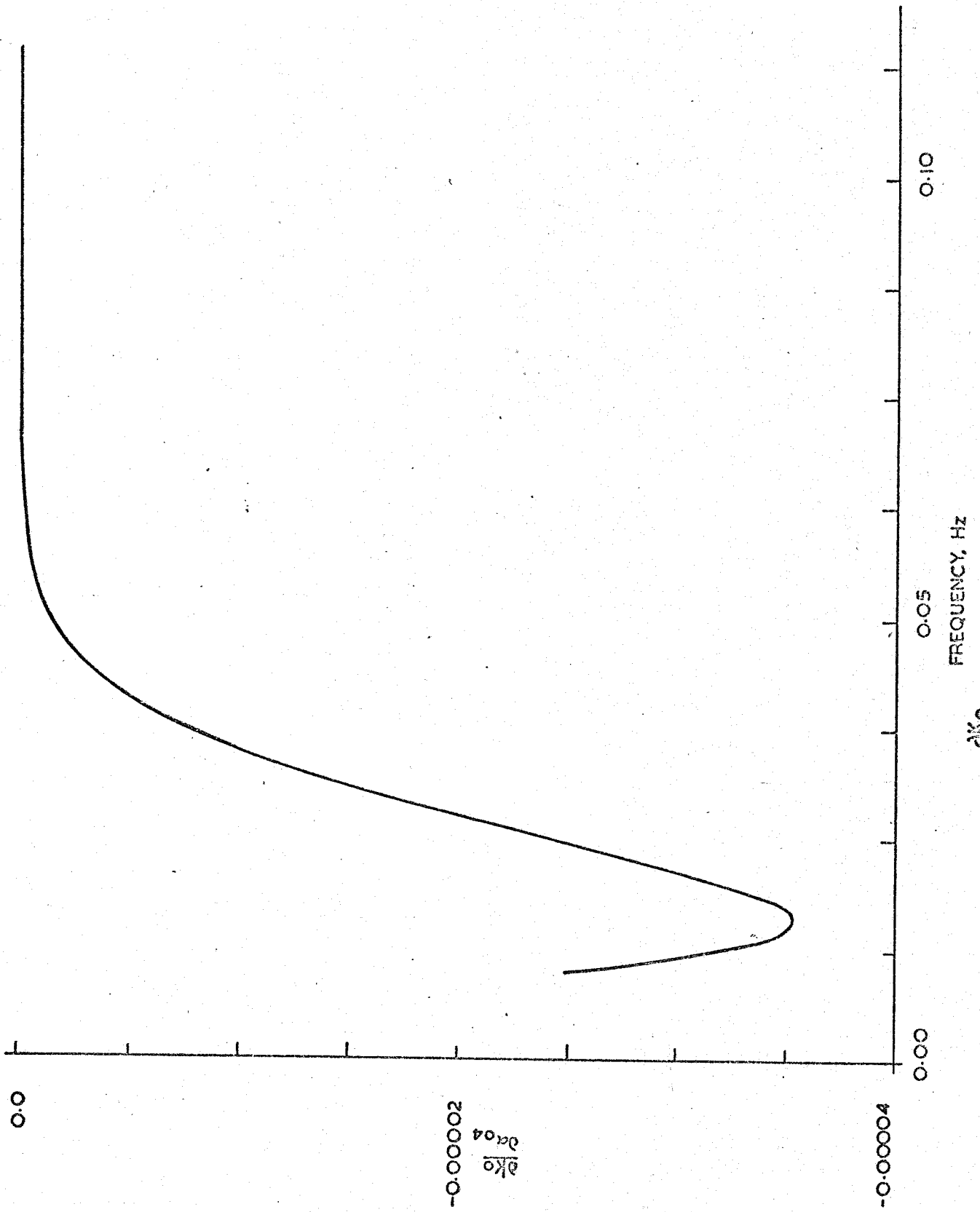


FIGURE 4.5 THE DERIVATIVE  $\frac{\partial k_0}{\partial z_0}$  FOR THE SIX LAYERED VELOCITY-DEPTH MODEL.

length into an homogeneous halfspace the vertical amplitude of motion has fallen to 0.19 of its value at the surface. For example a Rayleigh wave period 60s at a depth of 250 km is propagating with about 20% of its surface vertical amplitude. This depth value is regarded as the extreme limit of penetration of the waves used in this study; this is an obvious limit to the inversion range of depth.

The second comment arises because the deeper layer derivatives are much smaller than for shallower layers. For an homogeneous half space the shallower depths therefore have greater effect on the summation for  $\gamma(\omega)$ . For inversion over all frequencies into a depth model the upper layers are better resolved (because they are more heavily weighted by the derivatives). This is later of importance when direct "Hedgehog" inversion is used.

To summarise, the two sets of derivatives should be regarded as two dimensional weights varying with frequency and depth. When an attenuation model is postulated which varies with depth, the derivatives weight the model, shaping it and forming a result which may be compared to the observed.

#### 4.4 Simple Qualitative Inversion of the $Q_Y^{-1}(f)$ Data

Using the assumed velocity-depth structure, and the related partial derivatives, makes it possible to invert  $Q_Y^{-1}(f)$  into an attenuation model of  $Q_\alpha^{-1}$ ,  $Q_\beta^{-1}$  with depth. For the six layered attenuation structure to be used this requires twelve independent values of  $Q_{\alpha, \beta}^{-1}$ . It is desirable to reduce this number to six by assuming a simple relationship between  $Q_\alpha^{-1}$  and  $Q_\beta^{-1}$  for all layers. Anderson et al. (1965) and Kanamori (1970) have suggested the adhoc relations

$$Q_\beta^{-1} = 2.25 Q_\alpha^{-1} \quad 4.37 \text{ C1}$$

$$Q_\beta^{-1} = Q_\alpha^{-1} \quad 4.38 \text{ C2}$$

Burton and Kennet (1972) suggest using

$$Q_\beta^{-1} = \frac{1}{4} \left(\frac{\alpha}{\beta}\right)^2 Q_\alpha^{-1} \quad 4.39 \text{ C3}$$

because this has a physical interpretation: no attenuation attributable to the bulk modulus. The values of  $\frac{1}{4} \left(\frac{\alpha_1}{\beta_1}\right)^2$  and hence the ratio  $\frac{Q_{\beta 1}^{-1}}{Q_{\alpha 1}^{-1}}$  are listed in Table 4.1.

Not forgetting the influence the partial derivatives have on the calculation of  $Q_{\alpha}^{-1}(f)$  for the real earth we may now take equation 4.36 further. Using the condition, C1,  $Q_{\beta}^{-1} = 2.25 Q_{\alpha}^{-1}$  gives

$$Q_{\gamma}^{-1} = 3.25 Q_{\alpha}^{-1} \quad 4.40$$

A very simple qualitative inversion is now possible. The figures 3.1 to 3.6, and in particular 3.18 and 3.19 for average  $Q_{\gamma}^{-1}(f)$ , show that  $Q_{\gamma}^{-1}(f)$  for higher frequencies is about 0.003 but for lower frequencies it may reach 0.009. Using the approximation of 4.40 this gives

Depth	$Q_{\alpha}^{-1}$	$Q_{\beta}^{-1}$	$Q_{\gamma}^{-1}$	Frequency
Shallow	0.001	0.002	0.003	High
Deep	0.003	0.007	0.009	Low

Obviously the tentative conclusion is a region of greater attenuation at depth, which is only sampled by the penetrating low frequencies. The partial derivatives have been ignored in the above approximations, but the way in which they weight the deeper layers (previously described) will make larger values of  $Q^{-1}$  at depth difficult to resolve.

#### 4.5 Model Inversion of the $Q_{\gamma}^{-1}(f)$ data

It is possible to attempt inversion by trial and error. A model may be postulated, guided by the simple qualitative inversion above, and the  $Q_{\gamma}^{-1}(f)$  it would generate may be calculated. It was decided to model  $Q_{\alpha}^{-1}$  because this parameter is more abundant in the literature than  $Q_{\beta}^{-1}$ .

The computer program QRALEY (Appendix G) was written to calculate  $Q_{\gamma}^{-1}(f)$  for any postulated model of  $Q_{\alpha}^{-1}$  with depth and any simple relationship between  $Q_{\alpha}^{-1}$  and  $Q_{\beta}^{-1}$  may be used in this program.

A simple model (M1) was found which approximates the curve shape for the  $Q_{\gamma}^{-1}(f)$  values averaged for five atmospheric explosions shown

in Figure 3.19, that is the model generates roughly constant  $Q_Y^{-1}$  in the frequency range 0.03-0.09 Hz and  $Q_Y^{-1}$  increases for lower frequencies. This model shows a high value,  $Q_\alpha^{-1} = 0.008$ , for the deepest layer.

Model M1 was compared to four other models. All five models are listed in Table 4.2. The models attributed to Teng, Anderson et al. and Kanamori have been adapted (to fit the layers in this study) from the  $Q_\alpha$  values listed in Ibrahim's (1971) paper. The model M2 represents a simple decrease of attenuation with depth, this phenomenon might be expected due to increased compaction of material with depth. The control model M1 is regarded as a reasonable picture of the observed data. All five models were compared for the three conditional equations between  $Q_\alpha^{-1}$  and  $Q_\beta^{-1}$  specified by equations 4.37-4.39. The results are shown in Figures 4.6-4.8.

The models of Kanamori and M2 are untenable for all three conditions. Decreasing attenuation at low frequencies is found by M2, while the Kanamori values are too large. Teng's model is unsuitable given conditions C1 and C3 but using  $Q_\alpha^{-1} = Q_\beta^{-1}$  it is a possible model, although the onset of increasing  $Q_Y^{-1}$  at low frequencies occurs at too high a frequency (0.05 Hz). Anderson's model has possibilities but the peak at low frequencies, rather than a smooth increase of  $Q_Y^{-1}$ , tends to make it unacceptable.

#### 4.6 Conclusions

An expression has been obtained from which the specific attenuation factor  $Q_Y^{-1}(f)$  for Rayleigh waves may be calculated.

For the calculation of  $Q_Y^{-1}(f)$  it is necessary to assume a velocity-depth structure, for which partial derivatives of the type  $\frac{\partial k}{\partial a_{o1}}$  are calculated. An attenuation model for  $Q_\alpha^{-1}$  with depth is then postulated, and a condition of the type  $Q_{\beta 1}^{-1} = \frac{1}{4} \left(\frac{a_1}{\beta}\right)^2 Q_{\alpha 1}^{-1}$  assumed. The derivatives are regarded as weights which shape the attenuation model, forming a surface wave  $Q_Y^{-1}(f)$  from body wave  $Q_{\alpha, \beta}^{-1}(h)$ .

Thickness of Layer	Model 1		Model 2		Teng		Anderson et al.		Kanamori		
	$Q_{\alpha}^{-1}$	$Q_{\alpha}$	$Q_{\alpha}^{-1}$	$Q_{\alpha}$	$Q_{\alpha}^{-1}$	$Q_{\alpha}$	$Q_{\alpha}^{-1}$	$Q_{\alpha}$	$Q_{\alpha}^{-1}$	$Q_{\alpha}$	
h km											
14.0	.0025	450	.0045	450	.00222	1012	.00099	450	.00222	450	
22.0	.0025	450	.0040	450	.00222	1012	.00099	450	.00222	450	
22.0	.0025	255	.0035	255	.00392	135	.00741	60	.01667	60	
10.0	.0045	68	.0030	68	.01471	135	.00741	60	.01667	60	
55.0	.0015	95	.0025	95	.01053	195	.00513	87	.01149	87	
$\infty$	.0080	100	.0020	100	.01000	260	.00385	120	.00833	120	

Table 4.2 Attenuation models for  $Q_{\alpha}^{-1}$  as a function of depth. (The model types attributed to Teng, Anderson et al. and Kanamori are adapted from the  $Q_{\alpha}$  values listed by Ibrahim (1971).)

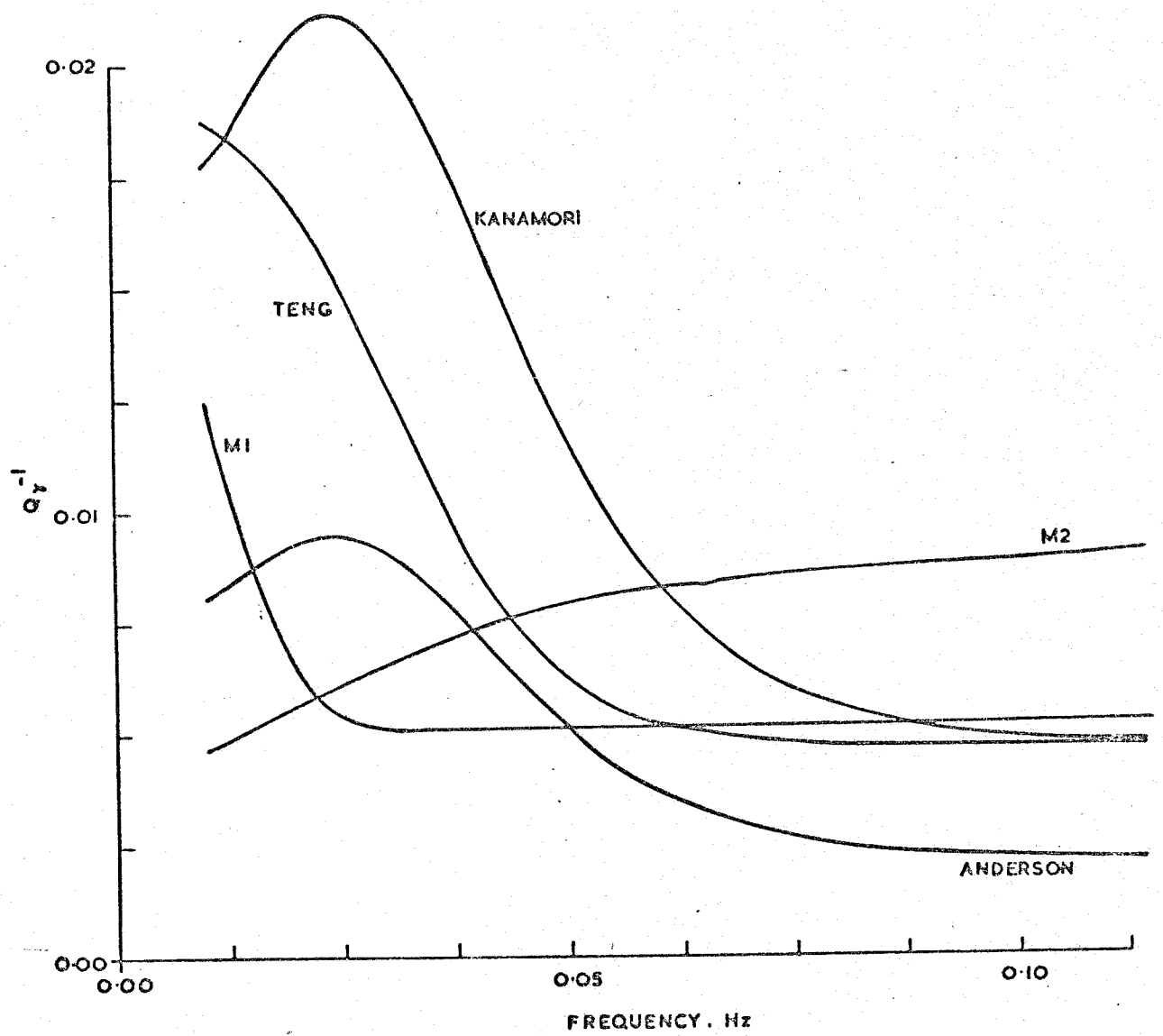


FIGURE 4.6 THEORETICAL RAYLEIGH WAVE  $Q_y^{-1}$  FOR MODELS USING  $Q_p^{-1} = 2.25 Q_s^{-1}$

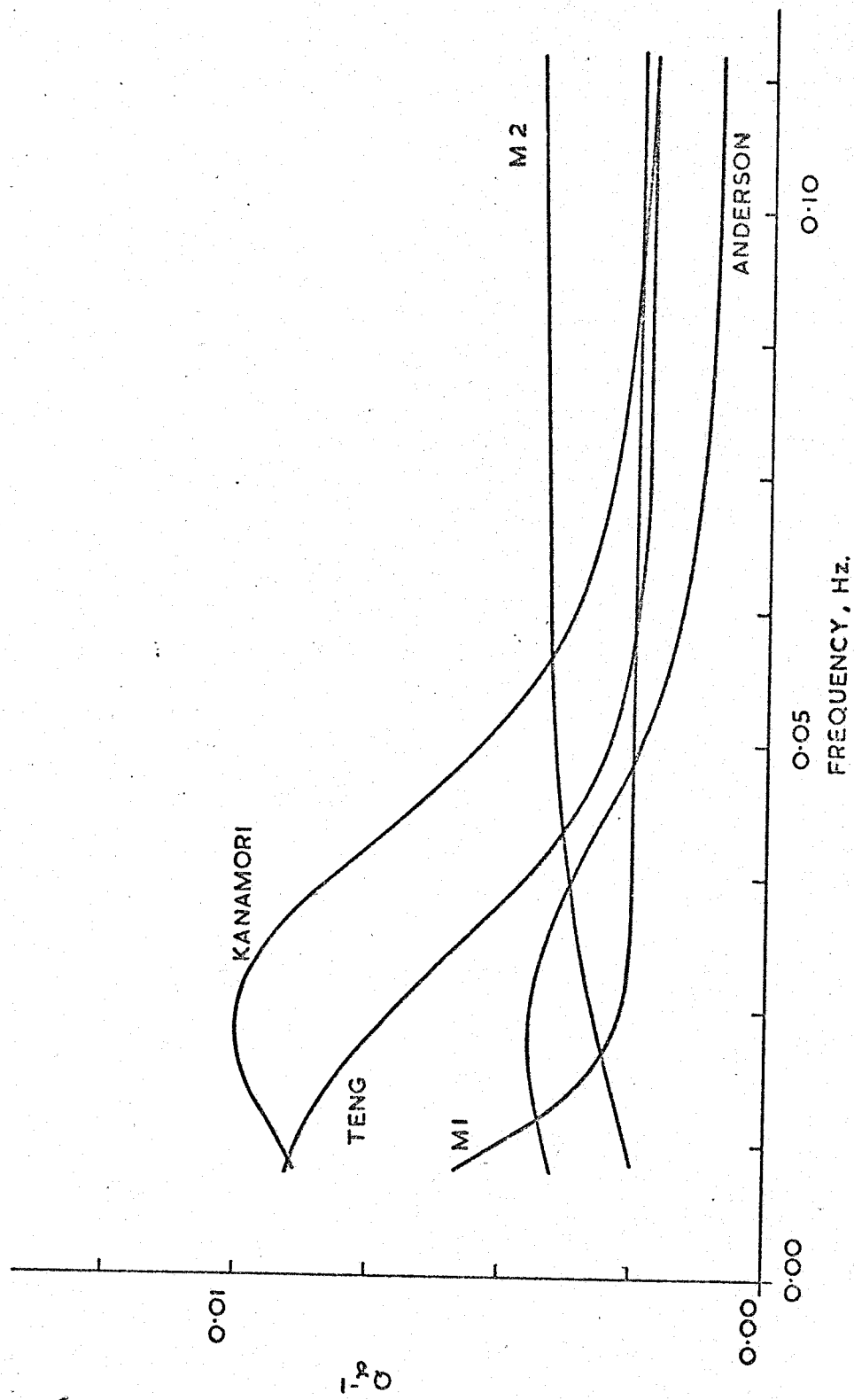


FIGURE 4.7 THEORETICAL RAYLEIGH WAVE  $Q_y^{-1}$  FOR MODELS USING  $Q_\beta^{-1} = Q_\alpha^{-1}$



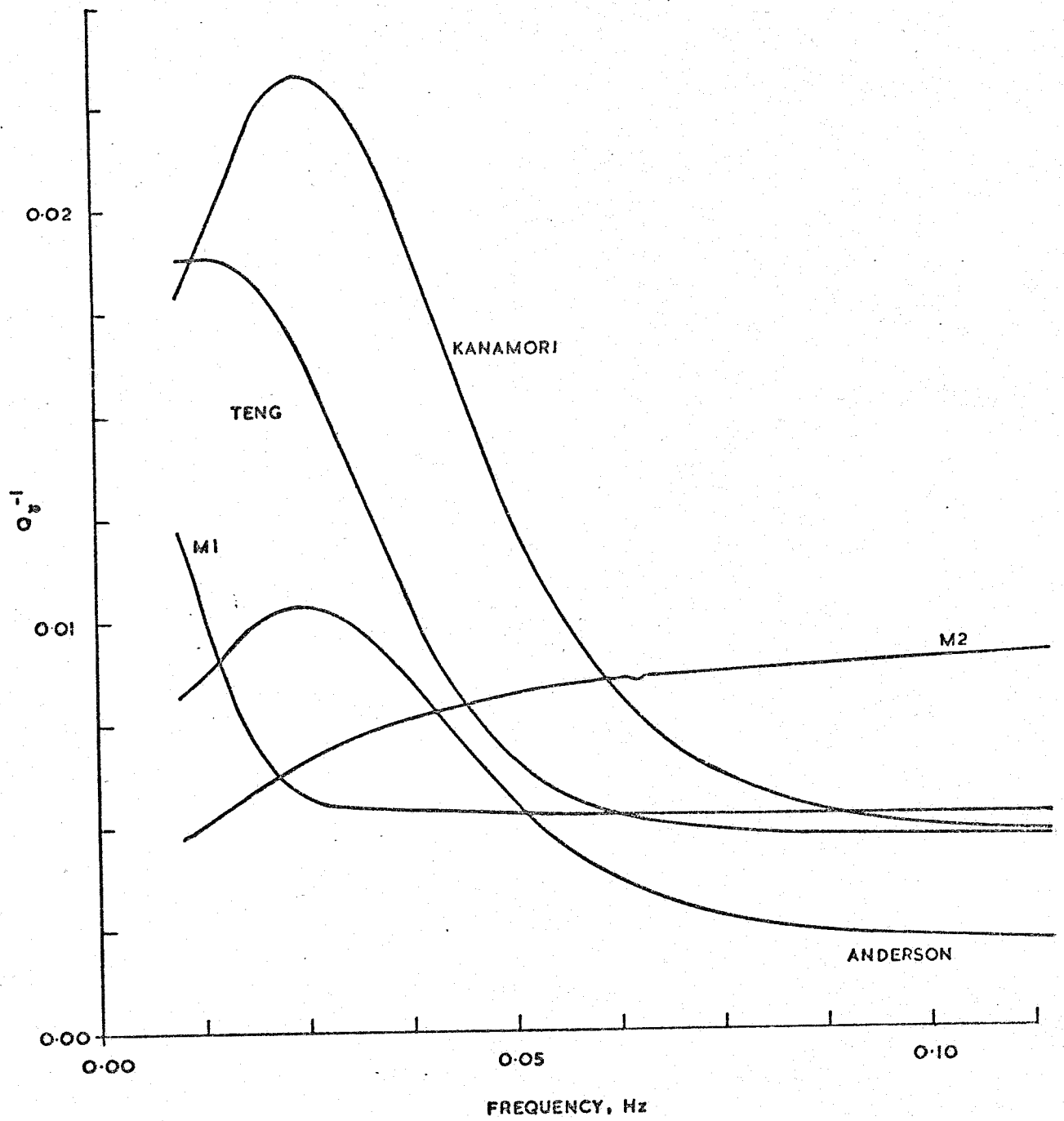


FIGURE 4.8 THEORETICAL RAYLEIGH WAVE  $Q_{\beta}^{-1}$  FOR MODELS USING  $Q_{\beta}^{-1} = \frac{3}{4} \left( \frac{\alpha_1}{\beta} \right)^2 Q_{\alpha}^{-1}$

A model M1 was found which approximates to the observed data. This model was compared to four other models, all of which were found to possess very individual characteristics. The model M1 was the best match to the data and condition C3

$$Q_{\beta}^{-1} = \frac{1}{4} \left(\frac{\alpha}{\beta}\right)^2 Q_{\alpha}^{-1}$$

was retained because it has physical meaning.

However trial and error model fitting of this nature is very inadequate because it gives little idea about the model accuracy. It is not possible to say by how much an individual layer in the model may be perturbed before the resulting  $Q_{\gamma}^{-1}(f)$  is incompatible with that observed. Also the accuracy of the observed data, expressed by the 95% confidence limits of figures 3.20 to 3.22 has been entirely ignored. A direct method of inversion, using this additional information, is desirable.

## CHAPTER 5

### 5.1 'Hedgehog' - Direct Inversion

#### 5.1.1 Introduction

Many data inversions - the matching of a particular depth dependent model to observed data at the surface of the earth - produce simple line models. The inversion attempts to show a simple one-to-one correspondence between surface results and depth dependent variables. This would only be possible for the present data if the inherent variability in the  $Q_Y^{-1}$  data, expressed by the confidence limits, was neglected. Any inversion of  $Q_Y^{-1}$  must produce a plot of  $Q_a^{-1}$ , varying with depth, and with a range of  $Q_a^{-1}$  values for any depth. It is important to realise that errors alone need not explain a range of  $Q_a^{-1}$  at a particular depth; it is realistic to expect a laterally inhomogeneous earth. The narrow confidence limits obtained in Chapter 3 have geophysical meaning and do not just contain experimental errors.

To invert the  $Q_Y^{-1}$  surface wave data it is necessary to postulate models in some form of  $Q$  space. "The difference between  $Q=\infty$  and  $Q=1450$  is not significant at present, since one is in fact comparing reciprocals of these quantities." This was stated by Knopoff (1969) and succinctly explains why all models considered here are in inverse  $Q$  space.

#### 5.1.2 "Hedgehog"

Any depth model in  $Q^{-1}$  space may be used to postulate  $Q_Y^{-1}$  at the surface by using the equations in Chapter 4. Once the postulated values for the surface have been obtained then a comparison may be made with the surface observed data.

It is necessary to distinguish between experimentally observed data and theoretically calculated values. The symbols  $Q_{Y0}^{-1}$  and  $Q_Y^{-1}$ , for observed and theoretical values respectively, make this distinction, and as a function of frequency  $Q_{Y0}^{-1}(f_i)$  will become  $Q_{Yoi}^{-1}$ . ( $i=1 \dots NFA$ ).

The goodness of fit for a particular model, compared to the observed data, may be quantitatively defined using the equations

$$\left| \frac{Q_{\gamma i}^{-1} - Q_{\gamma oi}^{-1}}{\Delta Q_{\gamma oi}^{-1}} \right| = a' \quad i=1 \quad \text{NFA} \quad 5.1$$

$$\left[ \frac{1}{\text{NFA}} \sum_{i=1}^{\text{NFA}} \left( \frac{Q_{\gamma i}^{-1} - Q_{\gamma oi}^{-1}}{\Delta Q_{\gamma oi}^{-1}} \right)^2 \right]^{\frac{1}{2}} = \sigma' \quad 5.2$$

The quantity  $\Delta Q_{\gamma oi}^{-1}$  relates to the confidence limits determined for each value of the observable  $Q_{\gamma oi}^{-1}$ . If  $a'$  and  $\sigma'$  are arbitrarily set to values  $a$  and  $\sigma$  and an inequality imposed on equations 5.1 and 5.2, then these equations either accept or reject a particular model (Burton and Kennett 1972).

The Monte-Carlo technique may be used to generate random models and equations 5.1, 5.2 used to select the acceptable ones. However, this shows no unity in the inversion models. Nor does it indicate, except by the density of acceptable models in  $Q^{-1}$  - depth space, any breadth of fit for a particular depth.

The Hedgehog program, once a good model has been found by Monte-Carlo in continuous valued  $Q^{-1}$  space, then moves onto a mesh or network of discrete values in  $Q^{-1}$  space. If the knot it has moved to is acceptable then all adjacent knots are tested until a boundary between good and bad models is reached. In this way the program determines a region of connected inversion solutions to the observed data and creates an area of fit rather than individual points. After completing one region the program returns to the Monte-Carlo technique to look for further solutions and regions outside those already found, until the entire region of search has been exhausted or sufficient models tested. The region of search is chosen by imposing geophysically realistic values on the  $Q^{-1}$  space for each layer of the model.

The values of  $\Delta Q_{\gamma oi}^{-1}$  calculated in Chapter 3 are the 95% confidence limits on  $Q_{\gamma oi}^{-1}$ , and values were determined for 79 frequencies. Altering  $a$  and  $\sigma$  changes the precision to which a model must fit the

experimental data. If  $a=1.0$  then models must lie within the 95% confidence limits. For other confidence levels the value of  $a$  depends upon the degrees of freedom for that particular event.

A typical Hedgehog network N1 used in this work is shown in Table 5.1. The values of  $\delta Q^{-1}$  are used to increment from  $Q_{LOW}^{-1}$  to  $Q_{HIGH}^{-1}$ . In all cases  $Q_{LOW}^{-1}$  was chosen as zero. It is possible to improve resolution of the inversion model by choosing a fine net, this presents problems because a fine net implies many knots and therefore many models to be tested. Monte-Carlo type inversion is only possible because the computation time involved in calculating  $Q_{\gamma i}^{-1}$  and testing against  $Q_{\gamma o i}^{-1}$  is minimal, 1000 models can be tested in 4 seconds. On one occasion a quarter million models were tested by the program in 15 minutes, however this did not facilitate inversion, because it also rejected the quarter million models! The precision to which the models fit the data, and the fineness of the net creating the models must be compatible.

## 5.2 Inversion

### 5.2.1 The General Model

The six layered velocity-depth model and partial derivatives of Chapter 4 are used. The relation

$$Q_{\beta l}^{-1} = \frac{1}{4} \left( \frac{\alpha_l}{\beta_l} \right)^2 Q_{\alpha l}^{-1} \quad l=1 \dots 6 \quad 5.3$$

is used for the six layers to reduce the number of  $Q^{-1}$  variables to six.

Inversion was attempted for three sets of  $Q_{\gamma o i}^{-1}$  data:

- 1 3NZA The average formed from the three atmospheric explosions at Novaya Zemlya (Figure 3.18).
- 2 2CA The average from the two atmospheric explosions at S Sinkiang Prov. China (Figure 3.18).
- 3 5A The average of all five atmospheric explosions (Figure 3.19)

The underground explosion was not included in 3NZA because it has been shown to be a different statistical population (Chapter 3). Table 3.1 shows

Table 5.1

## HEDGEHOG NETS

 $(Q_{\alpha}^{-1}$  Parameter Space)N1

Layer	$Q_{\alpha}^{-1}$ LOW	$Q_{\alpha}^{-1}$ HIGH	$\delta Q^{-1}$
1	0.0	0.01	.001
2	"	0.008	"
3	"	0.008	"
4	"	0.01	"
5	"	0.01	"
6	"	0.02	0.002

N2

Layer	$Q_{\alpha}^{-1}$ LOW	$Q_{\alpha}^{-1}$ HIGH	$\delta Q^{-1}$
1	0.0	.0105	.0015
2	"	.0075	"
3	"	"	"
4	"	.0105	"
5	"	.006	.001
6	"	.02	.002

N3

Layer	$Q_{\alpha}^{-1}$ LOW	$Q_{\alpha}^{-1}$ HIGH	$\delta Q^{-1}$
1	0.0	0.008	0.002
2	"	"	"
3	"	0.014	0.003
4	"	0.016	"
5	"	"	"
6	"	0.02	0.004

N4

Layer	$Q_{\alpha}^{-1}$ LOW	$Q_{\alpha}^{-1}$ HIGH	$\delta Q^{-1}$
1	0.0	.005	.002
2	"	"	"
3	"	.01	.003
4	"	"	"
5	"	.016	.004
6	"	.02	.005

N5

Layer	$Q_{\alpha}^{-1}$ LOW	$Q_{\alpha}^{-1}$ HIGH	$\delta Q^{-1}$
1	0.0	.008	.004
2	"	.008	.004
3	"	.012	.006
4	"	.012	.006
5	"	.005	.002
6	"	.020	.010

that these data sets only contain useful information up to a certain highest frequency. The frequency range used and therefore the number of  $Q_{\gamma oi}^{-1}$  values for each group is

$Q_{\gamma oi}^{-1}$ Data Set	Number of Stations	Frequency Range Hz	Number of $Q_{\gamma oi}^{-1}$ Values
3NZA	81	.0147-.0806	55
2CA	63	.0147-.0855	59
5A	144	.0147-.0830	57

For two reasons the removal of higher frequencies is beneficial for direct inversion. The depth of penetration for surface waves depends on wavelength. Therefore high frequencies will only contain information about the upper layers of the earth, whereas low frequencies contain information about both the upper layers and greater depths. Further, the shape of the weighting derivatives  $\frac{\partial k_o}{\partial \alpha_{01}}$ ,  $\frac{\partial k_o}{\partial \beta_{01}}$  (see Figures 4.3, 4.4) used to calculate theoretical  $Q_{\gamma i}^{-1}$  for the models, would heavily bias the resolution towards the upper layers, because of the large derivative values at high frequencies. Figure 5.1 for the major derivative  $\frac{\partial k_o}{\partial \beta_{01}}$  up to frequency .0623 Hz, shows more equal weighting for the various layers. To include high frequencies is to weight the inversion model towards the upper layers, at the expense of resolution at depth. A spread of energy throughout all layers is required for good inversion.

### 5.2.2 Inversion of 3NZA

The models were tested against the data for several levels of precision, also different nets were used to improve and confirm the results. The range of figures 5.2-5.5 show the inversion models, found using net N1, for different confidence levels on the observed data.

Figure 5.2 accepted models fitting within 90% confidence limits, a narrow band of fit, using  $a = 0.833$ . Only two Monte-Carlo models, and no Hedgehog connected region, are obtained out of the 80,000 random models

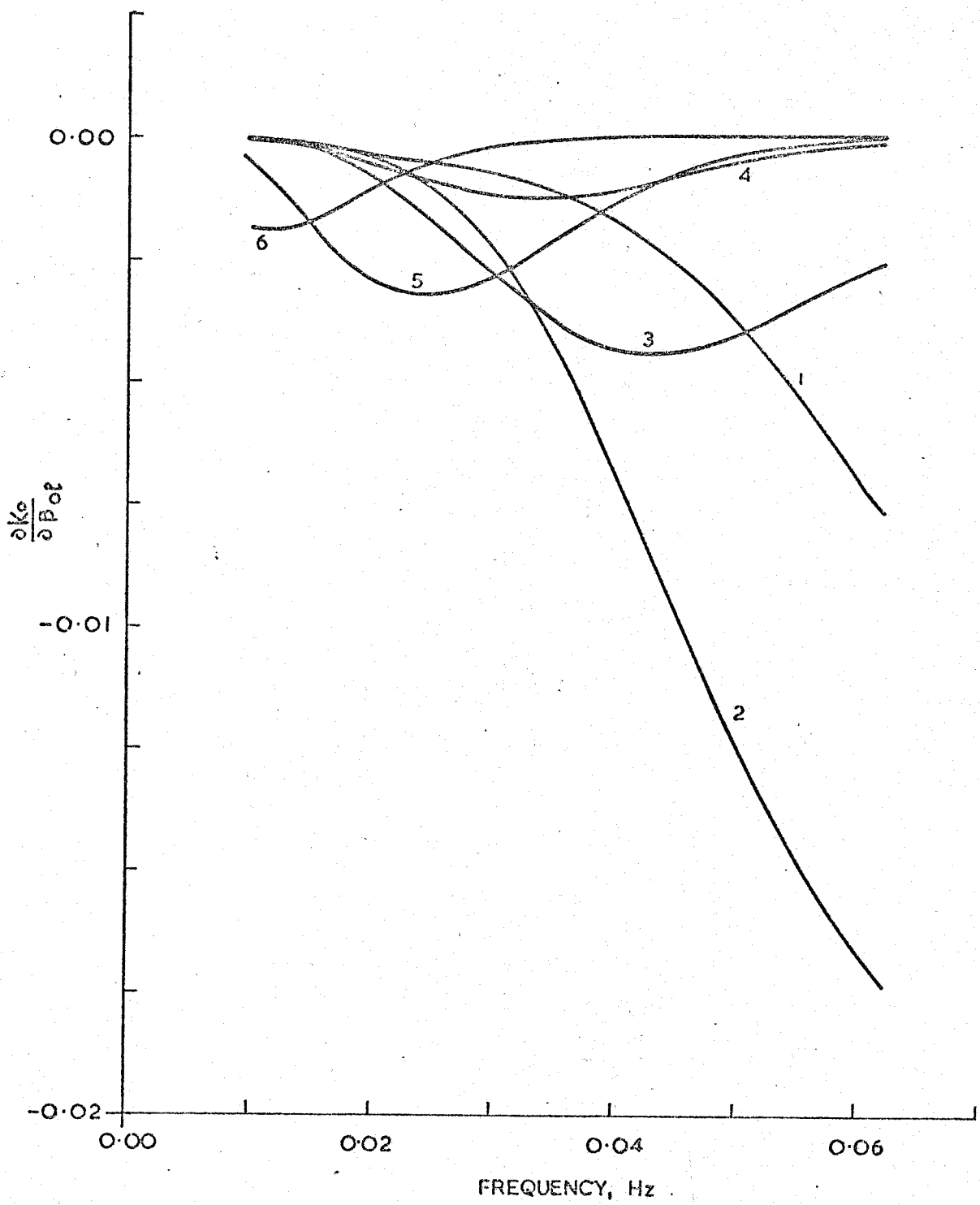


FIGURE 5.1 DERIVATIVES  $\frac{\partial k_o}{\partial \beta_{ol}}$  FOR 'HEDGEHOG' INVERSION



tested.

Two independent regions of fit are found using N1 and 95% confidence limits, these are shown in Figures 5.3 and 5.4. A fit to very broad confidence limits, 99%, was tried using nets N1 and N2. This produces Figures 5.5 and 5.6; execution of the program was finished in each case before the entire region had been delineated because far too many solution knots were being found to be of any use. The Hedgehog regions of Figures 5.3 and 5.4 represent the best inversion of the data from the Novaya Zemlya atmospheric explosions.

Three solutions, chosen as typical examples from the two Hedgehog regions, are shown in Figure 5.7. Table 5.2 lists the three models. All these models show a layer of high attenuation in the upper mantle, as did Burton and Kennett using one event. This again supports the theory of a highly attenuating zone corresponding to the Gutenberg low velocity zone, without assuming any such low velocity during model fitting.

Table 5.2 Three Typical Solutions for 3NZA

Layer	Model A		Model B		Model C		Depth to Layer Base km
	$Q_a^{-1}$	$Q_\beta^{-1}$	$Q_a^{-1}$	$Q_\beta^{-1}$	$Q_a^{-1}$	$Q_\beta^{-1}$	
1	.002	.00456	.001	.00228	.002	.00456	14
2	.002	.00458	.003	.00687	.002	.00458	36
3	.002	.00503	.001	.00252	.002	.00503	58
4	.002	.00501	.001	.00251	.006	.01504	68
5	.002	.00500	.003	.00749	.001	.0025	123
6	.008	.01762	.006	.01322	.008	.01762	$\infty$

Model A shows the upper 120 km to be of uniform low attenuation material, overlying the zone of high absorption. Model C shows a similar distribution but with a strongly attenuating perturbation around 70 km. This type of model was generally characteristic of the second Hedgehog region shown in Figure 5.4.

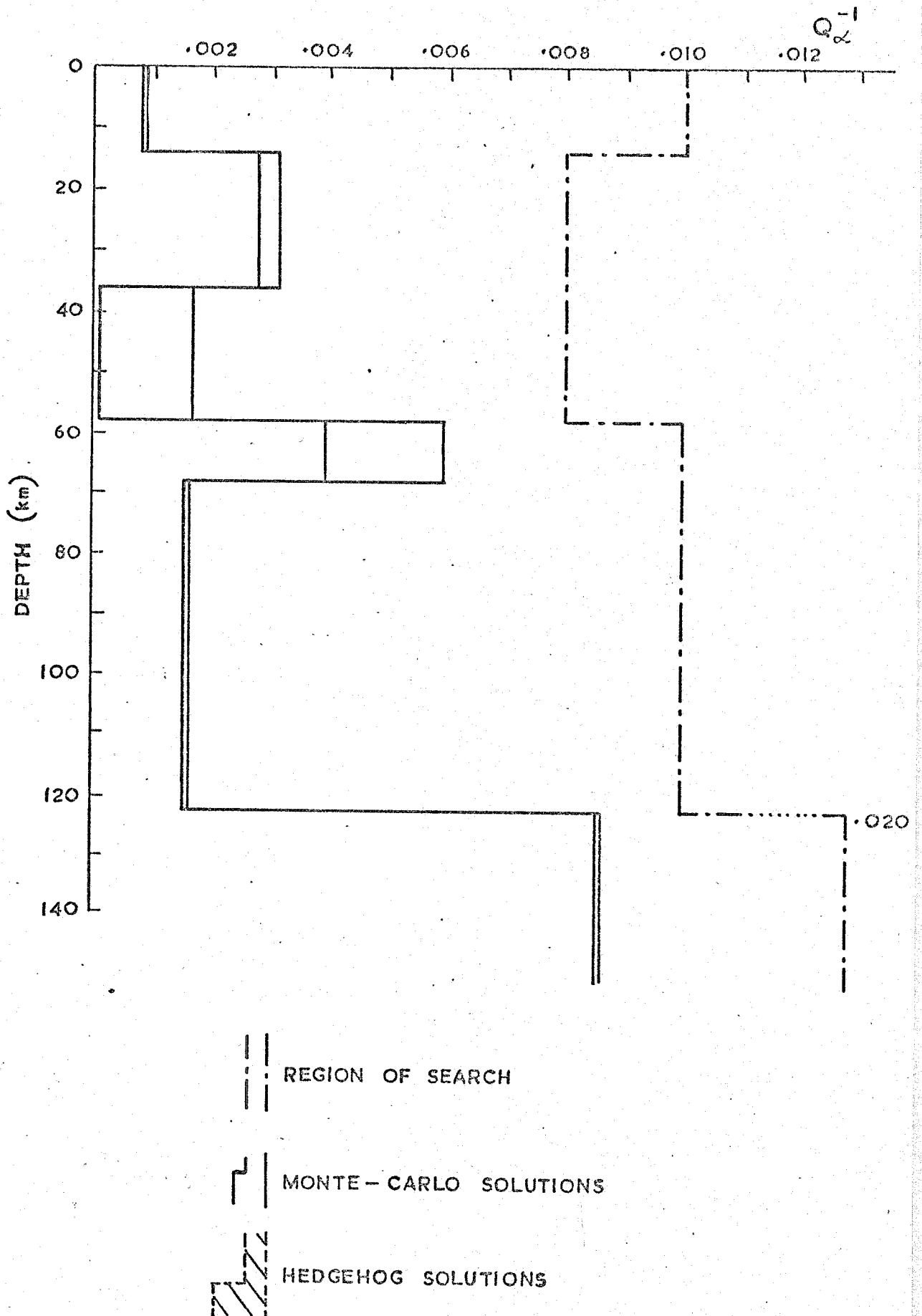


FIGURE 5.2 INVERSION OF THE AVERAGED NOVAYA ZEMLYA DATA (3NZA)  
 (90% CONFIDENCE LIMITS AND NET NI)

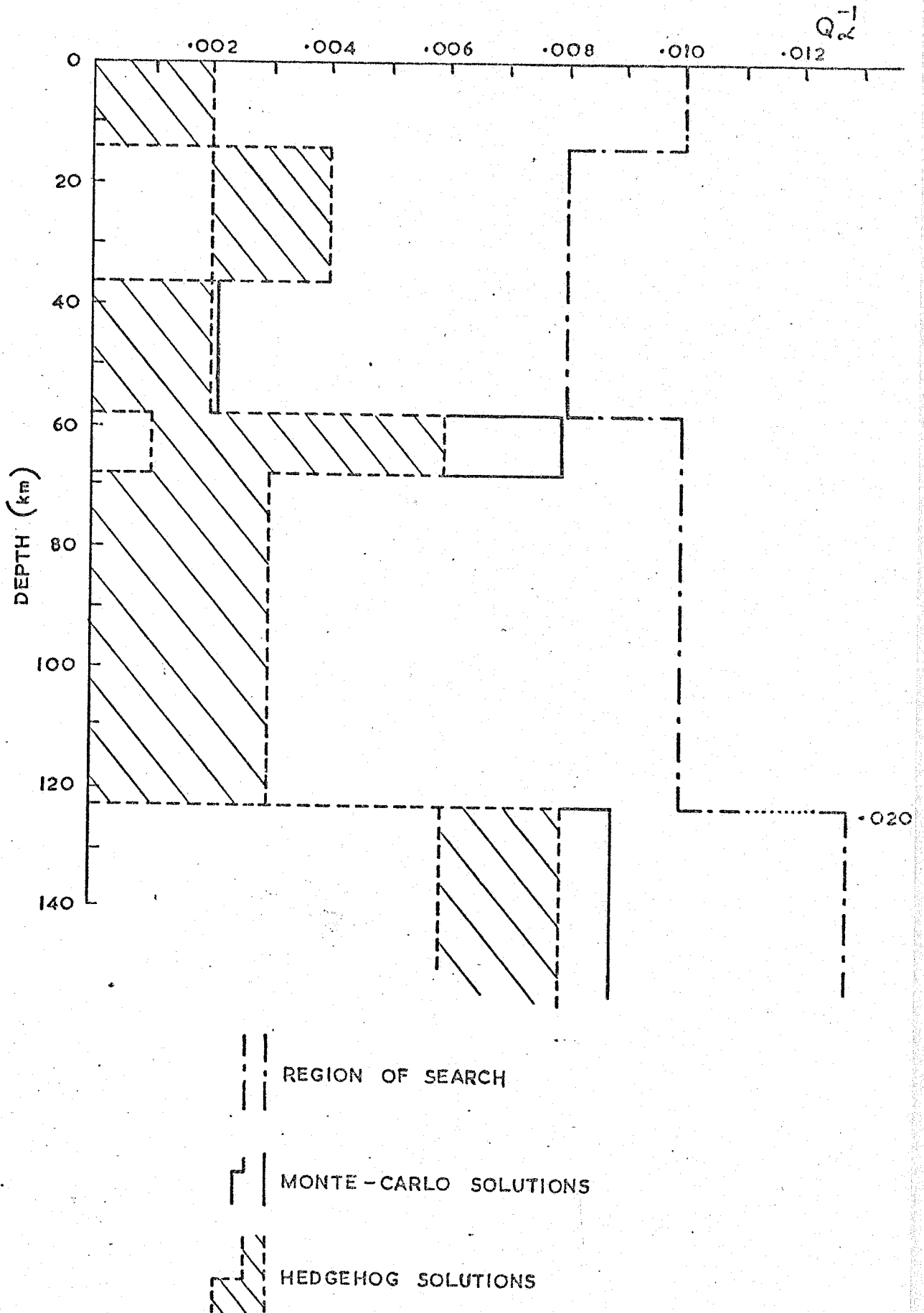


FIGURE 5.3 THE FIRST HEDGEHOG SOLUTION FOR 3NZA  
(95% CONFIDENCE LIMITS AND NET NI)

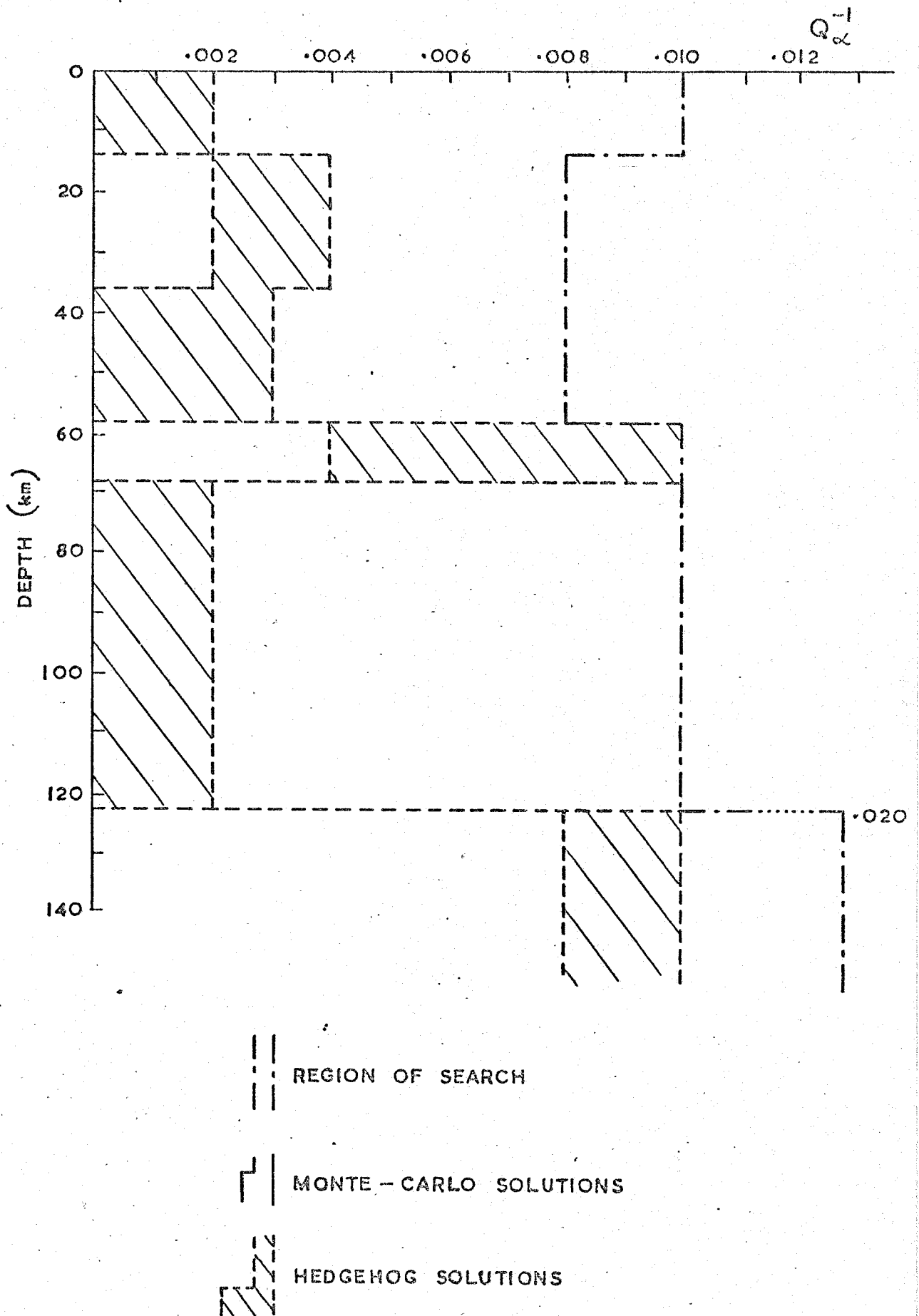
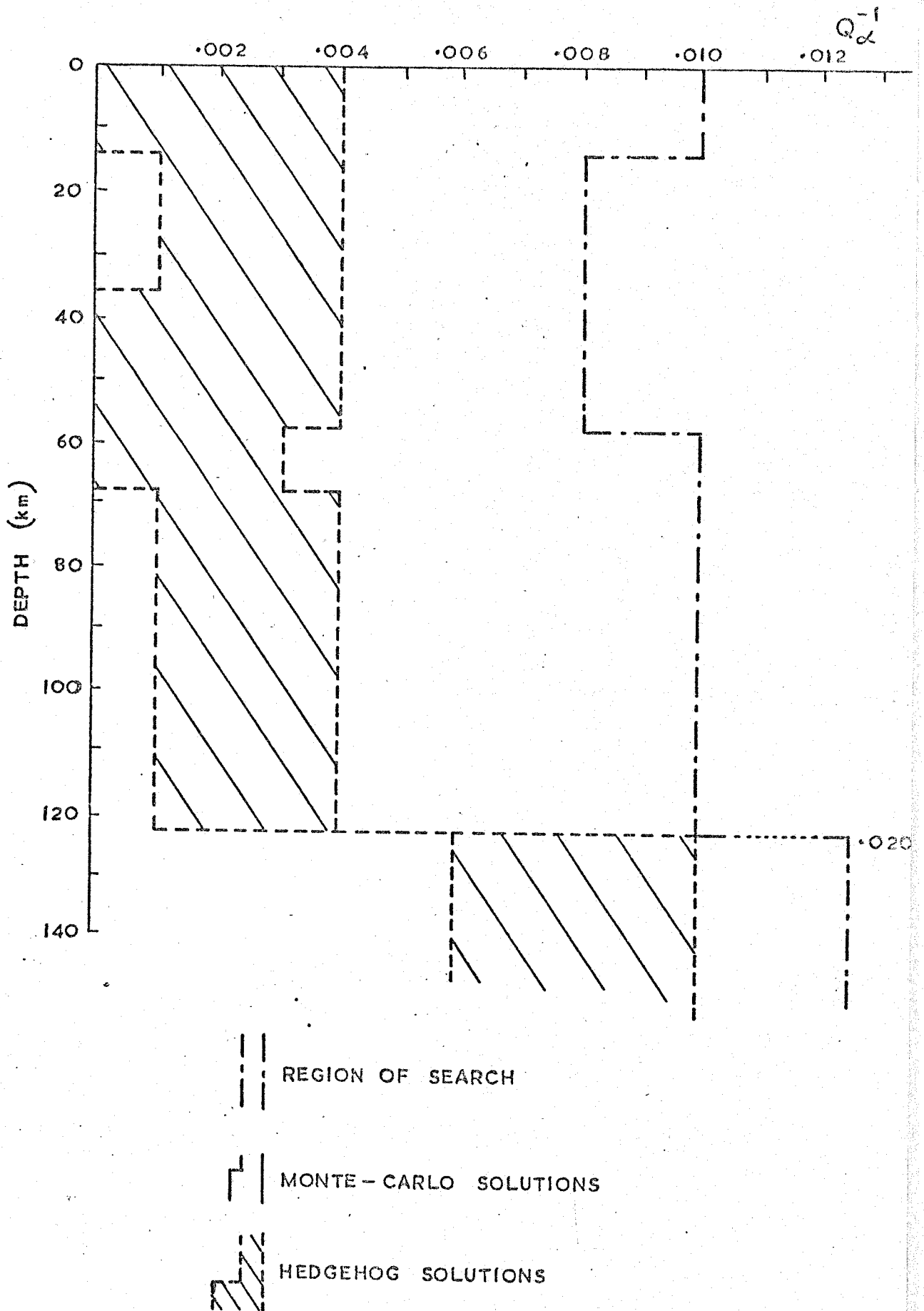
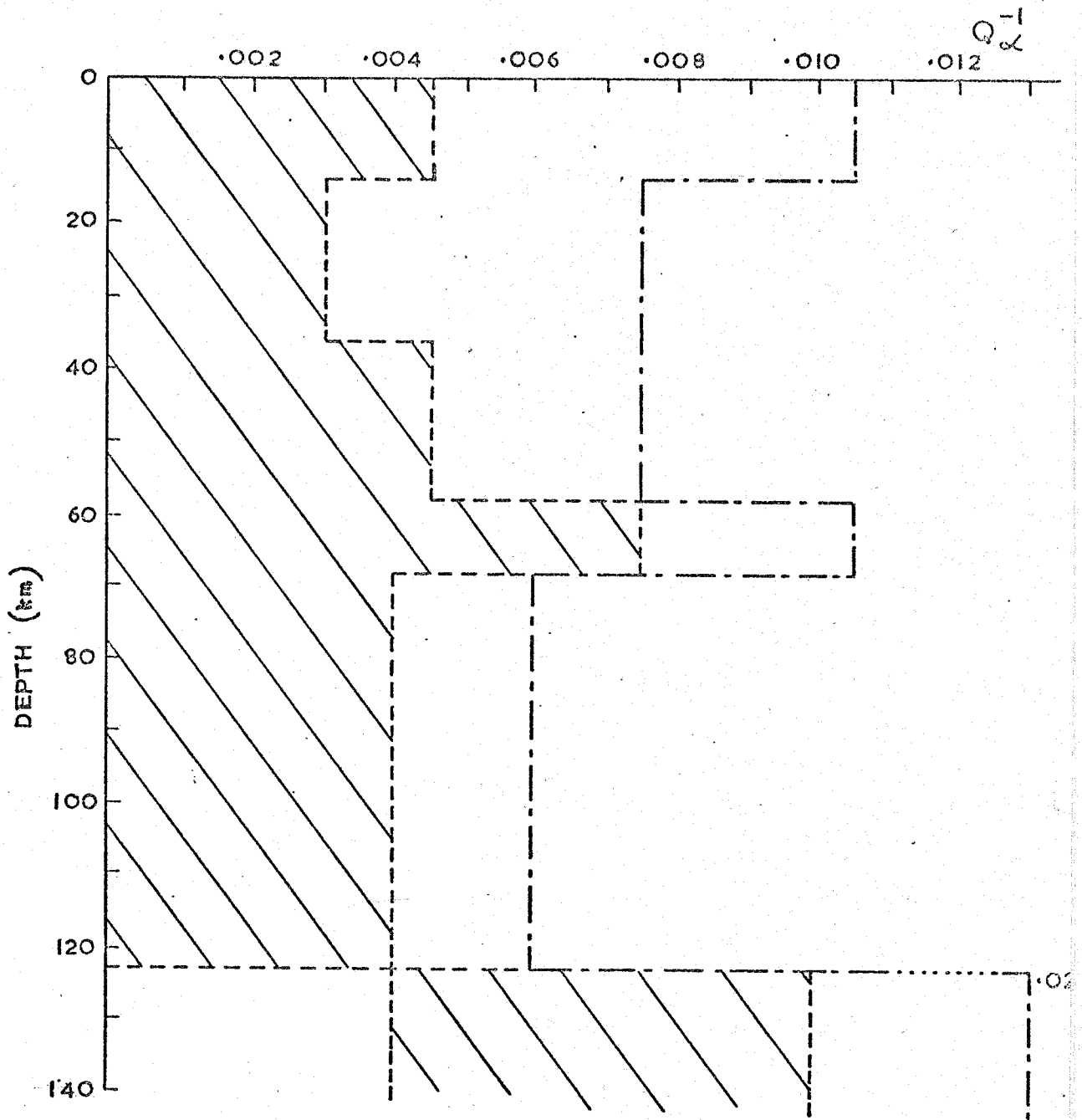
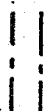




FIGURE 5.4 THE SECOND HEDGEHOG SOLUTION FOR 3 NZA  
 (95% CONFIDENCE LIMITS AND NET NI)



**FIGURE 5.5. ATTEMPTED INVERSION OF 3NZA**  
**(99% CONFIDENCE LIMITS AND NET MI)**



-  REGION OF SEARCH
-  MONTE-CARLO SOLUTIONS
-  HEDGEHOG SOLUTIONS

**FIGURE 5.6 ATTEMPTED INVERSION OF 3NZA**  
**(99% CONFIDENCE LIMITS AND NET H2)**

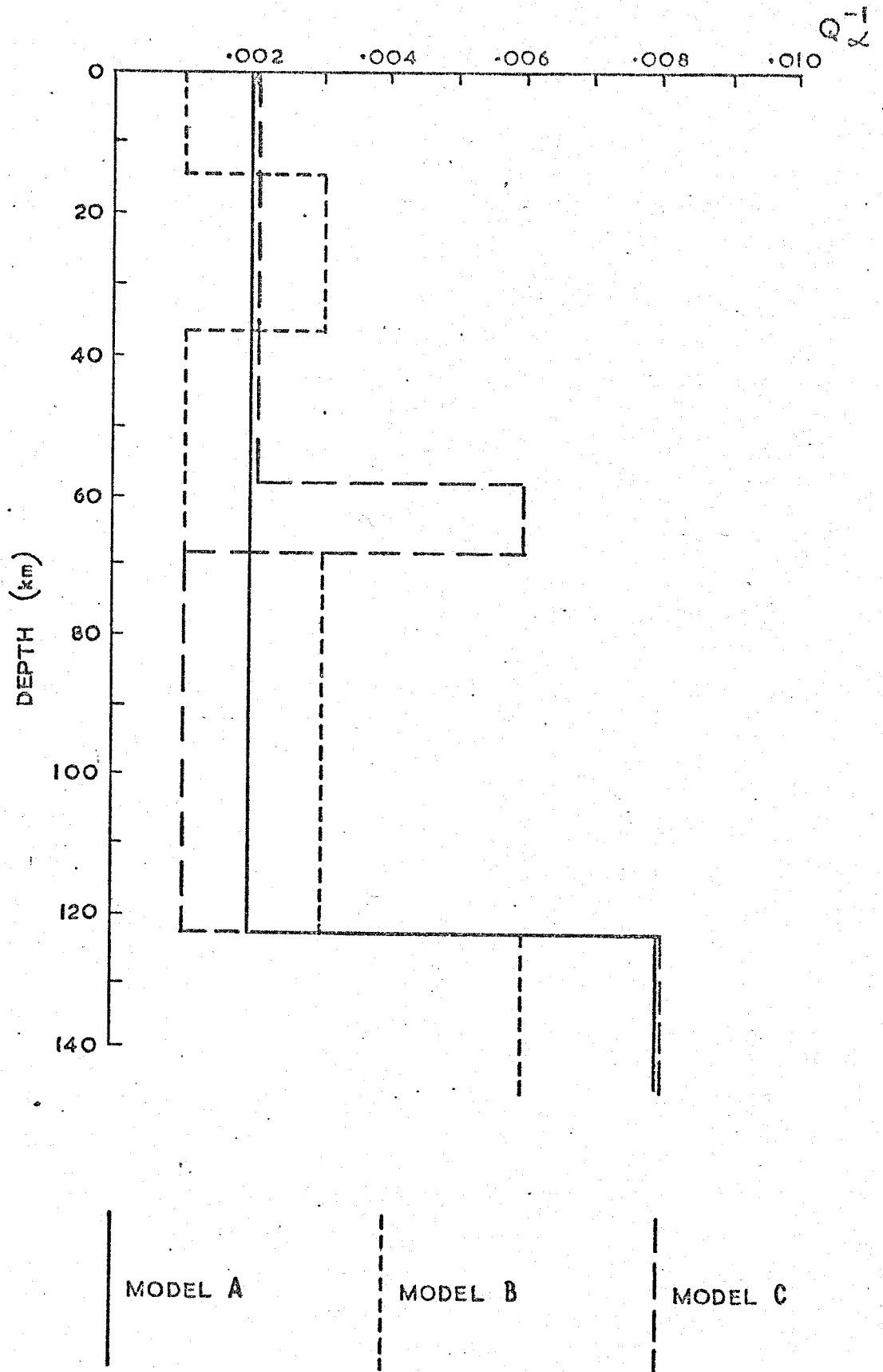


FIGURE 5.7 THREE TYPICAL INVERSION SOLUTIONS FOR 3MZA

The other model, B, shows a more gradual onset of the absorption zone below 70 km. Also, Model B shows a region of slight absorption around 30 km depth. This region is influenced by the combined effects of the Conrad and Mohorovicic discontinuities. Apart from any real changes of  $Q^{-1}$  in these regions a discontinuity will tend to increase the value of observed  $Q^{-1}$ . Any discontinuity will scatter and diffract energy, increasing the path length, and therefore magnifying the effectiveness of any spatial  $Q^{-1}$ . Such effects cannot be separated from the truly dissipative characteristic of the materials and must be included in these estimates. Model B shows a crust and uppermost mantle well suited to the propagation of seismic energy, overlying a region below 70 km of increasing dissipation until a "zone of low Q" is reached.

Burton and Kennett resolved a separate Hedgehog region which showed a zone of very high Q between 15 and 70 kms depth, this is because the region of search was described in Q rather than  $Q^{-1}$  space. Comparing the following sequencies of values explains this.

Q space	Q	100	300	500	700	900	1100
$Q^{-1}$ space	$Q^{-1}$	.01	.008	.006	.004	.002	0
Equivalent Q	Q	100	125	167	250	500	$\infty$

Models in Q space give better resolution at the high Q end of the range; however the step from Q=100 to Q=500 is far more significant than from 500 to 1100 and is not sufficiently well resolved. Because the attenuation factor per wavelength is  $\pi Q^{-1}$  models should preferably be in  $Q^{-1}$  space. This procedure more accurately describes the physical phenomenon of dissipation.

### 5.2.3 Inversion of 2CA and 5A

The inversion of these two data sets produced much poorer results than for 3NZA. Using the net N3 and 50% confidence limits for 2CA produced Figure 5.8, N4 and 40% confidence limits for 5A produced Figure 5.9. In



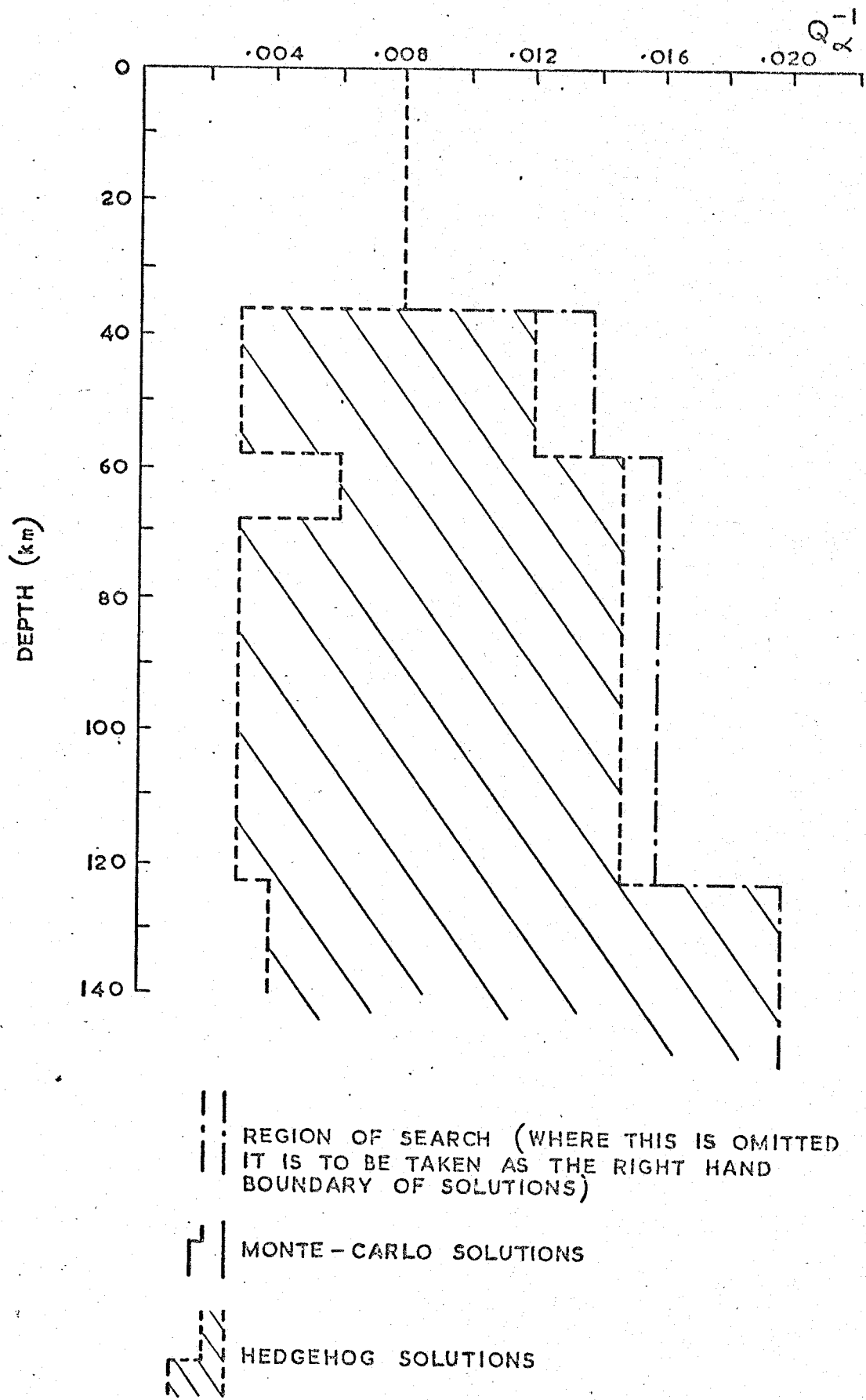


FIGURE 5.8 ATTEMPTED INVERSION OF THE AVERAGED SOUTHERN SINKIANG DATA (2CA) (50% CONFIDENCE LIMITS AND NET N3)

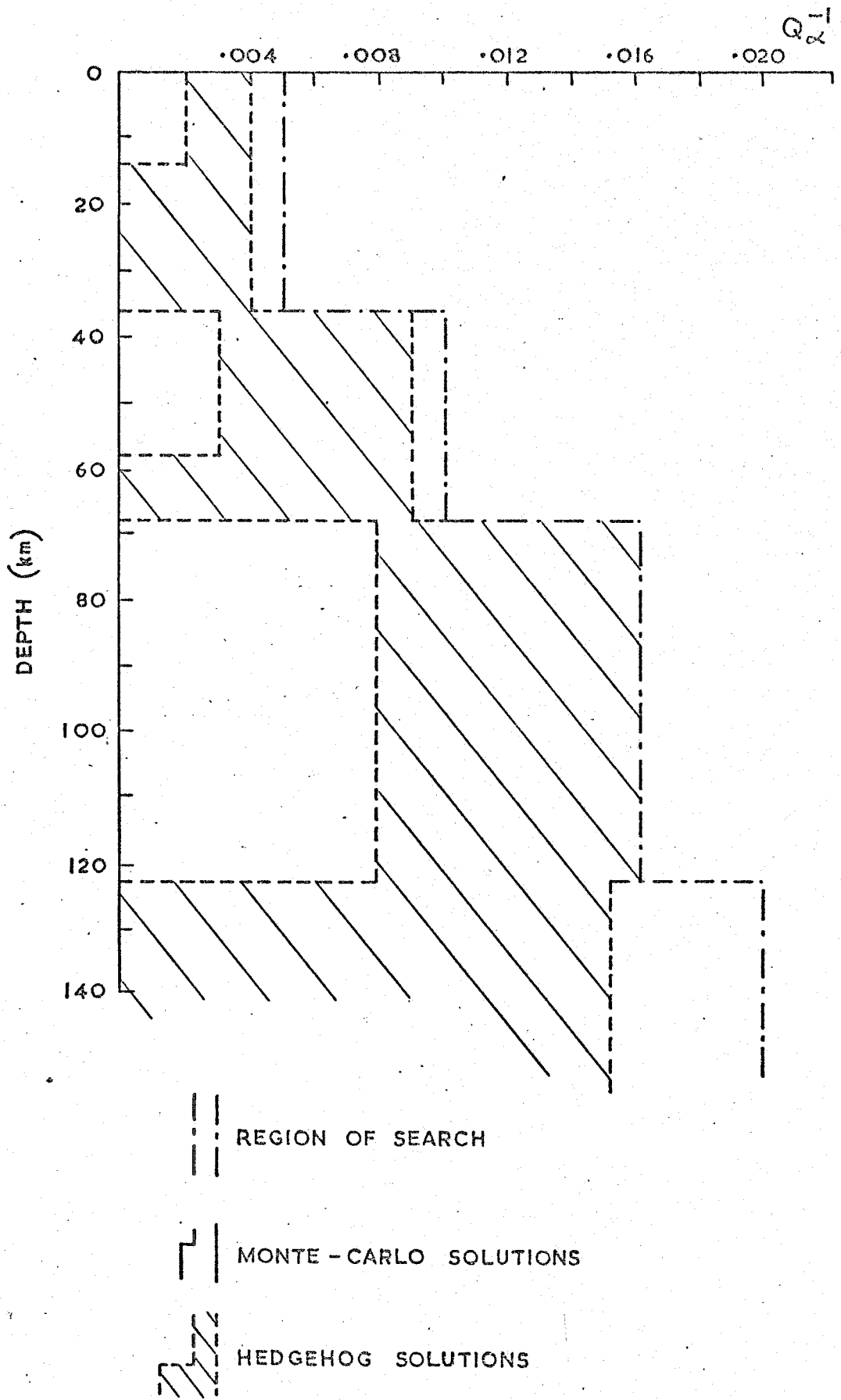


FIGURE 5.9 ATTEMPTED INVERSION OF THE AVERAGED ATMOSPHERIC EXPLOSION DATA (5A) (40% CONFIDENCE LIMITS AND NET N4)

both cases the entire region was not obtained because too many adequate knots were discovered before completion of the region. However, using 42.5% and 30% confidence limits for 2CA and 5A respectively, produced no solutions.

The conclusion is that the region of search and the nets used are inadequate to perform suitable inversion. Examination of Figure 3.18 for average  $Q_{\gamma_0}^{-1}$  from the two explosions in China provides an explanation. There is a minimum point around .038 Hz implying a region of very little dissipation. The minimum covers the frequency range .03-.05 Hz, outside this range normal values of  $Q_{\gamma_0}^{-1}$  are obtained. The rule has already been stated that the depth of penetration at a frequency corresponds to a wavelength, because the wave amplitude has fallen to 20% its surface value. This gives a range of depth penetration of about 80-130 kms. Frequencies higher than .05 Hz only penetrate to 80 km, and return normal values of  $Q_{\gamma_0}^{-1}$ . The lower frequencies which sample all zones of the earth above 130 km, return anomalously low values of  $Q_{\gamma_0}^{-1}$ . Obviously layer 5 of the inversion model (68-123 km) must consist of very low  $Q^{-1}$ . The nets N3 and N4 have not placed a sufficient constraint on the Hedgehog search in layer 5, and have allowed unrealistically large values of  $Q^{-1}$  for these depths to dominate the inversion. Further the lower frequencies, less than .03 Hz, which sample all depths of the model must be sampling very high  $Q^{-1}$  below 130 km to produce the  $Q_{\gamma_0}^{-1}$  values of Figure 3.18.

A further inversion was attempted using the net N5. This net restricts the  $Q^{-1}$  of layer 5 to a maximum value 0.005, also this net is coarser than those previously used. Inversion of 2C using 49.8% confidence limits produced Figure 5.10, and 33.2% confidence limits on 5A produced Figure 5.11. Some improvements are obtained but the picture is still unsatisfactory and the Hedgehog region ill defined. When the data from Southern Sinkiang is introduced we are led to the conclusion that the general model of section 5.2.1 must be questioned.

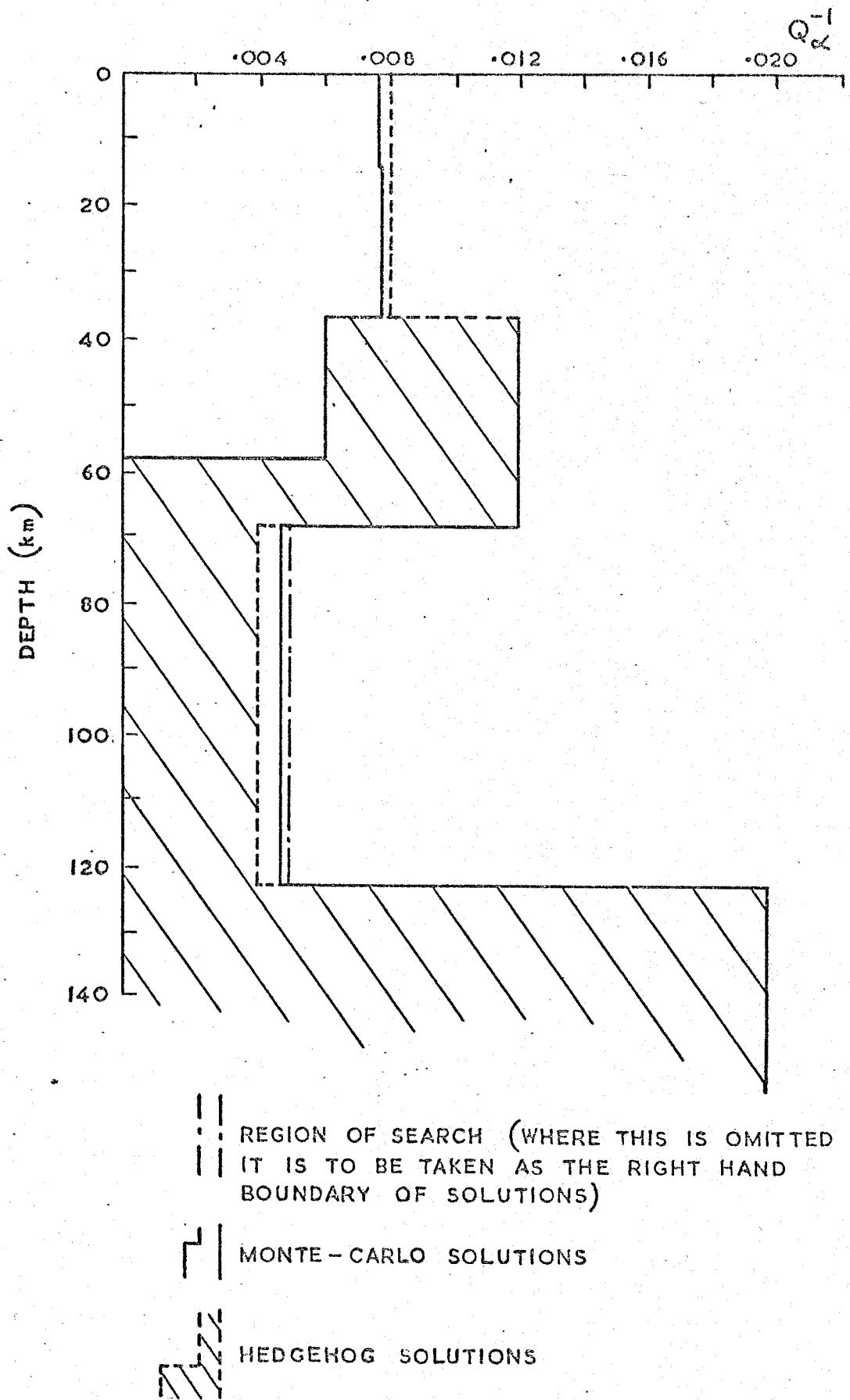


FIGURE 5.10 THE HEDGEHOG SOLUTION FOR 2 CA  
(49.0% CONFIDENCE LIMITS AND NET N5)

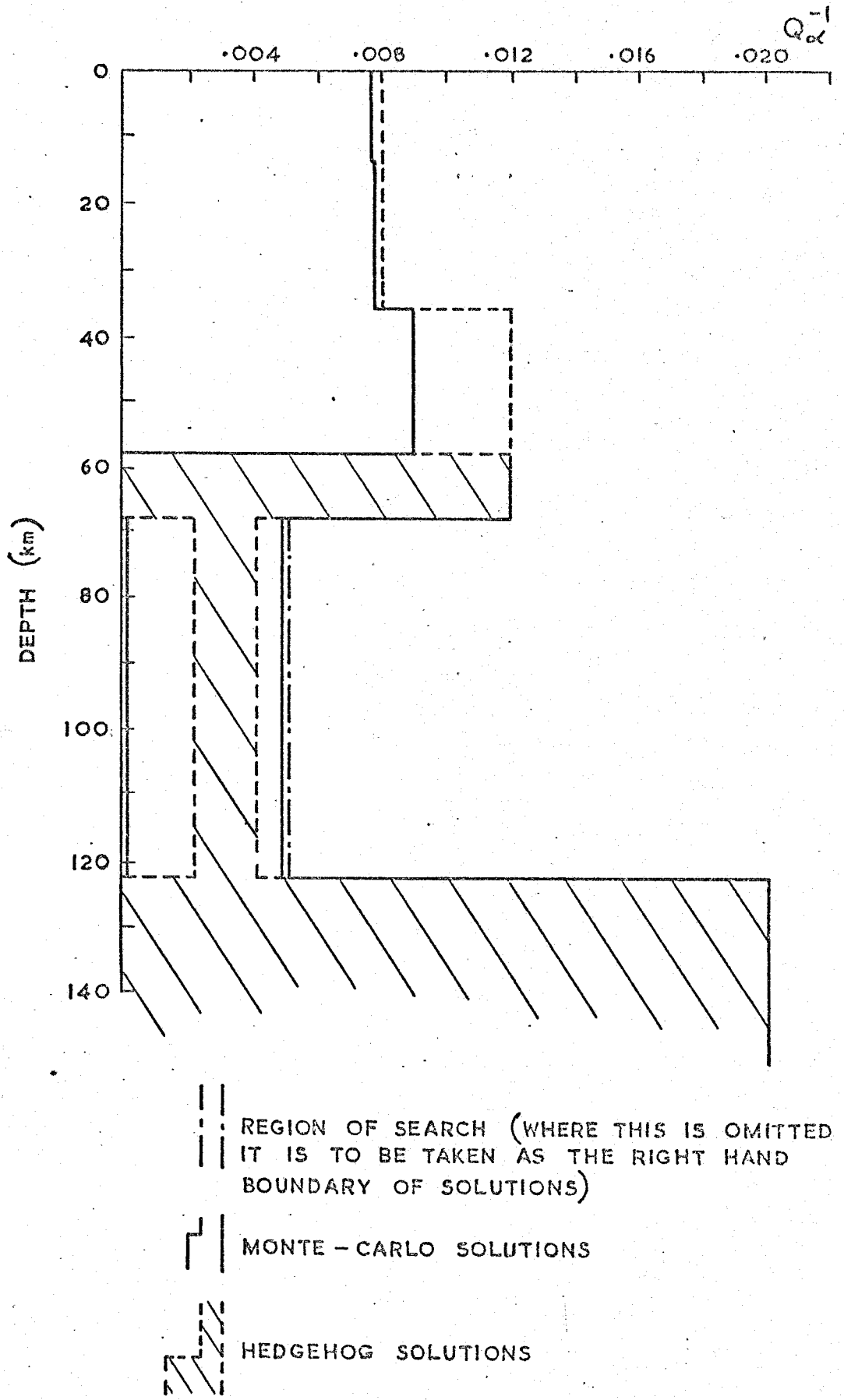


FIGURE 5.11 THE HEDGEHOG SOLUTION FOR 5A  
(33.2% CONFIDENCE LIMITS AND NET N5)

Local variations of the crustal thickness and lateral heterogeneity introduced by the Himalayas will influence the inversion. The paths from Southern Sinkiang to CHG, SNG, JER and IST have already been omitted due to particularly anomalous behaviour. So it is possible that the velocity-depth model (Figure 4.1) is inappropriate for the general region of the propagation paths around Southern Sinkiang. Also the assumed relation of  $Q_{\alpha}^{-1}$  to  $Q_{\beta}^{-1}$  (equation 5.3) is another limitation on the general inversion technique which may be inadequate for this region.

A future inversion which varies the parameters which are here fixed may well provide the solution.

### 5.3 Interpretation

Backus and Gilbert (1968) point out that the resolving power of any gross earth data is limited. The uncertainty of an earth parameter for a layered model will increase if an attempt is made to increase the depth resolution by using thinner layers. The delta-type resolution functions of Backus and Gilbert were calculated by Der et al. (1970) for the determination of shear velocity in the crust and upper mantle from surface wave observations. Der et al. concluded that a five layered model for the upper 130 km of the earth gave acceptable resolution and eliminated instability due to an excessive number of layers - the inversion model used here also has five layers and data obtained from the fundamental Rayleigh wave mode. Inclusion of a thin fourth layer (10 km) in the present inversion illustrates certain aspects of this resolution problem. The Hedgehog solutions of figures 5.3 and 5.4 show that the  $Q_{\alpha}^{-1}$  values in the fourth layer are the most uncertain, whereas  $Q_{\alpha}^{-1}$  is comparatively well resolved in the remaining thicker layers. With this resolution in mind it is possible to consider the implications of the  $Q^{-1}$  values in the various layers.

The major features of the three typical solutions for 3NZA (Figure 5.7) have already been described, but certain details of these models may not be adequately resolved. High  $Q^{-1}$  around 60 km in model C is uncertain,

as is the distinction between models A and B. All of the models show clearly resolved high values for  $Q^{-1}$  at depth, and model A may be regarded as the general continental  $Q^{-1}$  model which excludes any excessive detail. The inversion has provided substantial evidence for a zone of dissipation below about 120 km. If the usually accepted low velocity zone (Press 1970a) had been included the resolution of the discontinuity in  $Q^{-1}$  would have been further enhanced.

Press (1970b) failed to find low density associated with low shear velocity in the earth, and concluded that high density (3.5 gm/cc) was the rule over substantial intervals between depths of 70 km and 370 km. Both incipient melting of the rocks and interstitial water content may provide an explanation for a zone of low  $Q$  and low velocity associated with high density. The results of Born, illustrated in the introduction, show that a very small percentage of interstitial water occurring as a free phase in the rock causes a significant increase in the decrement (decrement is proportional to  $Q^{-1}$ ). Incipient melting will have a similar effect. Spetzler and Anderson (1968) examined the NaCl-H<sub>2</sub>O binary system and found that  $\alpha$ ,  $\beta$ ,  $Q_{\alpha}$  and  $Q_{\beta}$  vary slowly as the eutectic temperature is approached from below, and then suddenly drop at the eutectic by 9.5%, 13.5%, 48% and 37% respectively (1% NaCl). The shape of the liquid inclusions determines the amount of melt necessary to obtain the required velocities, 0.1% melt maybe sufficient and this would have a negligible effect on density.

If the oceanic geotherm is assumed, melting is not possible above 90 km (Anderson and Sammis 1970) unless water is present to reduce the solidus melting temperature. The continental geotherm gives much smaller temperatures at corresponding depths (approximately 250°C less) and therefore implies the solidus temperature is only reached at a greater depth. Lambert and Wyllie (1970a, b) have investigated a peridotite mantle model with 0.1% by weight of water and came to the conclusion that the "beginning of melting should occur at about 60 km for normal oceanic geothermal gradients,

and at about 110 km for normal shield geotherms".

Mineralogical variations may cause a low velocity zone but incipient melting is Green and Ringwood's (1970) preferred explanation. The region of anomalously high dissipation which is here found to start at the expected lithosphere-asthenosphere junction, combined with a low velocity zone, makes it difficult to conceive of an alternative explanation to incipient melting and interstitial water content. This lends support to Ringwood's (1969) concepts of the composition of the crust and upper mantle.

Ringwood's pyrolite model for the upper mantle in continental regions proposes a zone of dunite-peridotite over pyrolite, the transition occurring around 100-200 km. Partial melting causes the lower melting-point components to segregate upwards, and this is obviously influenced by variations of temperature with depth. Variations in seismic velocity may occur because of these chemical and physical zoning effects. However, these effects are not sufficient to explain the large shear wave velocity variations, and negative velocity gradients, which occur for the low velocity zone.

Incipient melting would cause a low velocity zone. However at depths of 100 km the pressure causes the degree of pyrolite melt to be very sensitive to temperature, and therefore unstable magmas might result. Water may stabilise this mechanism. A small quantity of water (0.1%) will lower the melting point and make it diffuse. A mechanism with a diffuse melting point is stable because a large temperature variation will only cause a small change in the degree of partial melt. Such a zone of incipient melting explains the anomalous dissipation found by the inversion for depths around 120 km, and why it may occur in conjunction with a low velocity zone.



## CHAPTER 6

### Concluding Comments

The inverse problem of seismology has been described by many people (Keilis-Borok and Yanovskaja 1967) but it is still very topical. Some measure of motion at the surface of the earth is obtained, the motion presumably caused by a particular source, and the problem is to obtain the variation within the earth of the elastic parameters  $k$  and  $\mu$  (bulk modulus and rigidity), the density  $\rho$  and the dissipation constant  $Q$ . These are the four fundamental quantities of seismology. From these the velocities of bodily waves (P and S) may be determined and related to travel times on the seismogram. An understanding of the often ignored second axis of the seismogram, amplitudes, requires knowledge of the attenuation constant  $Q$  and the generating source. However, velocities and density are often known to a few per cent whereas  $Q$  is rarely known so well - but it is still an equally fundamental and intrinsic property of rocks which influences the propagation of seismic waves as characterised by the seismogram. For example dynamic damping ( $Q$ ) allows us to calculate amplitude variation with distance from the source as a function of frequency. On the other hand static properties of rocks exemplified by creep also relate to the internal friction  $Q$  (Lomnitz 1957), and creep is very important on the geophysical time scale in regions of large tectonic stress - plate subduction zones are an obvious example. Further, a quantitative knowledge of the  $Q$  causing amplitude-distance variation by damping would help us to estimate source functions of various events and perhaps thereby elucidate the source mechanism. Source elucidation is important to seismology because such knowledge is necessary for earthquake prediction and control, and it is directly relevant to the earthquake-explosion discrimination problem.

Heterogeneity of the earth is also of great importance and this has appeared in several ways in this work. The average values of  $Q_{\gamma}^{-1}$  for the atmospheric explosions in Novaya Zemlya and China both show larger

values of  $Q_{\gamma}^{-1}$  at the lower frequencies, implying vertical heterogeneity in the form of a strongly dissipative layer at depth. Such a zone of "low Q" may be caused by incipient melting stabilised by the presence of small quantities of water, this is congruous with Ringwood's (1969) ideas concerning the low velocity zone of continental regions at the corresponding depth. Also the attenuation of Rayleigh waves for those propagation paths radiating from Novaya Zemlya is greater for all frequencies than for the paths investigated for the explosions in Southern Sinkiang Province, an example of lateral variation. Further, the attenuation-depth models attributable to several authors appear to be very dependent on the data source or region used.

The existence of a widespread low Q zone has wider implications in general geophysics. If plate theory is to be accepted then a discontinuity between the mobile lithosphere and the asthenosphere is a necessary prerequisite. A discontinuity caused by incipient melting, which implies low shear stress, would facilitate sliding motion. This discontinuity would be expected at different depths for oceanic and shield environments because the geothermal gradients differ. Kanamori (1970) has used surface wave phase velocity data to show that the major difference between the oceanic and shield environments must lie within the upper 200 km. Using the definition that the lithosphere ends where the shear velocity drops below 4.5 km/sec has led to thickness estimates of about 70 km for the suboceanic lithosphere and twice as much for the subshield lithosphere (Kanamori and Press 1970, Press 1970a). The discontinuity in Q around the depth of 120 km is perhaps a clear estimate of the thickness of the lithosphere under continental regions.

There is scope for extending the present technique into other regions where the all important assumption of the radially symmetric explosion source function would be equally useful. The French test site in the Pacific now gives the opportunity to determine oceanic  $Q^{-1}$  and the thickness of the suboceanic lithosphere. The large underground explosion CANNIKIN is of

sufficient yield (5 Mt) to give records with good signal-to-noise.

CANNIKIN is ideally situated in the Aleutian Island Arc to investigate the lateral variations of  $Q^{-1}$  both parallel and perpendicular to the arc and over oceanic and continental paths. Such data should be useful for the understanding of tectonic processes occurring at arcs.

It is also apparent that the lateral variations indicated by this work, and the extremities of the low  $Q$  zone, need resolving in greater detail. Perhaps body waves will provide this resolution. Frasier and Filson (1972) have determined P Wave  $Q_{\alpha}$  and obtained distinctly different results for different paths. Douglas et al. (1972) have shown the effects of anomalous dissipation manifest in particular seismogram records. Douglas et al. also state that with a knowledge of  $t_{Q_P}^{-1}$  (travel time  $t$  and  $Q_P^{-1}$  the average  $Q^{-1}$  for a particular path) the source function of explosions and earthquakes may be estimated; the difficulty is  $t_{Q_P}^{-1}$  is not usually known. It is difficult to estimate the source function itself, but a simple source parameter is available as the surface wave magnitude scale  $M_S$ . The amplitude  $A(T)$  of a surface wave at period  $T$  is measured in the time domain directly from the seismogram and used in estimating  $M_S$ . The  $M_S$  values are influenced by several phenomena; two of major importance are the nature of the source spectrum generating the waves and heterogeneity of the earth experienced by those waves. Obviously there will be considerable differences between earthquake and explosion spectra (Marshall 1970). Regional variations in surface wave amplitudes have also been demonstrated by Marshall and Basham (1972). These variations were mainly attributed to dispersion effects in the different paths sampled and so they introduced a strictly time domain path correction term  $P(T)$  to compensate the  $M_S$  values between different regions. A term allowing for geometrical spreading and dissipation with distance must also be included. Marshall and Basham used near surface events and measured  $A(T)$  from the most prominent period in the record which would therefore be around 20s, and so their distance dependent term could

assume a constant value of 300 for  $Q$ . But deep focus earthquakes appear very rich in long periods and this work has shown that  $Q_Y^{-1}$  increases for frequencies around 0.02 Hz (50s). A direct use of the  $Q_Y^{-1}$  values found here would be to adapt a magnitude scale for deep focus earthquakes to include a dissipation correction term dependent on the frequency.

The attenuation of bodily waves needs further research. More investigations are required into the relationship between  $Q_\alpha^{-1}$  and  $Q_\beta^{-1}$  using P and S waves. This is difficult because for a given frequency the wavelength of S waves is much shorter than for P waves, and therefore even if spatial  $Q^{-1}$  is the same for both, S will be attenuated far more with distance than P.

In this chapter an attempt has been made to indicate the general significance of the results obtained relative to earth structure. However the general need and usefulness of increased knowledge of  $Q^{-1}$  in many fields of research is still very much apparent.

## APPENDIX A

### The WWSSN Recording Stations Used for Each Event

All the WWSSN stations used for each event are listed. For an event the distance between each recording station and the hypocentre is expressed in degrees, radians and kilometres. These angular distances,  $\Delta^{\circ}$ , were calculated using the program GEDESS (Young and Gibbs, 1968).

The geometrical spreading term used to correct the amplitudes at each station is also listed. The term is  $(E \sin \Delta)^{1/2}$  where E, the radius of the earth, is taken to be 6371 km.

The maps in Figures A.1 to A.4 show the distribution of recording stations around each event.

A list is included expanding the station abbreviations for all the WWSSN stations used. This list also indicates the region where the station is sited.

NOVAYA ZEMLYA 27/9/62 ATMOSPHERIC 28 STATIONS

NSTAT = 28 NFA = 75 NFL = 40 T = 2.056

STATION	DATA NO.	DELTAD	DELTAR	DISTANCE(KMS)	SORT(E*SIN(DELTAR))
ALG/CC07	CC05	70.10	1.2235	7794.8	77.40
ALU/0010	CC07	36.60	0.6388	4069.7	61.63
ARE/0011	CC29	114.60	2.0001	12742.9	76.11
BEC/0015	CC35	65.90	1.1502	7227.7	76.26
BHP/CC17	CC37	91.80	1.6022	10207.7	75.80
BKS/CC18	CC39	63.10	1.1886	7572.4	76.88
BLA/CC19	CC41	64.40	1.1240	7160.9	75.80
BUG/0021	CC43	94.60	1.6546	10541.3	75.68
CAR/CC24	CC45	87.50	1.5272	9729.6	75.78
CJR/CC30	CC49	61.40	1.0716	6827.4	74.79
DAL/0032	CC51	71.20	1.2427	7517.1	77.66
HNR/0040	CC57	103.70	1.8099	11530.9	78.47
LGN/0056	CC61	59.20	1.0332	6582.7	73.98
LPB/CC60	CC63	113.90	1.9679	12465.1	76.32
LUB/CC62	CC65	71.00	1.2392	7894.8	77.61
PMG/CC86	CC73	100.30	1.7506	11152.8	75.17
QUE/CC92	CC17	44.80	0.7819	4581.5	67.00
KAB/CC94	CC75	96.70	1.6877	10752.5	75.55
TOL/0115	CC13	43.10	0.7522	4752.5	65.98
TRN/0118	CC77	86.10	1.5027	9573.9	75.73
LJP/CC25	CC47	24.30	0.4241	2702.0	51.20
GEL/CC43	CC55	65.30	1.1397	7261.0	76.08
IST/0050	CC09	35.10	0.6126	3902.9	60.53
REV/0052	CC59	9.00	0.1571	1000.8	31.57
KJN/0055	CC01	21.50	0.3752	2390.7	46.32
KDS/CC67	CC67	53.50	1.0210	6504.9	73.70
KOK/CC81	CC71	17.20	0.3002	1512.6	43.40
WES/0123	CC79	57.70	1.0071	6415.9	73.38

NOVAYA ZEMLYA 22/10/62 ATMOSPHERIC 27 STATIONS

NSTAT = 27 NFA = 79 NFL = 40 T = 2.060

STATION	DATA NO.	DELTAD	DELTAR	DISTANCE(KMS)	SORT(E*SIN(DELTAR))
ARE/0011	CC31	115.70	2.0193	12665.2	75.77
BAG/0014	CC81	67.50	1.1781	7505.7	76.72
BEC/0015	CC63	67.00	1.1694	7450.1	76.58
BHP/CC17	CC65	92.90	1.6214	10220.0	75.77
BLA/CC19	CC69	65.60	1.1449	7294.4	76.17
BUG/CC21	CC91	95.90	1.6738	10663.6	75.61
CAR/0024	CC93	83.60	1.5464	9851.9	75.81
DAL/0032	CC97	72.30	1.2619	8029.4	77.91
DUG/CC36	CC99	66.40	1.1589	7383.3	76.41
GEL/CC43	C101	66.40	1.1589	7383.3	76.41
LGN/0056	C103	60.10	1.0489	6682.8	74.32
LPB/CC60	C104	114.90	2.2054	12776.3	76.02
LUB/CC62	C105	72.10	1.2584	8017.1	77.86
MAL/0065	C106	46.50	0.8116	5170.6	67.98
MAN/CC66	C107	69.30	1.2095	7705.8	77.20
KJS/CC67	C108	59.60	1.0402	6627.2	74.13
NHA/CC76	C109	68.60	1.1973	7628.0	77.02
NJR/CC81	C110	17.20	0.3002	1512.6	43.40
GSC/CC85	C111	71.40	1.2462	7539.3	77.71
PMG/CC86	C112	59.60	1.1383	11075.0	76.26
QUE/CC92	C113	43.70	0.7627	4859.2	66.34
SCP/0101	C114	61.60	1.0751	6849.0	74.85
WES/0123	C115	58.80	1.0263	6538.3	72.82
ALU/CC07	CC21	71.20	1.2427	7517.1	77.66
BKS/CC18	CC67	69.00	1.2043	7672.4	77.12
LJP/CC25	CC55	24.60	0.4294	2725.4	51.50
KJN/0055	C102	21.90	0.3822	2435.2	46.75

NOVAYA ZEMLYA 24/12/62 ATMOSPHERIC 20 STATICS

NSTAT = 26 NFA = 75 NFL = 40 T = 2.064

STATION	DATA NO.	DELTAD	DELTAR	DISTANCE(KMS)	SORTIE*SI(DELTA)
AAE/0001	0025	63.50	1.1083	7060.5	75.51
ALQ/0007	0023	71.20	1.2427	7517.1	77.66
ARE/0011	0033	116.20	2.0281	12520.8	75.61
BEC/0015	0116	67.50	1.1781	7505.7	76.72
BHP/0017	0117	93.30	1.6264	10374.5	75.75
BKS/0018	0114	68.80	1.2028	7650.2	77.07
BLA/0019	0119	65.90	1.1502	7327.7	76.26
GDH/0040	0122	30.70	0.5358	3413.7	57.03
GDL/0043	0123	66.40	1.1589	7383.3	76.41
IST/0050	0125	35.30	0.6161	3925.2	60.68
KON/0055	0126	22.70	0.3662	2524.1	45.58
LPS/0060	0129	115.50	2.0159	12643.0	75.83
LPS/0061	0130	89.70	1.5656	9974.2	75.82
LNB/0065	0131	72.20	1.2601	8028.3	71.88
NAL/0065	0132	47.30	0.8255	5259.5	68.43
TJL/0115	0135	44.20	0.7714	4914.8	66.65
TRK/0118	0137	67.60	1.5289	9740.7	75.78
VAL/0121	0133	35.00	0.6109	3851.8	60.45
WIH/0124	0139	99.50	1.7366	11063.9	75.27
CAR/0024	0120	83.10	1.5551	9507.5	75.81
LAH/0050	0127	43.00	0.7505	4761.4	65.92
LON/0058	0123	59.90	1.0455	6660.6	74.24
MOS/0067	0133	59.90	1.0455	6660.6	74.24
QUE/0052	0135	43.80	0.7645	4670.3	66.41
ODP/0025	0121	25.30	0.4416	2813.2	52.18
HNR/0048	0124	102.50	1.7890	11257.5	76.87

NOVAYA ZEMLYA 7/11/68 UNDERGLAD 18 STATICS

NSTAT = 18 NFA = 75 NFL = 40 T = 2.120

STATION	DATA NO.	DELTAD	DELTAR	DISTANCE(KMS)	SORTIE*SI(DELTA)
ATL/0012	0143	69.93	1.2205	7775.5	77.36
BAG/0014	0144	67.51	1.1783	7506.8	76.72
BLA/0019	0145	65.57	1.1444	7291.0	76.16
CFG/0026	0146	59.85	1.0446	6655.0	74.22
CUP/0025	0147	24.57	0.4288	2722.1	51.47
ESK/0038	0148	29.23	0.5102	3250.2	55.78
FLU/0039	0149	65.60	1.1449	7254.4	76.17
IST/0050	0150	60.17	1.0502	6690.6	74.34
JER/0051	0152	34.70	0.6056	3858.5	60.22
KON/0055	0151	42.91	0.7489	4771.4	65.86
NAT/0064	0153	21.90	0.3822	2435.2	46.75
NSH/0071	0154	53.51	0.9339	5950.0	71.57
DAF/0082	0155	37.24	0.6500	4140.9	62.09
SHI/0104	0156	69.67	1.2160	7746.9	77.29
STU/0105	0158	43.84	0.7652	4674.8	66.43
TAB/0110	0159	31.68	0.5529	3522.7	57.84
LUR/0126	0160	35.66	0.6224	3965.2	60.94
	0161	34.47	0.6016	3832.9	60.05

CHINKY 17/6/67 24 STATIONS

NSTAT = 24 NFA = 75 NFL = 43 T = 2.070

STATION	DATA NO.	DELTAU	DELTAR	DISTANCE(KMS)	SORT IF #SIA (DELTAU)
KRK/0222	1CCC	42.00	0.7330	4670.2	65.29
TDL/0115	1CC6	67.81	1.1845	7540.1	76.81
SHK/0114	1CC7	34.41	0.6006	3826.2	61.00
STU/0109	1CC8	55.18	0.9631	6135.7	72.32
SHI/0104	1CC9	32.04	0.5592	2562.7	56.14
KTG/0100	1C12	58.85	1.0271	6543.6	72.84
PIU/0091	1C14	69.89	1.2198	7771.4	77.35
NUK/0081	1C18	43.63	0.7615	4651.4	66.30
ESK/0036	1C33	59.22	1.0336	6565.0	72.98
ATU/0012	1C40	49.55	0.8718	5554.2	66.83
TRI/0117	1CC5	53.57	0.9350	5556.7	71.60
SLU/0102	1C11	29.01	0.5063	3225.6	55.58
NJR/0075	1C19	52.33	0.9133	5818.8	71.01
NAI/0074	1C21	63.56	1.1093	7067.5	75.53
NAL/0065	1C23	69.38	1.2196	7770.3	77.34
KON/0055	1C25	51.18	0.8953	5650.9	70.45
KEV/0052	1C27	43.05	0.7514	4786.9	65.95
GDF/0040	1C31	67.04	1.1701	7454.5	74.56
CGP/0029	1C35	50.88	0.8880	5657.6	70.30
COL/0028	1C36	65.62	1.1453	7256.6	74.18
CHC/0027	1C37	70.19	1.2250	7804.6	78.42
BAG/0014	1C39	36.10	0.6301	4014.1	61.27
AUU/0010	1C41	55.22	0.9638	6140.2	72.34
AAE/0001	1042	54.86	0.9575	6100.1	72.18

SNG/0068	1022	34.81	0.6075	3870.7	60.31
CHG/0026	1038	23.27	0.4061	2587.5	50.17
JER/0051	1028	44.17	0.7709	4911.5	66.63
IST/0050	1029	44.99	0.7852	5002.7	67.11

CHINKY 25/5/65 39 STATIONS

NSTAT = 39 NFA = 79 NFL = 40 T = 2.026

STATION	DATA NO.	DELTAU	DELTAR	DISTANCE(KMS)	SORT IF #SIA (DELTAU)
AAE/0001	1043	54.86	0.9575	6100.1	72.18
AAU/0002	1044	97.16	1.6958	10803.7	79.51
ALQ/0007	1045	103.29	1.8027	11485.3	78.74
ARE/0011	1047	150.82	2.6323	16770.4	55.73
ATL/0012	1048	106.02	1.8504	11708.5	78.25
ATU/0013	1049	49.95	0.8718	5554.2	69.83
BEC/0015	1051	103.50	1.8064	11506.7	78.71
BKS/0018	1052	96.55	1.6851	10735.5	79.56
BLA/0019	1053	101.93	1.7790	11334.1	78.95
CAR/0024	1055	124.62	2.1750	13857.1	72.41
COR/0030	1058	90.10	1.5725	10018.7	79.82
DAV/0033	1059	46.35	0.8090	5153.5	67.90
DUG/0036	1061	96.94	1.6919	10775.2	79.53
FLO/0039	1062	100.88	1.7607	11217.3	79.10
GRH/0040	1063	67.04	1.1701	7454.5	76.59
GEO/0041	1064	99.85	1.7427	11102.6	79.23
IST/0050	1066	44.99	0.7852	5002.7	67.11
JER/0051	1067	44.17	0.7709	4911.5	66.63
KEV/0052	1068	43.05	0.7514	4786.9	65.95
MAT/0064	1072	37.82	0.6601	4205.4	62.50
NAI/0074	1074	63.56	1.1093	7067.5	75.53
KTG/0100	1077	58.85	1.0271	6543.6	73.84
TDL/0115	1080	67.81	1.1835	7540.1	76.81
TRI/0117	1081	53.57	0.9350	5556.7	71.60
AOL/0010	1046	55.22	0.9638	6140.2	72.34
BAG/0014	1054	36.10	0.6201	4014.1	61.27
BGG/0021	1054	132.47	2.3120	14730.0	68.55
CHG/0026	1056	23.27	0.4061	2587.5	50.17
COL/0028	1057	65.62	1.1453	7256.6	76.18
JCT/0035	1060	108.64	1.8961	12080.2	77.70
HCC/0045	1065	27.69	0.4833	3075.0	54.41
LAH/0056	1069	15.33	0.2676	1704.6	41.04
KBL/0057	1070	17.39	0.3035	1923.7	43.64
LDN/0058	1071	88.54	1.5453	9845.2	79.81
HAN/0066	1073	37.73	0.6585	4195.4	62.44
NJR/0075	1075	52.33	0.9133	5818.8	71.01
QUE/0092	1076	21.17	0.3695	2354.0	47.97
STU/0109	1078	55.18	0.9631	6135.7	72.32
TAB/0110	1079	33.30	0.5812	3702.8	59.14



ALEUTIAN ISLANDS 29/10/65 LCMG SHCT 9 STATICS

NSTAT = 5 NFA = 79 NFL = 40 T = 2.365

STATION	DATA NO.	DELTAD	DELTAR	DISTANCE(KMS)	SORT(E*SIN(DELTAR))
BLA/0019	20C1	67.70	1.1816	7527.9	76.78
CMC/0027	20C2	35.00	0.6109	3891.8	60.45
COL/0028	20C3	21.69	0.3786	2411.8	48.52
FLD/0039	20C4	61.13	1.0669	6797.3	74.69
HNR/0048	20C5	62.86	1.0971	6989.7	75.30
HAT/0064	20C6	32.55	0.5681	3619.4	58.55
NJR/0079	20C7	46.94	0.8193	5219.5	68.23
DGD/0082	20C8	67.77	1.1828	7535.7	76.79
PNK/0086	20C9	66.61	1.1626	7406.7	76.47

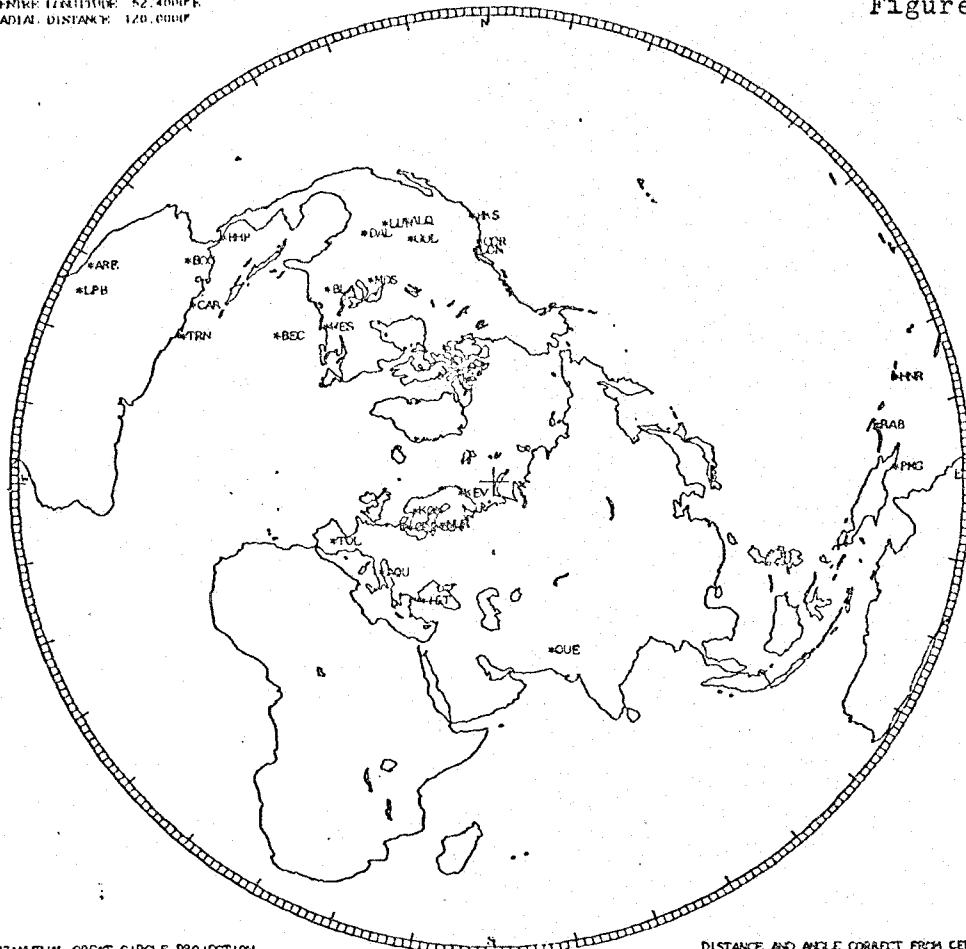
QUAKE 17/6/67 11 STATICS

NSTAT = 11 NFA = 79 NFU = 40 T = 2.260

STATION	DATA NO.	DELTAD	DELTAR	DISTANCE(KMS)	SORT(E*SIN(DELTAR))
SHA/0103	1010	38.41	0.6704	4271.0	62.91
QUI/0093	1013	26.59	0.4641	2956.7	53.40
GSC/0085	1015	41.19	0.7189	4580.1	64.77
OXF/0083	1016	41.39	0.7224	4602.4	64.90
KNA/0078	1020	28.53	0.4979	3172.4	55.16
KIP/0053	1026	58.22	1.0161	6473.8	73.59
GEO/0041	1030	50.17	0.8756	5578.6	65.95
FLU/0037	1032	45.08	0.7868	5012.7	67.17
DUG/0036	1034	45.10	0.7871	5014.9	67.18
TRN/0118	1004	45.66	0.7969	5077.2	67.50
TUC/0119	1003	37.06	0.6468	4120.9	61.96

TITLE: KAWAYA ZEM'YA 27/09/67 ATMOSPHERIC 28 STATIONS  
 CENTRE LATITUDE: 74.0000°N  
 CENTRE LONGITUDE: 52.0000°E  
 RADIAL DISTANCE: 120.0000

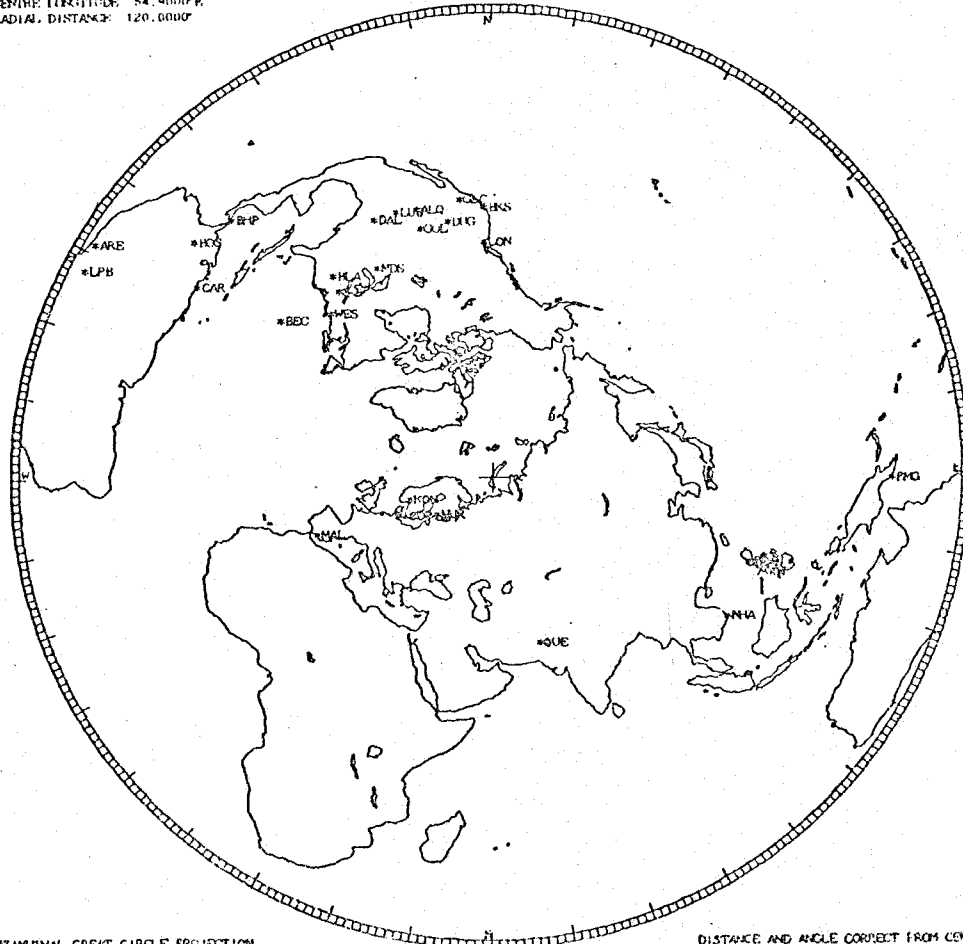
Figure A.1



AZIMUTHAL GREAT CIRCLE PROJECTION

DISTANCE AND ANGLE CORRECT FROM CENTRE

TITLE: KAWAYA ZEM'YA 22/10/67 ATMOSPHERIC 27 STATIONS  
 CENTRE LATITUDE: 73.0000°N  
 CENTRE LONGITUDE: 54.0000°E  
 RADIAL DISTANCE: 120.0000

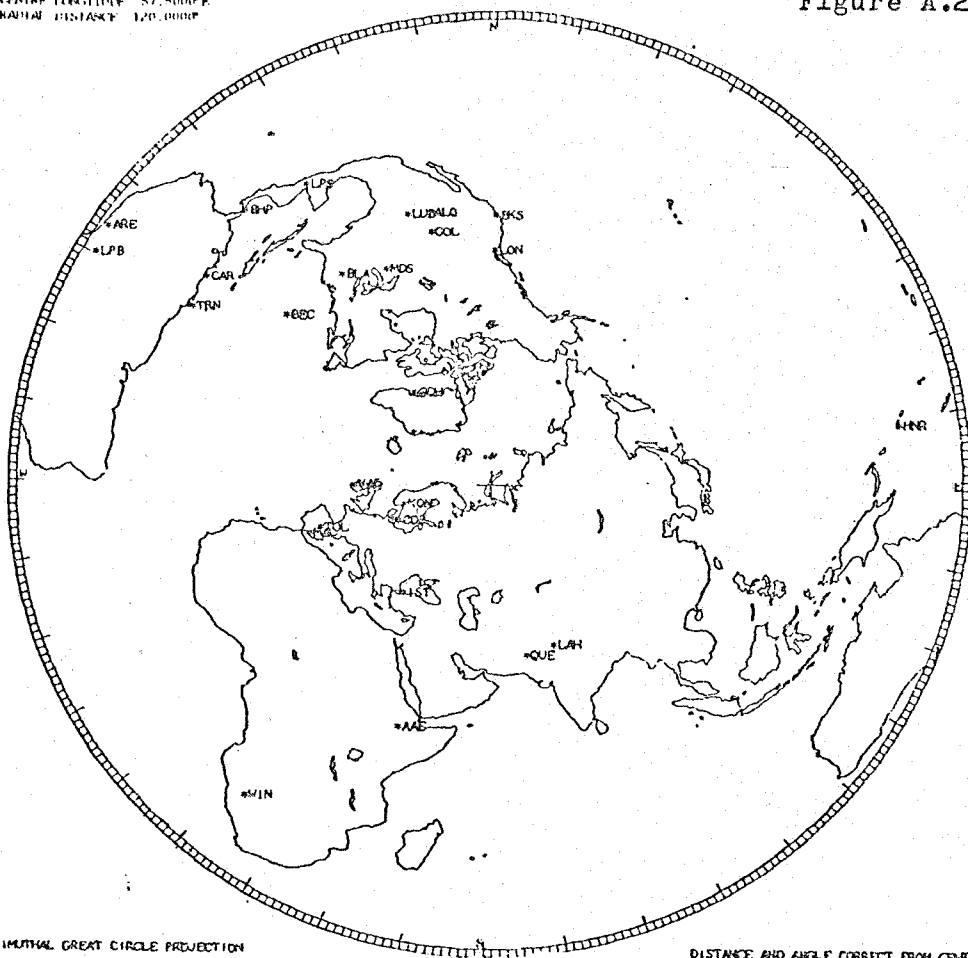


AZIMUTHAL GREAT CIRCLE PROJECTION

DISTANCE AND ANGLE CORRECT FROM CENTRE

TITLE NOVAYA ZEMLYA 24/12/67 AIRSUPPORT STATIONS  
 CENTRE LATITUDE 74.6000N  
 CENTRE LONGITUDE 57.5000E  
 RADIAL DISTANCE 120.000P

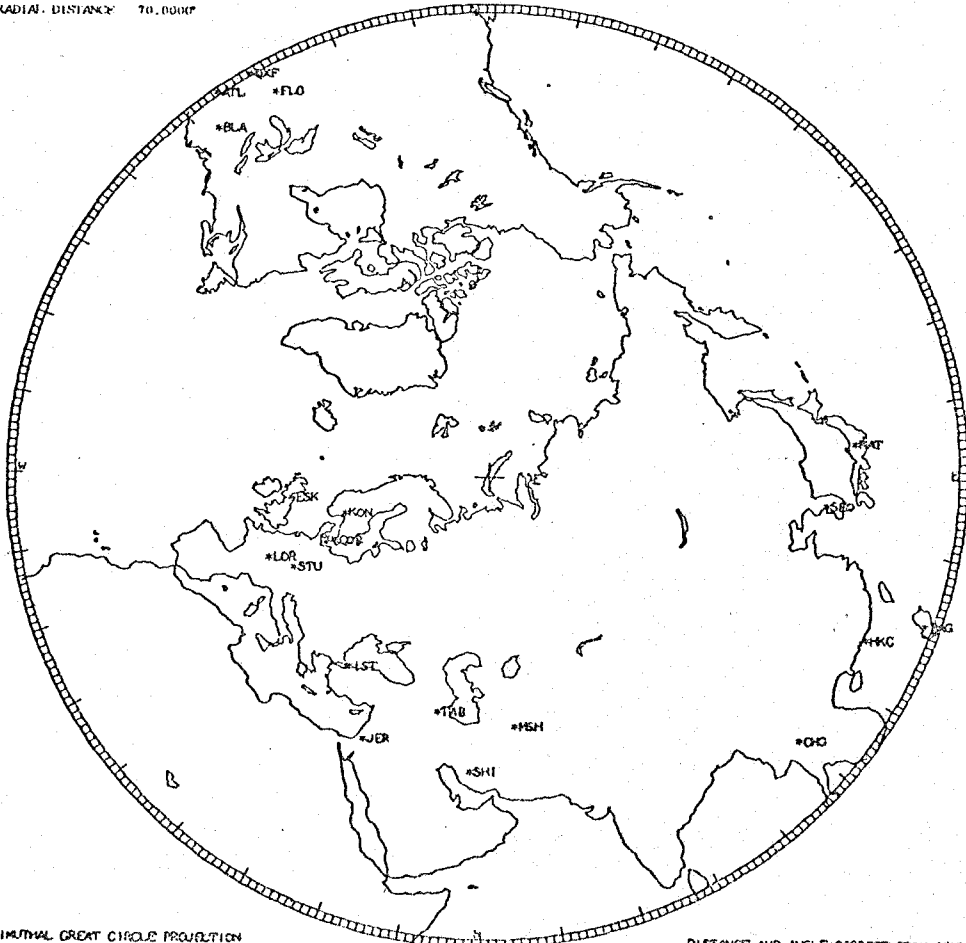
Figure A.2



AZIMUTHAL GREAT CIRCLE PROJECTION

DISTANCE AND ANGLE CORRECT FROM CENTRE

TITLE NOVAYA ZEMLYA 7/11/68 UNDERGROUND STATIONS (OF USE)  
 CENTRE LATITUDE 74.4000N  
 CENTRE LONGITUDE 54.9000E  
 RADIAL DISTANCE 70.000P

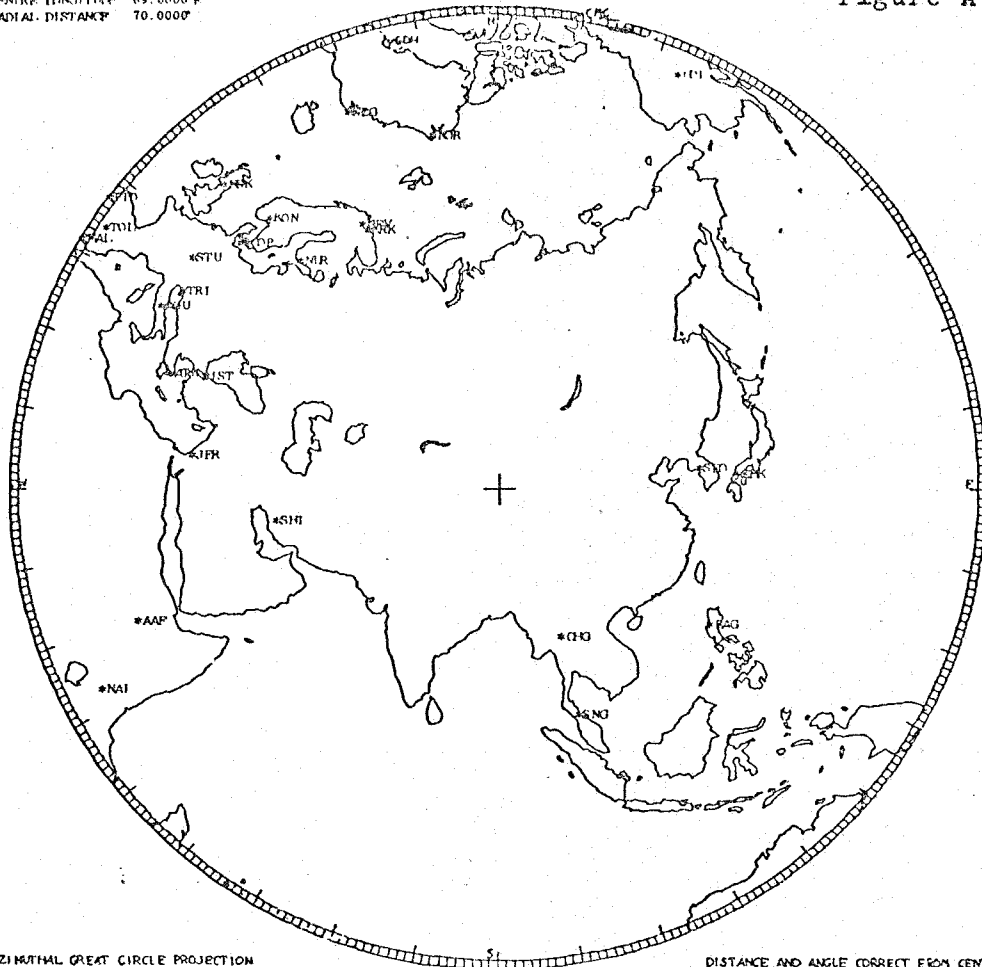


AZIMUTHAL GREAT CIRCLE PROJECTION

DISTANCE AND ANGLE CORRECT FROM CENTRE

TITLE S. SINKIANG PROV. CHINA 17/05/67 ATMOSPHERIC 28 STATIONS (24 USED)  
 CENTRE LATITUDE 40.7000°N  
 CENTRE LONGITUDE 89.6000°E  
 RADIAL DISTANCE 70.0000°

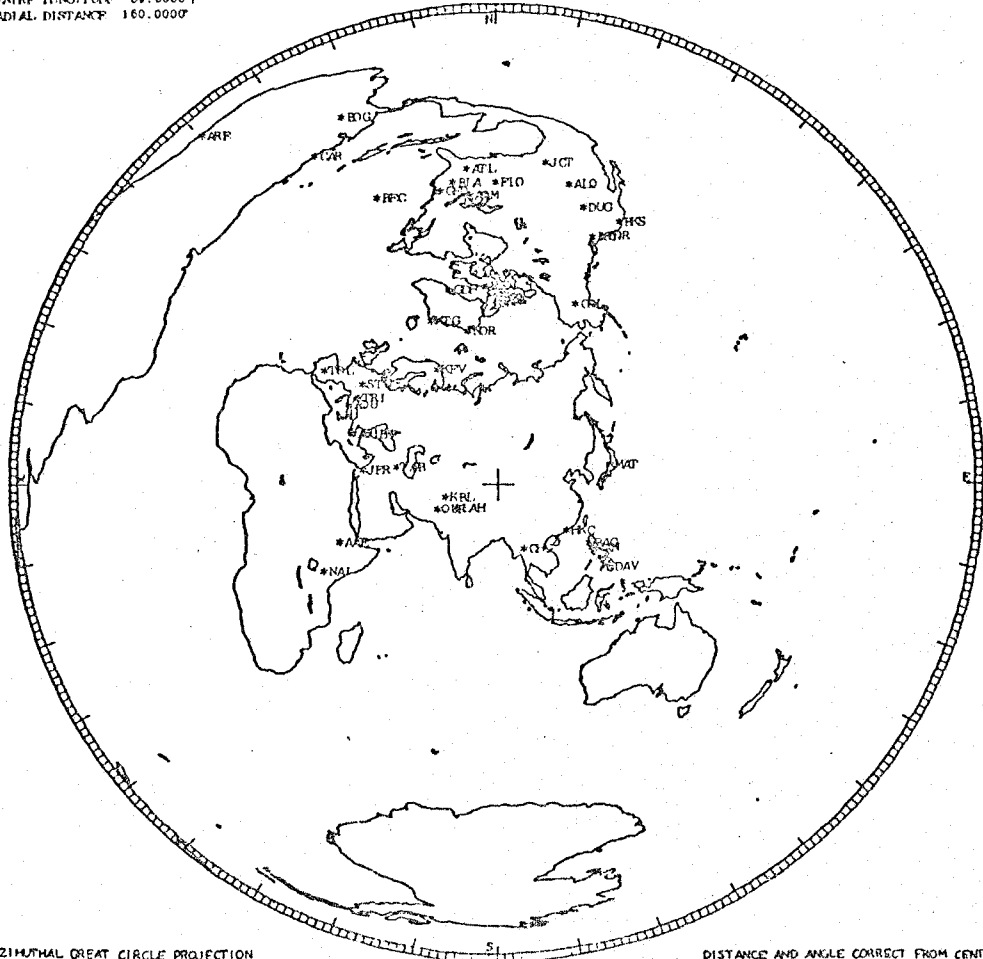
Figure A.3



AZIMUTHAL GREAT CIRCLE PROJECTION

DISTANCE AND ANGLE CORRECT FROM CENTRE

TITLE S. SINKIANG PROV. CHINA 29/09/69 ATMOSPHERIC 38 STATIONS  
 CENTRE LATITUDE 40.7000°N  
 CENTRE LONGITUDE 89.6000°E  
 RADIAL DISTANCE 160.0000°

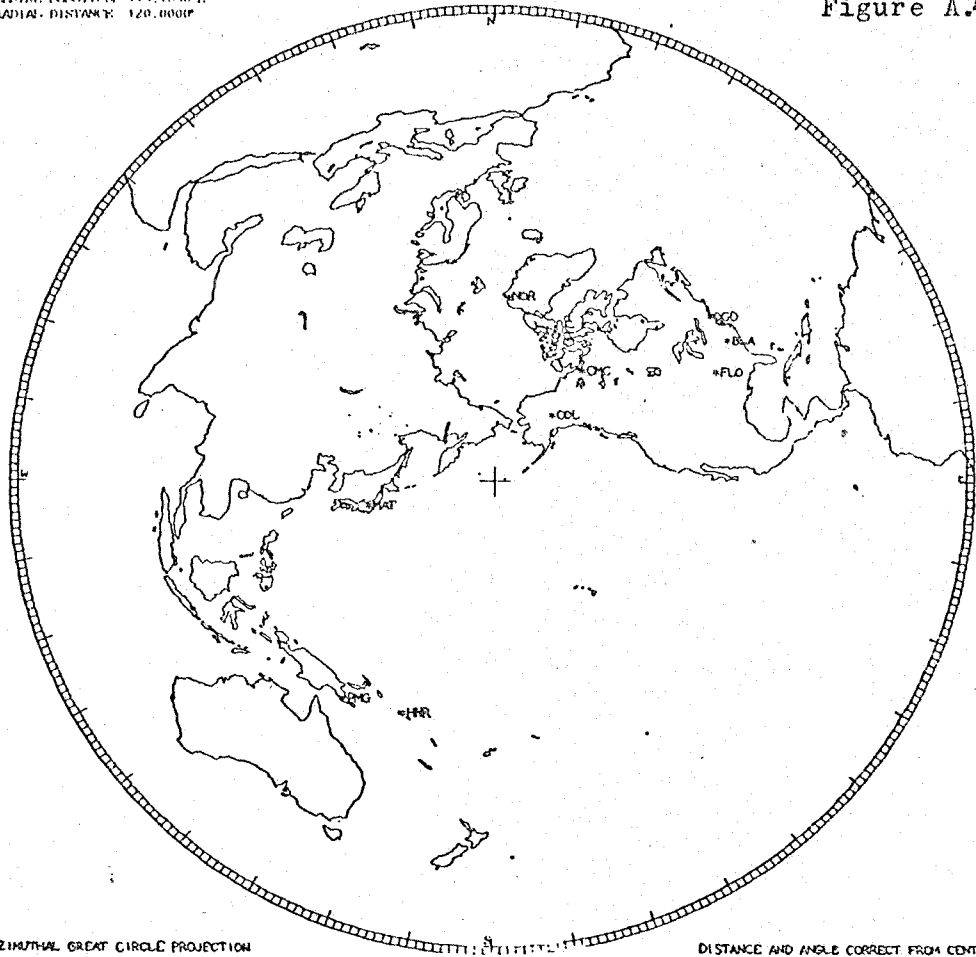


AZIMUTHAL GREAT CIRCLE PROJECTION

DISTANCE AND ANGLE CORRECT FROM CENTRE

TITLE ALPHEAN ISLANDS 29/10/65 UNDERGROUND 8 STATIONS (CLOSEST)  
 CENTRE LATITUDE 51.430°N  
 CENTRE LONGITUDE 179.180°E  
 RADIAL DISTANCE 120.000°

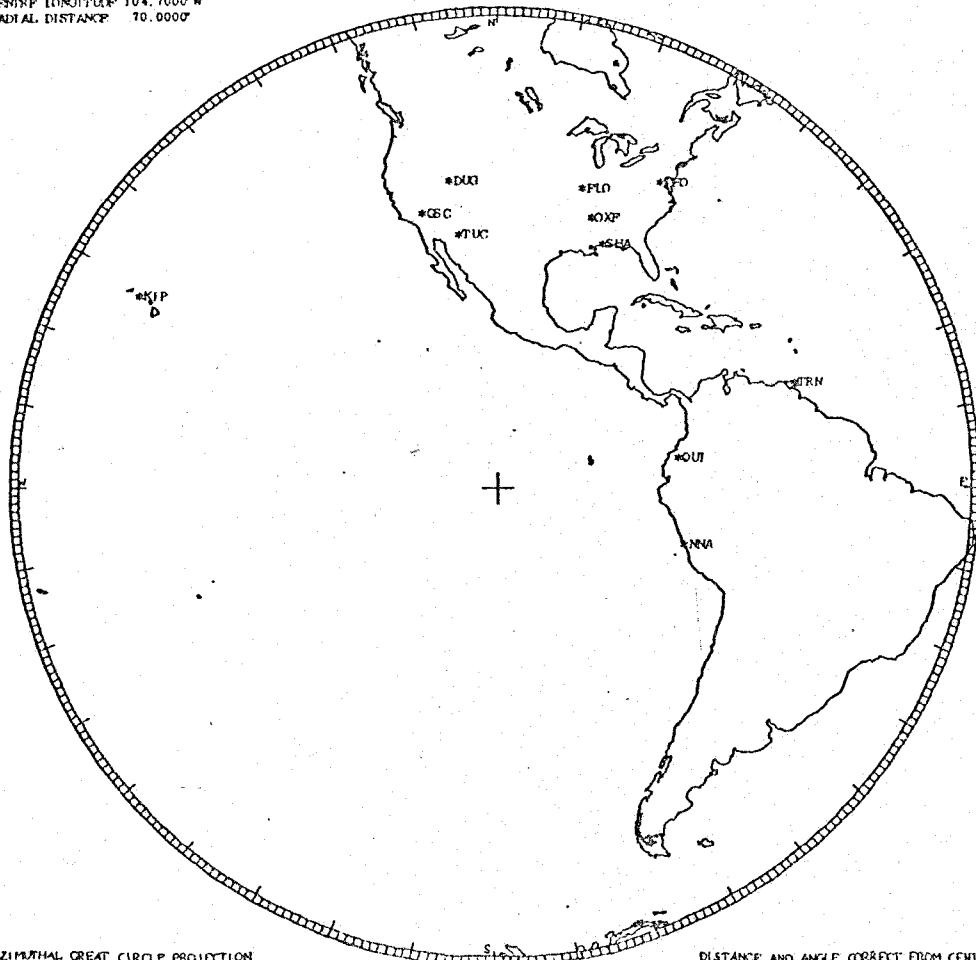
Figure A.4



AZIMUTHAL GREAT CIRCLE PROJECTION

DISTANCE AND ANGLE CORRECT FROM CENTRE

TITLE NORTHERN EASTER ISLAND 17/06/67 EARTHQUAKE 11 STATIONS  
 CENTRE LATITUDE 4.500°S  
 CENTRE LONGITUDE 104.700°W  
 RADIAL DISTANCE 70.000°



AZIMUTHAL GREAT CIRCLE PROJECTION

DISTANCE AND ANGLE CORRECT FROM CENTRE

World Wide Network of Standardized Seismograph Stations Used

In This Study

<u>Station Number</u>	<u>Station Name</u>	<u>Station Abbr.</u>
1	Addis Ababa, Ethiopia	AAE
2	Ann Arbor, Michigan	AAM
7	Albuquerque, New Mexico	ALQ
10	Aquila, Italy	AQU
11	Arequipa, Peru	ARE
12	Atlanta, Georgia	ATL
13	Athens, Greece	ATU
14	Baguio, Philippines	BAG
15	Bermuda, Colombia	BEC
17	Balboa Heights, Panama	BHP
18	Berkeley, (Strawberry) California	BKS
19	Blacksburg, Virginia	BLA
21	Bogota, Colombia	BOG
24	Caracus, Venezuela	CAR
26	Chiengmai, Thailand	CHG
27	Coppermine, Canada	CMC
28	College, (Fairbanks) Alaska	COL
29	Copenhagen, Denmark	COP
30	Corvallis, Oregon	COR
32	Dallas, Texas	DAL
33	Davao, Philippines	DAV
35	Junction, Texas	JCT
36	Dugway, Utah	DUG
38	Eskdalemuir, Scotland	ESK
39	Florissant, Missouri	FLO
40	Godhavn, Greenland	GDH
41	Georgetown, Washington, D.C.	GEO

<u>Station Number</u>	<u>Station Name</u>	<u>Station Abbr.</u>
43	Golden, Colorado	GOL
45	Hong Kong, China	HKC
48	Honiara, Guadalcanal, Solomon Is.	HNR
50	Istanbul, Turkey	IST
51	Jerusalem, Israel	JER
52	Kevo, Finland	KEV
53	Kipapa, Hawaii	KIP
55	Kongsberg, Norway	KON
56	Lahore, Pakistan	LAH
57	Kabul, Afghanistan	KBL
58	Longmire, Washington	LON
60	La Paz, Bolivia	LPB
61	La Palma, El Salvador	LPS
63	Lubbock, Texas	LUB
64	Matsushiro, Japan	MAT
65	Malaga, Spain	MAL
66	Manila, Philippines	MAN
67	Madison, Wisconsin	MDS
68	Songkla, Thailand	SNG
71	Meshed, Iran	MSH
74	Nairobi, Kenya	NAI
76	Nhatrang, South Vietnam	NHA
78	Nana, Peru	NNA
79	Nord, Greenland	NOR
81	Nurmijarvi, Finland	NUR
82	Ogdensburg, New Jersey	OGD
83	Oxford, Mississippi	OXF
85	Goldstone, California	GSC
86	Port Moresby, New Guinea	PMG

<u>Station Number</u>	<u>Station Name</u>	<u>Station Abbr.</u>
91	Porto, Portugal	PTO
92	Quetta, Pakistan	QUE
93	Quito, Ecuador	QUI
94	Rabaul, New Britain	RAB
100	Kap Tobin, Greenland	KTG
101	State College, Pennsylvania	SCP
102	Seoul, Korea	SEO
103	Spring Hill, Alabama	SHA
104	Shiraz, Iran	SHI
109	Stuttgart, Germany	STU
110	Tabriz, Iran	TAB
114	Shiraki, Japan	SHK
115	Toledo, Spain	TOL
117	Trieste, Italy	TRI
118	Trinidad, B.W.I.	TRN
119	Tucson, Arizona	TUC
121	Valentia, Ireland	VAL
123	Weston, Massachusetts	WES
124	Windhoek, South Africa	WIN
126	Lormes, France	LOR
222	Kirkenes, Norway	KRK



## APPENDIX B

### The Estimations of $Q_Y^{-1}$ from Seismic Rayleigh Waves

The values of the specific attenuation factor determined at 79 frequencies are listed for eight events, the values from the earthquake merely demonstrate the unsuitability of such an event. Confidence limits at the 95% level are also quoted.

For the eight individual events the intercept of the regression line is also listed. So for each amplitude-distance plot the regression line is entirely determined.

Three sets of average  $Q_Y^{-1}$  values are also included. The events averaged are

- 1 The three atmospheric explosions at Novaya Zemlya
- 2 The two atmospheric explosions at S Sinkiang Prov., China.
- 3 All five atmospheric explosions.

Graphs of all these  $Q_Y^{-1}$  values, and confidence limits, have been described in Chapter 3.

NUVAYA ZEMLYA 27/5/62 ATMOSPHERIC 28 STATICS

NSTAT = 28 NFA = 75 NFL = 40 T = 2.056

FREQ.(HZ)	INVERSE Q & LIMITS	INTERCEPT & LIMITS	FREQ.(HZ)	INVERSE Q & LIMITS	INTERCEPT & LIMITS
1	0.01465	0.0C715	2	0.01587	0.01118
3	0.01709	0.0C845	4	0.01831	0.0C891
5	0.01953	0.0C685	6	0.02075	0.0C775
7	0.02197	0.0C643	8	0.02319	0.0C0581
9	0.02441	0.0C491	10	0.02563	0.0C0434
11	0.02686	0.0C430	12	0.02808	0.0C0489
13	0.02930	0.0C526	14	0.03052	0.000531
15	0.03174	0.0C458	16	0.03296	0.0C0440
17	0.03418	0.0C425	18	0.03540	0.0C0440
19	0.03662	0.0C467	20	0.03784	0.0C0515
21	0.03906	0.0C0554	22	0.04028	0.000521
23	0.04150	0.0C429	24	0.04272	0.0C0358
25	0.04395	0.0C360	26	0.04517	0.0C0384
27	0.04639	0.0C359	28	0.04761	0.0C0409
29	0.04883	0.0C414	30	0.05005	0.0C0411
31	0.05127	0.0C485	32	0.05249	0.0C0547
33	0.05371	0.0C0505	34	0.05493	0.0C0445
35	0.05615	0.0C415	36	0.05737	0.0C0464
37	0.05859	0.0C527	38	0.05981	0.0C0542
39	0.06104	0.0C504	40	0.06226	0.0C0486
41	0.06348	0.0C471	42	0.06470	0.0C0441
43	0.06592	0.0C434	44	0.06714	0.0C0453
45	0.06836	0.0C454	46	0.06958	0.0C0464
47	0.07080	0.0C434	48	0.07202	0.0C0383
49	0.07324	0.0C353	50	0.07446	0.0C0421
51	0.07568	0.0C413	52	0.07690	0.0C0349
53	0.07813	0.0C368	54	0.07935	0.0C0345
55	0.08057	0.0C353	56	0.08179	0.0C0358
57	0.08301	0.0C371	58	0.08423	0.0C0339
59	0.08545	0.0C376	60	0.08667	0.0C0340
61	0.08789	0.0C337	62	0.08911	0.0C0341
63	0.09033	0.0C338	64	0.09155	0.0C0341
65	0.09277	0.0C306	66	0.09399	0.0C0305
67	0.09521	0.0C297	68	0.09644	0.0C0253
69	0.09766	0.0C240	70	0.09888	0.0C0250
71	0.10010	0.0C262	72	0.10132	0.0C0269
73	0.10254	0.0C0246	74	0.10376	0.0C0235
75	0.10498	0.0C0227	76	0.10620	0.0C0211
77	0.10742	0.0C199	78	0.10864	0.0C0183
79	0.10986	0.0C184			

NOVAYA ZEMLYA 22/IC/82 ATMOSPHERIC 27 STATICS

NSTAT = 27 NFA = 75 NFL = 40 T = 2.060

FREQ.(HZ)	INVERSE Q & LIMITS	INTERCEPT & LIMITS	FREQ.(HZ)	INVERSE Q & LIMITS	INTERCEPT & LIMITS
1	0.01465	C.CC7C5	2	0.01587	C.01021
3	0.01709	C.CC554	4	0.01831	C.01035
5	0.01953	C.CC555	6	0.02075	C.CC754
7	0.02157	C.CC549	8	0.02319	C.CC464
9	0.02411	C.CC450	10	0.02563	C.00366
11	0.02666	C.CC365	12	0.02808	C.CC412
13	0.02930	C.CC467	14	0.03052	C.00529
15	0.03174	C.CC411	16	0.03296	C.00324
17	0.03418	C.CC228	18	0.03540	C.00384
19	0.03662	C.CC354	20	0.03784	C.CC423
21	0.03906	C.CC574	22	0.04028	C.CC658
23	0.04150	C.CC523	24	0.04272	C.CC408
25	0.04395	C.CC414	26	0.04517	C.00443
27	0.04639	C.CC465	28	0.04761	C.CC485
29	0.04883	C.CC446	30	0.05005	C.CC431
31	0.05127	C.CC422	32	0.05249	C.CC357
33	0.05371	C.CC340	34	0.05493	C.00328
35	0.05615	C.CC381	36	0.05737	C.CC434
37	0.05859	C.CC460	38	0.05981	C.CC455
39	0.06104	C.CC468	40	0.06226	C.CC512
41	0.06348	C.CC501	42	0.06470	C.CC484
43	0.06592	C.CC448	44	0.06714	C.CC416
45	0.06836	C.CC420	46	0.06958	C.CC442
47	0.07080	C.CC382	48	0.07202	C.00341
49	0.07324	C.CC340	50	0.07446	C.CC378
51	0.07568	C.CC404	52	0.07690	C.CC404
53	0.07813	C.CC401	54	0.07935	C.CC416
55	0.08057	C.CC416	56	0.08179	C.CC372
57	0.08301	C.CC298	58	0.08423	C.CC273
59	0.08545	C.CC319	60	0.08667	C.CC304
61	0.08789	C.CC266	62	0.08911	C.CC255
63	0.09033	C.CC249	64	0.09155	C.CC269
65	0.09277	C.CC275	66	0.09399	C.CC248
67	0.09521	C.CC230	68	0.09644	C.00237
69	0.09766	C.CC250	70	0.09888	C.CC225
71	0.10010	C.CC150	72	0.10132	C.00148
73	0.10254	C.CC209	74	0.10376	C.CC200
75	0.10498	C.CC181	76	0.10620	C.CC186
77	0.10742	C.CC157	78	0.10864	C.CC183
79	0.10986	C.CC189			

NOVAYA ZEMLYA 24/12/62 ATMOSPHERIC 26 STATICS

NSTAT = 26 NFA = 75 NFL = 40 T = 2.064

FREQ.(MHz)	INVERSE Q & LIMITS	INTERCEPT & LIMITS	FREQ.(MHz)	INVERSE Q & LIMITS	INTERCEPT & LIMITS
1	0.01465	0.00551	2	0.01587	0.2373
3	0.01709	0.00451	4	0.01831	0.2269
5	0.01953	0.00359	6	0.02075	0.2021
7	0.02197	0.00300	8	0.02319	0.1895
9	0.02441	0.00230	10	0.02563	0.1633
11	0.02686	0.00204	12	0.02808	0.1622
13	0.02930	0.00193	14	0.03052	0.1700
15	0.03174	0.00181	16	0.03296	0.1771
17	0.03418	0.00248	18	0.03540	0.2670
19	0.03662	0.00256	20	0.03784	0.3479
21	0.03906	0.00301	22	0.04028	0.3842
23	0.04150	0.00263	24	0.04272	0.3675
25	0.04395	0.00231	26	0.04517	0.3466
27	0.04639	0.00246	28	0.04761	0.3994
29	0.04883	0.00247	30	0.05005	0.4253
31	0.05127	0.00240	32	0.05249	0.4408
33	0.05371	0.00225	34	0.05493	0.4405
35	0.05615	0.00215	36	0.05737	0.4323
37	0.05859	0.00199	38	0.05981	0.4189
39	0.06104	0.00205	40	0.06226	0.4495
41	0.06348	0.00186	42	0.06470	0.4223
43	0.06592	0.00183	44	0.06714	0.4254
45	0.06836	0.00174	46	0.06958	0.4215
47	0.07080	0.00165	48	0.07202	0.4245
49	0.07324	0.00148	50	0.07446	0.3753
51	0.07568	0.00135	52	0.07690	0.3663
53	0.07813	0.00145	54	0.07935	0.4026
55	0.08057	0.00182	56	0.08179	0.5065
57	0.08301	0.00160	58	0.08423	0.4501
59	0.08545	0.00166	60	0.08667	0.4784
61	0.08789	0.00170	62	0.08911	0.4999
63	0.09033	0.00157	64	0.09155	0.4746
65	0.09277	0.00137	66	0.09399	0.4311
67	0.09521	0.00108	68	0.09644	0.3521
69	0.09765	0.00129	70	0.09888	0.4285
71	0.10010	0.00253	72	0.10132	0.4199
73	0.10254	0.00160	74	0.10376	0.4314
75	0.10499	0.00154	76	0.10620	0.4995
77	0.10742	0.00197	78	0.10864	0.4354
79	0.10986	0.00175			3.4654
					0.4113



CHINKY 17/6/67 24 STATICS

NSTAT = 24 NFA = 75 NFL = 40 T = 2.070

FREQ.(HZ)	INVERSE Q & LIMITS	INTERCEPT & LIMITS	FREQ.(HZ)	INVERSE Q & LIMITS	INTERCEPT & LIMITS
1	0.01465	C.CC457	2	0.01587	C.CC262
3	0.01709	0.CC684	4	0.01831	0.CC459
5	0.01953	C.CC451	6	0.02075	C.CC354
7	0.02197	C.CC512	8	0.02319	C.CC936
9	0.02441	0.01035	10	0.02563	C.CC789
11	0.02686	C.CC832	12	0.02808	C.CC6C1
13	0.02930	0.CC538	14	0.03052	C.CC289
15	0.03174	C.CC472	16	0.03296	C.CC743
17	0.03418	0.CC615	18	0.03540	C.CC418
19	0.03662	C.CC335	20	0.03784	C.CC3C1
21	0.03906	0.CC425	22	0.04028	C.CC458
23	0.04150	C.CC532	24	0.04272	C.CC582
25	0.04395	0.CC531	26	0.04517	C.CC4C9
27	0.04639	C.CC3C3	28	0.04761	C.CC267
29	0.04883	0.CC245	30	0.05005	C.CC289
31	0.05127	C.CC423	32	0.05249	C.CC512
33	0.05371	C.CC5C6	34	0.05493	0.CC523
35	0.05615	C.CC5C8	36	0.05737	C.CC466
37	0.05859	0.CC452	38	0.05981	C.CC475
39	0.06104	C.CC485	40	0.06226	C.CC526
41	0.06348	C.CC588	42	0.06470	C.CC6C1
43	0.06592	0.CC6C2	44	0.06714	0.CC631
45	0.06836	0.CC637	46	0.06958	0.CC628
47	0.07080	0.CC483	48	0.07202	C.CC345
49	0.07324	C.CC357	50	0.07446	C.CC27C
51	0.07568	0.CC273	52	0.07690	0.CC26C
53	0.07813	0.CC213	54	0.07935	0.CC337
55	0.08057	0.CC316	56	0.08179	C.CC251
57	0.08301	0.CC260	58	0.08423	C.CC27C
59	0.08545	0.CC215	60	0.08667	C.CC155
61	0.08789	C.CC163	62	0.08911	0.CC176
63	0.09033	C.CC232	64	0.09155	C.CC318
65	0.09277	C.CC236	66	0.09399	C.CC278
67	0.09521	C.CC258	68	0.09644	C.CC225
69	0.09766	0.CC158	70	0.09888	C.CC234
71	0.10010	C.CC285	72	0.10132	C.CC25E
73	0.10254	0.CC223	74	0.10376	C.CC156
75	0.10498	C.CC2C5	76	0.10620	C.CC285
77	0.10742	0.CC240	78	0.10864	C.CC151
79	0.10986	0.CC667			

CHINKY 29/9/65 39 STATICS

NSTAT = 25 NFA = 79 NFL = 40 T = 2.026

FREQ.(HZ)	INVERSE Q & LIMITS	INTERCEPT & LIMITS	FREQ.(HZ)	INVERSE Q & LIMITS	INTERCEPT & LIMITS
1	C.01465	C.00612	C.00275	3.4906	0.1521
3	C.01709	C.00513	0.00217	3.3864	0.1369
5	C.01953	C.00702	0.00274	3.5440	0.1758
7	C.02197	C.00612	C.00202	3.6049	0.1536
9	C.02441	C.00495	C.00204	3.6135	0.1639
11	C.02686	C.00366	C.00182	3.6051	0.1641
13	C.02930	C.00325	0.00157	3.6599	0.1958
15	C.03174	C.00153	C.00151	3.5603	0.2103
17	C.03418	C.00116	0.00187	3.6056	0.2266
19	C.03662	C.00060	0.00156	3.5532	0.2587
21	C.03906	C.00037	C.00164	3.5110	0.2332
23	C.04150	C.00075	0.00137	3.5684	0.2103
25	C.04395	C.00171	C.00137	3.6425	0.2251
27	C.04639	C.00188	C.00130	3.6791	0.2281
29	C.04883	C.00203	0.00142	3.7075	0.2639
31	C.05127	C.00253	0.00141	3.7533	0.2766
33	C.05371	C.00257	0.00125	3.8197	0.2576
35	C.05615	0.00343	C.00139	3.8080	0.3010
37	C.05859	C.00314	0.00136	3.7018	0.3081
39	C.06104	C.00345	0.00121	3.7736	0.2855
41	C.06348	0.00310	0.00128	3.6348	0.2976
43	C.06592	C.00283	C.00119	3.5696	0.2976
45	C.06836	0.00238	0.00116	3.4461	0.3014
47	C.07080	C.00274	0.00101	3.4788	0.2698
49	C.07324	C.00229	0.00100	3.3498	0.2768
51	C.07568	0.00236	C.00056	3.3467	0.2692
53	C.07813	C.00250	C.00095	3.3209	0.2751
55	C.08057	C.00269	C.00082	3.4072	0.2425
57	C.08301	C.00261	0.00083	3.3466	0.2505
59	C.08545	C.00203	C.00082	3.2037	0.2555
61	C.08789	C.00199	C.00087	3.1418	0.2779
63	0.09033	C.00161	C.00081	3.0313	0.2670
65	C.09277	C.00149	C.00052	2.9834	0.3085
67	0.09521	0.00124	C.00087	2.9281	0.2980
69	C.09766	C.00155	C.00085	3.0534	0.3009
71	C.10010	C.00126	C.00077	3.0177	0.2783
73	C.10254	C.00110	C.00074	2.9183	0.2721
75	C.10498	C.00084	C.00069	2.8071	0.2644
77	C.10742	C.00091	C.00065	2.8225	0.2586
79	C.10986	C.00041	C.00062	2.6839	0.2415

FREQ.(HZ)	INVERSE Q & LIMITS	INTERCEPT & LIMITS
2	0.01587	C.00579
4	0.01831	C.00705
6	0.02075	C.00710
8	0.02319	C.00558
10	0.02563	C.00463
12	0.02808	C.00334
14	0.03052	C.00262
16	0.03296	C.00101
18	0.03540	C.00104
20	0.03784	C.00033
22	0.04028	0.00041
24	0.04272	C.00118
26	0.04517	C.00201
28	0.04761	C.00158
30	0.05005	C.00209
32	0.05249	C.00256
34	0.05493	0.00316
36	0.05737	C.00311
38	0.05981	C.00335
40	0.06226	C.00335
42	0.06470	C.00284
44	0.06714	C.00254
46	0.06958	C.00261
48	0.07202	0.00252
50	0.07446	C.00231
52	0.07690	C.00242
54	0.07935	C.00255
56	0.08179	C.00280
58	0.08423	0.00231
60	0.08667	0.00200
62	0.08911	C.00187
64	0.09155	C.00149
66	0.09399	0.00147
68	0.09644	C.00130
70	0.09888	C.00144
72	0.10132	C.00117
74	0.10376	C.00095
76	0.10620	C.00088
78	0.10864	C.00070

FREQ.(HZ)	INVERSE Q & LIMITS	INTERCEPT & LIMITS
3.4493	C.00262	0.1498
3.4798	C.00255	0.1584
3.6263	C.00260	0.1792
3.6088	C.00206	0.1584
3.6240	C.00201	0.1715
3.6252	C.00203	0.1920
3.6358	C.00187	0.1954
3.5477	C.00150	0.2193
3.6070	C.00150	0.2404
3.5080	C.00151	0.2629
3.5296	0.00144	0.2141
3.5983	C.00136	0.2168
3.6780	C.00137	0.2326
3.6965	C.00135	0.2439
3.7066	C.00145	0.2853
3.8176	C.00125	0.2595
3.8183	C.00125	0.2723
3.7180	C.00134	0.2963
3.7400	C.00125	0.2976
3.7452	C.00127	0.3024
3.5758	C.00123	0.3031
3.5009	C.00114	0.2902
3.4703	C.00110	0.2895
3.4259	C.00099	0.2705
3.3434	C.00095	0.2771
3.3187	C.00096	0.2734
3.3651	C.00083	0.2431
3.4179	C.00081	0.2432
3.2892	C.00084	0.2577
3.1578	0.00082	0.2599
3.1135	C.00082	0.2658
2.5737	C.00052	0.3040
2.5912	C.00081	0.2741
2.9530	C.00051	0.3154
3.0658	C.00075	0.2832
2.5765	C.00076	0.2754
2.8469	C.00072	0.2710
2.8226	C.00065	0.2661
2.7640	C.00070	0.2412





UJANE. 17/6/67 11 STATICS

INSTAT = 11 NFA = 75 NFU = 40 T = 2.260

FREQ.(HZ)	INVLKSE C & LIMITS	INTERCEPT & LIMITS	FREQ.(HZ)	INVERSE O & LIMITS	INTERCEPT & LIMITS
1	0.01465	0.02483	0.03801	0.9828	0.3679
3	0.01709	0.01005	0.03558	1.1631	3.9950
5	0.01953	0.00650	0.02688	0.8992	3.9759
7	0.02197	0.00921	0.01931	0.7255	4.0623
9	0.02441	0.00156	0.01228	0.5071	3.8465
11	0.02686	0.00066	0.01159	0.5310	3.7681
13	0.02930	-0.00016	0.01225	0.6172	3.7411
15	0.03174	-0.00016	0.01876	1.0349	3.7233
17	0.03418	0.00144	0.01884	1.1337	3.9393
19	0.03662	0.00063	0.01588	1.0213	3.8966
21	0.03906	0.00157	0.01337	0.9365	3.9714
23	0.04150	0.00345	0.01468	1.1263	4.0895
25	0.04395	0.00598	0.01526	1.2476	4.3824
27	0.04639	0.00855	0.01243	1.0796	4.4709
29	0.04883	0.01127	0.01066	0.9792	4.6856
31	0.05127	0.01390	0.01106	1.0720	4.6847
33	0.05371	0.01651	0.01125	1.1259	4.3435
35	0.05615	0.01917	0.00742	0.8086	4.8545
37	0.05859	0.02179	0.00660	0.7619	4.4288
39	0.06104	0.02442	0.00808	0.9783	4.3692
41	0.06348	0.02706	0.00783	1.0081	4.4539
43	0.06592	0.02969	0.00588	0.7902	4.3157
45	0.06836	0.03232	0.00607	0.8500	4.3521
47	0.07080	0.03495	0.00720	1.0547	4.4274
49	0.07324	0.03758	0.00663	1.0219	5.0194
51	0.07568	0.04021	0.00475	0.7795	4.3923
53	0.07813	0.04284	0.00475	0.8030	4.6208
55	0.08057	0.04547	0.00381	0.6729	4.7558
57	0.08301	0.04810	0.00544	1.0015	4.4966
59	0.08545	0.05073	0.00486	0.9469	3.7988
61	0.08789	0.05336	0.00412	0.8296	3.6124
63	0.09033	0.05600	0.00493	1.0249	3.7913
65	0.09277	0.05863	0.00507	1.0737	3.9214
67	0.09521	0.06126	0.00480	1.0519	3.8513
69	0.09766	0.06389	0.00428	0.9682	3.5448
71	0.10010	0.06652	0.00364	0.8235	3.7419
73	0.10254	0.06915	0.00472	1.0667	3.7840
75	0.10498	0.07178	0.00588	1.2440	3.6611
77	0.10742	0.07441	0.00311	0.7114	3.2874
79	0.10986	0.07704	0.00452	1.1377	3.4292
2	0.01587	0.02131	0.01587	0.01587	4.2560
4	0.01831	0.00492	0.00492	0.00492	3.8931
6	0.02075	0.01016	0.01016	0.01016	4.1103
8	0.02319	0.00329	0.00329	0.00329	3.8638
10	0.02563	0.00103	0.00103	0.00103	3.8335
12	0.02808	-0.000256	0.01124	0.01124	3.6761
14	0.03052	0.00015	0.01543	0.01543	3.7746
16	0.03296	0.00120	0.01607	0.01607	3.8613
18	0.03540	0.00068	0.01938	0.01938	3.8736
20	0.03784	0.00256	0.01391	0.01391	4.0310
22	0.04028	0.00179	0.01272	0.01272	3.5585
24	0.04272	0.00511	0.01777	0.01777	4.2529
26	0.04517	0.00634	0.01362	0.01362	4.4159
28	0.04761	0.00798	0.01131	0.01131	4.5763
30	0.05005	0.00861	0.00951	0.00951	4.6585
32	0.05249	0.00704	0.01165	0.01165	4.5177
34	0.05493	0.00840	0.00966	0.00966	4.8065
36	0.05737	0.00617	0.00694	0.00694	4.4695
38	0.05981	0.00619	0.00819	0.00819	4.3502
40	0.06226	0.00548	0.00776	0.00776	4.4517
42	0.06470	0.00526	0.00629	0.00629	4.4155
44	0.06714	0.00458	0.00620	0.00620	4.2523
46	0.06958	0.00516	0.00665	0.00665	4.3803
48	0.07202	0.00799	0.00731	0.00731	4.8363
50	0.07446	0.00681	0.00581	0.00581	4.7022
52	0.07690	0.00554	0.00432	0.00432	4.4636
54	0.07935	0.00707	0.00444	0.00444	4.7576
56	0.08179	0.00638	0.00464	0.00464	4.6790
58	0.08423	0.00440	0.00544	0.00544	4.2006
60	0.08667	0.00183	0.00519	0.00519	3.6561
62	0.08911	0.00165	0.00385	0.00385	3.7343
64	0.09155	0.00245	0.00552	0.00552	3.8453
66	0.09399	0.00316	0.00452	0.00452	3.9839
68	0.09644	0.00177	0.00467	0.00467	3.6977
70	0.09888	0.00117	0.00362	0.00362	3.4663
72	0.10132	0.00304	0.00421	0.00421	3.5130
74	0.10376	0.00165	0.00643	0.00643	3.6527
76	0.10620	0.00100	0.00414	0.00414	3.4210
78	0.10864	0.00087	0.00397	0.00397	3.3479

NOVAYA ZEMLYA 24/12/62 ATMOSPHERIC 26 STATIONS  
 NOVAYA ZEMLYA 27/9/62 ATMOSPHERIC 28 STATIONS  
 NOVAYA ZEMLYA 22/10/62 ATMOSPHERIC 27 STATIONS

	FREQ. (HZ)	INVERSE Q & LIMITS	FREQ. (HZ)	INVERSE Q & LIMITS
1	0.01465	0.007454 0.002240	2	0.01587 0.009868 0.002655
3	0.01709	0.008463 0.002440	4	0.01831 0.008792 0.002256
5	0.01953	0.007478 0.001752	6	0.02075 0.006789 0.001882
7	0.02197	0.005510 0.001819	8	0.02319 0.005025 0.001676
9	0.02441	0.004496 0.001498	10	0.02563 0.003868 0.001341
11	0.02686	0.003797 0.001293	12	0.02808 0.004420 0.001350
13	0.02930	0.004942 0.001296	14	0.03052 0.005215 0.001150
15	0.03174	0.004426 0.001094	16	0.03296 0.003634 0.001231
17	0.03418	0.003789 0.001407	18	0.03662 0.004028 0.001512
19	0.03662	0.004070 0.001493	20	0.03784 0.004664 0.001463
21	0.03906	0.005327 0.001513	22	0.04028 0.005466 0.001540
23	0.04150	0.004638 0.001493	24	0.04272 0.003946 0.001442
25	0.04395	0.004065 0.001385	26	0.04517 0.004082 0.001284
27	0.04639	0.004200 0.001213	28	0.04761 0.004372 0.001234
29	0.04883	0.004203 0.001239	30	0.05005 0.004157 0.001252
31	0.05127	0.004645 0.001204	32	0.05249 0.004848 0.001174
33	0.05371	0.004527 0.001199	34	0.05493 0.004174 0.001221
35	0.05615	0.004251 0.001189	36	0.05737 0.004714 0.001148
37	0.05859	0.004979 0.001040	38	0.05981 0.004911 0.000999
39	0.06104	0.004575 0.001047	40	0.06226 0.004425 0.001060
41	0.06348	0.004355 0.001039	42	0.06470 0.004326 0.001029
43	0.06592	0.004344 0.001056	44	0.06714 0.004466 0.001064
45	0.06836	0.004560 0.001021	46	0.06958 0.004638 0.001002
47	0.07080	0.004263 0.000974	48	0.07202 0.003994 0.000919
49	0.07324	0.003851 0.000977	50	0.07446 0.004132 0.000870
51	0.07568	0.004378 0.000859	52	0.07690 0.004451 0.000847
53	0.07813	0.004140 0.000811	54	0.07935 0.003930 0.000823
55	0.08057	0.003929 0.000862	56	0.08179 0.003784 0.000916
57	0.08301	0.003496 0.000907	58	0.08423 0.003397 0.000900
59	0.08545	0.003376 0.000897	60	0.08667 0.003216 0.000853
61	0.08789	0.003061 0.000829	62	0.08911 0.002968 0.000794
63	0.09033	0.002966 0.000739	64	0.09155 0.003092 0.000665
65	0.09277	0.002850 0.000668	66	0.09399 0.002616 0.000661
67	0.09521	0.002512 0.000618	68	0.09644 0.002473 0.000663
69	0.09766	0.002609 0.000691	70	0.09888 0.002579 0.000688
71	0.10010	0.002313 0.000650	72	0.10132 0.002095 0.000629
73	0.10254	0.002099 0.000590	74	0.10376 0.002064 0.000586
75	0.10498	0.001907 0.000621	76	0.10620 0.001819 0.000626
77	0.10742	0.001982 0.000585	78	0.10864 0.001866 0.000581
79	0.10986	0.001819 0.000584		

CHINKY 17/6/67 24 STATIONS  
 CHINKY 29/9/69 39 STATIONS

	FREQ. (HZ)	INVERSE Q	& LIMITS		FREQ. (HZ)	INVERSE Q	& LIMITS
1	0.01465	0.005988	0.002847	2	0.01587	0.005496	0.002528
3	0.01709	0.004783	0.002148	4	0.01831	0.006829	0.002605
5	0.01953	0.006800	0.002630	6	0.02075	0.006846	0.002326
7	0.02197	0.006068	0.001865	8	0.02319	0.005842	0.001916
9	0.02441	0.005346	0.001957	10	0.02563	0.004870	0.001952
11	0.02686	0.004008	0.001727	12	0.02808	0.003701	0.001817
13	0.02930	0.003417	0.001759	14	0.03052	0.002639	0.001688
15	0.03174	0.001791	0.001839	16	0.03296	0.001538	0.001763
17	0.03418	0.001587	0.001695	18	0.03540	0.001309	0.001690
19	0.03662	0.000845	0.001753	20	0.03784	0.000568	0.001871
21	0.03906	0.000704	0.001657	22	0.04028	0.000772	0.001467
23	0.04150	0.001147	0.001412	24	0.04272	0.001584	0.001364
25	0.04395	0.002032	0.001288	26	0.04517	0.002191	0.001273
27	0.04639	0.001980	0.001273	28	0.04761	0.002039	0.001325
29	0.04883	0.002069	0.001393	30	0.05005	0.002161	0.001389
31	0.05127	0.002694	0.001279	32	0.05249	0.003154	0.001192
33	0.05371	0.003161	0.001177	34	0.05493	0.003355	0.001223
35	0.05615	0.003585	0.001325	36	0.05737	0.003258	0.001275
37	0.05859	0.003272	0.001294	38	0.05981	0.003486	0.001248
39	0.06104	0.003592	0.001211	40	0.06226	0.003576	0.001201
41	0.06348	0.003383	0.001219	42	0.06470	0.003158	0.001168
43	0.06592	0.003148	0.001123	44	0.06714	0.002929	0.001069
45	0.06836	0.002795	0.001063	46	0.06958	0.002993	0.001012
47	0.07080	0.002952	0.000916	48	0.07202	0.002613	0.000987
49	0.07324	0.002418	0.000900	50	0.07446	0.002436	0.000941
51	0.07568	0.002401	0.000991	52	0.07690	0.002438	0.000997
53	0.07813	0.002567	0.000978	54	0.07935	0.002639	0.000850
55	0.08057	0.002743	0.000834	56	0.08179	0.002784	0.000919
57	0.08301	0.002608	0.000935	58	0.08423	0.002336	0.000887
59	0.08545	0.002043	0.000892	60	0.08667	0.001955	0.000891
61	0.08789	0.001956	0.000884	62	0.08911	0.001857	0.000847
63	0.09033	0.001684	0.000846	64	0.09155	0.001656	0.000900
65	0.09277	0.001679	0.000870	66	0.09399	0.001604	0.000809
67	0.09521	0.001384	0.000842	68	0.09644	0.001404	0.000864
69	0.09766	0.001595	0.000812	70	0.09888	0.001538	0.000742
71	0.10010	0.001431	0.000717	72	0.10132	0.001320	0.000718
73	0.10254	0.001216	0.000687	74	0.10376	0.001043	0.000668
75	0.10498	0.000962	0.000676	76	0.10620	0.001074	0.000692
77	0.10742	0.001060	0.000682	78	0.10864	0.000784	0.000663
79	0.10986	0.000439	0.000698				

NOVAYA ZEMLYA 24/12/62 ATMOSPHERIC 26 STATIONS  
 CHINKY 17/6/67 24 STATIONS  
 NOVAYA ZEMLYA 27/9/62 ATMOSPHERIC 28 STATIONS  
 NOVAYA ZEMLYA 22/10/62 ATMOSPHERIC 27 STATIONS  
 CHINKY 29/9/69 39 STATIONS

	FREQ. (HZ)	INVERSE Q & LIMITS		FRFQ. (HZ)	INVERSE Q & LIMITS
1	0.01465	0.006772 0.001755	2	0.01587	0.007490 0.001802
3	0.01709	0.006378 0.001591	4	0.01831	0.007803 0.001686
5	0.01953	0.007186 0.001492	6	0.02075	0.008617 0.001457
7	0.02197	0.005820 0.001277	8	0.02319	0.009433 0.001246
9	0.02441	0.004912 0.001195	10	0.02563	0.009141 0.001141
11	0.02686	0.003902 0.001045	12	0.02808	0.008063 0.001096
13	0.02930	0.004187 0.001058	14	0.03052	0.008941 0.000983
15	0.03174	0.003125 0.001021	16	0.03296	0.008606 0.001036
17	0.03418	0.002642 0.001045	18	0.03540	0.008277 0.001119
19	0.03662	0.002532 0.001142	20	0.03784	0.008614 0.001155
21	0.03906	0.003010 0.001102	22	0.04028	0.008154 0.001055
23	0.04150	0.002953 0.001022	24	0.04272	0.008203 0.000987
25	0.04395	0.003079 0.000941	26	0.04517	0.008163 0.000895
27	0.04639	0.003119 0.000867	28	0.04761	0.008236 0.000891
29	0.04883	0.003165 0.000914	30	0.05005	0.008208 0.000918
31	0.05127	0.003699 0.000865	32	0.05249	0.0084027 0.000827
33	0.05371	0.003866 0.000833	34	0.05493	0.008375 0.000855
35	0.05615	0.003925 0.000873	36	0.05737	0.0084005 0.000842
37	0.05859	0.004150 0.000808	38	0.05981	0.0084218 0.000777
39	0.06104	0.004096 0.000783	40	0.06226	0.0084009 0.000785
41	0.06348	0.003875 0.000783	42	0.06470	0.0083746 0.000763
43	0.06592	0.003750 0.000758	44	0.06714	0.0083704 0.000745
45	0.06836	0.003689 0.000726	46	0.06958	0.0083819 0.000703
47	0.07080	0.003612 0.000663	48	0.07202	0.0083259 0.000632
49	0.07324	0.003123 0.000631	50	0.07446	0.0083295 0.000630
51	0.07568	0.003410 0.000642	52	0.07690	0.0083461 0.000639
53	0.07813	0.003362 0.000620	54	0.07935	0.0083282 0.000583
55	0.08057	0.003329 0.000593	56	0.08179	0.0083286 0.000641
57	0.08301	0.003063 0.000643	58	0.08423	0.0082879 0.000626
59	0.08545	0.002726 0.000626	60	0.08667	0.0082602 0.000608
61	0.08789	0.002526 0.000596	62	0.08911	0.0082426 0.000572
63	0.09033	0.002337 0.000550	64	0.09155	0.0082395 0.000541
65	0.09277	0.002273 0.000532	66	0.09399	0.0082116 0.000509
67	0.09521	0.001954 0.000505	68	0.09644	0.0081945 0.000529
69	0.09766	0.002109 0.000521	70	0.09888	0.0082070 0.000498
71	0.10010	0.001888 0.000475	72	0.10132	0.0081718 0.000467
73	0.10254	0.001666 0.000442	74	0.10376	0.0081556 0.000435
75	0.10498	0.001430 0.000451	76	0.10620	0.0081445 0.000458
77	0.10742	0.001524 0.000440	78	0.10864	0.0081332 0.000432
79	0.10986	0.001144 0.000444			

## APPENDIX C

### The Instrument Response

Each Rayleigh wave train used in this work was recorded by a long period, vertical component instrument of the World-Wide Standard Seismograph Network (WWSSN). It is necessary to correct these seismograms for instrumental effects which influence both amplitude and phase. The corrections applied to the seismogram in the time domain for instrumental magnification and group delay time - which must necessarily be introduced - have been described by Brune, Nafe and Oliver (1960). The group delay time,  $t_u$ , at angular frequency  $\omega$  is

$$t_u = \frac{d\phi(\omega)}{d\omega}$$

where  $\phi(\omega)$  is the phase shift caused by the instrument. This usually amounts to several seconds and may significantly affect the measured group velocities.

In the frequency domain the complex seismogram spectrum  $A(\omega)$  is corrected for instrumental effects by using the complex instrumental transfer function  $I(\omega)$  and dividing at each frequency to form

$$A'(\omega) = \frac{A(\omega)}{I(\omega)}$$

$I(\omega)$  contains both amplitude and phase information and may be obtained by several methods, but not all are possible or convenient in the present case. If the seismograph system constants are known then  $I(\omega)$  may be calculated algebraically. Each seismogram contains a calibration pulse - the system response to a step of acceleration - this may be Fourier analysed and  $I(\omega)$  obtained directly. This latter process is difficult because it is difficult to digitise sharp calibration pulses to sufficient accuracy. Further, the calibration pulse is introduced while the seismometer is operational and recording ground motion, and therefore must contain noise superimposed onto the calibrating pulse. Alternatively the blanket response quoted by the WWSSN for all seismographs may be assumed. But

examination of calibration pulses on several film chips from different stations shows great differences in amplitude and phase response for different instruments. An individual correction for each seismogram is required. Mitchell and Landisman (1969) advocate a "least-squares inversion" technique to determine seismograph constants and hence  $I(\omega)$ , but this is too time consuming when 200 seismograms are involved. An alternative technique proposed by Espinosa, Sutton and Miller (1962, 1965) was eventually chosen.

Espinosa et al. (1965) have determined a set of analog standard transient responses to a step of acceleration which would be shown by a variety of instrument systems, each with specified characteristic parameters. Appendix VI of Espinosa et al. contains a computing program written by Brune which obtains  $I(\omega)$  by choosing the standard transient response, from a library of 78, which best matches the transient observed on the seismogram. A least squares deviation is calculated between six points measured from the observed transient and the analogous points on the standard library transients, the seismograph parameters corresponding to the best fitting transient are then used to calculate  $I(\omega)$ .

The six necessary measurements are shown in Figure C.1 which is taken from Espinosa et al. (1965). The time points  $P_1$  to  $P_6$  are measured from the initial break time of the calibration pulse. All the measurements are made from a baseline which takes into account the lateral motion of the recording pen on the drum. It is also necessary to know the mass of the seismometer (kg), the motor constant of the seismometer in newton/mA and the calibration current in mA. All the instruments have a seismometer mass of 11.2 kg and the motor constant and calibration current are marked on each film chip in the appropriate units.

Brune's program was adapted and incorporated into the subroutine WWSSN and is listed with the program TSAP (Burton and Blamey 1972). The measurements  $P_1$  to  $P_6$  were taken when the Rayleigh wave train was digitised

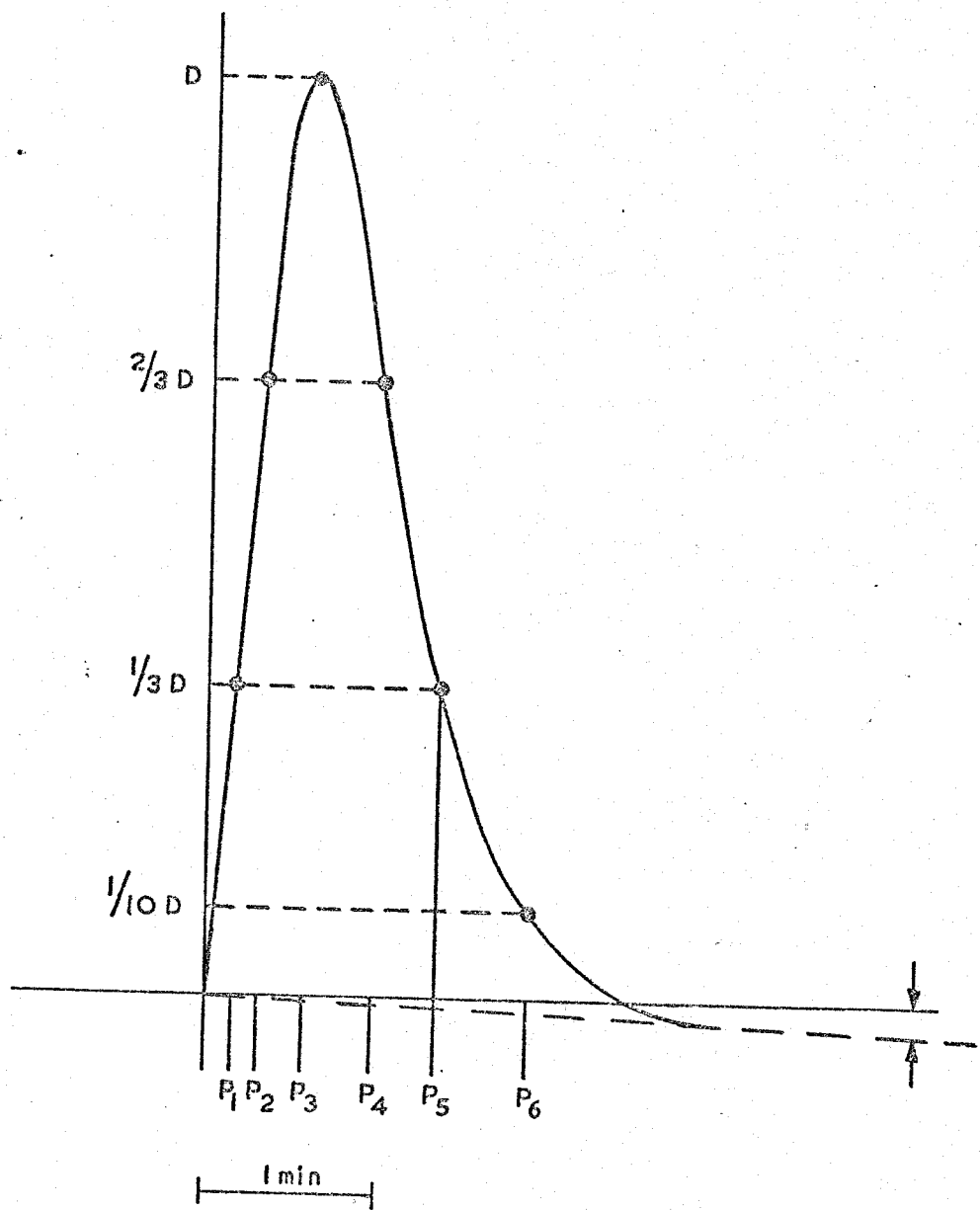


FIGURE C.1 TRANSIENT RESPONSE AS USED FOR COMPUTER COMPARISON WITH STANDARD TRANSIENT RESPONSE CASES

and the same digitising units of measure were used. These measurements are scaled to the appropriate absolute values within the subroutine WWSSN.

Four typical instrumental magnification curves calculated by this method are shown in Figure C.2. These correspond to the stations AAE, COP, MDS and QUE when they recorded the event NZA 24/12/62.

According to the film chips the nominal magnification at 20s period for these stations is 750, 750, 1500 and 3000 respectively. These absolute values of magnification have been ignored in Figure C.2 to illustrate the discrepancy between instruments of the position of the peak period response. This shows a surprising variation between systems which are supposedly standard. A blanket WWSSN instrumental response would have hidden this source of error and have been inappropriate in work requiring amplitude determinations for a wide range of recording stations.



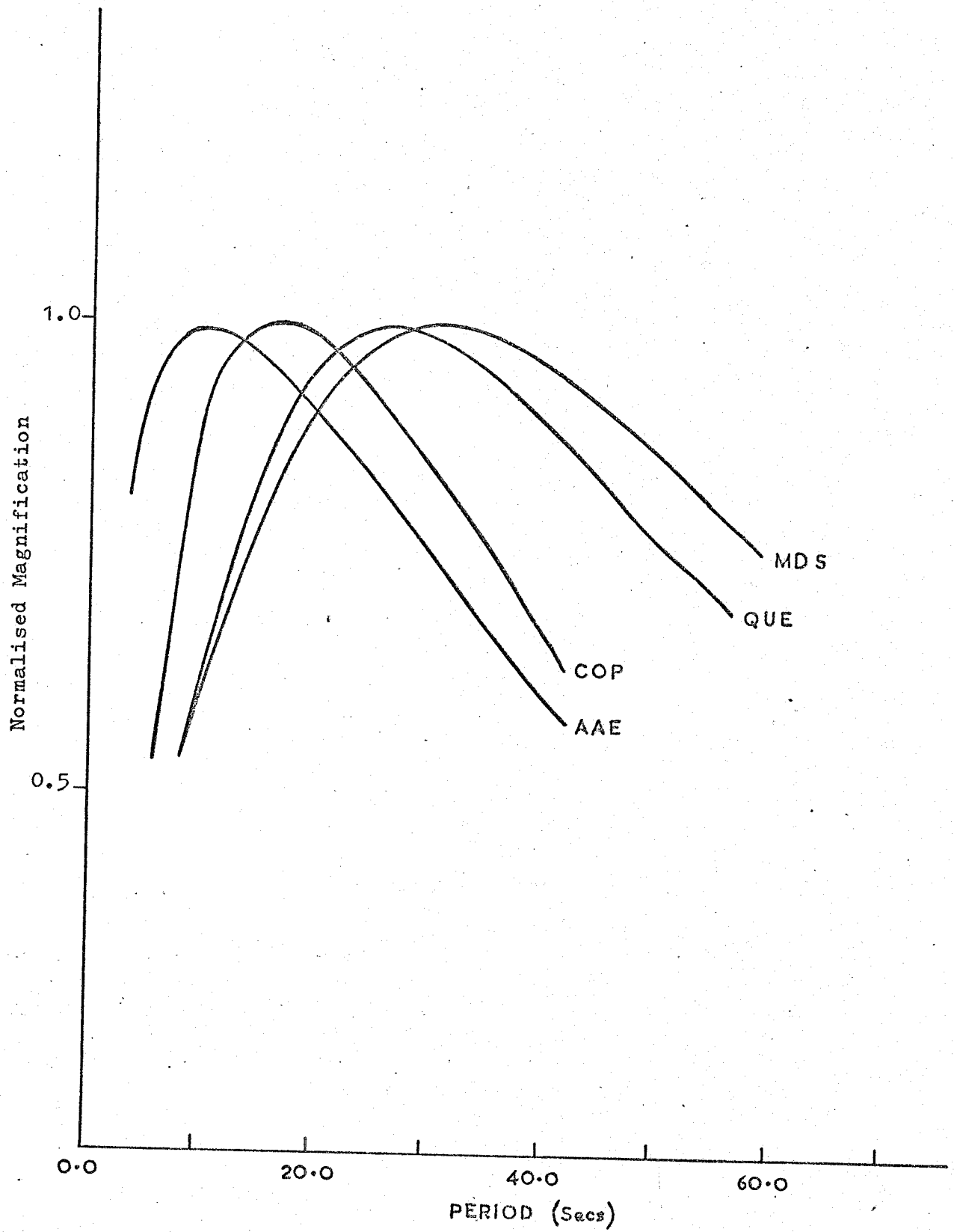


FIGURE C.2 WSSN INSTRUMENT MAGNIFICATIONS

## APPENDIX D

### Least Squares fitting of "the best" straight line

#### The "best line" appropriate to the experimental data

The variation of amplitude with distance for Rayleigh waves has already been expressed in a linear form. An amplitude term  $(\log_{10}(A\sqrt{E \sin \Delta}))$  plotted as the ordinate variable  $Y_i$  against a distance term  $\frac{\pi E \Delta f}{U} \log_{10} e$  or abscissa variable  $X_i$  yields values of the specific attenuation factor  $Q_Y^{-1}$ . The gradient of the plot is the negative value of  $Q_Y^{-1}$ . For each of the  $j$  events analysed there are  $n_j$  stations or  $n_j$  pairs of points  $(X_i, Y_i)$ . If  $a$  and  $b$  are the best estimates of the gradient and intercept formed from these points then

$$Y_i = aX_i + b \quad i=1 \text{-----} n_j \quad \text{D.1}$$

The method used to determine  $a$  and  $b$  depends on what is known about the errors in  $X_i$  and  $Y_i$ . Adcock (1880) determined  $a$  and  $b$  by minimising "the sum of the squares of the normals from the  $n$  points to the required line". However, this is a special case and has tacitly assumed that the weights  $w(X_i)$ ,  $w(Y_i)$  assigned to  $X_i$ ,  $Y_i$  are equal.

Other methods are particularly applicable to certain types of data. The papers by McIntyre et al. (1966) and Brooks et al. (1968) assume knowledge of errors or standard deviation at each point, that is for each point  $(X_i, Y_i)$  the values  $(\sigma_{X_i}, \sigma_{Y_i})$  are also known. For their application, determination of the best isochron for  $\text{Rb}^{87}/\text{Sr}^{86}$  isotope ratios, each ratio is itself the subject of an experiment and so the errors  $(\sigma_{X_i}, \sigma_{Y_i})$  are well determined at each point. Adjustments to obtain the best line are then made along the diagonal to the rectangle of sides  $\sigma_{X_i}, \sigma_{Y_i}$  at each point.

There are many possible simplifying assumptions, like the above, which can be made. The paper by D York (1967) depicts the geometrical implications of many of these assumptions. For example the often used assumptions that the  $X_i$  are exactly known ( $w(X_i) = \infty$ ) implies that all

adjustments made to obtain the required line are necessarily parallel to the y axis.

York (1966) has obtained a "least squares cubic" equation for the gradient  $a$  when both  $X_i$  and  $Y_i$  are subject to errors.

$$a^3 \sum_i \frac{W_i^2 U_i^2}{\omega(X_i)} - 2a^2 \sum_i \frac{W_i^2 U_i V_i}{\omega(X_i)} - a \left[ \sum_i W_i U_i^2 - \sum_i \frac{W_i^2 V_i^2}{\omega(X_i)} \right] + \sum_i W_i U_i V_i = 0 \quad D2$$

and

$$W_i = \frac{\omega(X_i) \omega(Y_i)}{a^2 \omega(Y_i) + \omega(X_i)} \quad D3$$

$$\bar{X} = \frac{\sum_i W_i X_i}{\sum_i W_i} \quad D4$$

$$\bar{Y} = \frac{\sum_i W_i Y_i}{\sum_i W_i} \quad D5$$

$$U_i = X_i - \bar{X} \quad D6$$

$$V_i = Y_i - \bar{Y} \quad D7$$

Obviously equation D.2 is not really a cubic, but an estimate of  $a$  in equation D.3 reduces it to one. Equation D.2 may then be solved for the gradient.

It is useful to rewrite equation D.3 as

$$W_i = \frac{\omega(Y_i)}{a^2 \left( \frac{\omega(Y_i)}{\omega(X_i)} \right) + 1} \quad D8$$

We expect values no greater than .01 for the specific attenuation factor,  $Q_Y^{-1}$ , of Rayleigh waves; this is of course equal to the gradient for the experimental data. Further, it has already been shown that errors in the amplitude term are far greater than in the distance term for the data used. Equation D.8 becomes

$$W_i = \frac{\omega(Y_i)}{10^{-4} \left( \frac{\omega(Y_i)}{\omega(X_i)} \right) + 1} \quad D9$$

with

$$\omega(Y_i) \ll \omega(X_i)$$

D.10

therefore

$$W_i \sim \omega(Y_i)$$

The errors caused by this approximation are obviously negligible for the present case.

Returning to equation D.2 we note that the first two terms are of order  $10^{-6}$  and  $10^{-4}$  respectively and contain the term  $1/\omega(X_i)$ , these may be safely neglected with respect to the third term which is of order  $10^{-2}$ . Equation D.2 therefore becomes

$$a \left[ \sum_i \omega(Y_i) U_i^2 - \sum_i \frac{(\omega(Y_i))^2 V_i^2}{\omega(X_i)} \right] = \sum_i \omega(Y_i) U_i V_i \quad \text{D.12}$$

and using condition D.10 the second term may again be neglected giving

$$a = \frac{\sum_i \omega(Y_i) U_i V_i}{\sum_i \omega(Y_i) U_i^2} \quad \text{D.13}$$

This result is the one which would be obtained from the simple regression of "y" on "x". The weights  $\omega(Y_i)$  were all set to unity because for the experimentally determined values of amplitude there was no reason to do otherwise.

#### Regression Formulae

The derivation of formulae relevant to regression calculations are to be found in many books on statistics, for example J T Ractliff's "Elements of Mathematical Statistics" (1967). The formulae used in this work are listed below.

The points on the regression line corresponding to  $(X_i, Y_i)$  are  $(x_{ir}, y_{ir})$  with  $x_{ir} = X_i$ , the line is

$$y_{ir} = a x_{ir} + b \quad \text{D.14}$$

In addition to the previous notation the regression formulae are written in terms of variances (var) and covariances (cov) whenever possible, because the abbreviations VAR and COV are used during calculations in the computer subroutine LSTSQR.

Formulae are listed in the order in which it is reasonable to calculate them for computing purposes.

$$\text{var}(X_i) = \frac{\sum_i U_i^2}{n_j} \quad \text{D.15}$$

$$\text{var}(Y_i) = \frac{\sum_i V_i^2}{n_j} \quad \text{D.16}$$

$$\text{cov}(X_i, Y_i) = \frac{\sum_i U_i V_i}{n_j} \quad \text{D.17}$$

$$a = \frac{\text{cov}(X_i, Y_i)}{\text{var}(X_i)} \quad \text{D.18}$$

$$b = \bar{Y}_i - a \bar{X}_i \quad \text{D.19}$$

the product-moment correlation coefficient, r

$$r = \frac{\text{cov}(X_i, Y_i)}{\sqrt{\text{var}(X_i)\text{var}(Y_i)}} \quad \text{D.20}$$

the residual sum of squares about the regression line, RSS

$$\text{RSS} = \sum_i (Y_i - y_{ir})^2 = (1-r^2)n \text{ var}(Y_i) \quad \text{D.21}$$

$$\text{var } a = \frac{(1-r^2)\text{var}(Y_i)}{(n-2)\text{var}(X_i)} \quad \text{D.22}$$

$$\text{var } b = \text{var } a \frac{\sum_i X_i^2}{n_j} \quad \text{D.23}$$

confidence limits on a and b require Student's "t" with  $n_j-2$  degrees of freedom at the appropriate confidence level and are

$$a \pm t \sqrt{\text{var } a} \quad \text{D.24}$$

and

$$b \pm t \sqrt{\text{var } b} \quad \text{D.25}$$

the scatter about the calculated regression line is

$$y_{ir} = a x_{ir} + b \pm t \sqrt{\frac{\text{RSS}}{n_j - 2}} \quad \text{D.26}$$

The subroutine LSTSQR is incorporated into the program AVD to determine values of the specific attenuation factor and confidence limits. Values of the correlation coefficient,  $r$ , indicate how reasonable a fit a line gives to the data. For zero correlation between the  $X_i$  and  $Y_i$

$$r \sqrt{\frac{(n_j - 2)}{(1 - r^2)}} \quad \text{D.27}$$

is distributed as Student's "t" with  $(n_j - 2)$  degrees of freedom. (Miller and Kahn, 1962, p112.) The significance of  $r$  for each line is calculated in this way.

The values of  $Q_Y^{-1}$  and confidence limits are listed in Appendix B for each event.

## APPENDIX E

### The Comparison of Two Regression Lines

For the two regression lines ( $j=1$  or  $2$ )

$$y_{1ir} = a_1 x_{1ir} + b_1 \quad \text{E.1}$$

$$y_{2ir} = a_2 x_{2ir} + b_2$$

with  $n_1, n_2$  points each it is often necessary to compare them to determine if the observables ( $X_{ji}, Y_{ji}$ ) come from the same population, have the same gradient  $a_j$  and the same intercept  $b_j$ . If all three comparisons show equality then the two lines are statistically the same line.

For amplitude-distance plots these comparisons will have geophysical significance. The first comparison will demonstrate if the energy from an event, at two frequencies or over two paths, has sampled similar environments. The further tests indicate if the attenuation differs and if the event size (or energy between frequencies) differs.

Statistics for making these comparisons are described by K A Brownlee (1965) and the relevant tests and formulae are listed below.

For each regression the residual sums of squares may be estimated as

$$\sum_i^{n_j} (y_{jir} - Y_{ji})^2 \quad \text{E.3}$$

$$= n_j \text{ var } (Y_j) - \frac{\text{cov}(X_j, Y_j)}{\text{var}(X_j)} \quad \text{E.4}$$

and the mean squares estimated as

$$S_j^2 = \frac{\sum_i (y_{jir} - Y_{ji})^2}{n_j - 2} \quad \text{E.5}$$

If the two sets of data are samples from the same population then the two values  $S_j^2$  are estimates of the same variance  $\sigma^2$  and Fisher's variance ratio "F" test may be performed to test this hypothesis.

$$F = \frac{S_1^2}{S_2^2} \quad \text{NFTEST} \quad \text{E.6}$$

If this test is passed  $\sigma^2$  is estimated by

$$S^2 = \frac{(n_1-2)S_1^2 + (n_2-2)S_2^2}{n_1-2 + n_2-2} \quad \text{E.7}$$

If the gradients are equal then  $a_1 - a_2$  is normally distributed about zero with variance

$$\text{var}(a_1 - a_2) = \frac{\sigma^2}{n_1 \text{var}(X_1)} + \frac{\sigma^2}{n_2 \text{var}(X_2)} \quad \text{E.8}$$

and the variable

$$S \left[ \left( \frac{1}{n_1 \text{var}(X_1)} \right) + \left( \frac{1}{n_2 \text{var}(X_2)} \right) \right]^{\frac{1}{2}} \quad \text{NATEST} \quad \text{E.9}$$

is distributed as t with  $(n_1 + n_2 - 4)$  degrees of freedom. This variable gives the second test.

If  $a_1$  and  $a_2$  are the same then a joint estimate may be obtained.

$$a = \frac{n_1 \text{cov}(X_1, Y_1) + n_2 \text{cov}(X_2, Y_2)}{n_1 \text{var}(X_1) + n_2 \text{var}(X_2)} \quad \text{E.10}$$

As might be expected this equation is similar to the analogous equation (D.18) for the gradient of a single regression line, for the comparison of two such lines the analogy must occur throughout.

The variance of the joint gradient is

$$\text{var}(a) = \frac{\sigma^2}{n_1 \text{var}(X_1) + n_2 \text{var}(X_2)} \quad \text{E.11}$$

and  $\sigma^2$  is estimated from the new residual sum of squares

$$\text{RSS} = n_1 \text{var}(Y_1) - \frac{n_1 (\text{cov}(X_1, Y_1))^2}{\text{var}(X_1)} + \left[ \begin{array}{l} \text{similar term} \\ \text{in } X_2, Y_2 \end{array} \right] \quad \text{E.12}$$

which has  $n_1 + n_2 - 3$  degrees of freedom, the analogy with the equations D.20 to D.22 is again obvious.

If the gradients are equal it is possible to test for complete equality of the lines, which depends on equality of the intercepts. The



statistic to be tested is

$$s \left[ \frac{1}{n_1} + \frac{1}{n_2} + \frac{(\bar{X}_1 - \bar{X}_2)^2}{(n_1 \text{var}(X_1) + n_2 \text{var}(X_2))} \right]^{1/2} \quad \text{NBTEST} \quad \text{E.13}$$

which is distributed as t with  $n_1 + n_2 - 3$  degrees of freedom. The new S is determined from the new RSS of equation E.12.

These statistics are used in the computer programs C2L and CNL. The terms NFTEST, NATEST and NBTEST are used in these programs to both indicate the result of a particular test and as a switch for subsequent tests. The values 0, 1 or 2 are assigned to NFTEST indicating that the test was failed, passed or not performed. Obviously, if the values 0 or 2 are obtained then subsequent tests may be switched off.

The Average Gradient for Several Regression Lines

The average  $Q_Y^{-1}$  values subsequently determined for several events ( $n_E$  events) required estimation of the average gradient for several regression lines. Such averages were determined irrespective of the individual population variances (the results of NFTEST) although any discrepancies were noted.

The formulae of Brownlee were generalised to give

$$a = \frac{\sum_j^{n_E} n_j \text{cov}(X_j, Y_j)}{\sum_j^{n_E} n_j \text{var}(X_j)} \quad \text{E.14}$$

with variance

$$\text{var}(a) = \frac{\sigma^2}{\sum_j^{n_E} n_j \text{var}(X_j)} \quad \text{E.15}$$

and  $\sigma^2$  is now estimated from the total of the residual sums of squares

$$\text{RSS} = \sum_j^{n_E} n_j \text{var}(Y_j) - \sum_j^{n_E} \frac{n_j (\text{cov}(X_j, Y_j))^2}{\text{var}(X_j)} \quad \text{E.16}$$

which has  $\sum_j^{n_E} (n_j - 1) - 1$  degrees of freedom.

These formulae are used in the program QBAR which is listed in Appendix G along with the programs C2L and CNL.

APPENDIX F

F1      Proof 1

To obtain the relation between the imaginary part of a bodily wave velocity and the specific attenuation factor:

For a body wave we have the wave propagation term

$$\exp [ i(\omega t - kx) ] \tag{F1.1}$$

where  $\omega$  is angular frequency,  $t$  is time,  $k$  the wave number and  $x$  is the distance travelled. The phase velocity  $\alpha = \omega/k$  and so we have

$$\exp [ i(\omega t - \frac{\omega x}{\alpha} ) ] \tag{F1.2}$$

and ignoring time dependence

$$\exp [ -i(\frac{\omega x}{\alpha} ) ] \tag{F1.3}$$

If the velocity  $\alpha$  is complex of the form

$$\alpha = \alpha_0 + I(\delta \alpha) \tag{F1.4}$$

then we have

$$\begin{aligned} & \exp \left[ -i \left( \frac{\omega x (\alpha_0 - I(\delta \alpha))}{\alpha_0^2} \right) \right] \\ &= \exp \left[ \frac{-i \omega x}{\alpha_0} \right] \exp \left[ \frac{-\omega x I(\delta \alpha)}{\alpha_0^2} \right] \end{aligned} \tag{F1.5}$$

and the attenuation coefficient,  $\gamma$ , is therefore

$$\gamma = \frac{-\omega I(\delta \alpha)}{\alpha_0^2} \tag{F1.6}$$

But the attenuation coefficient, in terms of the specific attenuation factor  $Q_\alpha^{-1}$  is

$$\gamma = \frac{-\pi f Q_\alpha^{-1}}{\alpha_0} \tag{F1.7}$$

where  $f$  is frequency, and so

$$I(\delta \alpha) = \frac{Q_\alpha^{-1} \alpha_0}{2} \tag{F1.8}$$

Dispersion and dissipation are causally linked. To obtain the relation between the real part of a body wave velocity and the specific attenuation factor:

Futterman's (1962) equations relating the real and imaginary parts of the refractive index  $n(\omega)$  are (Futterman's equations A-13<sup>1</sup> and A-14<sup>1</sup>)

$$R(n(\omega_1) - n(\infty)) = \frac{2}{\pi} P \int_0^{\infty} \frac{I(n(\omega)) \omega}{\omega^2 - \omega_1^2} d\omega \quad \text{F2.1}$$

$$R(n(0) - n(\infty)) = \frac{2}{\pi} P \int_0^{\infty} \frac{I(n(\omega))}{\omega} d\omega \quad \text{F2.2}$$

For a body wave velocity  $\alpha$  (compressional wave) with R and I parts we may write

$$\alpha = \alpha_0 + \delta\alpha \quad \text{F2.3}$$

where

$$\delta\alpha = R(\delta\alpha) + I(\delta\alpha) \quad \text{F2.4}$$

and using Futterman's formulation

$$R(\alpha(\omega_1) - \alpha(\infty)) = \frac{2}{\pi} P \int_0^{\infty} \frac{I(\alpha(\omega)) \omega}{\omega^2 - \omega_1^2} d\omega \quad \text{F2.5}$$

$$R(\alpha(0) - \alpha(\infty)) = \frac{2}{\pi} P \int_0^{\infty} \frac{I(\delta\alpha(\omega))}{\omega} d\omega \quad \text{F2.6}$$

Futterman makes the assumption that there is no attenuation for infinite frequencies, that is

$$\alpha(\infty) = \alpha_0 \quad \text{F2.7}$$

and so

$$R(\alpha(\omega_1) - \alpha(\infty)) = R(\delta\alpha(\omega_1)) \quad \text{F2.8}$$

$$R(\alpha(0) - \alpha(\infty)) = R(\delta\alpha(0)) \quad \text{F2.9}$$

If we make the assumption that the dispersive effect of dissipation is very small then

$$\alpha(\omega_1) \sim \alpha(0) \quad \text{F2.10}$$

and equation F2.6 is adequate to estimate  $R(\delta\alpha(\omega))$  which gives

$$R(\delta\alpha(\omega)) = \frac{2}{\pi} P \int_0^{\infty} \frac{I(\delta\alpha(\omega))}{\omega} d\omega \quad \text{F2.11}$$

but

$$I(\delta\alpha(\omega)) = \frac{Q_a^{-1} \alpha_0}{2} \quad \text{F2.12}$$

therefore

$$R(\delta\alpha(\omega)) = \frac{P}{\pi} \int_0^{\infty} \frac{Q_a^{-1} \alpha_0}{\omega} d\omega \quad \text{F2.13}$$

$$R(\delta\alpha(\omega)) = \frac{\alpha_0 Q_a^{-1}}{\pi} \ln \omega/\omega_0 \quad \text{F2.14}$$

The lower bound frequency  $\omega_0$  is inserted to eliminate the singularity.

Similarly, for shear waves of velocity  $\beta$

$$R(\delta\beta(\omega)) = \frac{\beta_0 Q_\beta^{-1}}{\pi} \ln \omega/\omega_0 \quad \text{F2.15}$$

## APPENDIX G

### Computer Program Listings

This appendix contains the listings of six programs used in this study. The large program TSAP, which determines spectral amplitudes and group velocities, is listed by Burton and Blamey (1972). The major subroutine HH of the Hedgehog inversion program was developed by Mr B L N Kennett and Dr V P Valus. Many of these programs produce graphs using a Stromberg-Carlson 4060 plotter; several of the routines used to produce graphs are taken or adapted from Young and Douglas (1968). All of the programs are written in Fortran IV for the AWRE IBM 360/75 computer.

The listing of each program starts with a comprehensive block of comment cards. These cards detail the purpose, method of use and the output of the program so only a brief description of each program is given here.

The six programs are:

1        AVD

This program takes the theoretical equation for the variation of Rayleigh wave amplitude with distance from an event and fits a simple regression line to the observed data. The variation of Rayleigh wave amplitude with distance is such that

$$\text{AMPLITUDE TERM} = Q_Y^{-1} \times \text{DISTANCE TERM} + \text{CONSTANT}$$

therefore the gradient of the regression line estimates  $Q_Y^{-1}$ . Confidence limits on  $Q_Y^{-1}$  are calculated. So that the various regression lines may be compared the program calculates the regression line parameters for future use, these are: the mean and variance of the abscissa and ordinate, and the covariance.

2        CNL

3        C2L

4

QBAR

These three programs use the theory and formulae of Appendix E. The data are the regression line parameters provided by the program AVD.

The program CNL uses the regression line data at each frequency from a single explosion. The regression line at one frequency is compared to the lines at every other frequency; this process cycles through all the frequencies in turn.

C2L compares the regression line data at one frequency from one explosion with the corresponding data at the same frequency from a second explosion. The data for two distinct explosions are therefore compared at all the available matching frequencies.

The last program of this set, QBAR, determines the average gradient for several regression lines. Average  $Q_Y^{-1}$  and confidence limits are therefore obtained for each frequency using several explosions instead of one, this is irrespective of the yield of the individual explosions.

5

QRALEY

Theoretical calculations of the specific attenuation function  $Q_Y^{-1}(f)$  of Rayleigh waves are carried out by this program for a chosen layered model. The model must comprise values of the body wave velocities and specific attenuation factors for each of the NOL layers, that is  $\alpha_i$ ,  $\beta_i$ ,  $Q_{\alpha i}^{-1}$ ,  $Q_{\beta i}^{-1}$  for  $i=1\dots NOL$ .

Three frequency dependent terms must also be known. The group velocity  $U(f)$  must be known for the layered model at each frequency of interest. Derivatives of the wavenumber,  $\frac{\partial k_o}{\partial \alpha_{o1}}$  and  $\frac{\partial k_o}{\partial \beta_{o1}}$ , must be known at each frequency and for each layer. Finally, a condition may be written into the program uniquely relating  $Q_{\alpha}^{-1}$  and  $Q_{\beta}^{-1}$ . The theory from which  $Q_Y^{-1}(f)$  is calculated is given in Chapter 4.

6

HEDGEHOG

The Hedgehog procedure inverts the observed Rayleigh wave specific attenuation factor  $Q_{Y_o}^{-1}(f)$ , which is frequency dependent, into a depth

dependent attenuation model for  $Q_a^{-1}$  and  $Q_\beta^{-1}$ . A velocity-depth model and values of  $U(f)$ ,  $\frac{\partial k_o}{\partial a_{ol}}$ ,  $\frac{\partial k_o}{\partial \beta_{ol}}$ , similar to those used in the modelling for QRALEY must also be assumed.

The Hedgehog process described by Burton and Kennett (1972) differs from usual Monte-Carlo techniques in that after obtaining an acceptable model by a random process the next model is not selected at random but is chosen by an organised process - the aim being to delineate a region of connected solutions rather than an assortment of haphazard and unconnected solutions.



Q AMPLITUDE/DISTANCE PLOTS AT SEVERAL FREQUENCIES.  
\*\*\*\*\*

CALCULATES THE SPECIFIC ATTENUATION FACTOR FOR RAYLEIGH WAVES.  
\*\*\*\*\*

THIS PROGRAM TAKES THE EQUATION

$$\text{LOG}(A \cdot \text{SQRT}(E \cdot \text{SIN}(\text{DELTA}))) = (QMI) \cdot (-\text{PI} \cdot E \cdot \text{DELTA} \cdot F / U) + \text{CONSTANT}$$

AND FITS

$$Y = QMI \cdot X + \text{CONSTANT}$$

WHICH IS A SIMPLE REGRESSION LINE

A SPECTRAL AMPLITUDE IN MICRON\*SECONDS  
E RADIUS OF EARTH = 6371KM  
DELTA ANGULAR SEPERATION OF EVENT-RECORDING SITE  
QMI THE SPECIFIC ATTENUATION FACTOR FOR RAYLEIGH WAVES  
F FREQUENCY HZ  
U GROUP VELOCITY KM/S

THE TERM SQRT(E\*SIN(DELTA)) CORRECTS A FOR GEOMETRICAL SPREADING

\*\*\*\*\*

INPUT  
\*\*\*\*\*

THE FOLLOWING CARDS ARE READ IN

1 AN SC4060 CARD REQUIRED FOR GRAPHICAL OUTPUT

2 TITLE(I) TITLE FOR THE EVENT BEING PROCESSED

3 NSTAT,NFA,NFU,T

NSTAT NUMBER OF STATIONS FOR THE EVENT  
NFA NUMBER OF AMPLITUDE VALUES,A,AT SPECTRAL FREQUENCIES FA  
NFU NUMBER OF GROUP VELOCITIES,U,AT SPECTRAL FREQUENCIES FU  
THE GROUP VELOCITY FREQUENCIES MUST CORRESPOND TO THE  
FIRST,THIRD,FIFTH AMPLITUDE FREQUENCY ETC.  
T STUDENT'S 'T' ON NSTAT-2 DEGREES OF FREEDOM TO DETERMINE  
CONFIDENCE LIMITS

4 STATN(I),DELTA(I),TITLEA(I)

STATN RECORDING STATION NAME  
DELTA DISTANCE (DEGREES) BETWEEN EVENT-RECORDING STATION

5 A BLOCK OF NFA CARDS,EACH CARD CONTAINING

FA(I),AMTRX(I,J)

FA FREQUENCY FOR THE SPECTRAL AMPLITUDES  
AMTRX THE SPECTRAL AMPLITUDES

6 A BLOCK OF NFU CARDS,EACH CARD CONTAINING

FU(I),UMTRX(I,J)

FU FREQUENCY FOR THE GROUP VELOCITIES  
UMTRX THE GROUP VELOCITY

THE BLOCK OF CARDS 4,5,6 IS REPEATED FOR EACH STATION,NSTAT BLOCKS

\*\*\*\*\*

OUTPUT  
\*\*\*\*\*

PRINTOUT  
\*\*\*\*\*

- 1 A SUMMARY OF STATION NAMES,EPICENTRE-STATION SEPERATION AND GEOMETRICAL SPREADING TERM
- 2 THE AMPLITUDE SPECTRUM AND GROUP VELOCITY FOR EACH STATION
- 3 THE AMPLITUDE/DISTANCE TERMS FOR EACH FREQUENCY AND THE BEST LINE FIT
- 4 A SUMMARY OF INVERSE Q,INTERCEPTS OF THE BEST LINE AND 95P.C. CONFIDENCE LIMITS FOR EACH FREQUENCY

PUNCHOUT  
\*\*\*\*\*

- 1 AMPLITUDE/DISTANCE TERMS FOR EACH FREQUENCY (IF REQUIRED)
- 2 INVERSE Q VALUES,INTERCEPTS AND 95P.C. CONFIDENCE LIMITS AT

EACH FREQUENCY  
3 REGRESSION PARAMETERS FOR EACH A/D LINE E.G. MEAN OF 'X' AND 'Y'  
VARIANCES AND COVARIANCE. CARDS USED IN PROGRAMS C2L AND CNL

GRAPHS  
\*\*\*\*\*

1 AMPLITUDE/DISTANCE FOR EACH FREQUENCY (IF REQUIRED)  
2 INVERSE Q VALUES AND 95P.C. CONFIDENCE LIMITS

\*\*\*\*\*  
\*\*\*\*\*

COMMON /GRFF/ TITLE(20), XMAX, XMIN, YMAX, YMIN, INDX, INDY, IND,  
1 JJOOT, ANSTRI, IF, XLIMIT, YLIMIT, SCALX, SCALY  
DIMENSION AMTRX(40,99),UMTRX(40,99),FA(99),FU(99),TITLEA(40),  
1 DELTA(40),DELTAR(40),GEOMSP(40),DIST(40),STATN(40),  
2 X2(40,99),Y2(40,99),X1(40),Y1(40),  
3 TEMPU(99),CML(59),QLIM(99),INT(99),INTLIM(99),  
4 XBAR(99),YBAR(99),VARX(99),VAKY(99),COVXY(99)  
REAL INT,INTLIM  
REAL\*8 TITLE,STATN,TITLEA  
REAL\*8 DUMMY,ELANK  
DATA BLANK/8H

CALL SCLIBR

PI=4.0\*ATAN(1.0)  
DTOR=PI/180.0  
E=6371.0  
DO 990 I=6,20  
TITLE(I)=BLANK

990 CONTINUE  
CALL DATIM(TITLE(16),DUMMY)

-----  
INPUT DATA  
-----

998 READ (5,1,END=999)(TITLE(I),I=6,15)  
1 FORMAT(10A8)  
PRINT 2,(TITLE(I),I=6,16)  
2 FORMAT(1H1,/,1CX,10A8,2CX,A8,/) )  
READ 10, NSTAT, NFA, NFL, T  
10 FORMAT(3I10,F10.5)  
PRINT 15, NSTAT, NFA, NFL, T  
15 FORMAT(10X, 'NSTAT =', I5, 5X, 'NFA =', I5, 5X, 'NFU =', I5, 5X, 'T =', F6.3)  
C  
20 READ 20, STATN(1), DELTA(1), TITLEA(1)  
FORMAT(A8, F12.5, 2X, A8)  
25 READ 25, (FA(I), AMTRX(I, I), I=1, NFA)  
25 FORMAT(2E15.7)  
25 READ 25, (FU(I), UMTRX(I, I), I=1, NFU)

DO 30 J=2, NSTAT  
READ 20, STATN(J), DELTA(J), TITLEA(J)  
READ 45, (AMTRX(J, I), I=1, NFA)  
READ 45, (UMTRX(J, I), I=1, NFU)  
45 FORMAT(15X, E15.7)  
30 CONTINUE

-----  
GEOMETRICAL SPREADING CORRECTION (GEOMSP).  
-----

DO 110 J=1, NSTAT  
DELTAR(J)=DTOR\*DELTA(J)  
DIST(J)=DELTAR(J)\*E  
GEOMSP(J)=SQRT(E\*SIN(DELTAR(J)))  
110 CONTINUE  
PRINT 46  
46 FORMAT(//, 1CX, 'STATION', 11X, 'DATA NO.', 11X, 'DELTAD', 12X, 'DELTAR',  
11X, 'DISTANCE (KFS)', 1CX, 'SQRT(E\*SIN(DELTAR))', //)  
PRINT 47, (STATN(J), TITLEA(J), DELTA(J), DELTAR(J), DIST(J), GEOMSP(J),  
1J=1, NSTAT)  
47 FORMAT(10X, A8, 12X, A8, 9X, F6.2, 12X, F6.4, 12X, F8.1, 12X, F12.2)

-----  
GROUP VELOCITY SET UP IN MATRIX UMTRX S.T. FREQUENCIES  
ARE SAME AS FOR AMPLITUDES.  
-----

DO 60 J=1, NSTAT  
DO 70 I=1, NFU  
TEMPU(I)=UMTRX(J, I)  
70 CONTINUE  
DO 80 I=2, NFU  
UMTRX(J, 2\*I-2)=(TEMPU(I)+TEMPU(I-1))/2.0  
UMTRX(J, 2\*I-1)=TEMPU(I)  
80 CONTINUE  
60 CONTINUE  
DO 65 J=1, NSTAT  
PRINT 66, STATN(J)  
66 FORMAT(1H1, //, 1CX, A8, //, 1CX, '-----', //, 1CX, '1. INDEX 2. FREQUENCY 3.  
AMPLITUDE 4. GROUP VELOCITY', //)  
PRINT 67, (I, FA(I), AMTRX(I, I), UMTRX(J, I), I=1, NFA)

```

67  FORMAT(3(16,F8.5,2E13.5))
65  CONTINUE
C
C-----
C
C  CALCULATE AMPLITUDE/DISTANCE TERMS FOR EACH FREQUENCY
C-----
C
      ELG10=0.42429
      FAC1=P1*ELG10
      DO 90 I=1,NFA
      FAC2=FAC1*FA(I)
      DO 100 J=1,NSTAT
      X2(J,I)=FAC2*DIST(J)/UMTRX(J,I)
100  CONTINUE
90  CONTINUE
      DO 120 I=1,NFA
      DO 130 J=1,NSTAT
      Y2(J,I)=ALOG10(AMTRX(J,I))+ALOG10(GEOMSP(J))
      X1(J,I)=X2(J,I)
      Y1(J,I)=Y2(J,I)
130  CONTINUE
      PRINT 125,FA(I)
125  FORMAT(1H1,/,10X,'AMPLITUDE/DISTANCE PLOT AT FREQUENCY =',F8.5,' (
      HZ)',//)
      PRINT 126,(J,X1(J),Y1(J),J=1,NSTAT)
126  FORMAT(3(15,2E15.7))
      PUNCH 127,FA(I)
127  FORMAT(F10.7,'HZ  AMPLITUDE/DISTANCE FACTORS')
      PUNCH 128,(X1(J),Y1(J),J,I,STATN(J),TITLEA(J),J=1,NSTAT)
128  FORMAT(2E15.7,15X,15,'A/C',2X,13,2X,48,4X,48)
C-----
C
C  INVERSE Q LEAST SQUARES VALUES.
C-----
C
C  'BEST LINE FIT'
C-----
C
      CALL LSTSOR(X1,Y1,NSTAT,CM1(I),INT(I),R,XBAR(I),YBAR(I),QLIM(I),
      INTLIM(I),SDYTPC,T,VARX(I),VARY(I),COVXY(I))
      QM1(I)=-QM1(I)
      ANSTR1=1.0
      YMAX=6.0
      YMIN=1.0
      CALL CARGRF(X1,Y1,NSTAT)
C
      CALL TSP(130,48,42)
      CALL C4020H
      PRINT 700
700  FORMAT('FREQUENCY(HZ) =')
      CALL C4020F(FA(I),7,4)
      CALL ENDFHE
120  CONTINUE
C
C  AMPLITUDE/DISTANCE PLOTS SUMMATION OVER ALL FREQUENCIES.
      DO 140 J=1,NSTAT
      X1(J)=0.0
      Y1(J)=0.0
      DO 150 I=1,NFA
      X1(J)=X1(J)+X2(J,I)
      Y1(J)=Y1(J)+AMTRX(J,I)*AMTRX(J,I)
150  CONTINUE
      X1(J)=X1(J)/NFA
      ANFA=NFA
      Y1(J)=0.5*ALOG10(Y1(J))+ALOG10(GEOMSP(J)/SORT(ANFA))
140  CONTINUE
      PRINT 135
135  FORMAT(1H1,/,10X,'AMPLITUDE/DISTANCE PLOTS SUMMATION',//)
      PRINT 126,(J,X1(J),Y1(J),J=1,NSTAT)
      PUNCH 136
136  FORMAT(15X,'AMPLITUDE/DISTANCE PLOTS SUMMATION')
      K=NFA+1
      PUNCH 128,(X1(J),Y1(J),J,K,STATN(J),TITLEA(J),J=1,NSTAT)
      CALL LSTSOR(X1,Y1,NSTAT,CM1(K),INT(K),R,XBAR(K),YBAR(K),QLIM(K),
      INTLIM(K),SDYTPC,T,VARX(K),VARY(K),COVXY(K))
      QM1(K)=-QM1(K)
      ANSTR1=1.0
      YMAX=6.0
      YMIN=1.0
      CALL CARGRF(X1,Y1,NSTAT)
C
      CALL TSP(130,48,42)
      CALL C4020H
      PRINT 701
701  FORMAT('AMPLITUDE/DISTANCE PLOTS SUMMATION')
      CALL ENDFHE
C-----
C
C  SUMMARY OF INVERSE Q VALUES AND CONFIDENCE LIMITS.
C-----
C
      PRINT 2,(TITLE(I),I=6,16)
      PRINT 15,NSTAT,NFA,NFL,T
      PRINT 160
160  FORMAT(/,2('      FREQ.(HZ)  INVERSE Q & LIMITS INTERCEPT & LI
      MITS      '),//)
      PRINT 170,(I,FA(I),CM1(I),QLIM(I),INT(I),INTLIM(I),I=1,NFA)
170  FORMAT(2(16,F5.5,F13.5,F9.5,F11.4,F8.4,10X))
C-----
C
C  PUNCHOUT
C-----

```

```

PUNCH 1,(TITLE(I),I=6,15)
PUNCH 10,NFA
PUNCH 190,(FA(I),CM1(I),CLIM(I),INT(I),INTLIM(I),I=1,NFA)
180 FORMAT(F10.7,5X,4E15.7,15)
CALL UGRAPH(FA,CM1,CLIM,NFA)
PUNCH 1,(TITLE(I),I=6,15)
PUNCH 10,NFA
PUNCH 190,(FA(I),NSTAT,XBAR(I),YBAR(I),VARX(I),VARY(I),COVXY(I),
I,I=1,NFA)
190 FORMAT(F7.5,1E3,5E13.5,15)
GO TO 998
999 CALL FINISH
RETURN
END

```

SUBROUTINE LSTSCR(X,Y,N,A,B,R,XBAR,YBAR,SDATPC,SDBTPC,SDYTPC,T,
IVARX,VARY,COVXY)

DETERMINES THE SIMPLE LINEAR REGRESSION LINE - 'THE BEST LINE'

\*\*\*\*\*

DIMENSION X(N),Y(N)

SUMX=0.0
SUMY=0.0
SUMXX=0.0
SUMYY=0.0
SUMXY=0.0

DO 10 I=1,N
SUMX=SUMX+X(I)
SUMY=SUMY+Y(I)
SUMXX=SUMXX+X(I)\*X(I)
SUMYY=SUMYY+Y(I)\*Y(I)
SUMXY=SUMXY+X(I)\*Y(I)
10 CONTINUE

EN=N
EN2=EN-2.0
XBAR=SUMX/EN
YBAR=SUMY/EN
VARX=SUMXX/EN-XBAR\*XBAR
VARY=SUMYY/EN-YBAR\*YBAR
COVXY=SUMXY/EN-XBAR\*YBAR
SDX=SQRT(VARX)
SDY=SQRT(VARY)

A=COVXY/VARX
B=YBAR-A\*XBAR
R=A\*SQRT(VARX/VARY)

RR=R\*R
RSS=EN\*VARY\*(1.0-RR)
PARAM=RSS/(EN2\*EN\*VARX)

SDYTPC=T\*SQRT(RSS/EN2)
SDATPC=T\*SQRT(PARAM)
SDBTPC=T\*SQRT((PARAM\*SUMXX)/EN)

STUDT=SQRT((RR\*EN2)/(1.0-RR))

PRINTOUT

PRINT 20,XBAR,VARX,SDX,YBAR,VARY,SDY,A,SDATPC,B,SDBTPC,
1R,STUDT,SDYTPC
20 FORMAT(//8X,'MEAN OF X =',F10.5,16X,'VARIANCE OF X =',F11.5,15X,
1'STANDARD DEVIATION OF X =',F10.5,16X,'MEAN OF Y =',F10.5,16X,
2'VARIANCE OF Y =',F10.5,16X,'STANDARD DEVIATION OF Y =',F10.5,
3'//,51X,'GRADIENT A =',F13.6,' +OR-',F13.6,16X,'INTERCEPT B =',
4F13.6,' +OR-',F13.6,16X,'PRODUCT MOMENT CORRELATION COEFFICIENT
5 =',F6.2,5X,'STUDENTS T =',F5.2,
65X,'SCATTER IN CALCULATED Y VALUES =',F10.5)

RETURN
END

SUBROUTINE UGRAPH(X,Y,Z,N)

GRAPHS VALUES OF U,Y(I),CONFIDENCE LIMITS,Z(I),AT FREQUENCIES X(I).

REQUIRES THE PROGRAM CARGRF TO PRODUCE GRAPHS.
SEE AWRE REPRRT NO. C-41/68 (J.B.YOUNG & A.DOUGLAS)

\*\*\*\*\*

COMMON /GRFF/ TITLE(20), XMAX, XMIN,YMAX, YMIN, INDX, INDY, IND,

```

11DOT, ANSTR1, IF, XLIMIT, YLIMIT, SCALX, SCALY
DIMENSION X(N), Y(N), Z(N), YLIM(2), XATLIM(2)
REAL*8 TITLE
IND=1
IDOT=0
ANSTR1=1.0
IF=3
XMAX=0.0
XMIN=0.0
YMAX=0.0175
YMIN=0.0
CALL CARGRF(X,Y,N)
NOW OVERGRAPH THE SP.C. LIMITS.
NEW CARGRF PARAMETERS.
IND=2
IDOT=32
ANSTR1=2.0
DO 190 I=1,N
YLIM(2)=Y(I)+Z(I)
YLIM(1)=Y(I)-Z(I)
XATLIM(2)=X(I)
XATLIM(1)=X(I)
CALL CARGRF(XATLIM,YLIM,2)
190 CONTINUE
RETURN
END

```

NEW CARGRF

FROM THE CALL CARGRF(X,Y,N) THIS PACKAGE PLOTS N POINTS THE CARTESIAN CO-ORDINATES OF THE ITH POINT BEING SPECIFIED AS X(I),Y(I)

THE OPTIONS ARE SET BY USING THE COMMON -

COMMON /GRFF/ TITLE(20), XMAX, XMIN, YMAX, YMIN, INDX, INDY, IND, 11DOT, ANSTR1, IF, XLIMIT, YLIMIT, SCALX, SCALY

THE TITLE ARRAY CARRIES INFORMATION FOR ANNOTATING THE OUTPUT GRAPH. THIS ARRAY MUST BE SET UP AS FOLLOWS -

TITLE(1) -) : )CONTAINS 24 HOLLERITH CHARACTERS GIVING THE UNITS OF THE ABSCISSAE

TITLE(4) -) : )CONTAINS 16 HOLLERITH CHARACTERS GIVING THE UNITS OF THE ORDINATE

TITLE(6) -) : )CONTAINS 80 HOLLERITH CHARACTERS GIVING A TITLE TO THE GRAPH

TITLE(16) -) )CONTAINS 8 HOLLERITH CHARACTERS GIVING DATE OF PROCESSING

TITLE(17) -) )CONTAINS 8 HOLLERITH CHARACTERS GIVING TIME OF PROCESSING

TITLE(18) -) )UNUSED

TITLE(20) -)

XMAX )SET BOTH EQUAL IF PROGRAM TO CHOOSE THE ABSCISSAE SCALE. OTHERWISE SET TO CHOSEN LIMITS OF ABSCISSAE SCALE

YMAX )SET BOTH EQUAL IF PROGRAM TO CHOOSE THE ORDINATE SCALE. OTHERWISE SET TO CHOSEN VALUES OF ORDINATE SCALE

INDX IS AN INDICATOR FOR PLOTTING THE ABSCISSAE ON A LOG SCALE  
INDX=1 ABSCISSAE ON LINEAR SCALE  
INDX=2 ABSCISSAE ON LOG SCALE

INDY IS A SIMILAR INDICATOR FOR THE ORDINATE SCALE

N.B. CONTENTS OF ARRAYS ARE MODIFIED USING LOG SCALE

IND IS AN INDICATOR FOR CONTROLLING FRAME CALLS -  
IND=1 CARGRF CALLS ADVFLM AND PLOTS ON A NEW FRAME  
=2 CARGRF PLOTS ON THE CURRENT FRAME

IDOT IS THE SC4020 CODE OF THE REQUIRED PLOTTING SYMBOL

ANSTR1 INDICATES WHETHER THE PLOTTED POINTS HAVE TO BE JOINED UP  
ANSTR1=1. POINTS NOT JOINED  
=2. POINTS JOINED

IF SPECIFIES TYPE OF OUTPUT  
IF=1 OUTPLT ON MICROFILM  
=2 OUTPLT ON HARD COPY  
=3 OUTPLT ON BOTH MICROFILM AND HARD COPY

REWRITTEN BY J.B.YOUNG FOR THE IBM 360/75 ON 03/04/72

SUBROUTINE CARGRF(X,Y,N)

DIMENSION X(N), Y(N)

```

COMMON /GRFF/ TITLE(2C), XMAX, XMIN, YMAX, YMIN, IND, INDY, IND,
1IDOT, ANSTR1, IF, XLIMIT, YLIMIT, SCALX, SCALY
C
REAL*8 TITLE,DATE
C
REAL*4 INSTR1,JCIN/4HJCIN/,BLANK/4H /
C
INTEGER*4 PLACEX,PLACEY,XPLOT1,XPLOT2,YPLOT1,YPLOT2,XPOS,YPOS
C
CALL DATIM( DATE, TITLE(17))
IF( IF)2,2,1
IF( IF-4)3,3,2
2 IF=3
3 IF( IND.NE.2)IND=1
IF( INDX.NE.2)INDX=1
IF( INDY.NE.2)INDY=1
IF( IDOT.GT.63)IDCT=48
INSTR1=JOIN
IF( ANSTR1.EQ.1.)INSTR1=BLANK
C
GO TO (30,1C),INDX
10 POSXT=POSMIN(X,N)
DO 20 I=1,N
IF( X(I).LT.POSXT)X(I)=POSXT
X(I)=ALOG10(X(I))
20 CONTINUE
30 GO TO (60,4C),INDY
40 POSYT=POSMIN(Y,N)
DO 50 I=1,N
IF( Y(I).LT.POSYT)Y(I)=POSYT
Y(I)=ALOG10(Y(I))
50 CONTINUE
C
60 GO TO (10C,20C),IND
C
100 IF( XMAX-XMIN)11C,12C,11C
110 XMX=XMAX
XMN=XMIN
GO TO 13C
120 CALL AMAX(X,N, XMX)
CALL AMIN(X,N, XMN)
130 IF( YMAX-YMIN)14C,15C,14C
140 YMX=YMAX
YMN=YMIN
GO TO 16C
150 CALL AMAX(Y,N, YMX)
CALL AMIN(Y,N, YMN)
160 CALL ADVFLM( IF)
C
200 CALL SCALEN(X, XLIMIT, SCALX, PLACEX, XFACTR, N, XMX, XMN)
CALL SCALEN(Y, YLIMIT, SCALY, PLACEY, YFACTR, N, YMX, YMN)
XPLOT1=(X(1)-XLIMIT)*SCALX+123.
YPLOT1=923.-(Y(1)-YLIMIT)*SCALY
IF( N.NE.2) IDCT=1
IF( N.GT.63) IDCT=0
CALL PLOT(XPLOT1, IDCT, YPLOT1)
DO 230 I=2,N
IF( N.NE.2) IDCT=1
IF( N.GT.63) IDCT=0
XPLOT2=(X(I)-XLIMIT)*SCALX+123.
YPLOT2=923.-(Y(I)-YLIMIT)*SCALY
CALL PLOT(XPLOT2, IDCT, YPLOT2)
IF( INSTR1=JOIN)220,21C,220
210 CALL VECTOR(XPLOT1, YPLOT1, XPLOT2, YPLOT2)
220 YPLOT1=YPLOT2
XPLOT1=XPLOT2
230 CONTINUE
C
GO TO (30C,40C),IND
C
300 CALL VECTOR(115,923,1003,923)
CALL VECTOR(123,931,123,43)
DO 310 I=1,11
XPOS=203+(I-1)*8C
YPOS=43+(I-1)*8C
CALL VECTOR(XPOS,923,XPOS,931)
CALL VECTOR(115,YPOS,123,YPOS)
310 CONTINUE
DO 370 I=1,3
XLIM=XLIMIT+FLOAT(I-1)*XFACTR*4.
GO TO (330,32C),INDX
320 XPOS=92+(I-1)*320
CALL TSP(XPOS,4E,942)
CALL C402CE(1C,**XLIM,11,4)
GO TO 340
330 XPOS=20+PLACEX*8+(I-1)*320
CALL TSP(XPOS,4E,942)
CALL C402OF(XLIM,13,PLACEX)
340 YPOS=915-(I-1)*32C
YLIM=YLIMIT+FLOAT(I-1)*YFACTR*4.
GO TO (36C,35C),INDY
350 CALL TSP(28,4E,YPOS)
CALL C402CE(1C,**YLIM,11,4)
GO TO 370
360 CALL TSP(12,4E,YPOS)
CALL C402OF(YLIM,13,PLACEY)
370 CONTINUE
C

```

```
IF(TITLE(16),NE,DATE)GC TO 400
CALL TSP(760,48,958)
CALL HORAM(TITLE(1),24)
CALL TSP(48,48,291)
CALL VERAM(TITLE(4),16)
CALL TSP(130,48,23)
CALL HORAM(TITLE(6),80)
```

C

```
400 RETURN
END
```

C

```
SUBROUTINE SCALE(X,XLIMIT,SCALX,IPLACE,FACTOR,N,XMAX,XMIN)
```

C

```
COMPUTES SCALING VALUES FOR CARGR
```

C

```
DIMENSION X(N)
DOUBLE PRECISION XRG,R,FACT,S
```

C

```
XRG=XMAX-XMIN
IF(XRG.LT..0000000001)XRG=1.000
```

C

```
R=0.000
1 IF(XRG.LT.(10.000**R+.0000000001)) GO TO 2
R=R+1.000
GO TO 1
```

1

```
2 FACT=(10.000**R*(R-1.000)*.000000000125)
S=0.000
```

2

```
3 IF(XRG.LE.FACT*(2.000**S)) GO TO 4
S=S+1.000
GO TO 3
```

3

```
4 FACTUR=(FACT*(2.000**S))*10.00-2
```

4

```
XLIMIT=FLOAT(IFIX(XMIN/FACTOR))*FACTOR
IF(XMIN.LT.XLIMIT)XLIMIT=XLIMIT-FACTOR
SCALX=80./FACTOR
IPLACE=12.-R
IF(IPLACE.LT.1)IPLACE=1
```

C

```
RETURN
END
FUNCTION POSMIN(X,N)
```

C

```
FINDS MINIMUM POSITIVE VALUE OF ARRAY X
```

C

C

C

C

```
DIMENSION X(N)
```

```
DO 1 KQ=1,N
IF(X(KQ).LE.0.0)GO TO 1
```

```
GO TO 5
```

```
1 CONTINUE
```

```
PRINT 6
```

```
6 FORMAT(132H1AN ARRAY FROM WHICH THE SMALLEST POSITIVE VALUE WAS RE  
QUESTED FOR GRAPHING WAS ALL NEGATIVE YOUR JOB HAS THEREFORE BEEN
```

```
2 TERMINATED)
```

```
CALL FINISH
```

```
CALL EXIT
```

```
5 KP=KQ
```

```
2 IF(KQ-N)3,4,4
```

```
3 KQ=KQ+1
```

```
IF(X(KQ).LE.0.0)GO TO 2
```

```
IF(X(KP)-X(KQ))2,5,5
```

```
4 POSMIN=X(KP)
```

```
RETURN
```

```
END
```

```
SUBROUTINE AMAX(X,N,XMAX)
```

C

```
FINDS MAXIMUM VALUE OF ARRAY X
```

C

C

C

C

```
DIMENSION X(N)
```

```
KQ = 1
```

```
2 KP = KQ
```

```
5 IF(KQ -N)3,4,4
```

```
3 KQ = KQ + 1
```

```
IF(X(KP) - X(KQ))2,5,5
```

```
4 XMAX = X(KP)
```

```
RETURN
```

```
END
```

```
SUBROUTINE AMIN(X,N,XMIN)
```

C

```
FINDS MINIMUM VALUE OF ARRAY X
```

C

C

C

C

```
DIMENSION X(N)
```

```
KQ = 1
```

```
5 KP = KQ
```

```
2 IF(KQ -N)3,4,4
```

```
3 KQ = KQ + 1
```

```
IF(X(KP) - X(KQ))2,5,5
```

```
4 XMIN = X(KP)
```

```
RETURN
```

```
END
```

MAIN MULTIPLE COMPARISON OF REGRESSION LINES.  
 \*\*\*\*\*

COMPARES RESIDUAL VARIANCES, GRADIENTS & INTERCEPTS FOR REGRESSION LINES

REFERENCE  
 \*\*\*\*\*

K.A. BROWNLEE 'STATISTICAL THEORY & METHODOLOGY' P349-- (WILEY 65)

A TYPICAL REGRESSION LINE IS OF THE FORM

$$Y = AX + B$$

Y VARIABLE WITH ERRORS  
 X INDEPENDENT VARIABLE, NO ERRORS  
 A GRADIENT  
 B INTERCEPT

TWO SUCH LINES ARE TO BE COMPARED, EACH LINE HAS N POINTS

PRINTS OUT MATRICES OF COMPARISON WHICH CONTAIN THE NUMBERS 0, 1 OR 2

COMPARISON=0	TEST FAILED	BAD COMPARISON
COMPARISON=1	TEST PASSED	GOOD COMPARISON
COMPARISON=2	TEST NOT CONDUCTED	NO COMPARISON

NFTEST TEST FOR EQUALITY OF RESIDUAL VARIANCES OF LINES  
 NATEST TEST FOR EQUALITY OF GRADIENTS OF LINES  
 NBTEST TEST FOR EQUALITY OF INTERCEPTS OF LINES

\*\*\*\*\*

INPUT  
 \*\*\*\*\*

1 TITLE(I)

A TITLE FOR THE DATA BEING PROCESSED

2 FTABL1, FTABL2, TA, TB

FTABL1 = FTABL2 = F(N-2, N-2)	FISHER'S 'F'
TA = T(2N-4)	STUDENT'S 'T'
TB = T(2N-3)	STUDENT'S 'T'

3 NFA

THE NUMBER OF REGRESSION LINES (THE NUMBER OF FREQUENCIES)

4 A BLOCK OF NFA CARDS, EACH CARD CONTAINING

FREQ(I), N, XBAR(I), YBAR(I), VARX(I), VARY(I), COVXY(I)

FREQ	FREQUENCY HZ
N	NUMBER OF POINTS FOR LINE, HENCE DEGREES OF FREEDOM
XBAR	MEAN OF 'X'
YBAR	MEAN OF 'Y'
VARX	VARIANCE OF 'X'
VARY	VARIANCE OF 'Y'
COVXY	COVARIANCE OF 'X' & 'Y'

\*\*\*\*\*

OUTPUT  
 \*\*\*\*\*

PRINTOUT  
 \*\*\*\*\*

- 1 THE INPUT DATA
- 2 THE NFTEST MATRIX-----COMPARISON OF VARIANCE
- 3 THE NATEST MATRIX-----COMPARISON OF GRADIENTS
- 4 THE NBTEST MATRIX-----COMPARISON OF INTERCEPTS

\*\*\*\*\*  
 \*\*\*\*\*

DIMENSION FREQ(79), XBAR(79), YBAR(79), VARX(79), VARY(79), COVXY(79),  
 1 A(79), F(79), VRSS(79),  
 2 NFTEST(79,79), NATEST(79,79), NBTEST(79,79),  
 3 TITLE(20)  
 REAL\*8 TITLE, DUMMY



```

C      CALL DATIM(TITLE(16),DUMMY)
C
C      INPUT DATA
C-----
998  READ(5,10,END=999)(TITLE(I),I=6,15)
    PRINT 85,(TITLE(I),I=6,16)
    READ 5,FTABL1,FTABL2,TA,TB
    PRINT5,FTABL1,FTABL2,TA,TB
5    FORMAT(4F10.5)
10   FORMAT(10A6)
    READ 20,NFA
    PRINT 20,NFA
20   FORMAT(1X,15)
    READ 30,(FREQ(I),N,XBAR(I),YBAR(I),VARX(I),VARY(I),COVXY(I),
1    I=1,NFA)
1    PRINT31,(FREQ(I),N,XBAR(I),YBAR(I),VARX(I),VARY(I),COVXY(I),
1    I=1,NFA)
30   FORMAT(F7.5,13,5F13.5)
31   FORMAT(1X,F7.5,13,5E13.5)
C-----
C
    DO 50 I=1,NFA
    DO 40 J=1,NFA
    NFTEST(I,J)=2
    NATEST(I,J)=2
    NBTEST(I,J)=2
40   CONTINUE
50   CONTINUE
    DO 60 I=1,NFA
    CALL REGR(N,XBAR(I),YBAR(I),VARX(I),VARY(I),COVXY(I),A(I),B(I),
1    VRSS(I))
60   CONTINUE
C
    DO 80 I=2,NFA
    K=I-1
    DO 70 J=1,K
    CALL FTLST(VRSS(I),VRSS(J),FTABL1,FTABL2,NFTEST(I,J),NSIZE,F)
    IF(NFTEST(I,J).EQ.1) CALL CLINES(
1    TA,TB,N,H,XBAR(I),XBAR(J),YBAR(I),YBAR(J),VARX(I),VARX(J),
2    VARY(I),VARY(J),
3    COVXY(I),COVXY(J),VRSS(I),VRSS(J),ANEW,VARA,
4    NATEST(I,J),NBTEST(I,J))
70   CONTINUE
80   CONTINUE
    PRINT 85,(TITLE(I),I=6,16)
    FORMAT(1H1,/,10X,10A6,20X,A8,/)
    PRINT 90
90   FORMAT(40X,'NFTEST MATRIX',/)
    DO 100 I=1,NFA
    PRINT 110,(NFTEST(I,J),J=1,I)
100  CONTINUE
110  FORMAT(10X,79I1)
    PRINT 85,(TITLE(I),I=6,16)
    PRINT 120
120  FORMAT(40X,'NATEST (GRADIENTS) MATRIX',/)
    DO 130 I=1,NFA
    PRINT 110,(NATEST(I,J),J=1,I)
130  CONTINUE
    PRINT 85,(TITLE(I),I=6,16)
    PRINT 140
140  FORMAT(40X,'NBTEST (INTERCEPTS) MATRIX',/)
    DO 150 I=1,NFA
    PRINT 110,(NBTEST(I,J),J=1,I)
150  CONTINUE
C
    GO TO 998
999  RETURN
    END
C
C
C
C
C      SUBROUTINE REGR(N,XBAR,YBAR,VARX,VARY,COVXY,A,B,VRSS)
C
C      FOR THE REGRESSION LINE 'Y = AX + B' THIS CALCULATES
C
C          A      THE GRADIENT
C          B      THE INTERCEPT
C          VRSS   THE VARIANCE OF THE RESIDUAL SUM OF SQUARES
C
C      GIVEN----
C
C          N      THE NUMBER OF LINE POINTS
C          XBAR   MEAN OF 'X'
C          YBAR   MEAN OF 'Y'
C          VARX   VARIANCE OF 'X'
C          VARY   VARIANCE OF 'Y'
C          COVXY  COVARIANCE OF 'X' & 'Y'
C
C      *****
C      *****
C
A=COVXY/VARX
B=YBAR-A*XBAR
FN=N
EN2=EN-2.0
RSS=EN*VARY-EN*A*COVXY
VRSS=RSS/EN2

```



MAIN COMPARISON OF PAIRED REGRESSION VALUES FOR NFA PAIRED LINES.  
\*\*\*\*\*

COMPARES RESIDUAL VARIANCES, GRADIENTS & INTERCEPTS FOR REGRESSION LINES

REFERENCE  
\*\*\*\*\*

K.A. BROWNLEE 'STATISTICAL THEORY & METHODOLOGY' P349-- (WILEY 65)

A TYPICAL REGRESSION LINE IS OF THE FORM

$Y = AX + B$

Y VARIABLE WITH ERRORS  
X INDEPENDENT VARIABLE, NO ERRORS  
A GRADIENT  
B INTERCEPT

TWO SUCH LINES ARE TO BE COMPARED, THE LINES HAVE N1 AND N2 POINTS

PRINTS OUT RESULTS OF COMPARISON WHICH ARE THE NUMBERS 0, 1 OR 2

COMPARISON=0 TEST FAILED BAD COMPARISON  
COMPARISON=1 TEST PASSED GOOD COMPARISON  
COMPARISON=2 TEST NOT CONDUCTED NO COMPARISON

FTTEST TEST FOR EQUALITY OF RESIDUAL VARIANCES OF LINES  
NATEST TEST FOR EQUALITY OF GRADIENTS OF LINES  
NBTEST TEST FOR EQUALITY OF INTERCEPTS OF LINES

\*\*\*\*\*

INPUT  
\*\*\*\*\*

1 TITLE(I)

A TITLE FOR THE REGRESSION DATA

2 NFA

THE NUMBER OF PAIRS OF LINES TO BE COMPARED

3 A BLOCK OF NFA CARDS, EACH CARD CONTAINING

FREQ(J), N(I), XBAR(I, J), YBAR(I, J), VARX(I, J), VARY(I, J), COVXY(I, J)

FREQ FREQUENCY HZ  
N NUMBER OF POINTS FOR LINE, HENCE DEGREES OF FREEDOM  
XBAR MEAN OF 'X'  
YBAR MEAN OF 'Y'  
VARX VARIANCE OF 'X'  
VARY VARIANCE OF 'Y'  
COVXY COVARIANCE OF 'X' & 'Y'

THE CARDS 1--3 ARE REPEATED FOR THE SECOND BLOCK OF DATA TO FORM  
NFA PAIRS OF LINES

4 FTABL1, FTABL2, TA, TB

FTABL1 = F(N1-2, N2-2) FISHER'S 'F'  
FTABL2 = F(N2-2, N1-2) FISHER'S 'F'  
TA = T(N1+N2-4) STUDENT'S 'T'  
TB = T(N1+N2-3) STUDENT'S 'T'

\*\*\*\*\*

OUTPUT  
\*\*\*\*\*

PRINTOUT  
\*\*\*\*\*

1 THE INPUT DATA  
2 A TABLE OF FREQUENCY VALUES, GRADIENT LINE 1, GRADIENT LINE 2,  
RESULTS OF FTTEST, NATEST AND NBTEST AND THE NEW RESULTANT GRADIENT  
(IF FORMED) AND CONFIDENCE LIMITS ON IT

\*\*\*\*\*  
\*\*\*\*\*

```

C
C
DIMENSION FREQ(79),
1 N(2), XBAR(2,79), YBAR(2,79), VARX(2,79), VARY(2,79),
2 COVXY(2,79), A(2,79), B(2,79), VRSS(2,79),
3 ANEW(79), VANEW(79), CONLIM(79),
4 NTEST(79), NATEST(79), NBTEST(79),
5 TITLE(2,20)
REAL*8 TITLE,DUMMY
998 DO 40 I=1,2
CALL DATIM(TITLE(I,16),DUMMY)
-----
C
C
C INPUT DATA
C
C
READ (5,10,END=999)(TITLE(I,J),J=6,15)
PRINT 65,(TITLE(I,J),J=6,16)
10 FORMAT(10A8)
READ 20,NFA
PRINT 20,NFA
20 FORMAT(1X,I9)
READ 30,(FREQ(J),N(I),XBAR(I,J),YBAR(I,J),VARX(I,J),VARY(I,J),
1COVXY(I,J),J=1,NFA)
PRINT 31,(FREQ(J),N(I),XBAR(I,J),YBAR(I,J),VARX(I,J),VARY(I,J),
1COVXY(I,J),J=1,NFA)
30 FORMAT(F7.5,I3,5F13.5)
31 FORMAT(1X,F7.5,I3,5F13.5)
40 CONTINUE
READ 50,FTABL1,FTABL2,TA,TB
PRINT 50,FTABL1,FTABL2,TA,TB
50 FORMAT(4F10.5)
-----
C
C
DO 60 J=1,NFA
NTEST(J)=2
NATEST(J)=2
NBTEST(J)=2
ANEW(J)=0.0
VANEW(J)=0.0
CONLIM(J)=0.0
60 CONTINUE
PRINT 65,(TITLE(1,I),I=6,16)
PRINT 66,(TITLE(2,I),I=6,16)
65 FORMAT(1H1,/,10X,10A8,20X,A8)
66 FORMAT(10X,10A8,20X,A8,/)
PRINT 67
67 FORMAT(25X,'FREQUENCY A1 A2 NTEST NATEST NB
1TEST NEW GRADIENT & LIMITS',/)
DO 90 J=1,NFA
DO 70 I=1,2
CALL REGR(N,I),XBAR(I,J),YBAR(I,J),VARX(I,J),VARY(I,J),COVXY(I,J),
1A(I,J),B(I,J),VRSS(I,J))
70 CONTINUE
CALL FTTEST(VRSS(1,J),VRSS(2,J),FTABL1,FTABL2,NTEST(J),NSIZE,F)
IF(NTEST(J).EQ.1) CALL CLINES
1(TA,TB,N(1),N(2),XBAR(1,J),XBAR(2,J),YBAR(1,J),YBAR(2,J),
2VARX(1,J),VARX(2,J),VARY(1,J),VARY(2,J),COVXY(1,J),COVXY(2,J),
3VRSS(1,J),VRSS(2,J),ANEW(J),VANEW(J),
4NATEST(J),NBTEST(J))
IF(NTEST(J).EQ.1) CONLIM(J)=TB*SQRT(VANEW(J))
PRINT 80,J,FREQ(J),A(1,J),A(2,J),NTEST(J),NATEST(J),NBTEST(J),
1ANEW(J),CONLIM(J)
80 FORMAT(10X,I10,3X,3F10.6,17,2I10,5X,2F10.6)
90 CONTINUE
GO TO 998
999 RETURN
END
C
C
C
C
SUBROUTINE REGR(N,XBAR,YBAR,VARX,VARY,COVXY,A,B,VRSS)
FOR THE REGRESSION LINE 'Y = AX + B' THIS CALCULATES
A THE GRADIENT
B THE INTERCEPT
VRSS THE VARIANCE OF THE RESIDUAL SUM OF SQUARES
GIVEN----
N THE NUMBER OF LINE POINTS
XBAR MEAN OF 'X'
YBAR MEAN OF 'Y'
VARX VARIANCE OF 'X'
VARY VARIANCE OF 'Y'
COVXY COVARIANCE OF 'X' & 'Y'
*****
*****
A=COVXY/VARX
B=YBAR-A*XBAR
EN=N
EN2=EN-2.0
RSS=EN*VARY-EN*A*COVXY
VRSS=RSS/EN2
RETURN
END

```



QBAR

AVERAGE GRADIENTS FOR A SET OF REGRESSION LINES-----AVERAGE QI  
\*\*\*\*\*

QI IS THE SPECIFIC ATTENUATION FACTOR FOR RAYLEIGH WAVES

THIS PROGRAM CALCULATES THE AVERAGE GRADIENT FOR SEVERAL SETS OF  
REGRESSION LINES

FOR NDATA BLOCKS OF DATA (EVENTS), EACH BLOCK CONTAINING NFA  
REGRESSION LINE PARAMETERS (FROM AMPLITUDE-DISTANCE PLOTS AT NFA  
FREQUENCIES) THE PROGRAM CALCULATES NFA AVERAGE GRADIENTS (AVERAGE  
INVERSE Q VALUES, QI, AT NFA FREQUENCIES) CONFIDENCE LIMITS ON THE  
AVERAGES ARE ALSO OBTAINED.

NOTE

\*\*\*\*

THIS PROGRAM REQUIRES THE SUBROUTINE-----

SUBROUTINE REGR(N,XBAR,YBAR,VARX,VARY,COVXY,A,B,VRSS)

\*\*\*\*\*

INPUT

\*\*\*\*

1 NDATA

THE NUMBER OF BLOCKS OF DATA(EVENTS) TO BE AVERAGED

2 TA

STUDENT'S 'T' TO DETERMINE CONFIDENCE LIMITS ON THE AVERAGE QI  
THE DEGREES OF FREEDOM ARE-----THE SUM OF THE NUMBER OF POINTS  
FOR EACH LINE, MINUS THE NUMBER OF EVENTS, MINUS ONE

3 TITLE(I,J)

A TITLE FOR ONE BLOCK OF REGRESSION DATA (FOR ONE EVENT)

4 NFA

THE NUMBER OF REGRESSION LINES PER EVENT (FOR FREQUENCIES F)  
NFA MUST BE THE SAME FOR EACH EVENT

5 A BLOCK OF NFA CARDS, EACH CARD CONTAINING

F(J),N(I),XBAR(I,J),YBAR(I,J),VARX(I,J),VARY(I,J),COVXY(I,J)

F FREQUENCY HZ

N NUMBER OF POINTS FOR LINE, HENCE DEGREES OF FREEDOM

XBAR MEAN OF 'X'

YBAR MEAN OF 'Y'

VARX VARIANCE OF 'X'

VARY VARIANCE OF 'Y'

COVXY COVARIANCE OF 'X' & 'Y'

THE CARDS 3--5 ARE REPEATED FOR EACH OF THE NDATA BLOCKS (EVENTS)  
TO FORM NFA AVERAGES

\*\*\*\*\*

OUTPUT

\*\*\*\*

PRINTOUT

\*\*\*\*\*

1 THE INPUT DATA

2 A TABLE OF FREQUENCY, AVERAGE QI AND CONFIDENCE LIMITS

PUNCHOUT

\*\*\*\*\*

1 THE AVERAGE VALUES OF QI AND CONFIDENCE LIMITS AT FREQUENCIES  
F ARE PUNCHED OUT

\*\*\*\*\*

DIMENSION F(80),  
N(9), XBAR(9,80), YBAR(9,80), VARX(9,80), VARY(9,80),

```

2COVXY(9,80),A(9,80),VRSS(9,80),
3ANEW(80),VANEW(80),CONLIM(80),
4TITLE(9,20),QRMI(80),
5ENM2(9),SQXX(9),SQYY(9),SQXY(9)
REAL*8 TITLE,DUMMY

```

C  
C  
C  
C  
C

-----  
INPUT DATA  
-----

```

998 READ (5,10,END=999) NDATA
10  FORMAT(1X,I9)
   PRINT11,NDATA
11  FORMAT(1H1,1X,I9)
   READ 20,TA
   PRINT31,TA
   DO 40 I=1,NDATA
   CALL DATIM(TITLE(I,16),DUMMY)
   READ 20,(TITLE(I,J),J=6,15)
   PRINT 25,(TITLE(I,J),J=6,16)
20  FORMAT(10A8)
25  FORMAT(1H1,10X,10A8,20X,A8)
   READ 10,NFA
   PRINT10,NFA
   READ 30,(F(J),N(I),XBAR(I,J),YBAR(I,J),VARX(I,J),VARY(I,J),
1COVXY(I,J),J=1,NFA)
   PRINT31,(F(J),N(I),XBAR(I,J),YBAR(I,J),VARX(I,J),VARY(I,J),
1COVXY(I,J),J=1,NFA)
30  FORMAT(F7.5,I3,5E13.5)
31  FORMAT(1X,F7.5,I3,5E13.5)
40  CONTINUE

```

C  
C  
C

```

DO 70 J=1,NFA
SQXXNU=0.0
SQYYNU=0.0
SQXYNU=0.0
DENOM =0.0
RSS =0.0
DO 60 I=1,NDATA
CALL REGR(N(I),XBAR(I,J),YBAR(I,J),VARX(I,J),VARY(I,J),CCVXY(I,J),
1 A(I,J),B,VRSS(I,J))
FN(I)=N(I)
ENM2(I)=EN(I)-2.0
SQXXNU=EN(I)*VARX(I,J)+SQXXNU
SQXYNU=EN(I)*COVXY(I,J)+SQXYNU
RSS=ENM2(I)*VRSS(I,J)+RSS
DENOM=ENM2(I)+DENOM
60  CONTINUE
ANEW(J)=SQXYNU/SQXXNU
QRMI(J)=-ANEW(J)
VANEW(J)=RSS/((DENOM+NDATA-1.0)*SQXXNU)
CONLIM(J)=TA*SQRT(VANEW(J))
70  CONTINUE

```

C  
C  
C

-----  
OUTPUT  
-----

C  
C  
C  
C  
C

-----  
PRINTOUT  
-----

```

DO 80 I=1,NDATA
IF(I .EQ.1) PRINT 25,(TITLE(1,J),J=6,16)
IF(I .NE.1) PRINT 26,(TITLE(1,J),J=6,16)
26  FORMAT(1X,10X,10A8,20X,A8)
80  CONTINUE
PRINT 85
85  FORMAT(/,2(26X,'FREQ.(HZ) INVERSE Q & LIMITS',10X),/)
PRINT 90,(I,F(I),QRMI(I),CONLIM(I),I=1,NFA)
90  FORMAT(2(20X,I5,F9.5,F11.6,F10.6,10X))

```

C  
C  
C  
C

-----  
PUNCHOUT  
-----

```

DO 92 I=1,NDATA
PUNCH 20,(TITLE(I,J),J=6,15)
PUNCH 95,(F(I),QRMI(I),CONLIM(I),I=1,NFA)
95  FORMAT(F10.7,5X,2E15.7,30X,I5)

```

C  
C  
C

-----  
GO TO 998  
RETURN  
END

ORALEY

ORALEY MAIN  
\*\*\*\*\*

THIS PROGRAM MAKES THEORETICAL CALCULATIONS OF THE ATTENUATION COEFFICIENT, GAMMA, AND THE SPECIFIC ATTENUATION FACTOR, QI, FOR RAYLEIGH WAVES AT NPERPT FREQUENCIES. AN ATTENUATION MODEL WITH NOL LAYERS IS REQUIRED.

THE PROGRAM USES THE EQUATIONS

$$\text{GAMMA} = \text{SUM OVER LAYERS} (0.5 * \text{DKBYDA} * \text{A} * \text{QAI} + 0.5 * \text{DKBYDB} * \text{B} * \text{QBI})$$

$$\text{QI} = (-\text{L} * \text{GAMMA}) / (\text{PI} * \text{FREQ})$$

GAMMA THE ATTENUATION COEFFICIENT  
A THE VELOCITY OF COMPRESSIONAL BODILY WAVES  
QAI THE SPECIFIC ATTENUATION FACTOR FOR COMPRESSIONAL WAVES  
DKBYDA THE PARTIAL DERIVATIVES OF THE WAVENUMBER, K, W.R.T. THE COMPRESSIONAL VELOCITY, A  
B THE VELOCITY OF SHEAR BODILY WAVES  
QBI THE SPECIFIC ATTENUATION FACTOR FOR SHEAR WAVES  
DKBYDB THE PARTIAL DERIVATIVES OF THE WAVENUMBER, K, W.R.T. THE SHEAR VELOCITY, B  
  
QI THE SPECIFIC ATTENUATION FACTOR FOR RAYLEIGH WAVES  
U THE GROUP VELOCITY  
FREQ FREQUENCY HZ

\*\*\*\*\*

INPUT  
\*\*\*\*\*

THE FOLLOWING CARDS ARE READ IN

- 1 AN SC4060 CARD TO PRODUCE GRAPHS
- 2 TITLE(I)  
A TITLE FOR THE MODEL UNDER CONSIDERATION
- 3 GRAPH1(I)  
A TITLE FOR THE GRAPH OF GAMMA AS A FUNCTION OF FREQUENCY
- 4 GRAPH2(I)  
A TITLE FOR THE GRAPH OF QI AS A FUNCTION OF FREQUENCY
- 5 NOL, NPERPT  
NOL THE NUMBER OF LAYERS IN THE MODEL  
NPERPT THE NUMBER OF FREQUENCIES TO BE USED
- 6 A BLOCK OF NOL CARDS, EACH CARD CONTAINING  
QAI(I), QBI(I)  
QAI THE SPECIFIC ATTENUATION FACTOR FOR COMPRESSIONAL WAVES IN EACH LAYER  
QBI THE SPECIFIC ATTENUATION FACTOR FOR SHEAR WAVES IN EACH LAYER
- 7 A BLOCK OF NOL CARDS, EACH CARD CONTAINING  
A(I), B(I)  
A COMPRESSIONAL BODILY WAVE VELOCITY FOR EACH LAYER  
B SHEAR BODILY WAVE VELOCITY FOR EACH LAYER
- 8 A BLOCK OF NPERPT CARDS, EACH CARD CONTAINING  
FREQ(I), U(I)  
FREQ FREQUENCY HZ  
U GROUP VELOCITY
- 9 A BLOCK OF NPERPT CARDS, EACH CARD CONTAINING NOL VALUES  
DKBYDA(I, J)  
DKBYDA PARTIAL DERIVATIVES OF THE WAVENUMBER, K, W.R.T. A FOR EACH LAYER AND AT EACH FREQUENCY
- 10 A BLOCK OF NPERPT CARDS, EACH CARD CONTAINING NOL VALUES  
DKBYDB(I, J)  
DKBYDB PARTIAL DERIVATIVES OF THE WAVENUMBER, K, W.R.T. B FOR EACH LAYER AND AT EACH FREQUENCY



NOTE THAT THE ABOVE CARDS 2 TO 10 MAY BE REPEATED FOR ANY NUMBER OF MODELS

\*\*\*\*\*

OUTPUT  
\*\*\*\*\*

PRINTOUT  
\*\*\*\*\*

- 1 THE ORIGINAL MODEL OF A,B,QAI,QBI
- 2 THE GROUP VELOCITY CURVE
- 3 A TABLE OF THE PARTIAL DERIVATIVES W.R.T. A
- 4 A TABLE OF THE PARTIAL DERIVATIVES W.R.T. B
- 5 A SUMMARY TABLE OF GAMMA AS A FUNCTION OF FREQUENCY
- 6 A SUMMARY TABLE OF QI AS A FUNCTION OF FREQUENCY

PUNCHOUT  
\*\*\*\*\*

- 1 THE VALUES OF QI AND FREQUENCY ARE PUNCHED OUT

GRAPHS  
\*\*\*\*\*

- 1 THE GROUP VELOCITY CURVE
- 2 THE ATTENUATION COEFFICIENT AS A FUNCTION OF FREQUENCY
- 3 THE SPECIFIC ATTENUATION FACTOR AS A FUNCTION OF FREQUENCY
- 4 THE DERIVATIVES FOR EACH LAYER AS A FUNCTION OF FREQUENCY (IF REQUIRED)

\*\*\*\*\*

```
DIMENSION U(90),PERIOD(90),GAMMA(90),QI(90),FREQ(90)
DIMENSION TITLE(20),GRAPH1(20),GRAPH2(20)
DIMENSION DERIVA(90),DERIVB(90)
COMMON /LAYE/A(20),B(20),QAI(20),QBI(20),DKBYDA(90,10),
1      CKBYDB(90,10),NOL
```

```
REAL*8 TITLE,GRAPH1,GRAPH2,DUMMY
CALL SCLIBR
NGRAPH=2
```

```
100 READ(5,1,END=999)(TITLE(I),I=6,15)
    READ 1,(GRAPH1(I),I=6,15)
    READ 1,(GRAPH2(I),I=6,15)
1   FORMAT(10A8)
    CALL DATIM(TITLE(16),DUMMY)
    CALL DATIM(GRAPH1(16),DUMMY)
    CALL DATIM(GRAPH2(16),DUMMY)
    PRINT 2,(TITLE(I),I=6,16)
2   FORMAT(1H1,///,20X,10A8,20X,A8)
```

-----  
INPUT DATA  
-----

```
3   READ 3,NOL,APERPT
    FORMAT(2I10)
    PRINT 4,NOL,NPERPT
4   FORMAT(///30X,'NLAYERS = ',15,10X,'NPERPT = ',15)
    READ 5,(QAI(I),QBI(I),I=1,NOL)
    READ 5,(A(I),B(I),I=1,NOL)
5   FORMAT(2F10.5)
    READ 6,(FREQ(I),U(I),I=1,NPERPT)
6   FORMAT(2F10.6)
    DO 7 I=1,NPERPT
    READ 9,(DKBYDA(I,J),J=1,NOL)
7   CONTINUE
    DO 8 I=1,NPERPT
    READ 9,(DKBYDB(I,J),J=1,NOL)
8   CONTINUE
9   FORMAT(6F12.9)
```

-----  
CONDITION  
-----

```
QBI(1)=2.29*QAI(1)
QBI(2)=2.29*QAI(2)
QBI(3)=2.51*QAI(3)
QBI(4)=2.51*QAI(4)
QBI(5)=2.51*QAI(5)
QBI(6)=2.19*QAI(6)
```

-----  
CALCULATION OF GAMMA FOR A PARTICULAR PERIOD.  
-----

```
DO 10 I=1,NPERPT
GAMMAT=0.0
CALL ATTEM(GAMMAT,I)
GAMMA(I)=GAMMAT
```



```

C
C
C
C
*****
*****
COMMON /LAYER/A(20),B(20),QAI(20),QBI(20),DKBYDA(90,10),
1 CKBYDB(90,10),NOL
C
1 CALCULATE GAMMAT
GAMMAT=0.0
DO 1 I=1,NOL
GAMMAT=GAMMAT+DKBYDA(NPER,I)*A(I)*0.5*QAI(I)
1 +DKBYDB(NPER,I)*B(I)*0.5*QBI(I)
C
1 CONTINUE
C
RETURN
END
C
C
C
C
SUBROUTINE GRAPH(X,Y,N,TITLE,NAME)
C
C
C
1 SUBROUTINE GRAPHS N VALUES OF X AGAINST Y.
2 IF NAME=0 THE GRAPH IS UNTITLED.
3 IF NAME=1 THEN TITLE MUST BE READ IN AND SDATE CALLED
BEFORE THIS SUBROUTINE IS CALLED.
4 CALL SCLIBR ESSENTIAL IN MAIN PROGRAM.
5 REQUIRES THE PROGRAM CARGRF TO PRODUCE GRAPHS.
SEE AKRE REPERT NO. C-41/68 (J.B.YOUNG & A.DOUGLAS)
C
*****
*****
COMMON /GRFF/ ATITLE(20),XMAX,XMIN,YMAX,YMIN,INDX,INDY,IND,IDOT,
ANSTR1,IF,XLIPIT,YLIPIT,SCALX,SCALY
C
DIMENSION X(N),Y(N)
DIMENSION TITLE(20),BTITLE(20)
REAL*8 TITLE,ATITLE,BTITLE,DUMMY,BLANK
C
DATA BLANK/8H /
DATA BTITLE/4CHFREQUENCY (HZ) AMPLITUDE /
C
DO 1 I=1,20
TITLE(I)=BLANK
CONTINUE
1
DO 5 I=1,5
TITLE(I)=BTITLE(I)
CONTINUE
5
C
IF (NAME.EQ.1) GO TO 2
DO 3 I=6,15
TITLE(I)=BLANK
CONTINUE
3
CALL DATIM(TITLE(16),DUMMY)
CONTINUE
2
DO 4 I=1,20
ATITLE(I)=TITLE(I)
CONTINUE
4
C
SET CARGRF PARAMETERS
C
INDX=1
INDY=1
IND=0
IDOT=42
ANSTR1=2.0
IF=3
C
XMAX=0.0
XMIN=0.0
YMAX=0.0
YMIN=0.0
C
CALL CARGRF(X,Y,N)
C
RETURN
END

```

HEDGEHOG

'HEDGEHOG' MAIN  
\*\*\*\*\*

THIS PROGRAM INVERTS THE OBSERVED SPECIFIC ATTENUATION FACTOR AS  
A FUNCTION OF FREQUENCY FOR RAYLEIGH WAVES INTO AN ATTENUATION  
MODEL AS A FUNCTION OF DEPTH

REFERENCE  
\*\*\*\*\*

P.W.BURTON & B.L.N.KENNETT 'UPPER MANTLE ZONE OF LOW Q'  
(NATURE PHYS. SCI. 238 PP87-90)

ACKNOWLEDGEMENTS  
\*\*\*\*\*

FOR THE SUBROUTINE HH---'HEHGEHOG'---THANKS TO B.L.N.KENNETT  
AND TO V.P.VALLUS

\*\*\*\*\*

INPUT  
\*\*\*\*\*

THE FOLLOWING CARDS ARE READ IN

1 TITLE(I)

A TITLE FOR THE DATA CURRENTLY BEING INVERTED

2 K

FOR K READ IN THE NUMBER OF LAYERS, NOL, IN THE MODEL

3 A BLOCK OF NOL CARDS, EACH CARD CONTAINING

LIMIT1(I), LIMIT2(I), STEP(I)

LIMIT1 THE LOWER LIMIT ON THE SPECIFIC ATTENUATION FACTOR  
FOR A LAYER (COMPRESSIONAL WAVES)

LIMIT2 THE UPPER LIMIT ON THE SPECIFIC ATTENUATION FACTOR  
FOR A LAYER (COMPRESSIONAL WAVES)

STEP THE INCREMENT USED TO STEP ALONG FROM LIMIT1 TO LIMIT2

4 STAPE, RANK, INT1, INT2, N, NMAX, ALG

SEE SUBROUTINE HH FOR EXPLANATION  
NMAX-N IS THE NUMBER OF MODELS TO BE TESTED

5 NOL, NPERPT

NOL THE NUMBER OF LAYERS IN THE MODEL  
NPERPT THE NUMBER OF FREQUENCIES TO BE USED

6 A BLOCK OF NOL CARDS, EACH CARD CONTAINING

A(I), B(I)

A COMPRESSIONAL BODILY WAVE VELOCITY FOR EACH LAYER  
B SHEAR BODILY WAVE VELOCITY FOR EACH LAYER

7 A BLOCK OF NPERPT CARDS, EACH CARD CONTAINING

FREQ(I), U(I)

FREQ FREQUENCY HZ  
U GROUP VELOCITY

8 A BLOCK OF NPERPT CARDS, EACH CARD CONTAINING NOL VALUES

DKBYDA(I, J)

DKBYDA PARTIAL DERIVATIVES OF THE WAVENUMBER, K, W.R.T. A FOR  
EACH LAYER AND AT EACH FREQUENCY

9 A BLOCK OF NPERPT CARDS, EACH CARD CONTAINING NOL VALUES

DKBYDB(I, J)

DKBYDB PARTIAL DERIVATIVES OF THE WAVENUMBER, K, W.R.T. B FOR  
EACH LAYER AND AT EACH FREQUENCY

10 A BLOCK OF NPERPT CARDS, EACH CARD CONTAINING

QMI(I), PRES(I)

QMI THE OBSERVED VALUES FOR THE SPECIFIC ATTENUATION  
FACTORS OF RAYLEIGH WAVES

PRES CONFIDENCE LIMITS ON THE QMI

11 ANAX, ASUM

PRECISION MEASURES ON THE FIT OF ANY MODEL TESTED  
SEE REFERENCE BURTON & KENNETT

\*\*\*\*\*

OUTPUT  
\*\*\*\*\*

PRINTOUT  
\*\*\*\*\*

THE PRINTOUT LISTS GOOD CONNECTED REGIONS FOUND BY 'HEDGEHOG' AND  
GOOD POINTS OUTSIDE THE CONNECTED REGIONS (FOUND BY MONTE-CARLO)

\*\*\*\*\*

INTEGER STAPE,RANK,ALG  
REAL LIMIT1(20),LIMIT2(20),STEP(20)  
COMMON /HHG/ K,LIMIT1,LIMIT2,STEP,STAPE,RANK,  
1 INT1,INT2,N,NMAX,ALG  
COMMON /LARA/A(20),B(20),DKBYDA(80,10),DKBYDB(80,10),NOL  
COMMON /PERJ/FREQ(80),U(80),NPERPT  
COMMON /TEMP/ TA(80,10),TG(80),QMI(80),PRES(80),ASUM,AMAX  
REAL\*8 TITLE(12)  
CALL DATIM(TITLE(11),TITLE(12))

-----  
INPUT DATA  
-----

1 READ 1,(TITLE(I),I=1,10)  
FORMAT(10A8)  
PRINT 2,(TITLE(I),I=1,11)  
2 FORMAT(1H1,/,/,1CX,10A8,2CX,A8,/) )  
READ(5,51) K  
51 FORMAT(13)  
READ(5,52) ((LIMIT1(I),LIMIT2(I),STEP(I)),I=1,K)  
52 FORMAT(3F10.5)  
READ(5,53) STAPE,RANK,INT1,INT2,N,NMAX,ALG  
53 FORMAT(7I6)  
C  
READ(5,103) NCL,NPERPT  
103 FORMAT(2I10)  
READ(5,105) (A(I),B(I),I=1,NOL)  
105 FORMAT(2F10.5)  
READ(5,106) (FREQ(I),U(I),I=1,NPERPT)  
106 FORMAT(2F10.6)  
DO 7 I=1,NPERPT  
READ(5,109) (CKBYDA(I,J),J=1,NOL)  
7 CONTINUE  
DO 8 I=1,NPERPT  
READ(5,109) (CKBYDB(I,J),J=1,NOL)  
8 CONTINUE  
109 FORMAT(6F12.9)  
READ(5,110) (QMI(I),PRES(I),I=1,NPERPT)  
READ(5,106) AMAX,ASUM  
110 FORMAT(15X,2E15.7)

-----  
PI = 4.0\*ATAN(1.0)  
DO 20 I=1,NPERPT  
TG(I)=-U(I)/(PI\*FREQ(I))  
DO 21 J=1,NOL  
TB = 0.5\*A(J)\*DKBYDA(I,J)  
TA(I,J) = TG+C.375\*A(J)\*A(J)\*DKBYDB(I,J)/B(J)  
21 CONTINUE  
20 CONTINUE

CALL HH  
RETURN  
END

SUBROUTINE EST(K,PCINT,RESULT) -  
SUBROUTINE OF COMPARISON FOR A POINT  
RESULT=0 IF PCINT IS GOOD ONE  
RESULT=1 IF PCINT IS BAD ONE

\*\*\*\*\*

SUBROUTINE EST(K,CAI,RESULT)  
INTEGER RESULT  
COMMON /LARA/A(20),B(20),DKBYDA(80,10),DKBYDB(80,10),NOL  
COMMON /PERJ/FREQ(80),U(80),NPERPT  
COMMON /TEMP/ TA(80,10),TG(80),QMI(80),PRES(80),ASUM,AMAX  
DIMENSION QAI(K),QBI(6),CRI(80)  
RESULT=1  
DO 30 I = 1,NCL



```

C      ISUM      -NUMBER OF VARIABLES OF A KNOT WHICH ARE
C      DIFFERENT ON TAKING ONE STEP FROM A KNOT
C      IN A LIST
C      CINT1     -CURRENT VALUE OF INTERVAL BETWEEN
C      WRITING ON A TAPE
C      CINT2     -CURRENT VALUE OF INTERVAL BETWEEN
C      PRINTING I1, I2, I4
C      I7       -SWITCHING VARIABLE ON COMPARISON OF
C      A KNOT AND ITS NEIGHBOUR IN LIST
C      N1       -CURRENT NUMBER OF POINT IN MONTE-CARLO
C      METHOD
C
C      *****
C      *****
C
C      SUBROUTINE HH
C
C      INTEGER RESULT, CRANK, CINT1, CINT2
C      REAL POINT(20),KNOT(20),LIST(100)
C      DIMENSION BKNOT(20),SI(20),II(20),LII(20)
C
C      THESE OPERATORS INTEGER, REAL, COMMON MUST BE REPEATED
C      IN MAIN PROGRAM
C      INTEGER STAPE,RANK,ALG
C      REAL LIM1(20),LIMIT2(20),STEP(20)
C      COMMON /HHG/ K,LIMIT1,LIMIT2,STEP,STAPE,RANK,INT1,INT2,
C      IN,NMAX,ALG
C
C      DATA I1/0/,I2/0/,I3/0/,I4/0/,I5/1/,I6/2/,N1/0/,
C      ICINT1/3/,CINT2/C/
C      N1=N1-1
C      IF (STAPE.EQ.C) GO TO 100
C      REWIND 2
C      READ(2)I1,I2,I3
C      K11=K*I1
C      READ (2) (LIST(I),I=1,K11)
C      WRITE(6,304) I1,I2,I3
304  FORMAT('TAPE WAS READ. I1=',I5,', I2=',I5,', I3=',I5)
C      IF(I1.EQ.I2)GO TO 100
C      IF(I1.NE.I2)GO TO 4
C      GO TO (2,3),I5
C      2 K11=K*I1
C      I4=0
C      REWIND 2
C      WRITE(2)I1,I2,I4
C      WRITE(2) (LIST(I),I=1,K11)
C      STAPE=1
C      WRITE(6,305) I1
305  FORMAT(' REGION ENDED. TAPE IS REWRITTEN.I1=',I5)
C      3 GO TO 100
C
C      CHOICE OF A NEW BASIC KNOT. PUTTING CONSTRUCTION OF
C      NEIGHBOUR KNOTS ON A STARTING LINE
C      4 K12=K*I2
C      DO 5 I=1,K
C      J1=K12+I
C      BKNOT(I)=LIST(J1)
C      5 SI(I)=-1.
205  CRANK=0
C      I4=0
C      I6=1
C
C      CHOICE OF A NEW NEIGHBOUR KNOT
C      6 IF(I6.NE.1)GO TO 1
C      7 IF(CRANK.NE.0)GO TO 15
C      8 CRANK=CRANK+1
C      IF(CRANK.LE.RANK)GO TO 9
C
C      RETURN TO CHOICE OF A NEW BASIC KNOT
C      IF(I5.NE.1)GO TO 208
C      IF(I2.LE.I1)I2=I2+1
208  I3=0
C      I6=2
C      GO TO 1
C      9 DO 10 I=1,CRANK
C      II(I)=I
C      10 LII(I)=K-CRANK+I
C      11 DO 12 I=1,K
C      12 KNUT(I)=BKNOT(I)
C      14 DO 214 I=1,CRANK
C      J=II(I)
C      KNUT(J)=BKNOT(J)+SI(I)*STEP(J)
C      IF((KNUT(J).LT.LIMIT1(J)).OR.(KNUT(J).GT.LIMIT2(J)))GO TO 15
214  CONTINUE
C      GO TO 19
C
C      PASSAGE TO A NEW NEIGHBOUR
C      15 I=CRANK
C      16 SI(I)=SI(I)+2
C      IF(SI(I).LT.2)GO TO 14
C      SI(I)=-1.
C      I=I-1
C      IF(I.NE.0)GO TO 16
C
C      I=CRANK
C      II(I)=II(I)+1
C      IF(II(I).LE.LII(I))GO TO 11
17  I=I-1
C      IF(I.EQ.0)GO TO 8
C      II(I)=II(I)+1

```

```

      IF(I1(I).GT.L11(I))GO TO 17
      JI=CRANK-1
      DO 18 J=1,JI
18     I1(J+1)=I1(J)+1
      GO TO 11
C
C     CHECK IF KNCT HAS OCCURED BEFORE
19     I7=1
20     IF(I2.EQ.0)GO TO 23
      DO 22 I=1,I2
      ISUM=0
      J1=K*(I-1)
      DO 21 J=1,K
      J2=J1+J
      R=(LIST(J2)-KNCT(J1))/STEP(J)
      IF(R.LT.0.)R=-R
      IF(R.LT.0.1)GO TO 21
      IF(R.GT.1.9)GO TO 22
      ISUM=ISUM+1
21     CONTINUE
      IF(ISUM.LE.RANK)GO TO 24
22     CONTINUE
23     GO TO (25,41), I7
24     GO TO (15,37), I7
C
C     ESTIMATION OF KNCT
25     IF(I4.GE.I3)GO TO 26
      I4=I4+1
      GO TO 15
26     CALL EST(K,KNCT,RESULT)
      I4=I4+1
      IF(RESULT.EQ.1)GO TO 26
      WRITE(6,315) RESULT,(KNCT(L),L=1,K)
315    FORMAT(/,' KNCT WAS ESTIMATED BY HEDGEHOG. RESULT=',I1/
      1,' KNCT=',1PE14.5,/(6X,1PE14.5))
      IF(RESULT.EQ.1)GO TO 28
C
C     PLACE GOOD KNCT IN A LIST
226    J=K*I1
      IF(J+K.GT.1000)GO TO 34
      DO 27 I=1,K
      J1=J+I
27     LIST(J1)=KNCT(I)
      I1=I1+1
      IF(I5.NE.1)I6=2
      I5=1
C
C     WRITING I1,I2,I4,LIST ON A TAPE
28     GO TO(228,30),I5
228    CINT1=CINT1+1
      IF(CINT1.LT.INT1)GO TO 30
29     K11=K*I1
      REWIND 2
      WRITE(2)I1,I2,I4
      WRITE(2)(LIST(I),I=1,K11)
      STAPE=1
      WRITE(6,318) I1,I2,I4
318    FORMAT(' TAPE WAS REWRITTEN. I1=',I5,', I2=',I5,', I3=',I5)
      CINT1=0
C
C     PRINTING I1,I2,I4
30     CINT2=CINT2+1
      IF(CINT2.LT.INT2)GO TO 33
31     WRITE(6,32) I1,I2,I4
32     FORMAT(' I1=',I5,5X,' I2=',I5,5X,' I3=',I5)
      CINT2=0
33     GO TO 6
C
C     LIST OVERFLOW
34     WRITE(6,35)
35     FORMAT(' TOO MANY KNCTS FOR A LIST. EXECUTION TERMINATED.')
      RETURN
C
C     HEDGEHOG OPERATION ON A KNOT FROM MONTE-CARLO TECHNIQUE
C     CHECK IF KNCT HAS OCCURED BEFORE
36     I7=2
      GO TO 20
37     WRITE(6,38) I,RESULT
38     FORMAT(' RANDOM KNCT IS NEIGHBOUR OF ',I5,' KNCT ',
      1,' IN A LIST. RESULT=',I1)
      GO TO 100
41     IF(RESULT.EQ.C)GO TO 226
      DO 42 I=1,K
      BKNOT (I)=KNCT(I)
42     S1(I)=-1
      WRITE(6,320) (BKNOT(L),L=1,K)
320    FORMAT(' BAD RANDOM KNCT WILL BE USED AS BKNOT'
      1/' BKNOT=',1PE14.5,/(7X,1PE14.5))
      I3=0
      I5=2
      GO TO 205
C
C     CHOICE OF NEW PCINT BY MONTE-CARLO METHOD
100    N1=N1+1
      IF(N1.LE.NMAX)GO TO 102
      WRITE(6,101) NMAX
101    FORMAT(' NUMBER OF RANDOM POINTS MORE THAN NMAX=',
      1I5,', EXECUTION TERMINATED.')
      RETURN
102    DO 103 I=1,K
103    POINT(I)=LIMIT1(I)+(LIMIT2(I)-LIMIT1(I))*FA01AS(I)
      IF(N1.LT.N)GO TO 100

```



```
GO TO (104,106,104,104,106), ALG
104 CALL EST(K,POINT,RESULT)
   IF(RESULT.EC.1)GO TO 100
   WRITE(6,105) N1,(POINT(I),I=1,K)
105 FORMAT(/' GOOD PCINT ',I5/(1PE14.5))
   IF(ALG.EQ.1)GO TO 100
C
106 DO 107 I=1,K
   J=(POINT(I)-LIMIT1(I))/STEP(I)+0.5
   R=J
107 KNOT(I)=LIMIT1(I)+STEP(I)*R
   CALL EST(K,KNOT,RESULT)
   IF(RESULT.EC.1)GO TO 110
   WRITE(6,108) N1,(KNOT(I),I=1,K)
108 FORMAT(/' GOOD KNOT ',I5/(1PE14.5))
109 GO TO (100,100,26,36,36), ALG
110 GO TO (100,100,26,100,100), ALG
   RETURN
   END
```

## REFERENCES

- Adcock, R. J. (1880). A Problem in Least Squares. *Analyst* 1880, 5, p53-54.
- Anderson, D. L., and Archambeau, C. B. (1964). The Anelasticity of the Earth. *J.G.R.* 69, 10, p2071-2084.
- Anderson, D. L., Ben-Menahem, A., and Archambeau, C. B. (1965). Attenuation of Seismic Energy in the Upper Mantle. *J.G.R.* 70, No 6, p1441-1448.
- Anderson, D. L., and Sammis, C. (1970). "Partial Melting in the Upper Mantle". *Phys. Earth Planet. Int.* 3, p41-50.
- Backus, G., and Gilbert, F. (1968). The Resolving Power of Gross Earth Data. *Geophys. J. Roy. Astr. Soc.* 16, p169-205.
- Barazangi, M., Isacks, B., and Oliver, J. (1972). Propagation of Seismic Waves through and Beneath the Lithosphere that Descends under the Tonga Island Arc. *J.G.R.* 77, 5, p952-958.
- Bath, M. (1968). *Mathematical Aspects of Seismology. Developments in Solid Earth Geophysics 4.* Elsevier Publishing Company.
- Bogert, R. P., Healy, M. J., and Tukey, J. W. (1962). The Quefrency Analysis of Time Series for Echoes: Cepstrum, Pseudo-Autocovariance, Cross-Cepstrum and Saphe Cracking. In 'Time Series Analysis' (Wiley), Ed. Rosenblatt, M. Ch. 15, p209-243, Appendix 1 (p240-242).
- Born, W. T. (1941). The Attenuation Constant of Earth Materials. *Geophysics*, 6, p132-148.
- Brooks, C., Wendt, I., and Harre, J. (1968). A Two-Error Regression Treatment and its Application to Rb-Sr and Initial  $Sr^{87}/Sr^{86}$  Ratios of Younger Variscan Granitic Rocks from the Schwarzwald Massif, Southwest Germany. *J.G.R.* 73, 18, p6071-6084.
- Brownlee, K. A. (1965). *Statistical Theory and Methodology in Science and Engineering.* Ch. 11, 2nd Edition, John Wiley and Sons.
- Brune, J. N. (1962). Attenuation of Dispersed Wave Trains. *BSSA* 52, 1, p109-112.

- Brune, J. N., Nafe, J. E., and Alsop, L. E. (1961). The Polar Phase Shift of Surface Waves on a Sphere. B.S.S.A. 51, 2, p247-257.
- Brune, J. N., Nafe, J. E., and Oliver, J. E. (1960). A Simplified Method for the Analysis and Synthesis of Dispersed Wave Trains. J.G.R. 65, 1, p287-304.
- Brune, J. N., and Oliver, J. E. (1959). The Seismic Noise of the Earth's Surface. B.S.S.A. 49, 4, p349-353.
- Buchbinder, G. G. R. (1972). Comments on Paper by Mansour Niazi, "Seismic Dissipation in Deep Seismic Zones from the Spectral Ratio of pP/P". J.G.R. Letters 77, 8, p1586-1587.
- Bullen, K. E. (1965). An Introduction to the Theory of Seismology. 3rd Edition. C.U.P.
- Burton, P. W., and Blamey, C. (1972). A Computer Program to Determine the Spectrum and a Dispersion Characteristic of a Transient Signal. HMSO, AWRE Report No O-48/72.
- Burton, P. W., and Kennett, B. L. N. (1972). Upper Mantle Zone of Low Q. Nature Phys.Sci. 238, 84, p87-90.
- Carpenter, E. W., and Davies, D. (1966). Frequency Dependent Seismic Phase Velocities; an Attempted Reconciliation between the Jeffreys/Bullen and the Gutenberg Models of the Upper Mantle. Nature 212, 5058, p134-135.
- Carpenter, E. W., and Marshall, P. D. (1970). Surface Waves Generated by Atmospheric Nuclear Explosions, United Kingdom Atomic Energy Authority. HMSO, AWRE Report No O-88/70.
- Carpenter, E. W., and Thirlaway, H. I. S. (1966). Proceedings of the Vesiac Special Study Conference on Seismic Signal Anomalies, Travel Times, Amplitudes and Pulse Shapes. Inst.Sci. and Technol., Univ. of Michigan. pp119-140.

- Der, Z., Masse, R., and Landisman, M. (1970). Effects of Observational Errors on the Resolution of Surface Waves at Intermediate Distances. *J.G.R.* 75, 17, p3399-3409.
- Douglas, A., Corbishley, D. J., Blamey, C., and Marshall, P. D. (1972). Estimating the Firing Depth of Underground Explosions. *Nature, Phys.Sci.* 237, 5349, p26-28.
- Douglas, A., Hudson, J. A., and Kembhavi, V. K. (1971). The Analysis of Surface Wave Spectra using a Reciprocity Theorem for Surface Waves. *Geophys.J.Roy.Astr.Soc.* 23, p207-223.
- Dziewonski, A., Bloch, S., and Landisman, M. (1969). A Technique for the Analysis of Transient Seismic Signals. *BSSA* 59, 1, p427-444.
- Enochson, L. D. and Otnes, R. K. (1968). Programming and Analysis for Digital Time Series Data. The Shock and Vibration Centre, Naval Research Laboratory, Washington DC.
- Espinosa, A. F., Sutton, G. H., and Miller, H. J. (1962). A Transient Technique for Seismograph Calibration. *BSSA* 52, 4, p767-779.
- Espinosa, A. F., Sutton, G. H., and Miller, H. J. (1965). A Transient Technique for Seismograph Calibration - Manual and Standard Set of Theoretical Transient Responses. Geophysics Laboratory, Inst, of Sci. and Tech., University of Michigan.
- Ewing, W. M., Jardetzky, W. S., and Press, F. (1957). Elastic Waves in Layered Media. McGraw-Hill.
- Frasier, C. W., and Filson, J. (1972). A Direct Measurement of the Earth's Short Period Attenuation Along a Teleseismic Ray Path. *J.G.R.* 77, 20, p3782-3787.
- Futterman, W. I. (1962). Dispersive Body Waves. *J.G.R.* 67, 13, p5279-5291.
- Goodman, N. R. (1960). Measuring Amplitude and Phase. *Journal of the Franklin Institute.* 270, p437-450.
- Green, D. H. and Ringwood, A. E. (1970). Mineralogy of peridotitic Composition under Upper Mantle Conditions. *Phys.Earth Planet.Int.* 3, p359-371.

- Haskell, N. A. (1953). The Dispersion of Surface Waves on Multilayered Media. B.S.S.A. 43, p17-34.
- Haskell, N. A. (1964). Radiation Pattern of Surface Waves from Point Sources in a Multi-Layered Medium. B.S.S.A. 54, 1, p377-393.
- Ibrahim, A. K. (1971). The Amplitude Ratio PcP/P and the Core-Mantle Boundary. Pure and Applied Geophysics (PAGEOPH) 91, 8, p114-133.
- Jackson, D. D., and Anderson, D. L. (1970). Physical Mechanisms of Seismic-Wave Attenuation. Revs. of Geophysics and Space Physics. 8, No 1, p1-64.
- Jeffreys, Sir Harold. (1961). Small Corrections in the Theory of Surface Waves. Geo.J.Roy.Astr.Soc. 6, No 1, p115-117.
- Kanamori, H. (1970). Velocity and Q of Mantle Waves. Phys.Earth Planet. Interiors. 2, p259-275.
- Kanamori, H. and Press, F. (1970). How Thick is the Lithosphere. Nature 226, p330-331.
- Keilis-Borok, V. I. and Yanovskaya, T. B. (1967). Inverse Problems of Seismology (Structural Review). Geophys.J.Roy.Astr.Soc. 13, p223-234.
- Knopoff, L. (1964). 'Q'. Revs of Geophysics, 2, No 4, p625-660.
- Knopoff, L. (1969). Attenuation of Seismic Waves in the Mantle. In 'The Earth's Crust and Upper Mantle'. American Geophysical Union. Geophysical Monograph 13, p273-275.
- Knopoff, L., Aki, K., Archambeau, C. B., Ben-Menahem, A., and Hudson, J. A. (1964). Attenuation of Dispersed Waves. J.G.R. Letters 69, 8, p1655-1657.
- Kolsky, H. (1953). Stress Waves in Solids. O.U.P.
- Kolsky, H. (1956). The Propagation of Stress Pulses in Viscoelastic Solids. Phil.Mag.Ser. 8, Vol 1, No 8, p693-710.
- Kovach, R. L., and Anderson, D. L. (1964). Attenuation of Shear Waves in the Upper and Lower Mantle. B.S.S.A. 54, p1855-1864.

- Lambert, I. B., and Wyllie, P. J. (1970a). Melting in the Deep Crust and Upper Mantle and the Nature of the Low-Velocity Layer. *Phys. Earth Planet. Int.* 3, p316-322.
- Lambert, I. B., and Wyllie, P. J. (1970b). Low Velocity Zone of the Earth's Mantle: Incipient Melting Caused by Water. *Science* 169, p764-766.
- Lomnitz, C. (1962). Application of the Logarithmic Creep Law to Stress Wave Attenuation in the Solid Earth. *J.G.R.* 67, p365-368.
- Marshall, P. D. (1970). Aspects of the Spectral Differences between Earthquakes and Underground Explosions. *Geophys. J. Roy. Astr. Soc.* 20, p397-416.
- Marshall, P. D., and Basham, P. W. (1972). Discrimination between Earthquakes and Underground Explosions Employing an Improved  $M_s$  Scale. *Geophys. J. Roy. Astr. Soc.* 28, p431-458.
- Marshall, P. D., and Burton, P. W. (1971). The Source-Layering Function of Underground Explosions and Earthquakes - An Application of a 'Common Path' Method. *Geophys. J. Roy. Astr. Soc.* 24, p533-537.
- Marshall, P. D., and Carpenter, E. W. (1966). Estimates of Q for Rayleigh Waves. *Geophys. J. Roy. Astr. Soc.* 10, p549-550.
- Marshall, P. D., Carpenter, E. W., Douglas, A., and Young, J. B. (1966). Some Seismic Results of the LONGSHOT Explosion. HMSO, AWRE Report No O-67/66.
- Marshall, P. D., Corbishley, D. J., and Gibbs, P. G. (1970). Some Seismic Results of the MILROW Underground Nuclear Explosion. HMSO, AWRE Report No O-47/70.
- Mason, W., and Kuo, J. T. (1971). Internal Friction of Pennsylvania Slate. *J.G.R.* 76, 8, p2084-2089.
- McIntyre, G. A., Brooks, C., Compston, W., and Turek, A. (1966). The Statistical Assessment of Rb-Sr Isochrons. *J.G.R.* 71, 22, p5459-5468.
- Miller, R. L., and Kahn, J. S. (1962). Statistical Analysis in the Geological Sciences. John Wiley and Sons.



- Mitchell, B. J. and Landisman, M. (1969). Electromagnetic Seismograph Constants by Least Squares Inversion. *B.S.S.A.* 59, 3, p1335-1348.
- Niazi, M. (1971). Seismic Dissipation in Deep Seismic Zones from the Spectral Ratio of pP/P. *J.G.R.* 76, 14, p3337-3343.
- Oliver, J. (1962). A Summary of Observed Seismic Surface Wave Dispersion. *B.S.S.A.* 52, 1, 81-86.
- Pekeris, C. L. (1948). The Theory of Propagation of Explosive Sound in Shallow Water. *Geol.Soc.Am.Mem.*, 27.
- Peselnick, L., and Zietz, I. (1959). Internal Friction of Fine Grained Limestones at Ultrasonic Frequencies. *Geophys.* 24, p285-296.
- Pinkerton, J. M. M. (1947). A Pulse Method for the Measurement of Ultrasonic Absorption in Liquids: Results for Water. *Nature* 160, p128-129.
- Press, F. (1970a). Regionalized Earth Models. *J.G.R.* 75, No 32, p6575-6581.
- Press, F. (1970b). Earth Models Consistent with Geophysical Data. *Phys.Earth and Planet.Int.* 3, p3-22.
- Press, F., and Healy, J. (1957). Absorption of Rayleigh Waves in Low-Loss Media. *Journal of Applied Physics.* 28, 11, p1323-1325.
- Ractliffe, J. F. (1967). Elements of Mathematical Statistics. 2nd Edition. O.U.P.
- Ringwood, A. E. (1969). Composition and Evolution of the Upper Mantle. In "The Earth's Crust and Upper Mantle". American Geophysical Union. Geophysical Monograph 13, p1-17.
- Robinson, E. A. (1966). Collection of Fortran II Programs for Filtering and Spectral Analysis of Single Channel Time Series. *Geophysical Prospecting* 14, Appendix 1 p42.
- Scheffe, H. (1964). The Analysis of Variance. John Wiley and Sons.
- Spetzler, H., and Anderson, D. L. (1968). The Effect of Temperature and Partial Melting on Velocity and Attenuation in a Simple Binary System. *J.G.R.* 73, No 18, p6051-6060.

- Strick, E. (1967). The Determination of  $Q$ , Dynamic Viscosity and Transient Creep Curves from Wave Propagation Measurements. *Geophys.J.Roy.Astr. Soc.* 13, p197-218.
- Takeuchi, H., Dorman, J., and Saito, M. (1964). Partial Derivatives of Surface Wave Phase Velocity with Respect to Physical Parameter Changes within the Earth. *J.G.R.* 69, 16, p3429-3441.
- Teng, T. L. (1968). Attenuation of Body Waves and the  $Q$  Structure of the Mantle. *J.G.R.* 73, p2195-2208.
- Teng, T. L. (1969). Attenuation of Body Waves and the  $Q$  Structure of the Mantle. *J.G.R.* 74, p6720-6722.
- Thomson, W. T. (1950). Transmission of Elastic Waves Through a Stratified Solid Medium. *Journal of Applied Physics.* 21, p89-93.
- Toksoz, M. N., Ben-Menahem, A., and Harkrider, D. G. (1964). Determination of Source Parameters of Explosions and Earthquakes by Amplitude Equalisation of Seismic Surface Waves. I Underground Nuclear Explosions. *J.G.R.* 69, p4355-4366.
- Handbook (1965). World Wide Standard Seismograph Network. Geophysics Laboratory. University of Michigan.
- Yamakawa, N., and Sato, Y. (1964).  $Q$  of Surface Waves. *Journal of Physics of the Earth.* 12, 1, p5-18.
- York, D., (1966). Least Squares Fitting of a Straight Line. *Canadian Journal of Physics* 44, p1079-1086.
- York, D. (1967). The Best Isochron. *Earth and Planet.Sci. Letters* 2, p479-482.
- Young, J. B., and Douglas, A. (1968). Map, Time Series and Other Plotting Routines for Use with the Stromberg-Carlson 4020 Plotter. HMSO, AWRE Report No O-41/68.
- Young, J. B., and Gibbs, P. G. (1968). GEDESS: A Series of Computer Programs for Deriving Information at Selected Seismic Recording Sites, for Signals from Known Hypocentres. HMSO, AWRE Report No O-54/68.



Zener, C. (1948). Elasticity and Anelasticity of Metals. Univer. of  
Chicago Press, Chicago, Illinois.



United Kingdom Atomic Energy Authority

AWRE, Aldermaston

AWRE REPORT NO. 048/72

A Computer Program to Determine the Spectrum and a Dispersion Characteristic of a Transient Signal

P W Burton  
C Blamey

C16

550.34:681.3.06  
681.3.06:550.34

TABLE OF CONTENTS

	<u>PAGE</u>
SUMMARY	3
1. INTRODUCTION	3
2. OUTLINE OF THE METHOD	4
3. PROGRAM SPECIFICATION	5
4. DATA	6
5. PROGRAM PROCEDURE	6
5.1 Spectral analysis	6
5.1.1 Preparation for Fourier analysis	6
5.1.2 The Fourier analysis	6
5.1.3 Absolute values	7
5.2 Dispersion	7
5.2.1 Preparation for filtering	7
5.2.2 The filter	7
5.2.3 Response to the filter	8
5.2.4 Group velocities	8
5.3 Output	8
6. PARAMETER CARDS	9
7. ACKNOWLEDGMENTS	11
FIGURES 1 - 8	12
APPENDIX A: COSINUSOIDAL AND COMPLEX TRANSFORMS	20
APPENDIX B: SCALING THE COOLEY-TUKEY CALCULATIONS AND THE SUBROUTINE COOL	23
APPENDIX C: THE ANALYTICAL SIGNAL FOR "ENVELOPE" DETERMINATION	25
APPENDIX D: MULTIPLE WINDOW FILTERING IN THE FREQUENCY DOMAIN TO DETERMINE DISPERSION	27
APPENDIX E: INSTRUMENTATION PACKAGE	28
APPENDIX F: PROGRAM LISTING	29
REFERENCES	74

## SUMMARY

The program described determines the Fourier amplitude and phase spectra, and the group velocity of a dispersed seismic surface wave signal (sampled at equal time intervals) as a function of frequency. Group velocity, a dispersion characteristic, is produced by a multiple filtering technique.

The program contains an option to generate and remove instrumental effects for World-Wide Standard Seismograph Network (WWSSN) types of instruments.

### 1. INTRODUCTION

The seismic surface waves generated by earthquakes and explosions are usually strongly dispersed (see for example figure 1), that is, the velocity at which the energy in the signal travels (the group velocity) is a function of frequency. This dispersion has two causes; the major contribution is a geometrical dispersion effect. The amplitudes of the longer period surface waves decay more slowly with depth than do the amplitudes of the shorter period components, but the group velocity of a surface wave component depends directly on the velocity of propagation of shear and compressional waves; these usually increase with depth in the earth. So the group velocity for the longer periods is usually greater than for shorter periods. If the wave propagation is not perfectly elastic a further minor degree of dispersion must exist as can be shown from arguments of causality.

In analysing surface waves one of the most important determinations is the relationship between group velocity and frequency. For example, from such a relationship it is possible to estimate the wave velocity, and therefore density, as a function of depth for the path followed by the surface waves between earthquake source and receiver. Various visual methods are available for determining the group velocity curve but in recent years computer techniques have refined these measurements and this report describes a program based on the method of Dziewonski et al. [1] which is an improvement on Dziewonski's original method.

The program was written as part of a study of the non-elastic attenuation effects on Rayleigh surface waves. This requires the evaluation of the absolute amplitude spectrum, as well as the group velocities, for a signal. A procedure to obtain the spectrum is thus included in the program. Further, because the recorded signals are usually distorted by recording instruments the program includes an option to remove these effects when they are known.

## 2. OUTLINE OF THE METHOD

To make the analyses the signal is passed through a series of narrow band-pass filters centred on different frequencies. The time when the amplitude of the filtered signal is maximum for each of the filtered records is then taken as the group arrival time of the group of frequencies in the signal centred on the centre frequency of the filter. Knowing the distance the signal has travelled from its source and the origin time of the earthquake (or explosion) the group velocity of each frequency can be computed. Group velocity, rather than the natural group arrival time, is used as the dispersion characteristic because it is independent of the distance between event and recording site. The group velocity curve obtained from the signal of figure 1 is shown in figure 5. An interesting feature of this curve is the extensive minimum section which implies that many frequencies arrive at the same time; this means that there will be a large amplitude spike in the time domain and this is easily identified in the time series of figure 1 (to the seismologist this is an Airy phase).

To analyse dispersion we are asking the question when does energy of frequency  $f$  (Hz) arrive? To answer this we need a narrow band-pass filter of mean frequency  $f$  and good joint frequency-time resolution to filter the time series. In choosing a narrow band filter a compromise must be made between a filter that is so narrow that the filtered signal is smeared out and the maximum amplitude is thus difficult to estimate in time, and a filter that is so wide that strong frequency components that lie well away from the filter centre frequency are nevertheless passed by the filter and possibly dominate the filtered signal (thus producing a spurious arrival time). In this program we follow Dziewonski et al. and use the Gaussian function as a filter because it optimises these conditions. A set of such filters is generated at different central frequencies; these are of constant  $Q$  (the ratio of peak frequency to bandwidth) to ensure uniform resolution for all  $f$ . For further discussion of optimum filter design see Inston et al. [2].

It is difficult to determine the maximum in each filtered signal even when the best filter is used because the filtered signal oscillates about zero. However, it is possible to determine the envelope to this oscillating signal by using the modulus of the analytic signal function (see appendix C). In practice it is usual to contour the envelope amplitudes as a function of group velocity and frequency. Such contouring creates a 2-D matrix which tabulates instantaneous envelope amplitudes as this function of group velocity and frequency.

Figures 6, 7 and 8 illustrate the procedure. Figure 6(a) is the signal generated by an atmospheric nuclear explosion at Novaya Zemlya, USSR, and recorded by a long period, vertical component seismometer at a WWSSN station at Kongsberg, Norway (a surface propagation distance of 2522 km). The signal-to-noise ratio is good for this record and it is assumed that this will be so for any record to be analysed. The dispersion in the signal is obvious visually and three frequencies,  $f_L$ ,  $f_I$  and  $f_H$ , are indicated. Scales of arrival time measured from the onset time of the event and the equivalent group velocity are shown below the seismogram and it is clear from this that the group velocity of  $f_L$  is about 3.2 km/s and for  $f_H$  about 2.5 km/s.

Figure 6(e) shows the record after filtering with a Gaussian filter centred on 0.033 Hz, the frequency of  $f_L$ , 6(f) is the Hilbert transform of 6(e) and 6(d) is the envelope of 6(e) obtained by forming the modulus of the analytic function from the filtered trace and its Hilbert transform. Similarly figure 7 shows the results of filtering the record with a filter centred on  $f_I$  and the corresponding envelope, while figure 8 is the result for  $f_H$ . Picking the peaks of the three envelopes gives a three point group velocity/frequency relationship of:-

$f_L$       0.033 Hz    3.17 km/s

$f_I$       0.051 Hz    2.64 km/s

$f_H$       0.088 Hz    2.55 km/s

Figure 4 shows envelope heights in db (normalised to 99 db) as the matrix function of group velocity and frequency. The group velocity/frequency curve stands out as a ridge on this plot.

To obtain the amplitude spectrum the original seismogram is Fourier transformed using a procedure based on the Cooley-Tukey algorithm (see appendices A and B). The amplitude and phase spectra of the Kongsberg record are shown in figures 2 and 3. At this stage the amplitude and phase response are uncorrected for the effects of the recording instrument. Given the instrument response its effects can be removed simply by dividing the observed complex spectrum by the instrument spectrum. As the signals we have analysed were recorded principally at WWSSN stations the program contains an option to generate and remove the effects of WWSSN long period recording systems. Details of the instrument calibration pulse and instrument parameters are read into the computer for each signal and this information is compared to a reference library of WWSSN instrument calibration pulses and parameters; the best match obtained is then used to generate the instrument response. The subroutine for obtaining these WWSSN instrument calibrations is based on a similar program written by J N Brune (see appendix E).

This program can be applied to other types of signal recorded by different instruments by inserting the relevant instrument transfer function. The program has been written to facilitate this exchange and the present instrument package may easily be replaced by another, or just omitted.

### 3.      PROGRAM SPECIFICATION

The program is written in Fortran IV for the AWRE IBM 360/75. When all the available options are included the required storage is 200k. Output is in the form of a paper printout and additional options are available for punched cards for the amplitude spectrum and group velocities, SC4060 graphical output and film. The maximum number of digits in the time series signal is 1024. The maximum size which may be requested for the group velocity/frequency matrix is 120/120.

#### 4. DATA

The time series has to be in digital form, with a constant sampling interval. The time between the event origin time and the first digit in the time series must be known, as must the distance between the event and recording site. (In this version this distance is expressed in degrees, measured round the great circle of propagation on the Earth's surface, and converted to kilometres within the program.)

#### 5. PROGRAM PROCEDURE

##### 5.1 Spectral analysis

##### 5.1.1 Preparation for Fourier analysis

The parameter cards (section 5) which specify the operations to be carried out and the digital time series, sampled at intervals of DELA seconds, are read in. The time series is stored in the array SEIS(I), cosine tapered at both ends and fitted to a mean baseline to reduce the Gibbs' phenomenon, and eliminate "square wave" effects caused by a time series superimposed onto a non-zero baseline. If required the seismogram may be inverted and/or samples removed from the front.

The NSEIS data points of the digital time series are now set to N points by adding zeros, where  $N = 2^{L+1}$  and L is the first integer which makes  $N \geq NSEIS$ . This condition is an intrinsic requirement of the Cooley-Tukey algorithm used in the Fast Fourier Transform routine COOL; the Fourier analysis procedure is then very rapid (4000 points in one second).

##### 5.1.2 The Fourier analysis

Cosine and sine transforms are obtained using COOL and these easily relate to the Fourier transform.

Harmonic frequencies are determined by the values of N and sampling interval DELA.

The Nyquist frequency is defined as

$$f_{NYQ} = \frac{1}{2.0 \times DELA} \text{ Hz,}$$

the fundamental frequency is

$$Df = \frac{f_{NYQ}}{NBY2} \text{ Hz (NBY2 = } \frac{N}{2}\text{)}$$

and the harmonic frequencies are

$$f_{i+1} = i \times Df \quad (0 \leq i \leq NBY2).$$

These frequencies are stored in array FREQ(I). The transform of SEIS(I) is stored in the complex array Z(I) (appendix B).

Expressions for the amplitude and phase at these frequencies are given in appendix A. No information is obtained for frequencies greater than  $f_{NYQ}$ . The amplitude and phase spectra obtained from the Kongsberg record are shown in figures 2 and 3.

### 5.1.3 Absolute values

If absolute values are required the instrument transfer function is formed by subroutine WWSSN and is stored in the complex array P(I) (appendix E). The instrument effect is removed by division at each frequency creating

$$Z'(I) = \frac{Z(I)}{P(I)}.$$

Spectral amplitudes and phases are recalculated and the spectrum may be smoothed if required. This completes spectral analysis of the time series.

## 5.2 Dispersion

### 5.2.1 Preparation for filtering

The velocity of travel to the first, VSF, and last, VSL, seismogram samples are computed and then the velocity to each digit in the time series is stored in the two-dimensional array TABLE (I,I) ( $0 \leq I \leq N$ ). The velocity array covering the range of interest is created and stored in VSTEP(I) by subtracting a chosen VSTEP from VSF, storing the result, and continuing until VSL is reached. There must not be more than 120 velocities.

### 5.2.2 The filter

Filter centre frequencies are chosen and stored in FREQC(I). These are chosen to correspond to a set of the harmonics selected at regular intervals from FREQ(I). The two arrays, FREQ(I) and VSTEP(I), specify the frequencies and group velocities for which instantaneous envelope amplitudes will subsequently be stored in the 2-D dispersion matrix.

The filter parameters BAND and DWF are used to shape the Gaussian filter function. BAND is dimensionless and gives the relative bandwidth for all the filters used (to preserve constant Q), that is

$$\text{BAND} = \frac{\text{FREQC}(I) - \text{Filter Low Frequency}}{\text{FREQC}(I)}$$

and a typical value is  $\text{BAND} = 0.20$ . The value of DWF specifies the decay rate, or roll-off, of the Gaussian filter. It is the ratio of the filter maximum amplitude at its central frequency to its amplitude at its lowest frequency, specified above by BAND.

This filter is created by subroutine GAUSSA at the harmonic frequencies FREQ(I), and is stored symmetrically in P(I) about FREQC(I).



### 5.2.3 Response to the filter

The analytic signal at a particular frequency (ie, the envelope components of the filter response to the seismogram, at a particular frequency) is formed by multiplication of  $Z'(I)$  and  $P(I)$ , storing the result in  $P'(I)$  and transforming to the time domain. The instantaneous amplitude of the analytic signal is obtained by forming the modulus of  $P'(I)$  and storing the values in TABLE (2,I) (appendix C).

We now have the situation of figure 6 where for a particular filter centre frequency (which is the same as an harmonic of the Fourier transform of the time series) we have two arrays - containing instantaneous amplitudes of the analytic signal and the corresponding velocity (obtained from arrival time). We are only interested in the selected velocities  $VSTEP(I)$  and therefore interpolate between the values of TABLE to obtain instantaneous amplitudes at the velocities of interest. Results are stored in one column of the 2-D matrix  $E(I,J)$ .

The sequence of operations, starting at creation of the filter, is repeated for each frequency of interest and the results stored in subsequent columns of  $E$ , which has a maximum size of  $120 \times 120$  (appendix D).

### 5.2.4 Group velocities

The maximum value of  $E$  is determined and set to 99 db, all other values of  $E$  being scaled relatively to give the matrix of figure 4. For each frequency of filter analysis, ie,  $FREQC(I)$ , the maximum value of the relevant column of  $E$  is obtained and the corresponding velocity is the group velocity (velocity of the maximum energy content at each frequency).

### 5.3 Output

There is a comprehensive printout consisting of:-

- (1) The input seismogram and parameters.
- (2) Spectral amplitudes and phases.
- (3) Instrumental magnification and phase.
- (4) Spectral amplitudes and phases after instrument removal.
- (5) The seismogram after instrument removal.
- (6) Filter information.
- (7) Group velocity against frequency.
- (8) The 2-D matrix  $E$  of instantaneous analytic signal amplitudes (in relative db) as a function of frequency and velocity (figure 4).

Also graphs [3] where relevant, on paper and film may be obtained and the smoothed spectral amplitudes and the group velocities punched out. The graphs used for figures 2, 3 and 5 are examples of this output.

## 6. PARAMETER CARDS

The data cards should be made up as follows with formats as specified in the listing of the program. The value +1 performs an option, 0 omits it, where appropriate.

- (1) An SC4060 card for graphics.
- (2) A block of 78 cards which are a reference library of WWSSN calibration pulses (appendix E).

The remaining block of cards should be repeated as many times as there are signals to be analysed.

- (1) TITLEA(I) A title card with columns 73 - 80 containing an identification label, eg, DATA 001.

- (2) STANAM(I) Name of recording station.

DELTAD Distance in degrees between event and recording station. Program uses  $1^\circ = 111.1$  km.

MHOUR )  
MIN ) GMT origin time of event in hours, minutes  
SEC ) and seconds.

MHRGMT )  
MINGMT ) GMT of first sample.  
SECGMT )

NSEIS Number of samples in time series.

- (3) DELA Sample interval in seconds.

IVSEIS Invert the seismogram.

NUMCUT Remove NUMCUT samples from the front of the seismogram and correct the first sample time by  $\text{NUMCUT} \times \text{DELA}$ .

NBASE Correct the seismogram to a mean baseline.

NCOSTP Cosine taper NCOSTP points at both ends of seismogram.

NCOMB Number of points in the comb used to smooth the Fourier amplitude spectrum. Set to an even number.

NAFLO Index number of the frequency array  $FREQ(I)$  referring to the lowest frequency of interest in the amplitude spectrum. All frequencies lower than  $NAFLO \times Df$  are removed.

NINSTR If this is set to 1 then remove the instrument effect.

NUGRUP Calculate group velocities.

NFLO Index number for  $FREQ(I)$  referring to the lowest frequency of interest,  $NFLO \times Df$ , for group velocity determination. Also  $NFLO$  must be greater than  $NAFLO$ .

NFHI Index number of the highest frequency of interest for group velocity determination.

NFSTEP The interval between adjacent frequencies of interest for group velocity determination is  $NFSTEP \times Df$ . Note filter central frequencies  $FREQC(I)$  are such that  $FREQC(I) = FREQ(NFLO-1) = NFLO \times Df$  etc.

BAND Dimensionless, relative bandwidth of Gaussian filter.

DWF Decay rate of Gaussian window function.

DV Velocity step along the seismogram. The velocities to the first and last seismogram samples,  $VSF$  and  $VSL$ , are known. This group velocity range is divided into 120, or less, values of group velocity by suitable choice of  $DV$ .

(4) NG1  
 ⋮  
 NG9  
 ⋮  
 NG15 Several graphs of the seismogram, amplitude, phase, instrument response and group velocity are available. These are described in detail in the program listing.

NP1 Punch out the smoothed amplitude/frequency spectrum of the seismogram.

NP2 Punch out the group velocity/frequency curve.

(5) FMT Read in the variable format used to input the seismogram.

Cards 6 and 7 if, and only if,  $NINSTR = 1$ .

(6) TITLEB A title card for the instrumentation data.

- (7) This card contains measurements from the WWSSN calibration pulse and WWSSN seismometer constants. If required, a full description of these parameters is in the program listing.
- (8) SEIS(I) The digital time series in format FMT containing NSEIS points and sampled every DELTA seconds.

7.

ACKNOWLEDGMENTS

We would like to thank Messrs J B Young and A Douglas for their help during the preparation of this program. We would also like to thank Messrs A Douglas and P D Marshall, and Dr. H L S Thirlaway for useful criticism of this text.

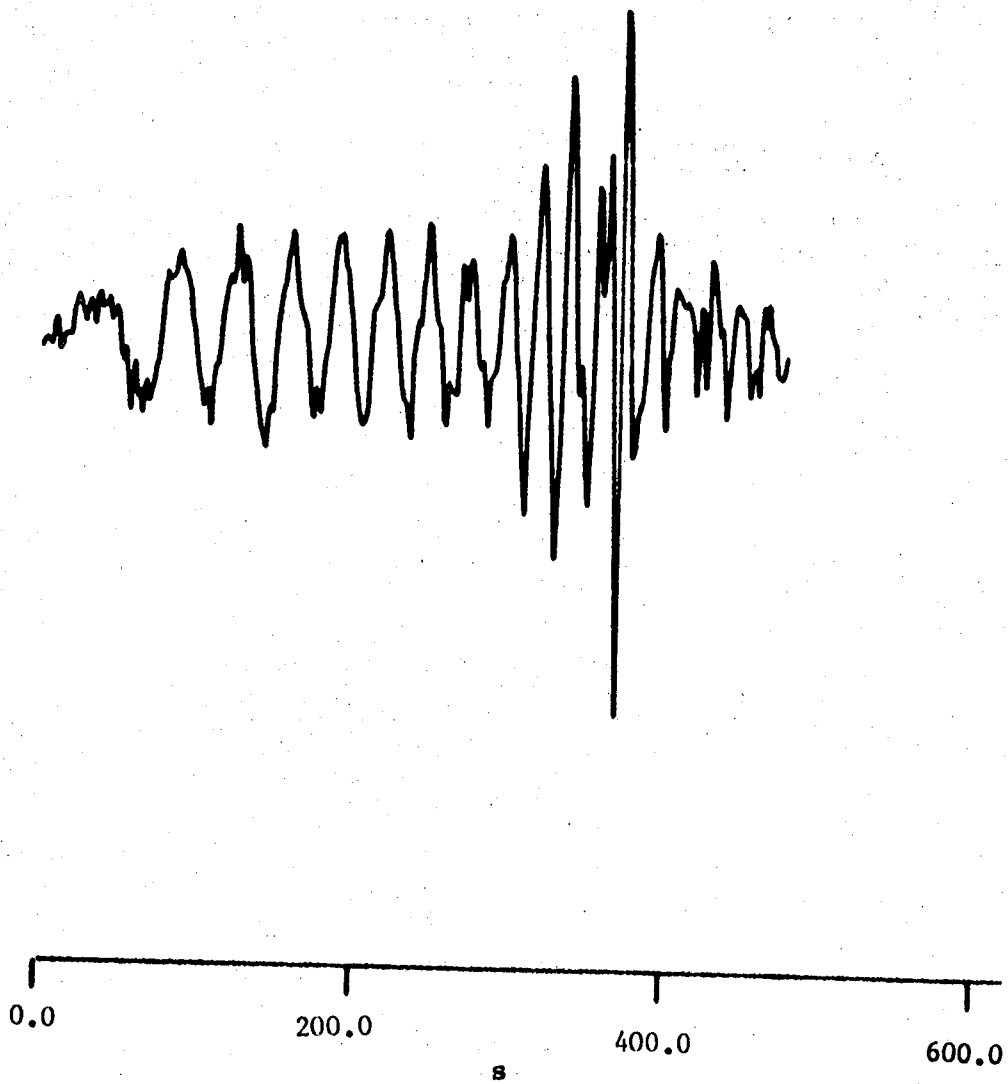


FIGURE 1. A SEISMIC RAYLEIGH WAVE FROM NOVAYA ZEMLYA WHICH WAS  
RECORDED AT KONGSBERG, NORWAY (DISTANCE IS 2522 km)

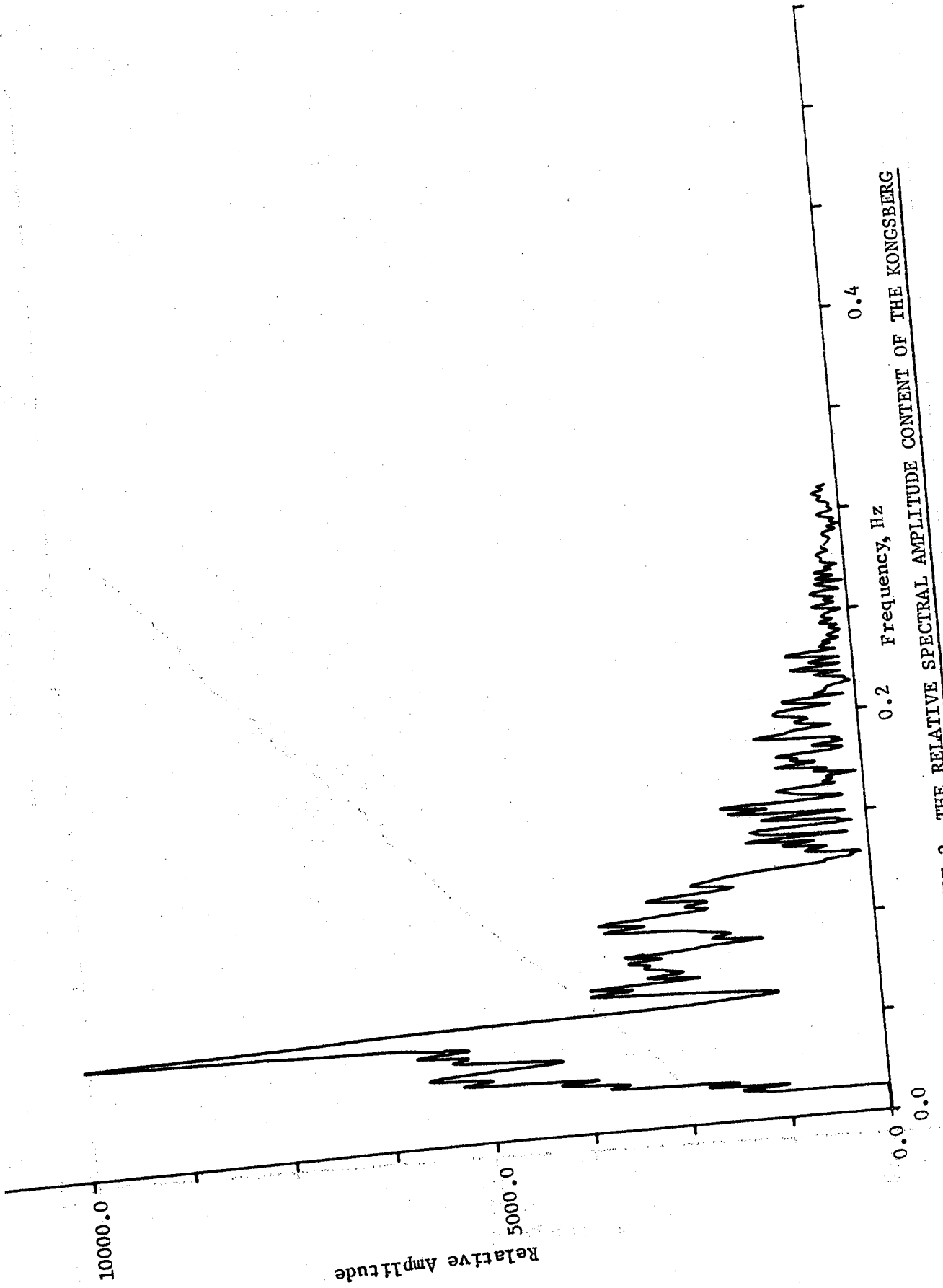


FIGURE 2. THE RELATIVE SPECTRAL AMPLITUDE CONTENT OF THE KONGSBERG RECORD

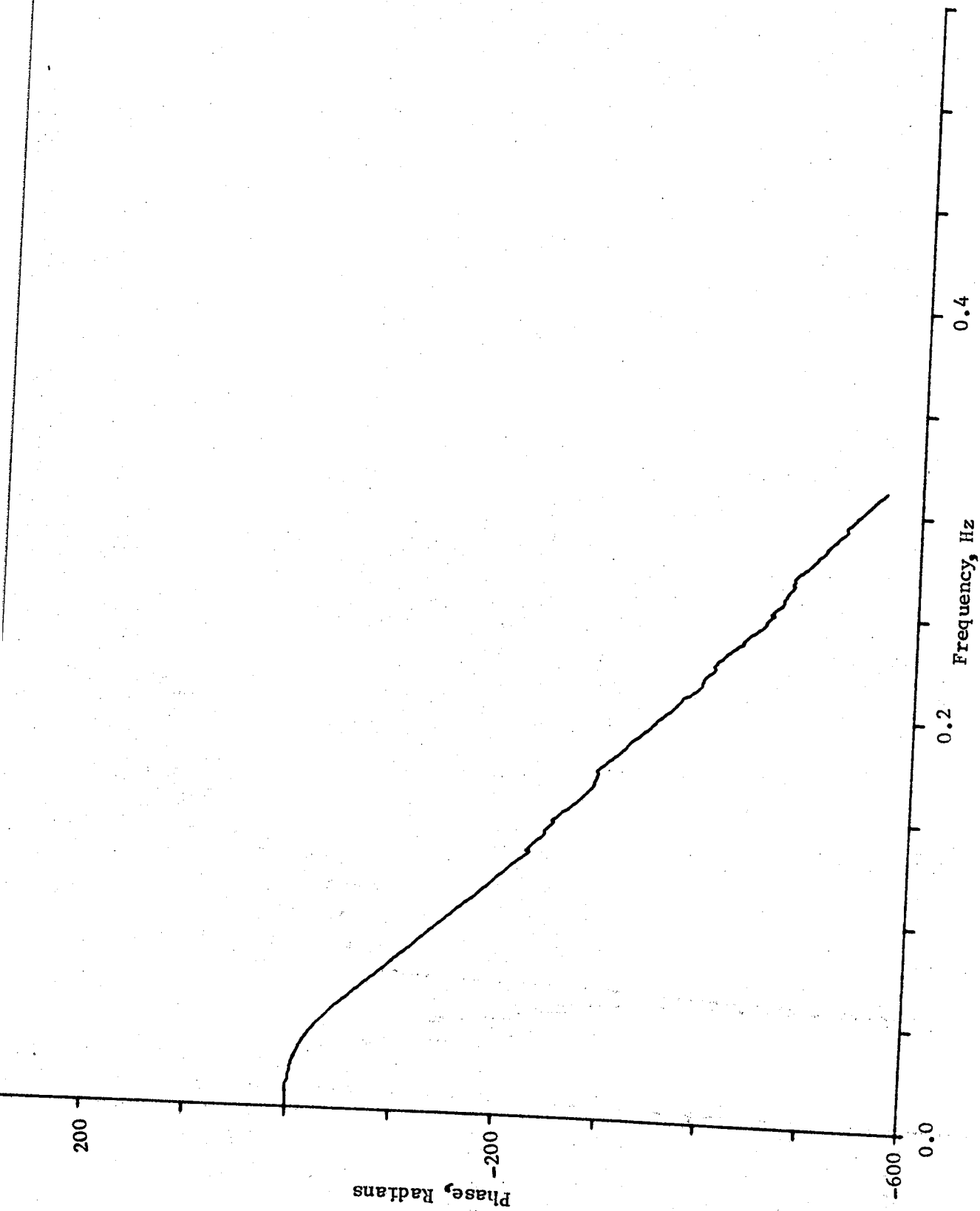


FIGURE 3. THE SPECTRAL PHASE CONTENT OF THE KONGSBERG RECORD

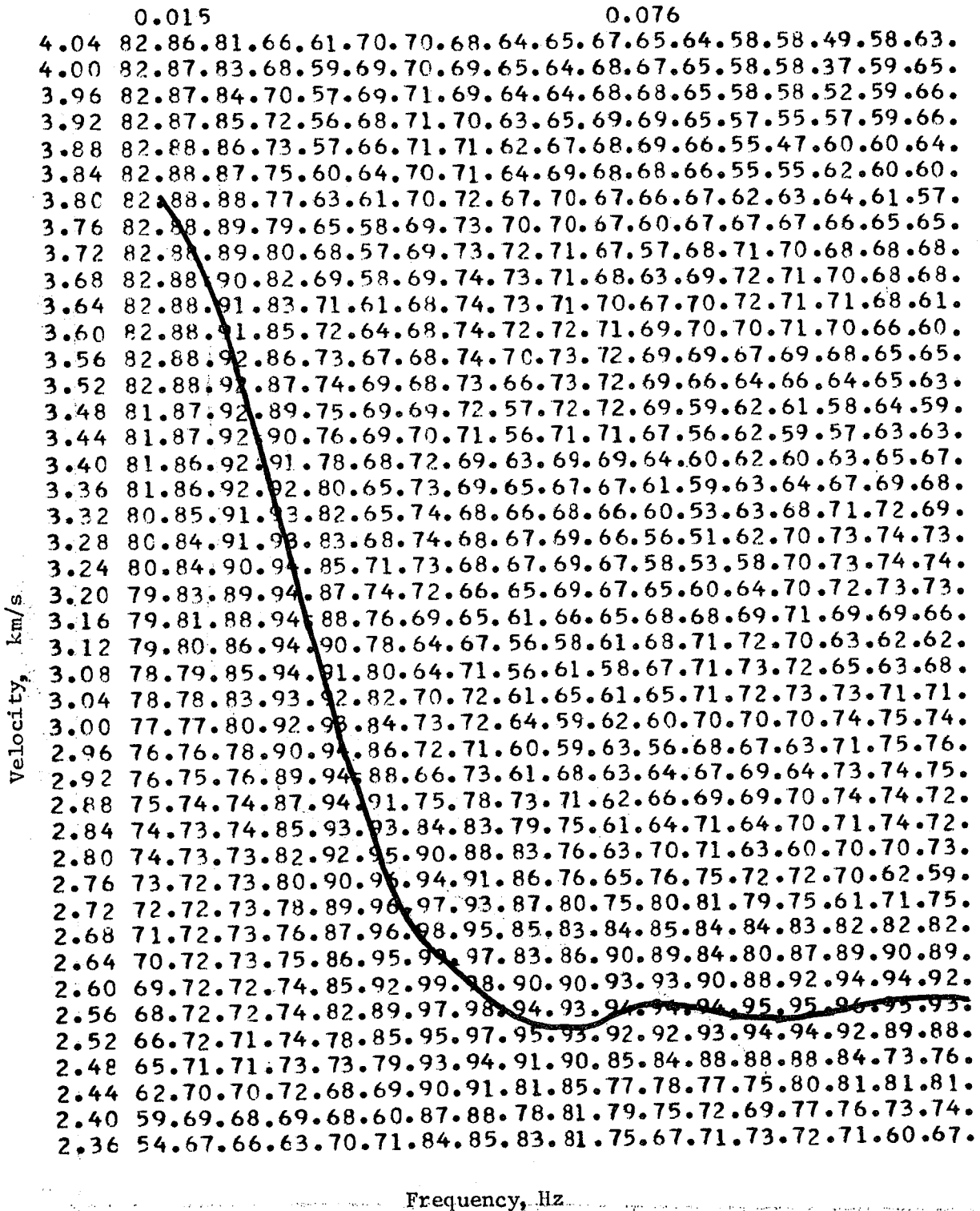


FIGURE 4. THE MATRIX E AND THE SELECTED GROUP VELOCITY CURVE  
(KONGSBERG RECORD)



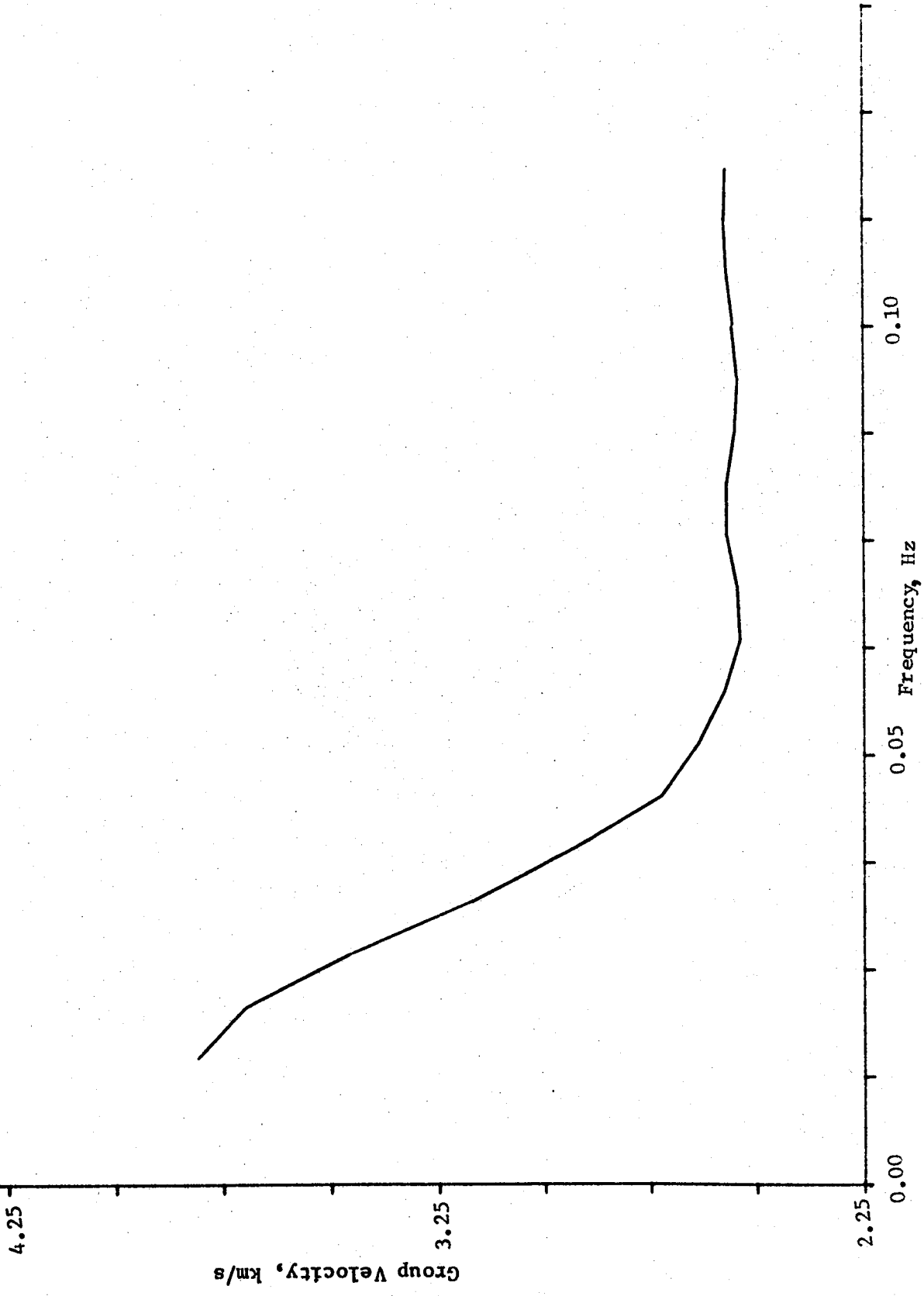


FIGURE 5. THE GROUP VELOCITY CURVE (KONGSBERG RECORD)

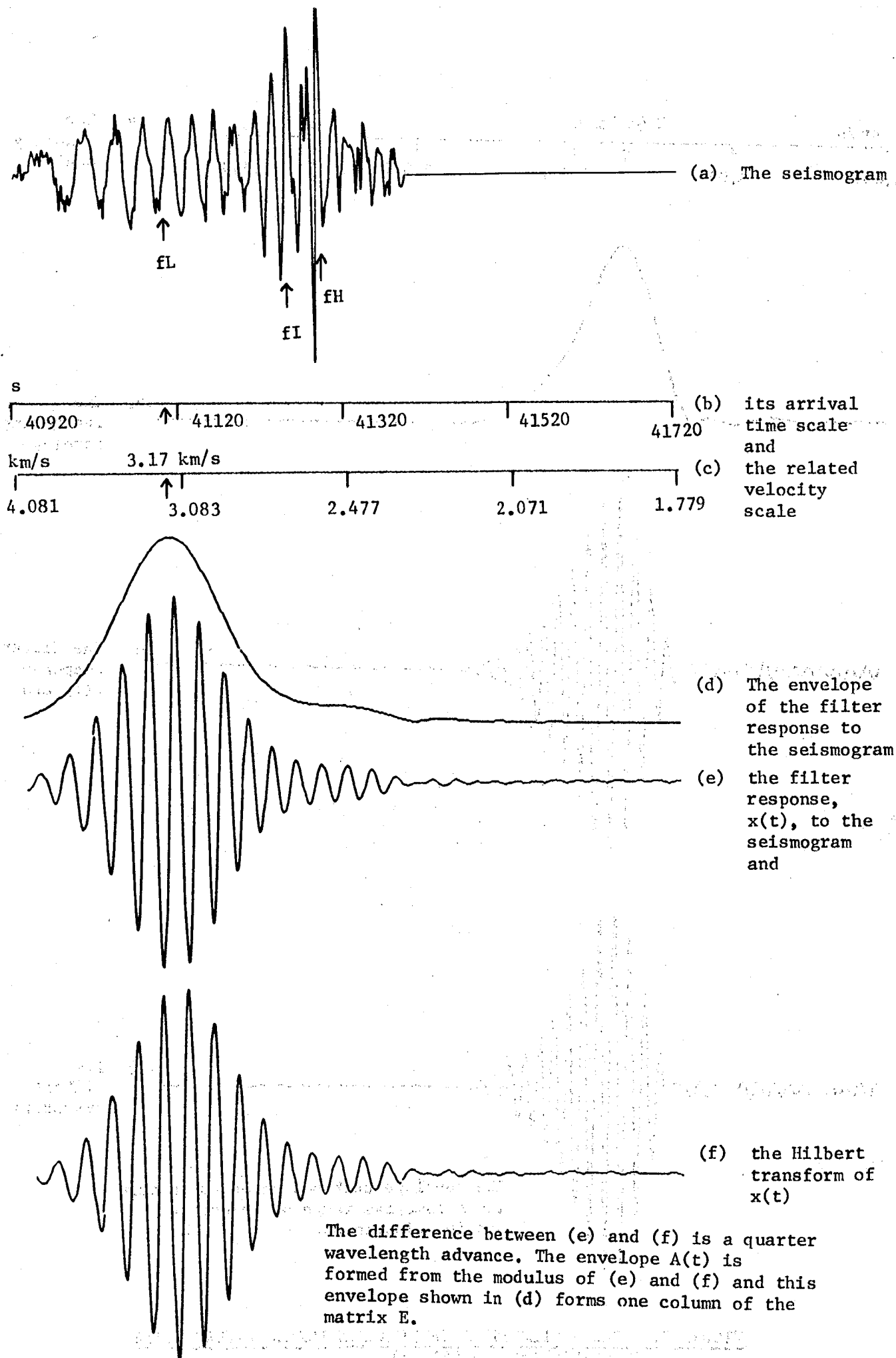
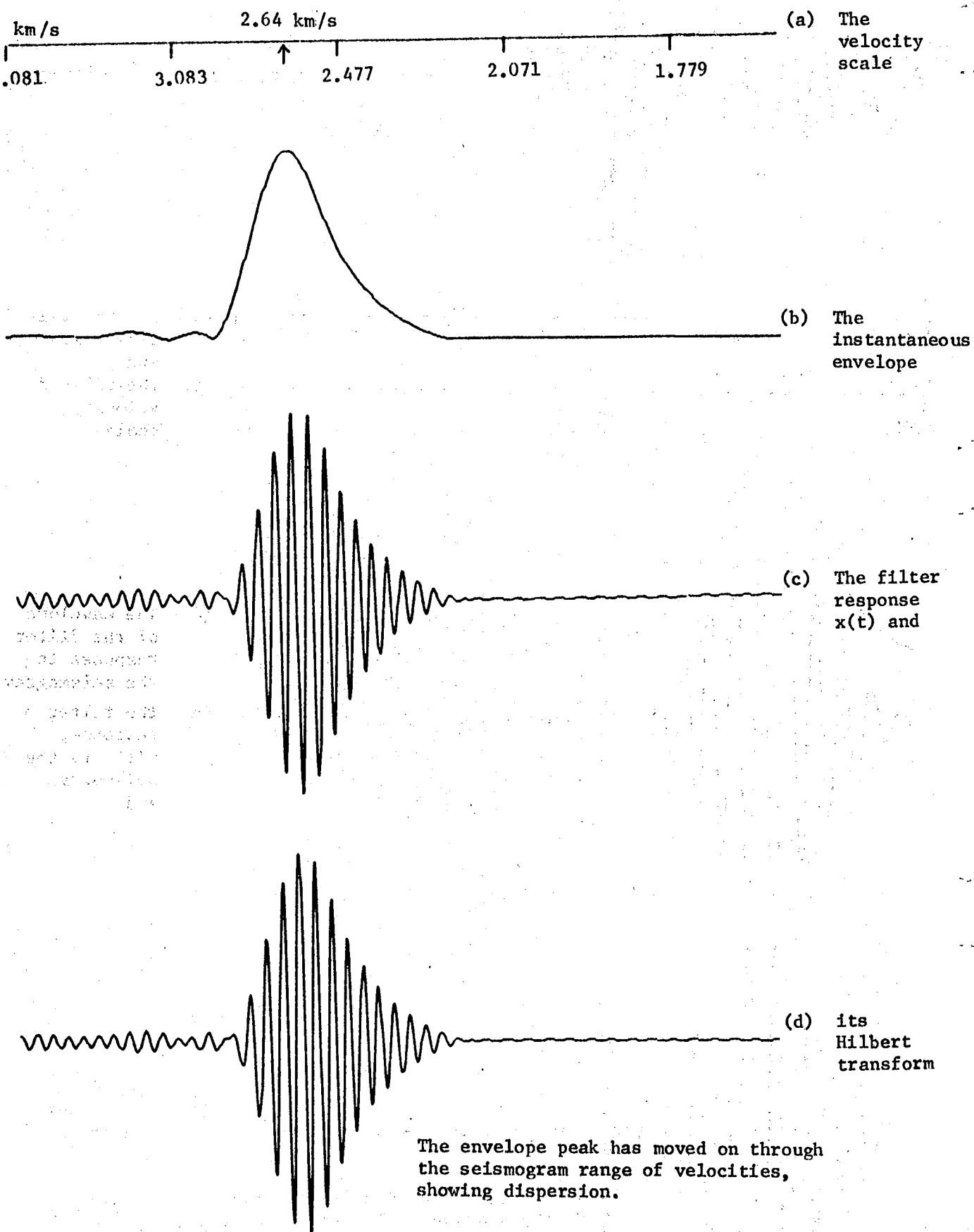


FIGURE 6. A GROUP VELOCITY DETERMINATION FOR A LOWER FREQUENCY  
( $f_L = 0.033$  Hz)



**FIGURE 7. A GROUP VELOCITY DETERMINATION FOR AN INTERMEDIATE FREQUENCY ( $f_1 = 0.051$  Hz)**

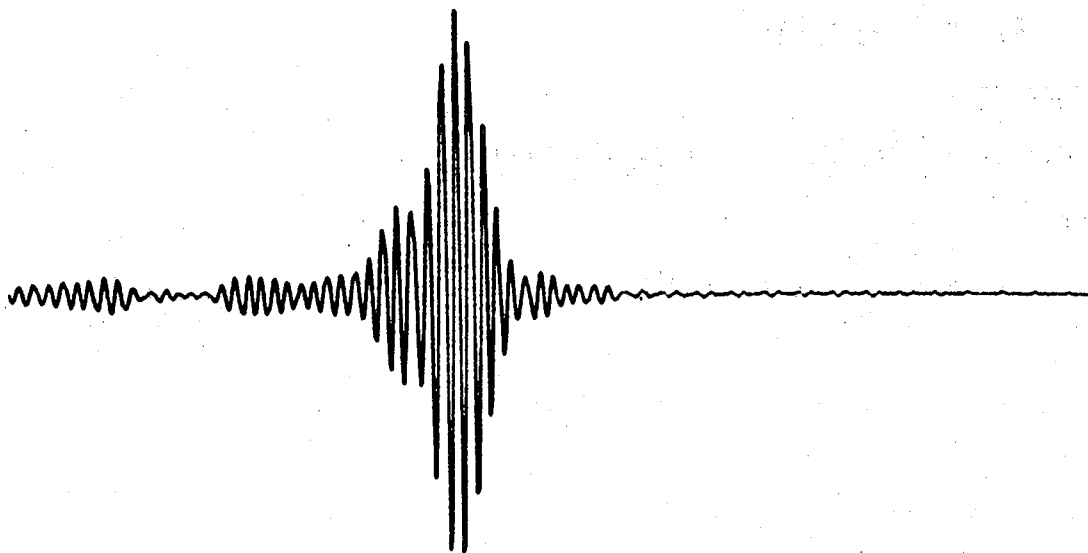
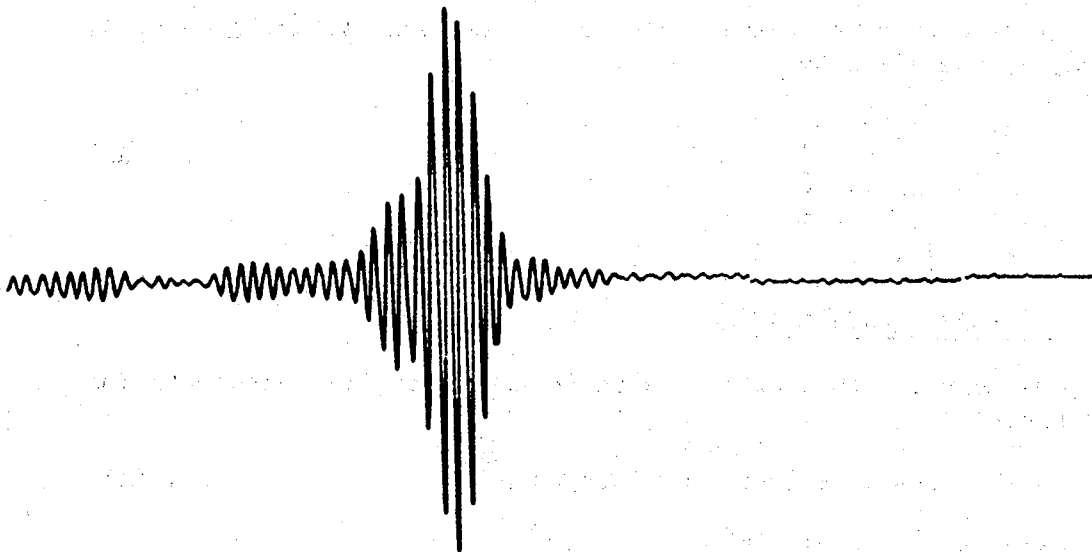
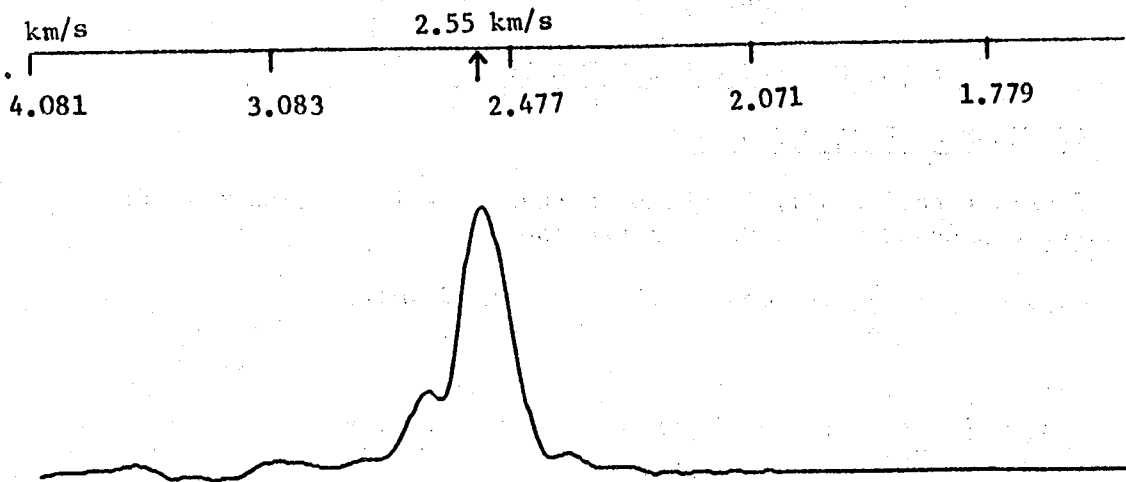


FIGURE 8. A GROUP VELOCITY DETERMINATION FOR A HIGHER FREQUENCY ( $f_H = 0.088$  Hz).  
FIGURES 7 AND 8 GIVE SIMILAR GROUP VELOCITIES BECAUSE THERE IS A MINIMUM  
TURNING POINT IN THE DISPERSION CURVE, FIGURE 5 (AN AIRY PHASE IN THE TIME DOMAIN).

APPENDIX A

COSINUSOIDAL AND COMPLEX TRANSFORMS

A1. CONTINUOUS, PERIODIC DATA

If the function  $x(t)$  is periodic (period =  $T$ , frequency =  $Df$ ) then it may be expressed as the Fourier series

$$x(t) = \frac{a_0}{2} + \sum_{j=1}^{\infty} (a_j \cos 2\pi j Df t + b_j \sin 2\pi j Df t) \quad \dots\dots(A1)$$

$$a_j = \frac{2}{T} \int_{-T/2}^{T/2} x(t) \cos 2\pi j Df t dt \quad j = 1 \dots\dots \infty$$

and similarly  $b_j$ . Orthogonality of cosinusoids easily gives the coefficients  $a_j, b_j$ .

In the frequency domain discrete line spectral amplitudes,  $A$ , and phase,  $\phi$ , are given by

$$\begin{aligned} A_j &= (a_j^2 + b_j^2)^{1/2} & ) \\ \phi_j &= \tan^{-1} \left( \frac{b_j}{a_j} \right) & ) \end{aligned} \quad \dots\dots(A2)$$

at  $f_j = j \times Df.$

A2. COMPLEX REPRESENTATION

De Moivre's theorem allows us to use a complex representation for (A1) since

$$e^{ip\theta} = \cos p\theta + i \sin p\theta \quad (\text{integer } p) \quad \dots\dots(A3)$$

$$x(t) = \sum_{j=-\infty}^{\infty} C_j e^{i2\pi j Df t},$$

where  $C_{\pm j} = \frac{1}{2} (a_j \mp b_j),$

or alternatively

$$C_j(f_j) = \frac{1}{2} (a_j(f_j) - \text{sign}(f_j) b_j(f_j))$$

therefore

$$C_j(f_j) = \frac{1}{T} \int_{-T/2}^{T/2} x(t) e^{-i2\pi j Df t} dt. \quad \dots\dots(A4)$$

A3. CONTINUOUS, NON-PERIODIC, TRANSIENT DATA

The traditional step is to allow the fundamental period to tend to infinity and produce a Fourier transform pair. The coefficients  $C_j(f_j)$  become the continuous functional  $X(f)$  and  $f_{j+1} - f_j \rightarrow 0$ . The Fourier transform pair to be used here may be obtained as

$$X(f) = \int_{-\infty}^{\infty} x(t)e^{-i2\pi ft} dt \quad \dots\dots(A5a)$$

$$x(t) = \int_{-\infty}^{\infty} X(f)e^{+i2\pi ft} df. \quad \dots\dots(A5b)$$

An important consequence of equation (A3) is that

$$(e^{ip\theta})^* = e^{-ip\theta}$$

and if  $x(t)$  is wholly real in equations (A4) and (A5a) it follows that

$$X^*(f) = X(-f)$$

and therefore values of the functional  $X(f)$  are dependently related about  $f = 0$ , and concern over calculations for negative frequencies is reduced.

A4. DISCRETE DATA OF FINITE LENGTH

We have the time series  $x(t)$  sampled at  $N$  points giving the values  $x_n$  ( $n = 0 \dots\dots N - 1$ ). There is a constant time interval  $Dt$  between adjacent values of  $x_n$  and adapting equation (A5a) gives

$$X(f_j) = Dt \sum_{n=0}^{N-1} x_n e^{-i2\pi f_j nDt}. \quad \dots\dots(A6)$$

It is apparent that  $X(f)$  now assumes discrete values at the frequencies  $f_j$  ( $|f_j| < \infty$ ).

Expanding (A6)

$$X(f_j) = Dt \sum_{n=0}^{N-1} x_n (\cos 2\pi f_j nDt - i \sin 2\pi f_j nDt)$$

and therefore

$$C_{sp}(f_j) = |\text{sign}(f_j)| Dt \sum_{n=0}^{N-1} x_n \cos 2\pi f_j nDt$$

$$S_{sp}(f_j) = \text{sign}(f_j) Dt \sum_{n=0}^{N-1} x_n \sin 2\pi f_j nDt$$

and again if  $x_n$  is real then  $X^*(f_j) = X(-f_j)$ .

The values of  $C_{sp}(f_j)$  and  $S_{sp}(f_j)$  must be evaluated at discrete frequencies  $f_j$ . For maximum information from the data, of length  $T$ , use

$$f_j = j \times Df = \frac{j}{T} = \frac{j}{N \times Dt} \quad |j| \leq \frac{N}{2}$$

and

$$f_{NYQ} = \frac{1}{2 \times Dt}$$

is the highest frequency, the Nyquist, which can be discriminated in the data. If no frequencies greater than  $f_{NYQ}$  are present in the continuous series  $x(t)$  then the above procedure exactly represents  $x(t)$  for all  $t$ , even though it was only sampled at times  $nDt$ .

The new expressions for amplitude and phase, which should be compared to equations (A2), are

$$\begin{aligned} A_j &= (Csp^2 + Ssp^2)^{\frac{1}{2}} && ) \\ \phi_j &= \tan^{-1} (- \text{sign} (f) \frac{Ssp}{Csp}) && ) \dots\dots(A7) \\ \text{at } f_j &= j \times Df. && ) \end{aligned}$$

It is worth noting that the dimensions of spectral amplitudes A are length  $\times$  time, eg, micron seconds.

APPENDIX B

SCALING THE COOLEY-TUKEY CALCULATIONS AND THE SUBROUTINE COOL

B1.        SCALING

Recursion formulae have been obtained which reduce computation time for Fourier transforms considerably. For discrete data of finite length we have equation (A6)

$$X(f_j) = Dt \sum_{n=0}^{N-1} x_n e^{-i2\pi f_j nDt}$$

and since  $f_j = \frac{j}{N \times Dt}$  we obtain

$$X(f_j) = Dt \sum_{n=0}^{N-1} x_n e^{-\frac{i2\pi jn}{N}} \quad |j| \leq \frac{N}{2}$$

Computational algorithms of the Cooley-Tukey type are derived from series of the type

$$Z_j = \sum_{n=0}^{N-1} Y_n e^{-\frac{i2\pi jn}{N}}, \quad \dots (B2)$$

where  $Z_j$  and  $Y_n$  are complex [4].

For machine computation equation (B2) gives results which are not unit dependent because the scale factor  $Dt$  has been omitted. Similarly on the reverse transform the factor  $Df$  is omitted. To obtain absolute values after applying COOL to the complex array  $Z(I)$ :-

- (1) Time to frequency, scale factor is  $Dt$  ( $Dt = DELA$ )

$$Z'(I) = Z(I) \times DELA.$$

- (2) Frequency to time, scale factor is  $Df = 1/NDt$

$$Z'(I) = \frac{Z(I)}{N \times DELA}.$$

B2.        SUBROUTINE COOL.

The digital time series  $x_n$  must have  $N$  points where  $N$  is some power of 2, that is,  $N = 2^L$ . An extra power of 2, as in this program, ensures that convolution formed by multiplication of two transforms in the frequency domain gives accurate values over the time domain range of interest [5]. Also  $x_n$  is stored in the real part of a complex array  $Z$ . The Fortran statement `CALL COOL (L, Z, +1)` performs the direct transform. On return from this call the storage in  $Z$  is:-

- (1)  $ReZ$  contains the cosine spectrum,  $Csp(f_j)$ .  
 (2)  $ImZ$  contains the sine spectrum  $Ssp(f_j)$ .



Also Z(1) contains the dc component to be set to zero. The components are folded about the array index number  $(N/2) + 1$ , NBY2P1, so that

$$Z(NBY2P1 + I) = Z^*(NBY2P1 - I)$$

for  $I = 0 \dots (N/2) - 1$ . Therefore the cosine spectrum is reflected symmetrically and the sine spectrum antisymmetrically. This creates negative frequency components in stores NBY2P1 + 1 to N of Z(I). Amplitude and phase are given by equation (A7).

Reverse transforms would be formed by storing components as they are obtained above, but calling COOL with -1.0 replacing +1.0. The time series is then returned in ReZ(I) [5].



(1) Calculate the Fourier transform of  $x(t)$ , obtaining the complex array  $Z(w)$ .

(2) Set the negative frequency components of  $Z$  to zero (ie, those with array indices greater than  $NBY2P1$  up to  $N$ ).

(3) Calculate the inverse Fourier transform of  $Z$  and hence revert to the time domain obtaining  $\hat{x}(t)$ , which is complex.

(4) Calculate instantaneous amplitudes of the envelope,  $|A(t)|$ , where

$$|A(t)| = (x(t)^2 + (Hx(t))^2)^{\frac{1}{2}}.$$

Note: The maximum value of  $|A(t)|$  is used to determine the group velocity at frequency  $f$  for which  $A(t)$  has been obtained. The values of  $|A(t)|$  for a particular filter frequency are stored in one column of the matrix  $E$ . Figures 6, 7 and 8 each show the use of this envelope for group velocity determination and how the envelope relates to its two components.

APPENDIX D

MULTIPLE WINDOW FILTERING IN THE FREQUENCY DOMAIN TO DETERMINE  
DISPERSION

D1. MULTIPLE FILTERING

A set of  $r$  passband filters of constant  $Q$ , that is, the ratio peak frequency to bandwidth is constant, and different centre peak frequencies  $f_j (1 \leq j \leq r)$ , is chosen. Therefore each filter "windows" a certain passband of the frequency spectrum [1].

Windowing the frequency spectrum of the time series around chosen frequencies allows us to measure signal amplitude as a function of both frequency and time of arrival of energy at that frequency. Time of arrival is easily related to a secondary quantity - group velocity - which is independent of the event to recording station separation. There are  $p$  values of group velocity,  $u_i (1 \leq i \leq p)$ . We have a two-dimensional,  $p \times r$ , matrix  $E(u, f)$  and chose the group velocity at frequency  $f_j$ , out of the  $p$  possible values  $u_i$ , to be such that  $E(u_i, f_j)$  is the maximum value of the column  $E(u, f_j)$ . This is done for all frequencies  $f_j$  to obtain the group velocity curve  $u(f_j) (1 \leq j \leq r)$ . This process is illustrated in the sequence of figures 6, 7 and 8 and the results are summarised by the matrix  $E$  in figure 4.

D2. THE FILTER

The filter chosen must have good resolution in both domains; we cannot sacrifice resolving power in one domain for improvement in the other. The Gaussian is chosen because for practical purposes the product of its resolution in the two domains is maximum [2,7].

The multiple filters are constant  $Q$  of relative bandwidth BAND. For the  $j$ th filter the upper and lower frequencies are:-

$$f_j^u = (1 + \text{BAND})f_j$$
$$f_j^l = (1 - \text{BAND})f_j.$$

The passband Gaussian filter for central frequency  $f_j$  is

$$W_j(f) = \begin{cases} 0 & ) f < f_j^l \\ e^{-\alpha \left(\frac{f-f_j}{f_j}\right)^2} & ) f_j^l \leq f \leq f_j^u \\ 0 & ) f > f_j^u \end{cases}$$

where ALPHA determines the resolution or filter roll-off. The filter roll-off is also specified by  $\beta$  where

$$\beta = \ln \left( \frac{W(f_j)}{W(f_j^1)} \right)$$

and therefore

$$\alpha = \frac{\beta}{\text{BAND}^2}$$

(The ratio  $W(f_j)/W(f_j^1)$  is read into the computer as the parameter DWF, for example, DWF = 10.0.) Each filter  $W_j(f)$  is chosen so that  $W(f_j) = 1$  at the central frequency.

The array of central frequencies  $f_j$  chosen for the filters is chosen to exactly correspond to harmonic frequencies obtained from the Fourier analysis of the time series. This eliminates errors in previous work which did not match these frequencies [1].

### D3. COMPUTATION

The Fourier transform of  $x(t)$  is contained in the complex array  $Z(I)$ , including the non-independent values for negative frequency components. A particular windowing filter is fed into the complex array  $P(I)$ ; this could be done for positive and negative frequency components. For the filter centred at  $f_j$  multiplication at each harmonic frequency achieves the required window filtering of the signal

$$Z'(I) = Z(I) \times P(I)$$

and inverse Fourier transform of  $Z'(I)$  would give the filtered seismogram at frequency  $f_j$ . This would be an oscillating signal of approximately mean frequency  $f_j$ , because for  $W_j(f)$  we have  $\bar{f} = f_j$  because the filter is symmetric about  $f_j$ .

Preferably we require the envelope, in the time domain, to  $Z'(I)$ ; this is obtained by setting the negative frequency components to zero (appendix C). This is simply accomplished by just storing the filter in the positive frequency range of  $P(I)$  before multiplication and transformation (appendix B, section B2).

## APPENDIX E

### INSTRUMENTATION PACKAGE

This is an adapted version of a program written by Brune. Full details will be found in the Vesiac report [8]. It is only applicable to long period WSSN instruments.

If the user wishes to consider an alternative instrument response he should do the following:-

- (1) Remove the 78 card library of calibration pulses and the subroutine SSLIBR which reads in this library.
- (2) Rewrite subroutine WSSN (TMCNRS) so that on return from this subroutine the complex array P(I) contains the new instrument transfer function. Also TMCNRS is the conversion factor from one arbitrary unit of displacement for the time series to microns.
- (3) The parameter cards 7 and 8 must be altered or removed, as appropriate for the new instrument.

APPENDIX F

PROGRAM LISTING

## TIME SERIES ANALYSIS PROGRAM

---

THE PROGRAM READS IN A DIGITAL SIGNAL SAMPLED AT EQUAL INTERVALS OF TIME. THE SIGNAL IS FOURIER ANALYSED PRODUCING SPECTRAL PHASE AND AMPLITUDE CONTENT AT THE HARMONIC FREQUENCIES. ABSOLUTE VALUES MAY BE OBTAINED BY REMOVING THE INSTRUMENT RESPONSE. A MULTIPLE FILTERING TECHNIQUE IS APPLIED TO PRODUCE A CHARACTERISTIC OF THE DISPERSION -- THE GROUP VELOCITY.

GENERAL REFERENCE -- DZIEWONSKI, BLOCH AND LANDISMAN 1969  
'A TECHNIQUE FOR THE ANALYSIS OF TRANSIENT SEISMIC SIGNALS'  
BULLETIN OF THE SEISMOLOGICAL SOCIETY OF AMERICA. 59, 1, P427-444.

THE ORIGINAL PURPOSE OF THE PROGRAM WAS TO ANALYSE RAYLEIGH WAVES FROM SEISMIC EVENTS.

---

### OUTPUT

---

#### PRINTOUT.

1. INPUT OPTICAL PARAMETERS AND INPUT SIGNAL DATA.
2. SPECTRAL AMPLITUDE AND PHASE AT THE HARMONIC FREQUENCIES.
3. INSTRUMENTAL MAGNIFICATION AND PHASE AT HARMONIC FREQUENCIES.
4. SPECTRAL AMPLITUDE AND PHASE AFTER INSTRUMENT REMOVAL.
5. THE SIGNAL AFTER INSTRUMENT REMOVAL.
6. INFORMATION ABOUT THE FILTERS.
7. GROUP VELOCITY V. FREQUENCY (KMS/SEC V. HZ)
8. THE 2-D MATRIX E -- INSTANTANEOUS ANALYTIC SIGNAL AMPLITUDES AS A FUNCTION OF FREQUENCY AND VELOCITY.

#### GRAPHS.

GRAPHS AT MOST OF THE ABOVE STAGES MAY BE REQUESTED FROM SC406C.

#### PUNCHOUT.

1. THE SMOOTHED FOURIER AMPLITUDE SPECTRUM V. FREQUENCY.
2. THE GROUP VELOCITY CURVE V. SELECTED HARMONIC FREQUENCIES.

MUCH OF THIS OUTPUT IS OPTICAL.

---



HARMONIC FREQUENCIES.

SIGNAL OF NSEIS SAMPLES AT INTERVALS DELA SECONDS. NSEIS SET TO N WHERE N/2 GREATER THAN OR EQUAL TO NSEIS AND IS A POWER OF 2.

1. FUNDAMENTAL FREQUENCY IS  $DF = 1/(N*DELA)$
2. FREQUENCY HARMONICS ARE  $FREQ(I) = (I-1)*DF$
3. THE NYQUIST FREQUENCY IS  $FNYQ = 1/(2*DELA)$

TO USE THIS PROGRAM.

THE PARAMETER CARDS AND DATA SHOULD BE PUNCHED AS FOLLOWS

CARD 1. THE RELEVANT SC4060 CARD.

CARD 2. A 78 CARD LIBRARY OF WSSN SEISMOMETER CALIBRATION PULSES.

CARD 3. FORMAT(10A8)

TITLEA TITLE FOR THE DATA. IN COLUMNS 73-80 PUNCH AN IDENTIFICATION LABEL E.G. DATA 001

CARD 4. FORMAT(8A1,F12.5,I2,I2,F3.1,3X,I2,I2,F3.1,3X,I10)

STANAM NAME OF THE RECORDING STATION.

DELTAD DISTANCE IN DEGREES BETWEEN EVENT AND RECORDING STATION. PROGRAM USES IDEGREE = 111.1 KMS.

MHOUR HOURS.  
MIN MINUTES. GMT ORIGIN TIME OF EVENT.  
SEC SECONDS.

MHRGMT HOURS.  
MINGMT MINUTES. GMT TIME OF FIRST SAMPLE.  
SECGMT SECONDS.

NSEIS NUMBER OF SAMPLES IN THE DIGITAL TIME SERIES. NOT MORE THAN 2048.

CARD 5. FORMAT(F5.1,11I5,3F5.2)

DELA INTERVAL BETWEEN SAMPLES (SECONDS).

IVSEIS INVERT THE SIGNAL. (IFF IVSEIS = 1)

NUMCLT REMOVE NUMCUT SAMPLES FROM THE FRONT OF THE SIGNAL AND CORRECT THE FIRST SAMPLE TIME BY NUMCUT\*DELA.

- NBASE CORRECT THE SIGNAL TO A MEAN BASELINE.  
(IF NBASE = 1)
- NCOSTP COSINE TAPER NCOSTP POINTS AT BOTH ENDS OF SIGNAL.
- NCOMB NUMBER OF POINTS IN THE COMB USED TO SMOOTH THE  
FOURIER AMPLITUDE SPECTRUM. MUST BE EVEN. THE COMB  
IS ADVANCED NCOMB/2 POINTS THROUGH THE SPECTRUM  
FOR EACH SMOOTHING OPERATION.
- NAFLC INDEX NO. FOR THE FREQUENCY ARRAY FREQ(I) WHICH  
REFERS TO THE LOWEST FREQUENCY OF INTEREST IN THE  
AMPLITUDE SPECTRUM. ALL FREQUENCIES LOWER THAN  
FREQ(NAFLC+1) = NAFLC\*DF ARE REMOVED.
- NINSTR REMOVE THE INSTRUMENT RESPONSE. (IFF NINSTR = 1)
- NLGRUP CALCULATE GROUP VELOCITIES. (IFF NUGRUP = 1)
- NFLO INDEX NO. FOR FREQ(I) REFERRING TO THE LOWEST  
FREQUENCY OF INTEREST, NFLO\*DF, FOR GROUP VELOCITY  
DETERMINATION. IGNORE FREQUENCY FREQ(NFLO) AND  
BELOW. NFLO MUST BE GREATER THAN NAFLC.
- NFHI INDEX NO. FOR FREQ(I) REFERRING TO THE HIGHEST  
FREQUENCY OF INTEREST, NFHI\*DF, FOR GROUP VELOCITY  
DETERMINATION. IGNORE FREQ(NFHI) AND ABOVE.
- NFSTEP INTERVAL BETWEEN ADJACENT FREQUENCIES FOR GROUP  
VELOCITY DETERMINATION IS NFSTEP\*DF.  
N.B. THESE ARE THE FILTER CENTRE FREQUENCIES FREQC  
SUCH THAT FREQC(1) = FREQ(NFLO+1) = NFLO\*DF ETC.
- BAND DIMENSIONLESS, RELATIVE BANDWIDTH OF GAUSS FILTER.
- DWF DECAY RATE GAUSSIAN FILTER WINDOWING FUNCTION.
- DV VELOCITY STEP ALONG THE SIGNAL. VELOCITY TO FIRST  
SAMPLE = VSF, TO LAST SAMPLE = VSL. CHOOSE DV TO  
DIVIDE VSF-VSL INTO AT MOST 120 VALUES OF VELOCITY

CARD 6. FORMAT(15I1,5X,2I1) SELECTION OF GRAPHS AS OUTPUT.

- NG1 INPUT SIGNAL.
- NG2 ADJUSTED SIGNAL PRIOR TO FOURIER ANALYSIS.
- NG3 SPECTRAL AMPLITUDE / FREQUENCY (HZ).
- NG4 SPECTRAL PHASE (RADIAN) / FREQUENCY (HZ).
- NG5 SEISMOMETER CALIBRATION PULSE (WSSN INSTRUMENT  
RESPONSE TO A STEP OF ACCELERATION).
- NG6 INSTRUMENT RESPONSE AMPLITUDE / FREQUENCY (HZ).
- NG7 INSTRUMENT RESPONSE PHASE (RADS.) / FREQUENCY (HZ)

- NG8 SIGNAL WITH INSTRUMENT EFFECT REMOVED.
- NG9 SPECTRAL AMPLITUDE (MICRONS\*SECS) / FREQUENCY (HZ)  
INSTRUMENT RESPONSE REMOVED.
- NG10 SPECTRAL PHASE (RADIAN) / FREQUENCY (HZ).  
INSTRUMENT RESPONSE REMOVED.
- NG11 SMOOTHED SPECTRAL AMPLITUDE / FREQUENCY (HZ).
- NG12 GROUP VELOCITY (KMS/SEC) / FREQUENCY (HZ).
- NG13 GROUP VELOCITY (KMS/SEC) / PERIOD (SECONDS).
- NG14 CONTOUR PLOT (AMPLITUDE CONTOURS AT 5DB. INTERVALS  
FOR THE GROUP VELOCITY / FREQUENCY MATRIX).
- NG15 NOT USED.

SELECTION OF PUNCHED CARDS AS OUTPUT.

- NP1 PUNCH OUT FREQUENCY / SMOOTHED AMPLITUDE (2E15.7)  
PLUS IDENTIFICATION LABELS AND A CARD COUNT.
- NP2 PUNCH OUT FREQUENCY / GROUP VELOCITY IN (2E15.7)  
PLUS IDENTIFICATION LABELS AND A CARD COUNT.

N.B. -- THESE OPTIONS ONLY CARRIED OUT WHEN THE OPTION  
PARAMETER IS SET TO 1 E.G. NG5 = 1.

CARD 7. FORMAT(10A8)

FMT VARIABLE FORMAT USED TO INPUT THE SIGNAL.

----- CARDS 8 AND 9 OMITTED UNLESS NINSTR = 1.

CARD 8. FORMAT(10A8)

TITLEB TITLE CARD FOR THE INSTRUMENT DATA.

CARD 9. FORMAT(10F5.1,22X,2I4) WSSN INSTRUMENT CALIBRATION DATA.

- Q11 TIME WHEN RISING PULSE IS 1/3 OF MAXIMUM HEIGHT.
- Q22 TIME WHEN RISING PULSE IS 2/3 OF MAXIMUM HEIGHT.
- Q33 TIME WHEN RISING PULSE IS AT MAXIMUM HEIGHT.
- Q44 TIME WHEN FALLING PULSE IS 2/3 ETC.
- Q55 TIME WHEN FALLING PULSE IS 1/3 ETC.
- Q66 TIME WHEN FALLING PULSE IS 1/10 ETC.

- FMASS SEISMOMETER MASS IN KGMS.
- G SEISMOMETER MOTOR CONSTANT (NEWTONS/MAMP).
- CLR CALIBRATION CURRENT (MAMP).
- DEFL MAXIMUM HEIGHT OF DEFLECTION (MM).

- LABEL LABEL OF PARTICULAR SEISMOGRAPH CONCERNED.
- NSCALE CHOICE OF TWO POSSIBLE SCALES WHICH CONVERT THE  
MEASURED VALUES OF Q11 ETC. AND DEFL FROM  
ARBITRARY UNITS INTO SECONDS AND MMS.

N.B. -- REMOVAL OF THIS PARTICULAR INSTRUMENT PROBABLY ONLY RELEVANT TO MY WORK. REFERENCE IS VESIAC SPECIAL REPORT NO. 4410-106-X 'A TRANSIENT TECHNIQUE FOR SEISMOGRAPH CALIBRATION-MANUAL AND STANDARD SET OF THEORETICAL TRANSIENT RESPONSES.' BY ESPINOSA, SUTTON AND MILLER. (OCTOBER 1965).

N.B. -- THIS PARTICULAR INSTRUMENT IS EASILY REPLACED. SEE 'C' REPORT.

----- CARDS 8 AND 9 OMITTED UNLESS NINSTR = 1.

CARD10. FORMAT IS FMT.

SEIS DIGITAL SIGNAL DATA. NOT MORE THAN 1024 POINTS.

CARDS 3 TO 10 REPEATED FOR ANY NUMBER OF SIGNALS.

MAIN

```
COMMON/C01/Z(2048),CZERO,P(2048)
COMMON/C02/SEIS(2048),FREQ(1024),AMP(1024),PHASE(1024)
COMMON/C03/STANAM(8),DELTA,DELTA,CRIGTM,GMTSEC
COMMON/C04/NSEIS,DELA,IVSEIS,NUMCUT,NBASE,NCOSTP,NCOMB,NAFLO,
1 NINSTR,NLGRUP,NFLG,NFHI,NFSTEP,BAND,CWF,DV,NAFLO1
COMMON/C05/NG1,NG2,NG3,NG4,NG5,NG6,NG7,NG8,NG9,NG10,NG11,NG12,NG13
1 ,NG14,NG15,NP1,NP2
COMMON/C06/TITLEA(20),DATE,BLANK,TITLEB(20)
COMMON/C09/Q1(78),Q2(78),Q3(78),Q4(78),Q5(78),Q6(78),HH1(78),HH2(7
18),SSIGMA(78),TT1(78),TT2(78),FAC(78),BA,CA,DA,TFAC(78)
COMMON/C10/G11,G22,G33,G44,G55,G66,FMASS,G,CUR,DEFL,LABEL,NSCALE
COMPLEX Z,CZERC,P
REAL*8 TITLEA,TITLEB,DATE,DUMMY,BLANK
DATA DUMMY,' '
BLANK=DUMMY
CALL SCLIBR
CALL TIMER
CALL SSLIBR
CZERO=CMPLX(0.0,0.0)
```

```
CALL DATIM(DATE,DUMMY)
100 READ(5,10,END=999)(TITLEA(I),I=6,15)
10 FORMAT(10A8)
PRINT 20,DATE
20 FORMAT(1H1,///,5X,'SURFACE WAVE ANALYSIS',90X,A8)
PRINT 30
30 FORMAT(5X,'-----',90X,'-----')
PRINT 40,(TITLEA(I),I=6,15)
40 FORMAT(20X,10A8//)
```

```

C
CALL INPLT
CALL TRACE1
IF(NINSTR.NE.1.AND.NG11.NE.1.AND.NP1.NE.1) GO TO 50
CALL TRACE2
50 IF(NUGRUP.NE.1) GO TO 60
CALL UGRUP

C
60 CALL ADVFLM(3)
CALL ENDFME
CALL TIMER
GO TO 100
999 CALL FINISH
END
SUBROUTINE SSLIBR

C
C READS IN LIBRARY OF WSSN CALIBRATION PULSE PARAMETERS.
C SEE VE SIAC REPORT.
C
COMMON/CC9/Q1(78),Q2(78),Q3(78),Q4(78),Q5(78),Q6(78),HH1(78),HH2(7
18),SSIGMA(78),TT1(78),TT2(78),FAC(78),BA,CA,DA,TFAC(78)
DO 1 I=1,78
READ 2,Q1(I),Q2(I),Q3(I),Q4(I),Q5(I),Q6(I),HH1(I),HH2(I),SSIGMA(I)
1,TT1(I),TT2(I),FAC(I),BA,CA,DA,TFAC(I)
2 FORMAT(16F5.1)
FAC(I)=(FAC(I)*DA)/(BA*CA)/2.0
1 CONTINUE
RETURN
END
SUBROUTINE INPLT

C
C READS IN INPUT PARAMETER OPTIONS AND THE INPUT SIGNAL.
C
COMMON/CC2/SEIS(2048)
COMMON/CC3/STANAM(8),DELTAD,DELTA,CRIGTM,GMTSEC
COMMON/CC4/NSEIS,DELA,IVSEIS,NUMCUT,NBASE,NCOSTP,NCOMB,NAFLO,
1 NINSTR,NUGRUP,NFLO,NFHI,NFSTEP,BAND,DWF,DV,NAFLO1
COMMON/CC5/NG1,NG2,NG3,NG4,NG5,NG6,NG7,NG8,NG9,NG10,NG11,NG12,NG13
1 ,NG14,NG15,NP1,NP2
COMMON/CC6/TITLEA(20),DATE,BLANK,TITLEB(20)
COMMON/CC10/Q11,Q22,Q33,Q44,Q55,Q66,FMASS,G,CUR,DEFL,LABEL,NSCALE
DIMENSION FMT(10)
REAL*8 TITLEA,TITLEB,FMT,BLANK,DATE
READ 10,STANAM,DELTAD,MHCUR,MIN,SEC,MHRGMT,MINGMT,SECGMT,NSEIS
10 FORMAT(8A1,F12.5,I2,I2,F3.1,3X,I2,I2,F3.1,3X,I10)
C
READ 20, DELA,IVSEIS,NUMCUT,NBASE,NCOSTP,NCOMB,NAFLO,NINSTR,
INUGRUP,NFLC,NFHI,NFSTEP,BAND,DWF,CV
20 FORMAT(F5.1,11I5,3F5.2)
ORIGTM=3600.0*FLCAT(MHCUR)+60.0*FLCAT(MIN)+SEC
GMTSEC=3600.0*FLCAT(MHRGMT)+60.0*FLCAT(MINGMT)+SECGMT
GMTLO=C.2*60.0*DELTAD+ORIGTM
GMTHI=1.0*60.0*DELTAD+CRIGTM
IF(GMTSEC.GE.GMTLC.AND.GMTSEC.LE.GMTHI) GO TO 30
PRINT 25
25 FORMAT(10X,'FAILED TIME TEST')
30 DELTA=DELTAD*111.1
PRINT 40,STANAM,DELTAD,DELTA,MHOUR,MIN,SEC,ORIGTM,
1 MHRGMT,MINGMT,SECGMT,GMTSEC

```

```

4C 31 FORMAT(//10X,'STATION NAME IS ',8A1,
1 //10X,'DISTANCE OF RECORDING STATION FROM EPICENTRE ',F10.
2 5,2X,'DEGREES',3X,'OR',3X,F10.4,1X,'KILOMETRES',
3 //10X,'ORIGIN TIME OF EVENT ',6X,I2,1X,'HOURS',3X,I2,1X,
4 'MINS',3X,F4.1,1X,'SECS',10X,'(IN SECONDS) = ',F11.3,
5 //10X,'GMT TIME OF FIRST SAMPLE ',2X,I2,1X,'HOURS',3X,I2,
6 1X,'MINS',3X,F4.1,1X,'SECS',10X,'(IN SECONDS) = ',F11.3)
PRINT5C,NSEIS,DELA,IVSEIS,NUMCUT,NBASE,NCOSTP,NCOMB,NAFLO,NINSTR,
1NUGRUP,NFLO,NFHI,NFSTEP,BAND,DWF,DV
5C FORMAT(//10X,'NSEIS = ',I5,10X,'DELA = ',F6.2,9X,'IVSEIS = ',
1 I5,10X,'NUMCUT = ',I5,
2 //10X,'NBASE = ',I5,10X,'NCOSTP = ',I5,10X,'NCOMB = ',
3 I5,10X,'NAFLO = ',I5,
4 //10X,'NINSTR = ',I5,10X,'NUGRUP = ',I5,10X,'NFLO = ',
5 I5,10X,'NFHI = ',I5,
6 //10X,'NFSTEP = ',I5,10X,'BAND = ',F6.2,9X,'DWF = ',
7 F6.2,9X,'DV = ',F6.2)
READ 60,NG1,NG2,NG3,NG4,NG5,NG6,NG7,NG8,NG9,NG10,NG11,NG12,NG13,
1 NG14,NG15,NP1,NP2
6C FORMAT(15I1,5X,2I1)
PRINT70,NG1,NG2,NG3,NG4,NG5,NG6,NG7,NG8,NG9,NG10,NG11,NG12,NG13,
1 NG14,NG15,NP1,NP2
7C FORMAT(//10X,'GRAPH AND PUNCH SELECTION',
1 //10X,5I1,1X,5I1,1X,5I1,2X,2I1)
READ 80,FMT
PRINT9C,FMT
8C FORMAT(10A8)
9C FORMAT(//10X,'INPUT FORMAT IS ',10A8)
IF(NINSTR.EQ.0) GO TO 110
READ 80,(TITLEB(I),I=6,15)
READ 100,Q11,Q22,Q33,Q44,Q55,Q66,FMASS,G,CUR,DEFL,LABEL,NSCALE
100 FORMAT(1CF5.1,22X,2I4)
110 READ FMT,(SEIS(I),I=1,NSEIS)
PRINT 120,(SEIS(I),I=1,NSEIS)
120 FORMAT(1H1//10X,'SEISMOGRAM ORIGINAL DATA',
1 //,(1X,12F10.0))
C
RETURN
END
SUBROUTINE TRACE1
C
C
C PREPARES THE SIGNAL FOR FOURIER ANALYSIS AND FOURIER ANALYSES IT.
COMMON/GRFF/TITLE(20),XMAX,XMIN,YMAX,YMIN,INDX,INDY,IND,IDOT,
1 ANSTR1,IF,XLIMIT,YLIMIT,SCALX,SCALY
COMMON/C01/7(2048),CZERC
COMMON/C02/SEIS(2048),FREQ(1024),AMP(1024),PHASE(1024)
COMMON/C03/STANAM(8),DELTAD,DELTA,ORIGTM,GMTSEC
COMMON/C04/NSEIS,DELA,IVSEIS,NUMCUT,NBASE,NCOSTP,NCOMB,NAFLO,
1 NINSTR,NUGRUP,NFLO,NFHI,NFSTEP,BAND,DWF,DV,NAFLO1
COMMON/C05/NG1,NG2,NG3,NG4,NG5,NG6,NG7,NG8,NG9,NG10,NG11,NG12,NG13
1 NG14,NG15,NP1,NP2
COMMON/C06/TITLEA(20),DATE,BLANK
COMMON/C07/N,NBY2,NBY2P1,NPCW2,FNYQ,CF
DIMENSION ATITLE(20),BTITLE(20),CTITLE(20)
REAL*8 TITLE,ATITLE,BTITLE,CTITLE,TITLEA,TYPMN,TYPE,BLANK,DATE
COMPLEX Z,CZERO
DATA ATITLE/'
SECCNDS SEISMOGRAM AF

```

ITER ANY ADJUSTMENTS IMMEDIATELY PRIOR TO TRANSFORMING BY FOURIER.

2 /\*  
DATA B TITLE / \*FREQUENCY (HZ)                    AMPLITUDE                    AMPLITUDE / E  
1 FREQUENCY (HZ) FOR ADJUSTED SEISMOGRAM.

2 /\*  
DATA C TITLE / \*FREQUENCY (HZ)                    PHASE (RADIANS) PHASE (RADIANS)  
1 / FREQUENCY (HZ) FOR ADJUSTED SEISMOGRAM.

2 /\*  
DATA TYPE MN / \*MEAN                    /\*  
A TITLE (16) = DATE  
B TITLE (16) = DATE  
C TITLE (16) = DATE  
C  
SET UP N  
NTEST = NSEIS - NUMCUT  
IF (NTEST.GT.2048) CALL EXIT  
N=2  
10 IF (NTEST.LE.N) GO TO 20  
N=2\*N  
GO TO 10  
20 N=2\*N  
IF (N.GT.2048) CALL EXIT  
CALL POW(N,NBY2,NBY2F1,NPCW2)  
FNYQ=1.C/(2.0\*DELA)  
DF=FNYQ/FLOAT(NBY2)  
PRINT 30,N,NBY2,NBY2F1,NPCW2,FNYQ,DF  
30 FORMAT (//10X,'N = ',I5,5X,'NBY2 = ',I5,5X,'NBY2F1 = ',I5,5X,  
1        'NPCW2 = ',I5,5X,'FNYQ = ',F9.5,5X,'DF = ',F9.6,/)

C  
FREQ(1)=C.C  
DO 40 I=2,NBY2  
FREQ(I)=FREQ(I-1)+DF  
40 CONTINUE  
IF (NG1.NE.1) GO TO 70  
DO 50 I=1,5  
TITLEA(I)=BLANK  
50 CONTINUE  
TITLEA(3)=A TITLE(3)  
DO 60 I=17,20  
TITLEA(I)=BLANK  
60 CONTINUE  
TITLEA(16)=DATE  
CALL TIMSER(TITLEA,SEIS,NSEIS,DELA,3)

C  
70 IF (IVSEIS.NE.1) GO TO 85  
DO 80 I=1,NSEIS  
SEIS(I)=-1.C\*SEIS(I)  
80 CONTINUE

C  
85 IF (NUMCLT.EQ.0) GO TO 95  
NSEIS=NSEIS-NUMCLT  
GMTSEC=GMTSEC+FLOAT(NUMCUT)\*DELA  
DO 90 I=1,NSEIS  
J=I+NUMCLT  
SEIS(I)=SEIS(J)  
90 CONTINUE

C  
95 IF (NBASE.EQ.0) GO TO 100  
IF (NBASE.EQ.1) TYPE=TYPEMN  
IP1=0  
CALL BASE(SEIS,NSEIS,TYPE,IP1)

```

C 100 IF(NCOSTP.EQ.0) GO TO 110
    PI=4.0*ATAN(1.0)
    CALL NPC STP(SEIS,NSEIS,NCSTP,1,PI)
C
C 110 NSE SP1=NSEIS+1
    DO 120 I=NSE SP1,N
    SEIS(I)=C.C
C 120 CONTINUE
C
C 130 IF(NG2.NE.1) GO TO 130
    CALL TIMSER(ATITLE,SEIS,N,DELA,3)
    FOURIER TRANSFORM OF SIGNAL.
    CALL ZRLOAD(N,SEIS,2)
    CALL COCL(NPCW2,2,+1.0)
    FILTER OUT LOW FREQUENCIES UP TO NAFLO*DF.
C 140 IF(NAFLO.EQ.0) NAFLO=1
    DO 140 I=1,NAFLO
    Z(I)=C ZERO
    AMP(I)=C.C
    PHASE(I)=C.C
C 140 CONTINUE
C
    NAFLO1=NAFLO+1
    DO 150 I=NAFLO1,NBY2
    Z(I)=DELA*Z(I)
    AMP(I)=CABS(Z(I))
    XA=-1.0*AIMAG(Z(I))
    XB=REAL(Z(I))
    IF(XA.EQ.0.C.OR.XB.EQ.0.0) GO TO 145
    PHASE(I)=ATAN2(XA,XB)
    GO TO 150
C 145 PHASE(I)=C.C
C 150 CONTINUE
    CALL FILLLP(NBY2P1,2)
C
C 160 IF(NG3.NE.1) GO TO 170
    DO 160 I=1,20
    TITLE(I)=BTITLE(I)
C 160 CONTINUE
    CALL CARGF(FREQ,AMP,NBY2)
C
C 170 IF(NG4.NE.1) GO TO 190
    DO 180 I=1,20
    TITLE(I)=CTITLE(I)
C 180 CONTINUE
    CALL DRUM(NBY2,PHASE)
    CALL CARGF(FREQ,PHASE,NBY2)
C 190 IF(NG3.NE.1.AND.NG4.NE.1) GO TO 210
    PRINT 200,(I,FREQ(I),AMP(I),PHASE(I),I=NAFLO1,NBY2,10)
C 200 FORMAT(1H1///8X,' SEISMICGRAM SPECTRUM',
1 //,2(8X,' FREQUENCY',6X,' AMPLITUDE',8X,' PHASE',5X),
2 //,2(I5,3E15.7))
C
C 210 RETURN
    END
    SUBROUTINE TRACE2

```



REMOVES THE INSTRUMENT EFFECT CALCULATED BY SUBROUTINE WWSSN AND  
SMOOTHS THE SPECTRAL AMPLITUDE / FREQUENCY GRAPH.

COMMON/GRFF/TITLE(20),XMAX,XMIN,YMAX,YMIN,INDX,INDY,IND,ICOT,  
1 ANSTR1,IF,XLIMIT,YLIMIT,SCALX,SCALY

COMMON/CC1/Z(2048),CZERC,P(2048)

COMMON/CO2/SEIS(2048),FREQ(1024),AMP(1024),PHASE(1024)

COMMON/CO3/STANAM(8),DELTAD

COMMON/CO4/NSEIS,DELA,IVSEIS,NUMCUT,NBASE,NCOSTP,NCOMB,NAFLO,  
1 NINSTR,NUGRUP,NFLO,NFHI,NFSTEP,BAND,DWF,DV,NAFLO1

COMMON/CO5/NG1,NG2,NG3,NG4,NG5,NG6,NG7,NG8,NG9,NG10,NG11,NG12,NG13  
1 ,NG14,NG15,NP1,NP2

COMMON/CC6/TITLEA(20),DATE,BLANK,TITLEB(20)

COMMON/CO7/N,NBY2,NBY2P1,NPOW2,FNYQ,DF

DIMENSION ATITLE(20),TIT1(5),TIT2(5)

REAL\*8 DATE,BLANK,TITLEA,TITLEB,ATITLE,TIT1,TIT2,TITLE

COMPLEX 7,CZERO,P

DATA ATITLE,'

SECCNDS

SEISMOGRAM WI

1TH EFFECT OF SEISMOMETER REMOVED.

2 //

DATA TIT1/'FREQUENCY (HZ)

AMP(MICRON\*SECS)'/

DATA TIT2/'PHASE (RADIAN) AMPLITUDE\*AMP-MAGNIFICATION'/

TITLE(16)=DATE

DO 10 I=1,N

P(I)=CZERO

SEIS(I)=0.0

10 CONTINUE

DO 20 I=6,15

TITLE(I)=TITLEA(I)

20 CONTINUE

IF(NINSTR.NE.1) GO TO 175

CALL WWSSN(TMCRNS)

DO 30 I=6,15

TITLE(I)=TITLEA(I)

30 CONTINUE

DO 80 I=NAFLO1,NBY2

IF(REAL(P(I)).EQ.0.0.AND.AIMAG(P(I)).EQ.0.0) GO TO 40

Z(I)=Z(I)/P(I)

GO TO 50

40 Z(I)=CZERO

50 AMP(I)=TMCRNS\*CABS(Z(I))

XA=-1.0\*AIMAG(Z(I))

XB=REAL(Z(I))

IF(XA.EQ.0.0.OR.XB.EQ.0.0) GO TO 60

PHASE(I)=ATAN2(XA,XB)

GO TO 80

60 PHASE(I)=0.0

PRINT 70,I,XA,XB

70 FORMAT(//10X,I5,2F10.5)

80 CONTINUE

CALL FILLUP(NBY2P1,Z)

IF(NG8.NE.1) GO TO 130

DO 90 I=1,NBY2

P(I)=TMCRNS\*Z(I)

90 CONTINUE

CALL FILLUP(NBY2P1,P)

CALL COOL(NPOW2,P,-1.0)

DO 100 I=1,N

P(I)=P(I)/(DELA\*FLCAT(N))

SEIS(I)=REAL(P(I))

```

100 CONTINUE
110 PRINT 110, (SEIS(I), I=1, NSEIS)
110 FORMAT(1H1///10X, 'SEISMOGRAM WITHOUT INSTRUMENT (MICRONS)', //,
1 (1X, 12F10.3))
A TITLE(16)=DATE
DO 120 I=1, 20
A TITLE(I)=BLANK
120 CONTINUE
IF=3
CALL TIMSER(ATITLE, SEIS, N, DELA, IF)

C
130 DO 140 I=1, 5
TITLE(I)=TITLE(I)
140 CONTINUE
IF(NG9.NE.1) GO TO 160
NM=NB Y2-NAFLC1
CALL CARGRF(FREQ(NAFLC1), AMP(NAFLC1), NM)
160 IF(NG10.NE.1) GO TO 165
TITLE(4)=TITLE(1)
TITLE(5)=TITLE(2)
CALL DRUM(NB Y2, PHASE)
CALL CARGRF(FREQ(NAFLC1), PHASE(NAFLC1), NM)
165 PRINT 170, (I, FREQ(I), AMP(I), PHASE(I), I=NAFLC1, NB Y2, 10)
170 FORMAT(1H1///8X, 'SEISMOGRAM SPECTRUM WITHOUT INSTRUMENT',
1 //, 2(8X, 'FREQUENCY', 6X, 'AMPLITUDE', 8X, 'PHASE', 5X),
2 //, 2(15, 3E15.7))
175 IF(NG11.NE.1.AND.NF1.NE.1) GO TO 280
NSHIFT=NCCMB/2
INDF=1
CALL SMOOTH(AMP, FREQ, NB Y2, NCCMB, NSHIFT, KNFL, INDF)
PRINT 180, (I, FREQ(I), AMP(I), I=1, KNFL)
180 FORMAT(1H1/8X, 'SMOOTHED AMPLITUDE SPECTRUM',
1 //, 3(8X, 'FREQUENCY', 6X, 'AMPLITUDE', 3X),
2 //, 3(15, 2E15.7))
IF(NG11.NE.1) GO TO 190
TITLE(4)=TITLE(1)
TITLE(5)=TITLE(1)
IF(NINSTR.EQ.1) GO TO 185
TITLE(4)=TITLE(3)
TITLE(5)=BLANK
185 CALL CARGRF(FREQ, AMP, KNFL)
190 IF(NP1.NE.1) GO TO 280
PUNCH SMOOTHED AMP./FREQ. SPECTRUM IN (2E15.7).
220 PUNCH 220, STANAM, DELTAD, TITLEA(15)
FORMAT(8A1, F12.5, 2X, A8)
NL=1
NH=KNFL
FLO=NFLO*DF
FHI=NFHI*DF
230 IF(FREQ(NL).GE.FLO) GO TO 240
NL=NL+1
GO TO 230
240 IF(FREQ(NH).LE.FHI) GO TO 250
NH=NH-1
GO TO 240
250 PUNCH 260, (FREQ(I), AMP(I), I, STANAM, TITLEA(15), I=NL, NH)
260 FORMAT(2E15.7, 15X, I5, 'A', 9X, 8A1, 4X, A8)
PRINT 270, NL, NH
270 FORMAT(/10X, 'FREQUENCY RANGE OF PUNCHED OUT SPECTRUM',
1 //10X, 'NL =', I4, 5X, 'NH =', I4)
280 RETURN
END

```

1 SUBROUTINE WSSN(TMCRNS)

2 CALCULATES THE THEORETICAL INSTRUMENT RESPONSE MATCHING NEAREST  
3 TO THE OBSERVED DATA. SEE VESIAC REPORT.

4 COMMON/GRFF/TITLE(20),XMAX,XMIN,YMAX,YMIN,INDX,INCY,IND,IDOT,  
5 ANSTR1,IF,XLIMIT,YLIMIT,SCALX,SCALY

6 COMMON/CC1/2(2048),CZERC,P(2048)

7 COMMON/CO2/SEIS(2048),FREQ(1024),AMP(1024),PHASE(1024)

8 COMMON/CO4/NSEIS,DELA,IVSEIS,NUMCUT,NBASE,NCOSTP,NCOMB,NAFLO,  
9 NINSTR,NUGRUP,NFLC,NFHI,NFSTEP,BAND,CWF,DV,NAFLO1

10 COMMON/CO5/NG1,NG2,NG3,NG4,NG5,NG6,NG7,NG8,NG9,NG10,NG11,NG12,NG13  
11,NG14,NG15,NP1,NP2

12 COMMON/CO6/TITLEA(20),DATE,BLANK,TITLEB(20)

13 COMMON/CO7/N,NBY2,NBY2P1,NPGW2,FNYG,CF

14 COMMON/CO9/Q1(78),Q2(78),Q3(78),Q4(78),Q5(78),Q6(78),HH1(78),HH2(7  
15 8),SSIGMA(78),TT1(78),TT2(78),FAC(78),BA,CA,DA,TFAC(78)

16 COMMON/C10/Q11,Q22,Q33,Q44,Q55,Q66,FMASS,G,CUR,DEFL,LABEL,NSCALE  
17 COMPLEX Z,CZERC,P,AYEM,PCW

18 DIMENSION ATITLE(7),RMS(78)  
19 REAL\*8 TITLEA,DATE,BLANK,TITLEB,ATITLE,TITLE

20 AYEM=CMPLX(0.0,-1.0)

21 DATA ATITLE/'FREQUENCY (HZ) SECONDS AMP-MAGNIFICATION PHASE (RADIAN  
22 S) ' //

23 PRINT 10,(TITLEB(I),I=6,15)

24 FORMAT(1H1///10X,'SEISMOMETER CALIBRATION PULSE (RESPONSE TO A ST  
25 IEP OF ACCELERATION). '///,

26 1CX,10A8//)

27 PI=4.0\*ATAN(1.0)

28 TITLE(16)=DATE

29 AMP(1)=C.C

30 PHASE(1)=C.C

31 P(1)=CZERO

32 NSCALE FOR MY OWN USE ONLY WITH A.G.I. DATA  
33 THERE ARE TWO DIFFERENT WSSN FILM CHIP SCALES

34 TWO SCALE FACTORS FOR A.G.I. DATA ARE  
35 1. 1 A.G.I. UNIT = 0.32258 SECS. (SCALE1)

36 2. 1 A.G.I. UNIT = 0.16313 SECS. (SCALE2)

37 SCALE=0.32258  
38 IF(NSCALE.EQ.2) SCALE=0.16313

39 Q11=SCALE\*Q11

40 Q22=SCALE\*Q22

41 Q33=SCALE\*Q33

42 Q44=SCALE\*Q44

43 Q55=SCALE\*Q55

44 Q66=SCALE\*Q66

45 FOR MY A.G.I. DATA 1 UNIT DISPLACEMENT IN Y = 0.08 MM.

46 DEFL=0.C8\*DEFL  
47 PRINT 20,LABEL,NSCALE,Q11,Q22,Q33,Q44,Q55,Q66,FMASS,G,CUR,DEFL

48 FORMAT(10X'CALIBRATION PULSE DATA LABEL NUMBER =',I5/  
49 10X'NSCALE =',I4,//

50 1 12X,'Q11 G Q22 Q33 Q44 Q55 Q66

51 2 9X,10(F8.4,2X),// CUR DEFL, //

52 IF(Q33.NE.C.0) GO TO 40

53 PRINT 3C

54 FORMAT(/10X,'Q33 = 0.0')

55 CALL EXIT

56 NLIBR=78

57 PRINT 50,NLIBR

50 FORMAT(10X, 'NUMBER OF LIBRARY SEISMOGRAPHS =', I5, /)

C DO 90 I=1, NLIBR  
A=((Q1(I)-Q11)/Q11)\*\*2  
B=((Q2(I)-Q22)/Q22)\*\*2  
C=((Q3(I)-Q33)/Q33)\*\*2  
D=((Q4(I)-Q44)/Q44)\*\*2  
E=((Q5(I)-Q55)/Q55)\*\*2

C IF(Q66) 70,60,70

60 F=C.0

GO TO 80

70 F=((Q6(I)-Q66)/Q66)\*\*2

80 RMS(I)=SQRT(A+B+C+D+E+F)

90 CONTINUE

C CALL AMINN(RMS, NLIBR, RMSMIN, NMIN)  
BEST FITTING LIBRARY SEISMOGRAPH CHARACTERISTICS.

K=NMIN

H1=HH1(K)

H2=HH2(K)

SIGMA=SSIGMA(K)

T1=TT1(K)

T2=TT2(K)

TTFAC=TFAC(K)

FFAC=FAC(K)

100 PRINT 100, K, RMSMIN

1 FORMAT(10X, 'BEST FITTING LIBRARY SEISMOGRAPH IS NUMBER', I5, /  
10X, 'WITH R.M.S. DEVIATION =', F10.6/)

C B2=4.0\*H1\*H2\*(1.0-SIGMA)\*\*2  
C1=T1/T2

C U=TTFAC/T1

D1=C1\*C1\*(U\*\*4)-(1.0+(C1+B2)\*C1)\*(U\*\*2)+1.0

D2=2.0\*U\*((C1\*H1+H2)\*C1\*U\*U-(H1+C1\*H2))

F1=U/SQRT(D1\*D1+D2\*D2)

FMFAC=(FMASS\*DEFL\*FFAC)/(G\*CUR\*F1)  
CALCULATE AMPLITUDE RESPONSE (MAGNIFICATION) AND PHASE.

C DO 110 I=2, NBY2

U=1.0/(FREQ(I)\*T1)

D1=C1\*C1\*(U\*\*4)-(1.0+(C1+B2)\*C1)\*(U\*\*2)+1.0

D2=2.0\*U\*((C1\*H1+H2)\*C1\*U\*U-(H1+C1\*H2))

F1=U/SQRT(D1\*D1+D2\*D2)

AMP(I)=F1\*FMFAC

PHASE(I)=ATAN(D1/D2)

IF(D2.GE.0.0) PHASE(I)=PHASE(I)+PI

PHASE(I)=PHASE(I)+PI

P(I)=CMPLX(AMP(I)\*CCS(PHASE(I)), -1.0\*AMP(I)\*SIN(PHASE(I)))

110 CONTINUE

C IF(NG5.NE.1.AND.NG6.NE.1.AND.NG7.NE.1) GO TO 180

DO 120 I=5, 15

TITLE(I)=TITLEB(I)

120 CONTINUE

IF(NG5.NE.1) GO TO 160

DO 130 I=2, NBY2

POW=(2.0\*PI\*FREQ(I))\*\*(-3.0)

P(I)=-1.0\*AYEN\*P(I)\*PCW

```

130 CONTINUE
CALL FILLUP(NBY2PI,P)
C   FREQ TO TIME.
CALL COOL(NPCW2,P,-1.0)
DO 140 I=1,N
P(I)=P(I)/(DELA*FLCAT(N))
SEIS(I)=REAL(P(I))
140 CONTINUE
TITLE(3)=ATITLE(3)
IF=3
CALL TIMSER(TITLE,SEIS,N,DELA,IF)
C
DO 150 I=2,NBY2
P(I)=CMPLX(AMP(I)*CCS(PHASE(I)),-1.0*AMP(I)*SIN(PHASE(I)))
150 CONTINUE
P(I)=CZERO
C
160 IF(NG6.NE.1.AND.NG7.NE.1) GO TO 200
NM=NBY2-NAFLO1
TITLE(1)=ATITLE(1)
TITLE(2)=ATITLE(2)
TITLE(3)=BLANK
IF(NG6.NE.1) GO TO 170
TITLE(4)=ATITLE(4)
TITLE(5)=ATITLE(5)
CALL CARGRF(FREQ(NAFLO1),AMP(NAFLO1),NM)
C
170 IF(NG7.NE.1) GO TO 180
TITLE(4)=ATITLE(6)
TITLE(5)=ATITLE(7)
CALL DRUM(NBY2,PHASE)
CALL CARGRF(FREQ(NAFLO1),PHASE(NAFLO1),NM)
180 PRINT 19C,(I,FREQ(I),AMP(I),PHASE(I),I=NAFLO1,NBY2,10)
190 FORMAT(1H1//8X,'INSTRUMENT RESPONSE',
1 //,2(8X),'FREQUENCY',6X,'AMPLITUDE',8X,'PHASE',5X),
2 //,2(15,3E15.7))
C
200 TMCNRS=80.0
DO 210 I=1,NBY2
J=NBY2+I
SEIS(I)=0.0
SEIS(J)=0.0
AMP(I)=0.0
PHASE(I)=0.0
210 CONTINUE
RETURN
END
SUBROUTINE UGRUP
PERFORMS THE MULTIPLE FILTERING ANALYSIS TO PRODUCE THE DISPERSION
CHARACTERISTIC AS A FUNCTION OF FREQUENCY AND VELOCITY OF ARRIVAL
I.E. THE 2-D MATRIX E.
COMMON/CC1/Z(2048),CZERC,P(2048)
COMMON/CC8/E(120,120)
COMMON/CC4/NSEIS,DELA,IVSEIS,NUFCUT,NBASE,NCOSTP,NCOMB,NAFLO,
1 NI NSTR,NUGRUP,NFLO,NFHI,NFSTEP,BAND,CWF,DV,NAFLO1

```

```
COMMON/CC7/N,NBY2,NBY2P1,NPOW2,FNYG,DF
COMMON/CO3/STANAM(8),DELTAD,DELTA,CRIGTM,GMTSEC
COMMON/CO2/SEIS(2048),FREQ(1024),AMP(1024),PHASE(1024)
DIMENSION VSTEP(120),FREQC(120),TABLE(2,2048)
COMPLEX Z,CZERO,P
EQUIVALENCE (VSTEP(1),SEIS(1)),
              (FREQC(1),SEIS(121)),
              (TABLE(1,1),SEIS(1025))
```

```
1
2 DO 5 I=1,1024
  J=1024+I
  SEIS(I)=C.C
  SEIS(J)=C.C
  FREQ(I)=C.C
  AMP(I)=C.C
  PHASE(I)=C.C
```

```
5 CONTINUE
  VELOCITY TO FIRST & LAST SAMPLES.
```

```
C TF=GMTSEC
  VSF=DELTA/(TF-CRIGTM)
  TL=GMTSEC+FLOAT(N-1)*DELA
  VSL=DELTA/(TL-CRIGTM)
  PRINT 1C,CRIGTM,GMTSEC,TL,VSF,VSL
  FORMAT(1H1//10X,'GRUP VELOCITY CALCULATION',
```

```
10 /10X,'-----',
  1 /10X,'CRIGIN TIME OF EVENT IS ',F10.2,2X,'SECONDS',
  2 /10X,'TIME OF FIRST SAMPLE IS ',F10.2,2X,'SECONDS',
  3 /10X,'TIME OF LAST SAMPLE IS ',F10.2,2X,'SECONDS',
  4 /10X,'VELCCITY TO FIRST SAMPLE IS ',F7.3,1X,'KMS/SEC',
  5 /10X,'VELCCITY TO LAST SAMPLE IS ',F7.3,1X,'KMS/SEC')
  VELOCITY TO EACH E(I). (EACH DIGIT IN TIME SERIES)
```

```
C DO 20 I=1,N
  K=N-I+1
  TABLE(1,I)=DELTA/(GMTSEC+FLOAT(K-1)*DELA-CRIGTM)
```

```
20 CONTINUE
  MAKE SURE NO. OF VELOCITIES IS LE TO 120.
```

```
C IF(VSF.GT.5.0) VSF=5.0
  30 NLIM=(VSF-VSL)/DV
  IF(NLIM.LE.120) GC TO 40
  DV=2.0*DV
  GO TO 30
```

```
C 40 K=1
  VSTEP(1)=VSF-DV
  50 IF(VSTEP(K).LE.VSL) GC TO 60
  K=K+1
```

```
VSTEP(K)=VSTEP(K-1)-DV
  GO TO 50
```

```
60 NROW=K-1
  PRINT 7C,NROW
```

```
70 FORMAT(/10X,'NO. OF VELOCITY STEPS = NROW = ',I5)
  SET UP FILTER VALUES.
```

```
C BETA=ALOG(DWF)
  ALPHA=BETA/BAND**2
  PRINT 8C,BETA,ALPHA,DF
```

```
80 FORMAT(/10X,'BETA = ',F8.3,5X,'ALPHA = ',F8.3,5X,'FUNDAMENTAL DF = ',F8.6)
```

```
C CALL ZERO2D(E,120,120)
```

```

C
C
C   CHOOSE CENTRE FREQUENCIES.
    NCOL=1
    IF(NFLO.LT.NAFLC1) CALL EXIT
    FREQC(1)=NFLO*DF
    NFC TWO=NFLO+NFSTEP
    DO 90 I=NFCTWC,NFHI,NFSTEP
    NCOL=NCOL+1
    FREQC(NCOL)=FREQC(NCOL-1)+NFSTEP*CF
90  CONTINUE
    PRINT 100,NCOL
100  FORMAT(/10X,'NUMBER OF FREQUENCY STEPS = NCOL =',I5)
C
    IF(NCOL.GT.120) CALL EXIT
    DO 140 J=1,NCOL
    JCOL=J
    CALL GALSSA(FREQC(J),ALPHA,JCOL)
    DO 110 I=1,N
    P(I)=P(I)*Z(I)
110  CONTINUE
    CALL COOL(NPCW2,P,-1.0)
    DO 120 I=1,N
    K=N-I+1
    TABLE(2,I)=CABS(P(K))/(FLCAT(NBY2)*DELA)
120  CONTINUE
C
    DO 130 I=1,NROW
    CALL LOCK(I,2,N,TABLE,VSTEP(I),E(J,I))
130  CONTINUE
140  CONTINUE
C
    CALL UEMTRX(NROW,NCOL)
    RETURN
    END
SUBROUTINE GALSSA(FC,ALPHA,JCOL)
C
C   CREATES IN THE FREQUENCY DOMAIN A BANDPASS GAUSSIAN FILTER OF
C   SPECIFIED 'Q'.
C
COMMON/CC1/2(2048),CZERO,P(2048)
COMMON/CC2/N,NBY2,NBY2P1,NPCW2,FNYQ,DF
COMMON/CC3/NSEIS,DELA,IVSEIS,NFLO,NFHI,NFSTEP,BAND,CWF,DV,NAFLO1
1  NINSTR,NUGRUP,NFLO,NFHI,NFSTEP,BAND,CWF,DV,NAFLO1
COMPLEX Z,CZERO,P,CFXCNE
C   CFXONE=(1.0,0.0)
DO 10 I=1,N
P(I)=CZERO
10  CONTINUE
LMI=FC/DF+0.5
L=LMI+1

FLO=(1.0-BAND)*FC
FHI=(1.0+BAND)*FC
LL=(FC-FLO)/DF+0.5
CHECK FILTER IS WITHIN TIME SERIES.
IF((FC-FLCAT(LL)*DF).GT.0.0.AND.(FC+FLCAT(LL)*DF).LT.FNYQ)GO TO 30
PRINT 20,FC,LL
20  FORMAT(/10X,'FC =',F10.5,5X,'LL =',I5)
CALL EXIT

```

```

30 P(L)=CPXCNE
C CHECK FILTER WIDTH.
IF(LL.GE.1) GO TO 50
40 PRINT 4C,LL
FORMAT(/10X,'CHECK PARAMETER BAND. LL =',15)
CALL EXIT
50 FF=FC
DO 60 I=1,LL
J=L-I
K=L+I
FF=FF-DF
PONENT=-ALPHA*((FF-FC)/FC)**2
P(J)=CMPLX(EXP(PCNENT),0.0)
P(K)=P(J)
60 CONTINUE
NFILT=2*LL+1

C
70 IF(JCOL.EQ.1) PRINT 70
FORMAT(/10X,'FC=FILTER CENTRE FREQUENCY (HZ) FC=(L-1)*DF',
1 /10X,'L=FREQUENCY ARRAY INDEX NO. CORRESPONDING TO FC',
2 /10X,'FLC & FHI ARE FILTER BAND LIMITS FLO=(1-BAND)*FC',
3 /10X,'NFILT=NO. OF FILTER POINTS',
4 /16X,'NCCL',9X,'L',10X,'FC',13X,'FLO',10X,'FHI',12X,'NFILT'
5 )
PRINT 8C,JCOL,L,FC,FLC,FHI,NFILT
80 FORMAT(2(5X,I5),3(5X,F10.5),5X,I5)

C
RETURN
END
SUBROUTINE LENTRX(NRCW,NCCL)

C
C PRODUCES THE GROUP VELOCITY / FREQUENCY CURVE FROM E BY OBTAINING
C THE VELOCITY OF THE MAXIMUM ENERGY ARRIVAL AT EACH FREQUENCY.
C SCALES THE MATRIX E RELATIVE TO A MAXIMUM VALUE OF 99DB.
C
COMMON/GRFF/TITLE(20),XMAX,XMIN,YMAX,YMIN,INDX,INDY,IND,IDDT,
1 ANSTR1,IF,XLIMIT,YLIMIT,SCALX,SCALY
COMMON/C02/SEIS(1024)
COMMON/C03/STANAM(8)
1 COMMON/C04/NSEIS,DELA,IVSEIS,NUMCUT,NBASE,NCOSTP,NCOMB,NAFLO,
NI NSTR,NGRUP,NFLO,NFHI,NFSTEP,BAND,CWF,DV,NAFLO1
COMMON/C05/NG1,NG2,NG3,NG4,NG5,NG6,NG7,NG8,NG9,NG10,NG11,NG12,NG13
1 ,NG14,NG15,NP1,NP2
COMMON/C06/TITLEA(20),DATE,BLANK
COMMON/C08/E(120,120)
1 DIMENSION VSTEP(120),FREQC(120),X(120),Y(120),U(120),PERIOD(120),
ATITLE(6)
2 REAL*8 ATITLE,TITLE,TITLEA,DATE,BLANK
3 EQUIVALENCE (VSTEP(1),SEIS(1)),
4 (FREQC(1),SEIS(121)),
5 (X(1),SEIS(241)),
(Y(1),SEIS(361)),
(L(1),SEIS(481)),
(PERIOD(1),SEIS(601))
DATA ATITLE/'FREQUENCY (HZ) PERIOD (SECONDS)GRP.VEL. KMS/SEC'/
DO 10 I=1,NROW
X(I)=VSTEP(I)

```



```

1C  CONTINUE
    EMAX=C.C
    DO 40 J=1,NCOL
    DO 20 I=1,NROW
    Y(I)=E(J,I)
2C  CONTINUE
    CALL AMAXN(Y,NROW,L(J),IR)
    YMAX=ABS(L(J))
    IF(EMAX.GE.YMAX) GC TC 30
    IRM=IR
    JCM=J
    EMAX=YMAX
C   QUADRATIC FIT ABOUT MAXIMUM VALUE.
3C  XO=X(IR)
    A=0.5*(Y(IR-1)+Y(IR+1)-2.0*Y(IR))
    B=0.5*(-Y(IR-1)+Y(IR+1))
    C=Y(IR)
    PERIOD(J)=1.0/FRECC(J)
    U(J)=XO+C.5*B/A*DV
4C  CONTINUE
    PRINT 5C,(J,FRECC(J),PERIOD(J),U(J),J=1,NCOL)
5C  FORMAT(1H1/20X,'FREQUENCY (HZ) & PERIOD (SECS)/GROUP VELOCITY (KMS
1/SECS) ',
2     //,3(7X,'FREQUENCY',5X,'PERIOD',5X,'U VELOCITY '),
3     //,3(14,3E13.5))
    PRINT 6C,EMAX,IRM,JCM
6C  FORMAT(/10X,'EMAX =',E15.7,5X,'IRM =',I5,5X,'ICM =',I5)
    DO 70 I=6,16
    TITLE(I)=TITLEA(I)
7C  CONTINUE
    TITLE(3)=BLANK
    TITLE(4)=ATITLE(5)
    TITLE(5)=ATITLE(6)
    IF(NG12.NE.1) GC TC 80
    TITLE(1)=ATITLE(1)
    TITLE(2)=ATITLE(2)
    CALL CARGRF(FRECC,U,NCOL)
8C  IF(NG13.NE.1) GC TC 90
    TITLE(1)=ATITLE(3)
    TITLE(2)=ATITLE(4)
    CALL CARGRF(PERIOD,U,NCOL)
9C  IF(NP2.NE.1) GC TC 130
C   PUNCH FREQUENCY (HZ) AND GROUP VELOCITY (KMS/SEC) IN (2E15.7).
    PUNCH 120,(FRECC(I),L(I),I,STANAM,TITLEA(15),I=1,NCOL)
12C  FORMAT(2E15.7,15X,I5,'U',9X,8A1,4X,A8)
C
13C  DO 150 J=1,NCOL
    DO 140 I=1,NROW
    F(J,I)=20.0*ALOG10(E(J,I)/EMAX)+99.0
14C  CONTINUE
15C  CONTINUE
    PRINT OUT E MATRIX.
    N42=(NCOL-1)/42+1
    DO 200 IZ=1,N42
    NLOW=(IZ-1)*42+1
    NHY=NLOW+41
    IF(NHY.GT.NCOL) NHY=NCOL
    PRINT 16C
16C  FORMAT(1H1//50X,'MATRIX OF E(I)',///)
    IF(IZ.EQ.1) PRINT 17C,(FRECC(I),I=1,NHY,10)

```

```
17C FORMAT(7X,F5.3,4(25X,F5.3))
DO 180 I=1,ARCW
PRINT 190,VSTEP(I),(E(J,I),J=NLCW,NHY)
18C CONTINUE
19C FORMAT(1X,F4.2,1X,42F3.0)
20C CONTINUE
```

```
C
IF(NG14.NE.1) GO TO 210
CALL CENTUR(E,NCCL,ARCW,120,5.0,5.0,100.0,3)
21C RETURN
END
SUBROUTINE COCL(N,XX,SIGNI)
```

```
THIS SUBROUTINE WAS PROGRAMMED BY I.MACLEOD, DEPT. OF
ENGINEERING PHYSICS,A.N.U. AND HAS BORROWED FROM D.MCCOWAN'S
COOL AND IBM'S HARM.
```

```
SINGLE PRECISION VERSION MODIFIED BY J.B.YOUNG FOR THE 360/75.
```

```
C
C
C
C
C
C
C
DIMENSION W(14),XX(1),NBIT(20),JNT(20)
```

```
C
C
C
C
C
C
C
INTEGER OFFSET
```

```
C
C
C
C
C
C
C
DATA NX/0/
```

```
C
C
C
C
C
C
C
IF(NX.GT.0)GO TO 100
ROOT2=SQRT(2.0)
PI2=8.0*ATAN(1.0)
```

```
C
100 NX=2**N
NX2=NX+NX
NX2LS1=NX2-1
NX2LS2=NX2-2
NXON8=NX/8
NXON4=NXON8+NXON8
NXON2=NXON4+NXON4
CON1=PI2/FLCAT(NX)
IF(SIGNI.GT.0.0)GO TO 120
```

```
C
DO 110 K=1,NX2LS1,2
XX(K+1)=-XX(K+1)
```

```
110 CONTINUE
```

```
C
120 DO 130 K=1,N
JNT(K)=2**(N-K)
```

```
130 CONTINUE
```

```
C
LSTART=N-N/3*3+1
IF(LSTART.EQ.1)GO TO 200
IF(LSTART.EQ.2)GO TO 150
LBLOK2=NXON2
L2BLOK=LBLOK2-1
```

```
C
DO 140 K0=1,L2BLOK,2
K1=K0+LBLOK2
K2=K1+LBLOK2
K3=K2+LBLOK2
ACR=XX(K0)+XX(K2)
```

```

ACI = XX(KC+1) + XX(K2+1)
AIR = XX(KC) - XX(K2)
AII = XX(KC+1) - XX(K2+1)
A2R = XX(K1) + XX(K3)
A2I = XX(K1+1) + XX(K3+1)
A3R = XX(K1) - XX(K3)
A3I = XX(K1+1) - XX(K3+1)
XX(KC) = ACR + A2R
XX(KC+1) = ACI + A2I
XX(K1) = ACR - A2R
XX(K1+1) = ACI - A2I
XX(K2) = AIR - A3I
XX(K2+1) = AII + A3R
XX(K3) = AIR + A3I
XX(K3+1) = AII - A3R

```

```

14C CONTINUE
GO TO 200

```

```

15C LBLOCK2 = NX
L2BLOCK = LBLOCK2 - 1
DO 160 KC = 1, L2BLOCK, 2
K1 = KC + LBLOCK2
AIR = XX(K1)
AII = XX(K1+1)
XX(K1) = XX(KC) - AIR
XX(K1+1) = XX(KC+1) - AII
XX(KC) = XX(KC) + AIR
XX(KC+1) = XX(KC+1) + AII
16C CONTINUE

```

```

200 DO 300 M = LSTART, N, 3
LBLOCK2 = NX / 2 ** (M + 1)
L2BLOCK = LBLOCK2 - 1
LBLOCK1 = L2BLOCK - 1
LBLOCK8 = LBLOCK2 * 8
LBLAST = NX2 - LBLOCK8 + 1

```

```

DO 210 K = 4, N
NBIT(K) = 0

```

```

210 CONTINUE

```

```

NW = 0

```

```

DO 290 OFFSET = 1, LBLAST, LBLOCK8
IF (OFFSET.EQ.1) GO TO 220
ARG = CON1 * FLCA1(NW)
W(1) = COS(ARG)
W(2) = SIN(ARG)
CSSQA = W(1) * W(1)
W(3) = CSSQA + CSSQA - 1.0
W(4) = W(1) * W(2)
W(4) = W(4) + W(4)
W(5) = W(3) * W(1) - W(4) * W(2)
W(6) = W(4) * W(1) + W(3) * W(2)
CSSQ2A = W(3) * W(3)
W(7) = CSSQ2A + CSSQ2A - 1.0
W(8) = W(4) * W(3)
W(8) = W(8) + W(8)

```

W(9)=W(7)\*W(1)-W(8)\*W(2)  
W(10)=W(8)\*W(1)+W(7)\*W(2)  
CSSQ3A=W(5)\*W(5)  
W(11)=CSSQ3A+CSSQ3A-1.0  
W(12)=W(6)\*W(5)  
W(12)=W(12)+W(12)  
W(13)=W(7)\*W(5)-W(8)\*W(6)  
W(14)=W(8)\*W(5)+W(7)\*W(6)  
LBLOKO=OFF SET+LBLCK1

22C  
C

DO 260 KO=OFF SET, LBLCKG, 2  
K1=K0+LBLCK2  
K2=K1+LBLCK2  
K3=K2+LBLCK2  
K4=K3+LBLCK2  
K5=K4+LBLCK2  
K6=K5+LBLCK2  
K7=K6+LBLCK2  
XKOWR=XX(K0)  
XKOWI=XX(K0+1)  
IF (OFF SET.NE.1) GO TO 240  
XK1WR=XX(K1)  
XK1WI=XX(K1+1)  
XK2WR=XX(K2)  
XK2WI=XX(K2+1)  
XK3WR=XX(K3)  
XK3WI=XX(K3+1)  
XK4WR=XX(K4)  
XK4WI=XX(K4+1)  
XK5WR=XX(K5)  
XK5WI=XX(K5+1)  
XK6WR=XX(K6)  
XK6WI=XX(K6+1)  
XK7WR=XX(K7)  
XK7WI=XX(K7+1)

24C GO TO 250  
XK1WR=XX(K1)\*W(1)-XX(K1+1)\*W(2)  
XK1WI=XX(K1)\*W(2)+XX(K1+1)\*W(1)  
XK2WR=XX(K2)\*W(3)-XX(K2+1)\*W(4)  
XK2WI=XX(K2)\*W(4)+XX(K2+1)\*W(3)  
XK3WR=XX(K3)\*W(5)-XX(K3+1)\*W(6)  
XK3WI=XX(K3)\*W(6)+XX(K3+1)\*W(5)  
XK4WR=XX(K4)\*W(7)-XX(K4+1)\*W(8)  
XK4WI=XX(K4)\*W(8)+XX(K4+1)\*W(7)  
XK5WR=XX(K5)\*W(9)-XX(K5+1)\*W(10)  
XK5WI=XX(K5)\*W(10)+XX(K5+1)\*W(9)  
XK6WR=XX(K6)\*W(11)-XX(K6+1)\*W(12)  
XK6WI=XX(K6)\*W(12)+XX(K6+1)\*W(11)  
XK7WR=XX(K7)\*W(13)-XX(K7+1)\*W(14)  
XK7WI=XX(K7)\*W(14)+XX(K7+1)\*W(13)

25C A OR=XKOWR+XK4WR  
A OI=XKOWI+XK4WI  
A 1R=XK1WR+XK5WR  
A 1I=XK1WI+XK5WI  
A 2R=XK2WR+XK6WR  
A 2I=XK2WI+XK6WI  
A 3R=XK3WR+XK7WR  
A 3I=XK3WI+XK7WI  
A 4R=A OR+A2R  
A 4I=A OI+A2I

A 5R = A CR - A 2R  
 A 5I = A CI - A 2I  
 A 6R = A 1R + A 3R  
 A 6I = A 1I + A 3I  
 A 7R = A 3I - A 1I  
 A 7I = A 1R - A 3R  
 XX(K0) = A 4R + A 6R  
 XX(K0+1) = A 4I + A 6I  
 XX(K1) = A 4R - A 6R  
 XX(K1+1) = A 4I - A 6I  
 XX(K2) = A 5R + A 7R  
 XX(K2+1) = A 5I + A 7I  
 XX(K3) = A 5R - A 7R  
 XX(K3+1) = A 5I - A 7I  
 A CR = XK C WR - XK 4 WR  
 A CI = XK C WI - XK 4 WI  
 A 8R = XK 1 WR - XK 5 WR  
 A 8I = XK 1 WI - XK 5 WI  
 A 1R = A 8R - A 8I  
 A 1I = A 8R + A 8I  
 A 2R = XK 6 WI - XK 2 WI  
 A 2I = XK 2 WR - XK 6 WR  
 A 6R = XK 3 WR - XK 7 WR  
 A 6I = XK 3 WI - XK 7 WI  
 A 3R = A 8R - A 8I  
 A 3I = A 8R + A 8I  
 A 4R = A 0R + A 2R  
 A 4I = A 0I + A 2I  
 A 5R = A 0R - A 2R  
 A 5I = A 0I - A 2I  
 A 6R = (A 1R - A 3I) / RCCT2  
 A 6I = (A 1I + A 3R) / RCCT2  
 A 7R = (A 3R - A 1I) / RCCT2  
 A 7I = (A 3I + A 1R) / RCCT2  
 XX(K4) = A 4R + A 6R  
 XX(K4+1) = A 4I + A 6I  
 XX(K5) = A 4R - A 6R  
 XX(K5+1) = A 4I - A 6I  
 XX(K6) = A 5R + A 7R  
 XX(K6+1) = A 5I + A 7I  
 XX(K7) = A 5R - A 7R  
 XX(K7+1) = A 5I - A 7I

26C CONTINUE

DO 280 K=4,N  
 IF(NBIT(K).NE.0)GC TC 270  
 NBIT(K)=1  
 NW=NW+JNT(K)  
 GO TO 290  
 NBIT(K)=0  
 NW=NW-JNT(K)  
 CONTINUE

27C

28C CONTINUE

29C CONTINUE

30C CONTINUE

NW=0

DO 310 K=1,N  
 JNT(K)=JNT(K)+JNT(K)  
 NBIT(K)=0

310 CONTINUE

C

```
K=0
IF(NW.LE.K)GO TC 320
HOLDR=XX(NW+1)
HOLDI=XX(NW+2)
XX(NW+1)=XX(1)
XX(NW+2)=XX(2)
XX(1)=HOLDR
XX(2)=HOLDI
```

C

```
320 DO 340 M=1,N
IF(NBIT(M).NE.0)GO TC 330
NBIT(M)=1
NW=NW+JNT(M)
GO TO 350
```

```
330 NBIT(M)=0
NW=NW-JNT(M)
```

```
340 CONTINUE
```

C

```
350 DO 390 K=2,NX2LS2,2
IF(NW.LE.K)GO TC 360
HOLDR=XX(NW+1)
HOLDI=XX(NW+2)
XX(NW+1)=XX(K+1)
XX(NW+2)=XX(K+2)
XX(K+1)=HOLDR
XX(K+2)=HOLDI
```

C

```
360 DO 380 M=1,N
IF(NBIT(M).NE.0)GO TC 370
NBIT(M)=1
NW=NW+JNT(M)
GO TO 390
```

```
370 NBIT(M)=0
NW=NW-JNT(M)
```

```
380 CONTINUE
```

C

```
390 CONTINUE
```

C

```
IF(SIGNI.GT.0.0)GO TC 420
```

C

```
DO 410 K=1,NX2LS1,2
XX(K+1)=-XX(K+1)
```

```
410 CONTINUE
```

C

C

```
420 RETURN
END
SUBROUTINE POW(N,NBY2,NBY2P1,NPOW2)
```

C

C

```
NBY2=N/2
NBY2P1=NBY2+1
A=(N-1)/2
NPOW2=A*LOG10(A)/ALCG10(2.0)+2.0
RETURN
END
SUBROUTINE ZRLOAD(N,X,Z)
```

```

C
C
DIMENSION X(N),Z(N)
COMPLEX Z
DO 1 I=1,N
Z(I)=CMPLX(X(I),C.O)
1 CONTINUE
RETURN
END
SUBROUTINE FILLUP(NCPTS,Z)

```

```

C
C
DIMENSION Z(1)
COMPLEX Z,CZERO
CZERO=CMPLX(C.O,0.O)
AN=NOPTS-2
N=ALOG10(AN)/ALOG10(2.O)+1.O
N1=(2**N)+1
N2=2*(N+1)
N1M1=N1-1
DO 1 I=2,N1M1
NN=N2-I+2
Z(NN)=CCNJG(Z(I))
1 CONTINUE
Z(N1)=CZERO
RETURN
END

```

GENERAL USER SUBROUTINE TIMER

---

```

C
C
C
C
FROM THE CALL - CALL TIMER
THE TIME FROM THE LAST CALL TIMER IS PRINTED OUT
THE FIRST CALL SETS UP TIMER

```

```

SUBROUTINE TIMER
DATA DIFF /0./
IF(DIFF) 2,1,2

```

```

1 CALL CLOCK(DIFF)
DIFF=DIFF*60.
RETURN

```

```

2 CALL CLOCK(TIME)
TIME=TIME*60.
DIFF=TIME-DIFF
PRINT 3, DIFF

```

```

3 FORMAT(8CX,29HTIME ELAPSED FROM LAST CALL =,F10.4,8H SECONDS)
DIFF=TIME
RETURN

```

```

C
END
SUBROUTINE BASE (X,N,TYPE, IPI)

```

```

C
C
DIMENSION X(N)
REAL*8 MEAN,TYPE
DATA MEAN/8HMEAN /

```

\*\*\*

IND=3-----COSINE TAPER COSINE TAPER BACK END OF CURVE

X-----IS THE ARRAY.

N-----IS THE NUMBER OF POINTS IN THE ARRAY.

NO -----IS THE STARTING NUMBER.

DIMENSION X(N)

ANG = NO-1

PHI = PI/ANG

CPHI = COS(PHI)

SPHI = SIN(PHI)

CTHET1 = 1.

STHET1 = 0.

CTHET2 = 1.

STHET2 = 0.

DO 1 I = 1,NO

GO TO (2,3,4),IND

2 IA = N-I+1

3 IN=I

GO TO 5

4 IN = N-I+1

5 X(IN) = 0.5\*X(IN)\*(1. - CTHET2)

GO TO (6,9,9),IND

6 X(IA) = 0.5\*X(IA)\*(1. - CTHET2)

9 CALL SINCCS(CPHI,SPHI,CTHET1,STHET1,CTHET2,STHET2)

1 CONTINUE

RETURN

END

SUBROUTINE SINCCS (CPHI,SPHI,CTHET1,STHET1,CTHET2,STHET2)

CTHET2 = CTHET1\*CPHI - STHET1\*SPHI

STHET2 = STHET1\*CPHI + CTHET1\*SPHI

CTHET1 = CTHET2

STHET1 = STHET2

RETURN

END

SUBROUTINE DRUM(LPHZ,PHZ)

DRUM MAKES PHASE CURVE CONTINUOUS

DIMENSION PHZ(LPHZ)

PI=4.0\*ATAN(1.0)

PI2=2.0\*PI

PJ=0.

DO 40 I=2,LPHZ

IF(ABS(PHZ(I)+PJ-PHZ(I-1))-PI)40,40,10

10 IF(PHZ(I)+PJ-PHZ(I-1))20,40,30

20 PJ=PJ+PI2

GO TO 40



```

C
  SUMX = C
  SUMIX = C
  AN = N
  IF(TYPE - MEAN)1,2,1
1  IND = 1
  GO TO 3
2  IND = 2
3  DO 4 I = 1,N
  AI = I
  SUMX = SUMX + X(I)
  GO TO (5,4),IND
5  SUMIX = SUMIX + AI*X(I)
4  CONTINUE
  XBAR = SUMX/AN
  GO TO (6,7),IND
6  XINTO = (((4.*AN)+2.)*SUMX-6.*SUMIX)/(AN*(AN-1.))
  PHI = ((12.*SUMIX)-6.*(AN+1.)*SUMX)/(AN*(AN+1.)*(AN-1.))
  DO 20 I = 1,N
  AI = I
  X(I) = X(I) - AI*PHI - XINTO
20 CONTINUE
  PRINT 10, PHI, XBAR
10 FORMAT(/ /4X,49HDATA HAS BEEN CORRECTED TO LEAST SQUARES BASELINE /
14X,32HGRADIENT OF LEAST SQUARES LINE =,F10.5,8X,14HMEAN OF DATA =
2F10.5)
  GO TO 8

```

```

C
7  DO 30 I = 1,N
  X(I) = X(I) - XBAR
30 CONTINUE
  PRINT 11, XBAR
11 FORMAT(/ /4X,4CHDATA HAS BEEN CORRECTED TO MEAN BASELINE//4X,
114HMEAN OF DATA =,F10.4)
  SUMX2 = C
  SUMX3 = C
  DO 9 I = 1,N
  X2 = X(I)*X(I)
  SUMX2 = SUMX2 + X2
  SUMX3 = SUMX3 + X2*X(I)
9  CONTINUE
  VARX = SUMX2/AN
  A3MNT = SUMX3/AN
  SKEW = (A3MNT*A3MNT)/(VARX**3.)
  PRINT 12, VARX, SKEW
12 FORMAT(/4X,18HVARIANCE OF DATA =,E10.4,8X,10H SKEWNESS =,F10.4)
  IP1 = IP1 + 1
  GO TO (14,15),IP1
15 PRINT 16,(I, X(I), I = 1,N)
16 FORMAT(/ /4X,24HTHE BASELINED DATA IS --//5(4X,6HSAMPLE,4X,4HX(I),
13X)/(5(4X,I5,2X,F10.5)))
C
14 RETURN
  END
  SUBROUTINE NPCSTP(X,N,NC,IND,PI)

```

```

C
C -----
C
C IND=1-----CCSINE TAPER BOTH ENDS OF CURVE.
C IND=2-----CCSINE TAPER FRONT END OF CURVE.

```

```

30 PJ=PJ-PI2
40 PHZ(I)=PHZ(I)+PJ
RETURN
END
SUBROUTINE SMOOTH (X,F,N,NB,NS,KN,IND)

```

```

*****

```

```

INPUT PARAMETERS AND RETURNED DATA.

```

```

*****

```

```

X=ARRAY TO BE SMOOTHED (SAY) AMPLITUDES.

```

```

F=ARRAY OF CORRESPONDING (SAY) FREQUENCIES.

```

```

N=NUMBER OF POINTS IN ARRAY X.

```

```

NB=NUMBER OF FREQUENCY BANDS TO BE INCLUDED IN EACH SMOOTHED VALUE
----SET TO AN EVEN NUMBER.

```

```

NS=NUMBER OF FREQUENCY BANDS BETWEEN STEPS (E.G. NB=16 , NS=8 ).

```

```

KN=NUMBER OF SMOOTHED POINTS FED BACK.

```

```

IND=1 SMOOTH X AND F .
    =2 SMOOTH X ONLY.

```

```

*****
*****

```

```

DIMENSION X(N), F(N)

```

```

NN=N/NB
NN=NB*(NN-1)+1

```

```

DO 1 K=1,NN,NS
KN=(K-1)/NS+1
SUM=0.
DO 2 I=1,NB
II=I+K-1
IF (II.GE.N) II=N-1
SUM=(X(II)+X(II+1))*0.5+SUM
2 CONTINUE
KB=K+NB
IF (KB.GT.N) KB=N
X(KN)=SUM/FLOAT(NB)
GO TO (3,1),IND
3 F(KN)=(F(K)+F(KB))*0.5
1 CONTINUE

```

```

RETURN
END
SUBROUTINE ZERO2D (X,IFIRST,J2ND)

```

```

SETS DOUBLE ARRAY TO ZERO

```

```

DIMENSION X(IFIRST,J2ND)
DO 1 J=1,J2ND
DO 2 I=1,IFIRST
X(I,J)=0.0

```

```

2 CONTINUE
1 CONTINUE
  RETURN
  END
  SUBROUTINE LOCK(IARGUM,N,N,TABLE,VALIN,VALOT)

C
C *****
C IMPORTANT NCTE
C *****
C   TABLE(1,I) VALUES MUST BE IN INCREASING ORDER OF MAGNITUDE.
C
C IARGUM IS THE INDEX OF THE CURRENT VALUE BEING LOOKED UP IN THE
C TABLE.
C VALIN IS A VALUE OF THE VARIABLE STORED IN THE FIRST
C COLUMN OF TABLE, AND VALOT IS THE CORRESPONDING VALUE OF THE
C VARIABLE STORED IN THE SECOND COLUMN OF TABLE.
C
C
C DIMENSION TABLE(N,N)
C
C   NM1=N-1
C   DO 1 IT=1,NM1
C     IF(TABLE(1,IT)-VALIN)1,2,3
C   1 CONTINUE
C
C   PRINT 600,VALIN,IARGUM
C 600 FORMAT(1H0,20X,13HL00K ARGUMENT F10.3,13H NOT IN TABLE, *IARGUM=*,
C 1 I7)
C
C   CALL EXIT
C
C   2 VALOT=TABLE(2,IT)
C   RETURN
C   3 DIFF1=TABLE(1,IT-1)-VALIN
C   DIFF2=TABLE(1,IT-2)-VALIN
C   DIFF3=TABLE(1,IT)-VALIN
C   DIFF4=TABLE(1,IT+1)-VALIN
C   4 TERM4=(TABLE(2,IT-1)*DIFF3-TABLE(2,IT)*DIFF1)/(DIFF3-DIFF1)
C   TERM1=(DIFF3*(TABLE(2,IT-2)*DIFF1-TABLE(2,IT-1)*DIFF2))/(DIFF1-DIF
C IF 2)
C   TERM3=(DIFF4*(TERM1-(DIFF2*TERM4)))/(DIFF3-DIFF2)
C   5 TERM1=DIFF4*TERM4
C   TERM2=(DIFF1*(TABLE(2,IT)*DIFF4-TABLE(2,IT+1)*DIFF3))/(DIFF4-DIFF3
C 1)
C   TERM4=(DIFF2*(TERM1-TERM2))/(DIFF4-DIFF1)
C   VALOT=(TERM3-TERM4)/(DIFF4-DIFF2)
C
C
C   6 RETURN
C   END
  SUBROUTINE AMAXN(X,N,XMAX,KP)
C
C DIMENSION X(N)
C KQ=1
C 2 KP=KQ
C 5 IF(KQ-N)3,4,4
C 3 KQ=KQ+1
C IF(X(KP)-X(KQ))2,5,5
C 4 XMAX=X(KP)
C RETURN
C END
  SUBROUTINE AMINN(X,N,XMIN,KP)

```

C  
C  
DIMENSION X(N)

KQ=1

2 KP=KQ

5 IF (KQ-N) 3,4,4

3 KQ=KQ+1

IF (X(KP)-X(KQ)) 5,5,2

4 XMIN=X(KP)

RETURN

END

SUBROUTINE TIMSER(TITLE,X,N,DELA,IF)

C  
C  
C THIS ROUTINE PLOTS N VALUES OF THE ARRAY X. DELA IS THE  
C SAMPLING INTERVAL AND IF IS AN INDICATOR WHICH SPECIFIES THE TYPE  
C OF SC4020 OUTPUT REQUIRED.

IF IF=1 OUTPUT IS ON MICROFILM

IF IF=2 OUTPUT IS ON HARD COPY

IF IF=3 OUTPUT IS ON BOTH MICROFILM AND HARD COPY.

C  
C  
C TITLE IS A 20 ELEMENT ARRAY CARRYING DATA FOR ANNOTATING THE  
C OUTPUT GRAPHS. THE TITLE ARRAY IS SET UP AS FOLLOWS

C  
C  
C TITLE (1) - UNUSED

C  
C  
C TITLE (2) - UNUSED

C  
C  
C TITLE (3) - CONTAINS 8 HOLLERITH CHARACTERS GIVING THE UNITS  
C OF THE TIME SERIES E.G. SECONDS

C  
C  
C TITLE (4) - UNUSED

C  
C  
C TITLE (5) - UNUSED

C  
C  
C TITLE (6) -)

C  
C  
C . )CONTAINS 80 HOLLERITH CHARACTERS GIVING A TITLE TO  
C . )THE GRAPH

C  
C  
C TITLE (15) -)

C  
C  
C TITLE (16) CONTAINS 8 HOLLERITH CHARACTERS GIVING DATE

C  
C  
C TITLE (17) -)

C  
C  
C . )CONTAINS 24 HOLLERITH CHARACTERS GIVING A SUBTITLE

C  
C  
C TITLE (19) -) TO THE GRAPH

C  
C  
C TITLE (20) - UNUSED

C  
C  
C SUBROUTINE TIMSER(TITLE,X,N,DELA,IF)

C  
C  
C DIMENSION X(N), TITLE(20)

REAL\*8 TITLE,SECS

DATA SECS/8HSECS /

CALL AMAX(X,N,XMAX)

CALL AMIN(X,N,XMIN)

XRG=XMAX-XMIN

RANGE=300./XRG

IF(DELA.EQ..04444.AND.TITLE(3).EQ.SECS)GO TO 20

S=6.

IF(N.LE.100)S=7.

R=0.

3 IF(DELA.LT.(10.\*\*R\*.0000001))GO TO 2

R=R+1.

GO TO 3

2 IF(R.LT.1.)GO TO 99

INTER = 10.\*\* (8.-R)\*DELA + 0.5

AINTER = FLCAT(INTER)/(10.\*\* (S-R))

ANXL=(6.\*AINTER)/DELA

GO TO 4

\*X

```

C
2C AINTER=5.
   ANXL=675.
C
4  NXL=ANXL
   NXS=3*NXL
   CONST=800./ANXL
   NT=N/NXS
   NT=NT+1
C
DO 10 I=1,NT
CALL ADVFLM(IF)
IBEGIN=(I-1)*NXS+1
IEND=NXS
IF(I*NXS.GT.N)IEND=N-((I-1)*NXS)
CALL RECORF(X(IBEGIN),1,IEND,XMIN,RANGE,CONST,AINTER,TITLE,NXL)
10 CONTINUE
C
CALL ENDFME
99 RETURN
END
SUBROUTINE RECORF(X,IBEGIN,IEND,XMIN,RANGE,CONST,AINTER,TITLE,NXL)
C
C
INTEGER BASE,PCS,BASEL,BASEY,AMARK,XPLOT1,XPLOT2,TPLOT1,TPLOT2
DIMENSION X(IEND),TITLE(20)
REAL*8 TITLE
***
CALL TSP(120,48,8)
C
DO 1 I=6,15
CALL HORAM(TITLE(I),8)
CONTINUE
CALL TSP(120,48,24)
DO 30 I=17,19
CALL HORAM(TITLE(I),8)
30 CONTINUE
C
DO 5 I=1,3
BASE=340*I-170
CALL VECTOR(111,BASE,911,BASE)
POS=BASE+40
CALL TSP(801,48,PCS)
CALL HORAM(TITLE(3),8)
BASEL=BASE+12
BASEY=BASE+20
C
DO 10 J=1,7
ANMBR=FLOAT(J-1)*AINTER
AMARK=(FLOAT((J-1)*5)*80.)/3. + 111.
CALL VECTOR(AMARK,BASE,AMARK,BASEL)
AMARK=AMARK-40
CALL TSP(AMARK,48,BASEY)
CALL C4C2CF(ANMBR,6,1)
10 CONTINUE
5 CONTINUE

```

```

C
C
IBEG11=IBEGIN+1
XPL0T1=32C.-(X(IBEGIN)-XMIN)*RANGE
TPL0T1=111.
DO 15 I=IBEG11,IEND
I LINE=(I-1)/NXL+1
XPL0T2=34C.*FLCAT(I LINE)-(X(I)-XMIN)*RANGE-20.
TPL0T2=FLOAT(I-IBEGIN-((I LINE-1)*NXL))*CONST+111.
IF(I.EQ.(NXL+1).OR.I.EQ.(2*NXL+1))GO TO 20
CALL VECTOR(TPL0T1,XPL0T1,TPL0T2,XPL0T2)
20 XPL0T1=XPL0T2
TPL0T1=TPL0T2
15 CONTINUE

```

```

C
CALL TSP(939,48,23)
CALL HORAN(TITLE(16),8)

```

```

C
RETURN
END
SUBROUTINE CARGRF(X,Y,N)

```

THIS PACKAGE PLOTS N POINTS THE CARTESIAN CO-ORDINATES OF THE JTH POINT BEING SPECIFIED AS X(J),Y(J). THE PACKAGE USES THE COMMON --

COMMON /GRFF/ TITLE(20), XMAX, XMIN, YMAX, YMIN, INDX, INDY, IND, IIDOT, ANSTR1, IF, XLIMIT, YLIMIT, SCALX, SCALY

THE TITLE ARRAY CARRIES INFORMATION FOR ANNOTATING THE OUTPUT GRAPH. THIS ARRAY IS SET UP AS FOLLOWS -

- TITLE (1) -)
  - . )CONTAINS 24 HOLLERITH CHARACTERS GIVING THE UNITS
- TITLE (3) -) OF THE ABSCISSAE
- TITLE (4) )CONTAINS 16 HOLLERITH CHARACTERS GIVING THE UNITS
- TITLE (5) ) OF THE ORDINATE
- TITLE (6) -)
  - . )CONTAINS 80 HOLLERITH CHARACTERS GIVING A TITLE TO
  - . ) THE GRAPH
- TITLE (15) -)
- TITLE (16) -CONTAINS 8 HOLLERITH CHARACTERS GIVING DATE OF PROCESSING
- TITLE (17) -CONTAINS 8 HOLLERITH CHARACTERS GIVING TIME OF PROCESSING
- TITLE (18) -)
  - . )UNUSED
- TITLE (20) -)

XMAX ) SET BOTH EQUAL IF PROGRAM TO CHOOSE THE ABSCISSAE SCALE.  
 XMIN ) OTHERWISE SET TO CHOSEN LIMITS OF ABSCISSAE SCALE

YMAX ) SET BOTH EQUAL IF PROGRAM TO CHOOSE THE ORDINATE SCALE.  
 YMIN ) OTHERWISE SET TO CHOSEN VALUES OF ORDINATE SCALE

INDX IS AN INDICATOR FOR PLOTTING THE ABSCISSAE ON A LOG SCALE  
INDX=1 ABSCISSAE ON LINEAR SCALE  
INDX=2 ABSCISSAE ON LOG SCALE

INDY IS A SIMILAR INDICATOR FOR THE ORDINATE SCALE

N.B. CONTENTS OF ARRAYS ARE MODIFIED USING LOG SCALE.

IND IS AN INDICATOR FOR CONTROLLING FRAME CALLS -  
IND=1 CARGRF CALLS ADVFLM AND ENDFME  
=2 CARGRF CALLS ENDFME BUT NOT ADVFLM

IDOT IS THE SC4020 CODE OF THE REQUIRED PLOTTING SYMBOL

ANSTR1 INDICATES WHETHER THE PLOTTED POINTS HAVE TO BE JOINED UP  
ANSTR1=1. POINTS NOT JOINED  
=2. POINTS JOINED

IF SPECIFIES TYPE OF OUTPUT  
IF=1 OUTPUT ON MICROFILM  
=2 OUTPUT ON HARD COPY  
=3 OUTPUT ON BOTH MICROFILM AND HARD COPY

SUBROUTINE CARGRF(X,Y,N)

DIMENSION X(N), Y(N)

COMMON /GRFF/ TITLE(20), XMAX, XMIN, YMAX, YMIN, INDX, INDY, IND,  
IIDOT, ANSTR1, IF, XLIMIT, YLIMIT, SCALX, SCALY

REAL\*8 TITLE, AJCIN, BLANK, INSTR1, DATE, TIME

INTEGER PLACEX, PLACEY, XPLOT1, XPLOT2, YPLOT1, YPLOT2

DATA AJCIN/8HJCI N /, BLANK/8H /

CALL DATIM(DATE, TIME)

IF(IF)2,2,1

IF(IF-4)3,3,2

IF=3

IF(IND.NE.2) IND=1

IF(INDX.NE.2) INDX=1

IF(INDY.NE.2) INDY=1

IF(IDOT.GT.63) IDOT=48

INSTR1=AJCIN

IF(ANSTR1.EQ.1.) INSTR1=BLANK

GO TO (55,60), INDX

60 POSXT=POSMIN(X,N)

POSX=ALOG10(POSXT)

POSXT=POSXT\*0.9999

DO 201 I=1,N

IF(X(I).LE.C.0) X(I)=POSXT

```

201 CONTINUE
CALL CLOG(X,N)
55 GO TO (65,70),INDY
70 POSYT=POSMIN(Y,N)
POSY=ALOG10(PCSYT)
POSYT=POSYT*C.9999
DO 202 I=1,N
IF(Y(I).LE.C.0)Y(I)=PCSYT
202 CONTINUE
CALL CLOG(Y,N)
65 IF((XMAX-XMIN).GT.1.0E-7)GO TO 66
CALL AMAX(X,N,XX)
CALL AMIN(X,N,XXN)
IF((XX-XXN).LT.1.0E-7)XX=XX+1.0E-7
GO TO 67
66 XX=XMAX
XXN=XMIN
67 IF((YMAX-YMIN).GT.1.0E-7)GO TO 68
CALL AMAX(Y,N,YY)
CALL AMIN(Y,N,YYN)
IF((YY-YYN).LT.1.0E-7)YY=YY+1.0E-7
GO TO 200
68 YY=YMAX
YYN=YMIN
200 GO TO (888,889),IND
888 CALL ADVFLM(IF)
889 CALL EXPHVY(123,27,923)
CALL SCALN(X,XLIMIT,SCALX,PLACEX,XFACTOR,N,XX,XXN)
CALL SCALN(Y,YLIMIT,SCALY,PLACEY,YFACTOR,N,YY,YYN)
GO TO (777,778),IND
777 CALL VECTOR(115,923,1003,923)
CALL VECTOR(123,931,123,43)

```

C

```

DO 5 I=1,11
FACTOR=FLOAT(I-1)*80.
XSCAL=203.+FACTOR
YSCAL=43.+FACTOR
CALL VECTOR(XSCAL,923,XSCAL,931)
CALL VECTOR(115,YSCAL,123,YSCAL)
5 CONTINUE

```

C

```

778 IGUIDE = 1
IDRAW = 1
IF(INDX.EQ.2.AND.X(1).LT.PCSX)IGUIDE=2
IF(INDY.EQ.2.AND.Y(1).LT.PCSY)IGUIDE=2
GO TO (998,999),IGUIDE
998 XPLCT1=(X(1)-XLIMIT)*SCALX + 123.
YPLCT1=923.-((Y(1)-YLIMIT)*SCALY)
CALL PLOT(XPLCT1,IDCT,YPLCT1)
IDRAW=2
IF(INSTR1.NE.AJCI)IDRAW=1
999 IGUIDE=1

```

C

```

DO 10 I=2,N
IF(INDY.EQ.2.AND.Y(I).LT.PCSY)IGUIDE=2
IF(INDX.EQ.2.AND.X(I).LT.PCSX)IGUIDE=2
GO TO (997,996),IGUIDE
997 XPLCT2=(X(I)-XLIMIT)*SCALX + 123.
YPLCT2=923.-((Y(I)-YLIMIT)*SCALY)
CALL PLOT(XPLCT2,IDCT,YPLCT2)
GO TO (995,994),IDRAW

```



```

994 CALL VECTOR(XPLOT1,YPLOT1,XPLOT2,YPLOT2)
995 YPLOT1=YPLOT2
    XPLOT1=XPLOT2
    IGUIDE=1
    IDRAW=2
    IF(INSTR1.NE.AJCIN)IDRAW=1
    GO TO 10
996 IDRAW=1
    IGUIDE=1
10  CONTINUE

```

```

C
C
GO TO (779,780),IND
779 Y4=4.*YFACTR
    X4 = 4.*XFACTR

```

```

C
DO 30 I=1,3
  F=(I-1)
  YLIM=YLIMIT+F*Y4
  GO TO (21,31),INDY
31  YLIM=10.**YLIM
32  XLIM=XLIMIT+F*X4
  GO TO (22,32),INDX
32  XLIM=10.**XLIM
33  YPOS=915.-F*320.
  XPOS=52.+F*320.
  CALL TSP(12,48,YPCS)
  GO TO (23,33),INDY
33  CALL C4020E(YLIM,11,2)
  GO TO 41
34  CALL C4020F(YLIM,13,PLACEY)
41  CALL TSP(XPCS,48,942)
  GO TO (24,34),INDX
34  CALL C4020E(XLIM,11,2)
  GO TO 30
24  CALL C4020F(XLIM,13,PLACEX)
30  CONTINUE

```

```

C
C
IF(TITLE(16).NE.DATE)GO TO 780

```

```

CALL TSP(48,48,291)
CALL VERAM(TITLE(4),16)
CALL TSP(760,48,958)
CALL HORAM(TITLE(1),24)
CALL TSP(130,48,23)
CALL HORAM(TITLE(6),80)

```

```

C
C
780 CALL ENDFME
    RETURN
    END
FUNCTION PCSMIN(X,N)

```

```

FINDS MINIMUM POSITIVE VALUE OF ARRAY X

```

```

DIMENSION X(N)

```

```

C
IND = 0
DO 10 I=1,N
IF(X(I).LE.0.0)GO TO 10
IND=I
GO TO 1
10 CONTINUE
1 IF(IND.NE.0)GO TO 7
PRINT 20
20 FORMAT(132H1AN ARRAY FROM WHICH THE SMALLEST POSITIVE VALUE WAS RE
1QUESTED FOR GRAPHING WAS ALL NEGATIVE YOUR JOB HAS THEREFORE BEEN
2 TERMINATED)
CALL FINISH
CALL EXIT
7 KQ=IND
5 KP=KQ
2 IF(KQ-N)3,4,4
3 KQ=KQ+1
IF(X(KQ).LE.0.0)GO TO 2
IF(X(KP)-X(KQ))2,5,5
4 POSMIN=X(KP)
RETURN
END
SUBROUTINE CLOG(X,N)

```

```

C
C
C
C
C
CONVERTS ARRAY X TO COMMON LOGS

```

```

DIMENSION X(N)

```

```

DO 1 I = 1,N
X(I) = ALOG10(X(I))
1 CONTINUE
RETURN
END
SUBROUTINE SCALEN(X,XLIMIT,SCALX,IPLACE,FACTOR,N,XMAX,XMIN)

```

```

C
C
C
C
COMPUTES SCALING VALUES FOR CARGRF

```

```

DIMENSION X(N)
DOUBLE PRECISION XRG,R,FACT,S

```

```

XRG=XMAX-XMIN

```

```

C
1 R=0.000
IF(XRG.LT.(10.000**R*.0000000001)) GO TO 2
R=R+1.000
GO TO 1
2 IF(R.LT.1.000) GO TO 5
FACT=(10.000**(R-1.000)*.000000000125)
S=0.000
3 IF(XRG.LE.FACT*(2.000**S)) GO TO 4
S=S+1.000
GO TO 3
4 FACTOR=(FACT*(2.000**S))*10.00-2

```

```

C
XLIMIT=XMIN/FACTOR
LIMITX=XLIMIT-.99999
XLIMIT=FLOAT(LIMITX)*FACTOR
IF(XMIN.LT.XLIMIT) XLIMIT=XLIMIT-FACTOR
SCALX=80./FACTOR

```

```
IPLACE=13.-R
IF (IPLACE.LT.1) IPLACE=1
```

```
RETURN
END
SUBROUTINE AMAX (X,N,XMAX)
```

```
FINDS MAXIMUM VALUE OF ARRAY X
```

```
DIMENSION X(N)
KQ = 1
2 KP = KQ
5 IF (KQ - N) 3,4,4
3 KQ = KQ + 1
IF (X(KP) - X(KQ)) 2,5,5
4 XMAX = X(KP)
RETURN
END
SUBROUTINE AMIN (X,N,XMIN)
```

```
FINDS MINIMUM VALUE OF ARRAY X
```

```
DIMENSION X(N)
KQ = 1
5 KP = KQ
2 IF (KQ - N) 3,4,4
3 KQ = KQ + 1
IF (X(KP) - X(KQ)) 2,5,5
4 XMIN = X(KP)
RETURN
END
SUBROUTINE CONTR (A,NX,NY,N,CSTEP,CLOW,CHIGH,IF)
```

```
DIMENSION A(N,N)
CALL ADVFLP(IF)
HX=10.2/FLOAT(NX)
HY=10.2/FLOAT(NY)
QX=C.02
QY=C.02
DC=CSTEP
C3=CLOW
C4=CHIGH
C1=C4+DC
C2=C1+DC
CALL OBC7A (A,DC,C1,C2,C3,C4,NX,NY,HX,HY,QX,QY,0.,1,N)
CALL ENDFME
RETURN
END
SUBROUTINE CBO7A (F,DC,C1,C2,C3,C4,NX,NY,HX,HY,QX,QY,COSS,NQ,IDF)
```

```
DIMENSION F (IDF, IDF)
COMMON /CNT/ OX,CY,COSS,SING,DX,DY,CX,CY,X,Y,A,B,C,D,CON,IHL,IHK
IHL=1
IHK=2
IHO=3
CEN=100.
OX = QX
OY = QY
```



3 PAUL.W.BURTON & BLACKNEST

9.	12.5	25.	42.	56.	71.50.8	.8	0.	30.	100.	43.100.	320181.3.	C48C4C.00
8.	12.	24.	41.	58.	80.50.8	1.	0.	30.	100.	39.200.	320161.C.	C48C4C.00
7.50C	11.50C	22.50C	42.00C	65.00C	103.00.8001.5000.00030.00100.032.000.						320134.C.	C48C4C.00
6.50C	10.00C	20.00C	54.00C	69.0203.00.8003.0000.00030.00100.038.000.							640149.CC.	C96C4C.00
5.00C	7.50C	19.00C	88.00C	210.0420.00.8006.0000.00030.00100.020.200.							640147.8.	192C4C.00
8.50C	13.50C	26.00C	44.00C	59.0073.501.0000.8000.00030.00100.035.200.							320148.8.	C48C4C.CC
8.00C	13.50C	25.00C	45.00C	63.0087.501.0001.0000.00030.00100.036.000.							320148.8.	C48C4C.00
7.50C	12.00C	24.00C	48.50C	78.00126.01.0001.5000.00030.00100.026.000.							320148.5.	C64C4C.00
6.00C	10.00C	23.50C	67.00C	132.0243.01.0003.0000.00030.00100.015.000.							320163.8.	128C4C.00
5.00C	8.50C	24.00C	106.0243.0468.01.0006.0000.00030.00100.015.300.								640130.5.	192C4C.CC
9.50C	15.50C	30.50C	50.50C	67.0084.001.5000.8000.00030.00100.048.200.							640148.5.	C48C4C.CC
8.50C	14.00C	28.50C	51.50C	72.0099.001.5001.0000.00030.00100.044.000.							640172.C.	C64C4C.00
8.00C	13.00C	28.50C	59.00C	90.00140.01.5001.5000.00030.00100.035.000.							640192.8.	C96C4C.00
7.50C	12.00C	32.00C	82.00C	147.0260.01.5003.0000.00030.00100.020.200.							640146.3.	128C4C.00
6.00C	11.00C	36.00C	127.0260.0484.01.5006.0000.00030.00100.021.001.								280162.C.	256C4C.00
10.50C	18.00C	36.00C	62.50C	84.00113.03.0000.8000.00030.00100.039.201.							020149.5.	C64C4C.CC
10.00C	17.50C	37.00C	68.50C	96.00133.03.0001.0000.00030.00100.035.701.							020195.C.	C96C4C.00
8.50C	17.50C	49.00C	113.5184.0291.03.0003.0000.00030.00100.028.301.								020147.8.	C96C4C.CC
10.00C	17.00C	40.00C	80.50C	120.0175.03.0001.5000.00030.00100.016.701.							020183.8.	192C4C.00
8.50C	19.00C	61.00C	162.0292.0509.03.0006.0000.00030.00100.08.9001.								020148.C.	256C4C.CC
9.00C	14.50C	28.50C	48.50C	67.0092.001.0001.0000.00035.00100.077.000.							640196.4.	048C4C.00
9.50C	16.00C	31.50C	56.00C	77.00105.01.5001.0000.00035.00100.052.000.							640167.3.	C48C4C.00
10.00C	17.00C	35.50C	62.50C	86.00118.03.0001.0000.00035.00100.033.800.							640198.4.	C64C4C.CC
7.50C	11.50C	21.50C	35.50C	47.0058.501.0000.8000.00030.0075.0034.600.							320161.5.	C64C4C.00
7.00C	11.50C	22.00C	37.50C	52.0070.001.0001.0000.00030.0075.0029.300.							320139.0.	C64C4C.00
7.00C	10.50C	21.50C	40.50C	63.00100.01.0001.5000.00030.0075.0021.400.							320156.8.	C96C4C.00
5.50C	9.50C	21.50C	56.00C	105.0187.01.0003.0000.00030.0075.0022.600.							640176.2.	192C4C.00
4.50C	8.00C	23.00C	86.50C	185.0357.01.0006.0000.00030.0075.0011.400.							640127.3.	256C4C.00
7.50C	12.50C	24.00C	40.00C	54.0069.001.5000.8000.00030.0075.0046.000.							640204.C.	C96C4C.00
7.00C	11.50C	24.00C	43.00C	60.0081.001.5001.0000.00030.0075.0039.800.							640176.2.	096C4C.00
7.00C	11.50C	24.50C	50.00C	75.00113.01.5001.5000.00030.0075.0029.000.							640176.3.	128C4C.00
5.50C	9.50C	26.50C	68.00C	118.0201.01.5003.0000.00030.0075.0015.500.							640154.8.	192C4C.CC
5.50C	10.50C	33.50C	103.0203.0375.01.5006.0000.00030.0075.0015.801.								280116.1.	256C4C.00
9.00C	15.00C	30.00C	52.50C	72.00101.03.0000.8000.00030.0075.0037.201.							020144.3.	096C4C.CC
8.50C	15.00C	30.50C	57.00C	81.00117.03.0001.0000.00030.0075.0032.101.							020169.C.	128C4C.CC
7.50C	14.00C	34.00C	69.00C	101.0148.03.0001.5000.00030.0075.0023.401.							020196.6.	192C4C.00
7.50C	15.50C	44.00C	98.00C	154.0237.03.0003.0000.00030.0075.0012.501.							020165.C.	256C4C.CC
8.00C	17.50C	55.00C	141.0243.0414.03.0006.0000.00030.0075.0012.802.								040149.5.	384C4C.CC
7.50C	11.50C	21.00C	34.00C	54.5056.000.8000.8000.00030.0075.0041.000.							320173.C.	C64C4C.00
7.00C	11.00C	19.50C	34.00C	47.0065.000.8001.0000.00030.0075.0036.100.							320153.C.	C64C4C.00
6.50C	10.00C	19.00C	36.00C	58.0096.000.8001.5000.00030.0075.0025.600.							320170.7.	C96C4C.00
4.50C	8.00C	23.50C	47.50C	95.50176.00.8003.0000.00030.0075.0014.00.							320193.C.	192C4C.CC
4.00C	8.00C	23.50C	47.50C	95.50176.00.8003.0000.00030.0075.0014.00.							320193.C.	192C4C.CC
8.0	12.5	24.5	44.5	62.5	87.001.0	1.0	0.0	25.	100.	50.200.	640141.7.	C64C4C.CC
8.0	13.0	27.5	49.0	57.5	92.001.5	1.0	0.0	25.	100.	35.800.	640193.5.	C96C4C.00
9.5	17.	34.5	62.5	87.0	119.03.0	1.0	0.0	25.	100.	18.800.	640150.C.	096C4C.00
9.5	15.5	30.5	52.0	68.5	86.003.0	0.8	0.0	15.	100.	18.201.	020146.2.	192C4C.00
7.5	13.5	29.5	52.5	74.	102.03.0	1.0	0.0	15.	100.	16.801.	020126.3.	192C4C.00
7.0	13.	29.5	60.0	92.0	142.03.0	1.5	0.0	15.	100.	27.402.	040188.C.	384C4C.CC
6.0	11.5	32.0	84.0	148.	255.03.0	3.0	0.0	15.	100.	15.302.	040144.8.	512C4C.00
4.5	10.0	37.5	125.	5250.	468.03.0	6.0	0.0	15.	100.	8.3002.	040166.81.	0244C.00
7.0	12.0	24.5	42.0	56.5	72.001.5	0.8	0.0	15.	100.	31.301.	020173.8.	192C4C.CC
6.5	11.0	23.0	42.5	62.0	88.001.5	1.0	0.0	15.	100.	28.401.	020150.1.	192C4C.00
5.5	9.0	22.0	48.0	77.0	128.01.5	1.5	0.0	15.	100.	22.501.	020148.8.	256C4C.CC
4.5	8.0	22.0	65.5	130.	0237.01.5	3.0	0.0	15.	100.	26.002.	040164.9.	512C4C.CC
3.0	6.5	23.	107.	239.	467.01.5	6.0	0.0	15.	100.	13.602.	040175.71.	0244C.00

6.0	10.5	21.5	39.0	53.0	69.0	01.0	0.8	0.0	15.	100.	35.700.	960182.2.192040.00
5.5	9.5	20.0	39.5	57.0	82.0	01.0	1.0	0.0	15.	100.	33.000.	960160.0.192040.00
5.5	8.5	19.0	42.5	72.0	120.0	01.0	1.5	0.0	15.	100.	26.200.	960159.8.256040.00
4.5	7.0	16.5	56.5	121.	233.0	01.0	3.0	0.0	15.	100.	17.001.	020176.0.512040.00
5.0	9.0	20.0	37.0	52.0	68.0	00.8	0.8	0.0	15.	100.	39.300.	960187.2.192040.00
5.0	8.0	18.0	37.0	55.0	80.0	00.8	1.0	0.0	15.	100.	35.500.	960162.0.192040.00
4.5	7.5	16.5	39.5	69.0	120.0	00.8	1.5	0.0	15.	100.	28.000.	960162.0.256040.00
4.5	6.5	14.5	53.0	117.	229.0	00.8	3.0	0.0	15.	100.	21.601.	280180.0.512040.00
4.5	7.5	15.5	28.5	39.5	52.0	00.8	0.8	0.0	15.	75.	37.000.	960187.2.256040.00
4.5	6.5	14.5	28.5	42.0	61.0	00.8	1.0	0.0	15.	75.0	32.200.	960163.8.256040.00
4.5	6.5	13.5	30.0	52.5	90.0	00.8	1.5	0.0	15.	75.	23.300.	960181.5.384040.00
3.5	5.0	12.0	40.5	90.0	173.0	00.8	3.0	0.0	15.	75.	17.501.	280199.0.768040.00
5.0	8.5	17.0	30.0	40.0	52.5	01.0	0.8	0.0	15.	75.	34.300.	960180.0.256040.00
4.0	7.5	16.0	30.0	44.0	64.0	00.1.0	1.0	0.0	15.	75.	29.900.	960155.0.256040.00
3.5	6.5	15.0	32.5	55.5	92.0	00.1.0	1.5	0.0	15.	75.	20.700.	960172.7.384040.00
5.5	9.0	19.0	33.0	44.5	57.0	00.1.5	0.8	0.0	15.	75.	30.001.	020166.0.256040.00
5.0	9.0	19.5	35.0	49.0	68.0	00.1.5	1.0	0.0	15.	75.	25.201.	020142.6.256040.00
4.5	8.0	18.0	38.5	60.5	99.0	00.1.5	1.5	0.0	15.	75.	20.301.	020159.7.384040.00
6.5	11.5	24.5	40.5	54.5	65.5	03.0	0.8	0.0	15.	75.	34.302.	040200.0.384040.00
6.5	11.5	24.0	45.0	63.0	87.0	03.0	1.0	0.0	15.	75.	29.202.	040165.8.384040.00
6.5	10.5	25.5	52.5	79.0	119.0	03.0	1.5	0.0	15.	75.	21.002.	040165.8.512040.00
8.5	11.0	30.0	73.5	124.	209.0	03.0	3.0	0.0	15.	75.	11.502.	040146.2.768040.00

122362 1704 0055 04 INCREMENT=10 (AN EXAMPLE OF A COMPLETE DATA SET) 0126  
 KON/0055 22.7 111142. 1122000 300  
 1.6 0 0 1 10 8 22 1 1 24 198 10 .2 10. .04  
 11111111111111 11  
 (12F5.0)

122362 1704 0055 04 CALIBRATION PULSE OF SEISMG DATA NUMBER 0126															0126	2
41.	80.	170.	346.	557.	896.	11.2	.096	.08	942.	4998	5000	5015	5015		C1260001	
5000	5001	5010	5011	5007	5005	5029	5032	4998	5044	5027	5060				C1260002	
5013	5013	5040	5058	5052	5040	5029	5045	5053	5044	5027	5060				C1260003	
5061	5047	5049	5048	5056	5032	5045	5037	4995	4989	5001	4966				C1260004	
4934	4970	4985	4948	4955	4929	4956	4964	4944	4962	4981	4988				C1260005	
5015	5046	5071	5085	5078	5076	5077	5082	5101	5106	5088	5085				C1260006	
5064	5029	5020	4991	4970	4957	4936	4950	4955	4915	4959	4980				C1260007	
4980	5002	5036	5069	5081	5073	5086	5135	5106	5072	5100	5096				C1260008	
5066	5002	4978	4956	4931	4912	4890	4926	4936	4931	4991	5025				C1260009	
5047	5064	5071	5100	5115	5129	5101	5072	5051	5032	5025	4986				C1260010	
4937	4925	4956	4946	4929	4968	4990	5003	5040	5075	5105	5125				C1260011	
5128	5094	5087	5058	5034	5001	4958	4938	4920	4918	4922	4936				C1260012	
4993	5042	5049	5058	5085	5127	5132	5115	5091	5054	5036	4994				C1260013	
4962	4946	4942	4925	4905	4992	5032	5029	5070	5095	5142	5140				C1260014	
5089	5054	5032	5029	4995	4926	4920	4966	4959	4957	5036	5100				C1260015	
5095	5062	5100	5107	5085	5040	4991	4985	4992	4961	4921	4973				C1260016	
4980	4992	5029	5082	5085	5105	5135	5130	5087	5006	4974	4910				C1260017	
4860	4824	4916	5021	5086	5124	5187	5215	5181	5107	5005	4936				C1260018	
4856	4775	4828	4892	4988	5138	5315	5287	5162	5006	4960	4991				C1260019	
4967	4866	4836	4896	4953	5062	5190	5187	5070	5121	5226	5140				C1260020	
4992	4785	4600	4838	5225	5389	5362	5220	4986	4887	4895	4934				C1260021	
4953	4984	5038	5083	5101	5112	5138	5132	5062	4955	4920	4996				C1260022	
5008	5058	5078	5067	5058	5056	5062	5056	5047	5031	4958	4995				C1260023	
5055	5054	4966	5011	5109	5103	5051	5026	5033	4992	4932	4962				C1260024	
4996	5029	5057	5060	5049	5048	5042	5002	4956	4985	4987	4958				C1260025	
5032	5057	5035	5060	5027	5020	5013	4981	4977	4978	4986	5000				C1260025	

## REFERENCES

1. A Dziewonski, S Bloch and M Landisman: "A Technique for the Analysis of Transient Seismic Signals". BSSA, 59, 1, 427-444 (February 1969)
2. H H Inston, P D Marshall and C Blamey: "Optimisation of Filter Bandwidth in Spectral Analysis of Wavetrains". Geophys J Roy Astr Soc, 23, 243-250 (1971)
3. J B Young and A Douglas: "Map, Time Series and other Plotting Routines for Use with the Stromberg-Carlson 4020 Plotter". AWRE Report 041/68 (1968)
4. L D Enochson and R K Otnes: "Programming and Analysis for Digital Time Series Data". The Shock and Vibration Information Centre, United States Department of Defense (1968)
5. D W McCowan: "Finite Fourier Transform Theory and its Application to the Computation of Convolutions, Correlations and Spectra". Earth Sciences Division, Teledyne Industries Inc, Alexandria, Virginia. Memorandum No 8-66 (1966)
6. R Bracewell: "The Fourier Transform and its Applications". McGraw-Hill (1965)
7. J E W Kuye: "The Effect of Frequency Tapers on the Transfer Function of the Band Pass Filter". In preparation
8. A J Espinosa, J H Sutton and H J Miller: "A Transient Technique for Seismograph Calibration - Manual and Standard Set of Theoretical Transient Responses". Vesiac Special Report No 4410-106-X (October 1965)

The Source-Layering Function of Underground Explosions and Earthquakes—An Application of a 'Common Path' Method

R. D. Marshall and R. W. Braton

REPRINTED FROM

*Geophys. J. R. astr. Soc.* (1971) 24, 533-537

REISSUED BY

BLACKWELL SCIENTIFIC PUBLICATIONS

OXFORD AND EDINBURGH

PRINTED IN ENGLAND BY

C. R. HODGSON & SON LTD., LONDON





## Letter to the Editors

# The Source-Layering Function of Underground Explosions and Earthquakes—an Application of a 'Common Path' Method

P. D. Marshall and P. W. Burton

(Received 1971 August 10)

The vertical component of surface motion,  $R(\omega)$ , created by a Rayleigh wave in a layered medium, at a point distant  $r$  from a source, is given by the expression:

$$R(\omega) = \frac{K}{r^{\frac{1}{2}}} \cdot L(\omega, d) * I(\omega) * A(\omega) * S(\omega)$$

where  $K$  is a constant and  $L(\omega, d)$ ,  $I(\omega)$  and  $S(\omega)$  represent the amplitude response of the layered medium as a function of frequency and source depth  $d$ , the amplitude response of the instrument, the absorption term and the source spectral function respectively. The Rayleigh wave amplitude  $R(\omega)$  is expressed in the angular frequency domain (Toksöz, Ben-Menahem & Harkrider 1964).

For a closed system comprising a single epicentre, path and recording station:

$$\frac{S(\omega) * L(\omega, d)}{R(\omega)} = \frac{r^{\frac{1}{2}}}{K \cdot I(\omega) * A(\omega)} = \alpha(\omega)$$

is a function of frequency only, and constant at a given frequency;  $\alpha(\omega)$  is a characteristic of the system and independent of the source. Any two events which occur at the same epicentre have a common path parameter  $\alpha(\omega)$  and therefore are related by the expression

$$\frac{S_1(\omega) * L_1(\omega, d)}{R_1(\omega)} = \frac{S_2(\omega) * L_2(\omega, d)}{R_2(\omega)} \quad (1)$$

The terms  $R_1(\omega)$  and  $R_2(\omega)$  can be obtained by Fourier analysis of the Rayleigh wave trains. This gives a means of relating the spectral source-layering functions  $S(\omega) * L(\omega, d)$  for two events; the terms for absorption, scattering and lateral refraction along the path and the instrument are eliminated.

It is usually difficult to assess the source-layering term. This paper suggests the comparison of a known with an unknown source, by means of the common path method to solve the problem.

The source spectrum for atmospheric explosions has been published by Carpenter & Marshall (1970) using data from the large explosions fired over Novaya Zemlya in 1962. Since 1964 large underground explosions have taken place very close to these epicentres. Rewriting relation (1) for these two types of event leads to:

$$S_u(\omega) * L_u(\omega, d) = \frac{R_u(\omega) * S_A(\omega) * L_A(\omega, 0)}{R_A(\omega)} \quad (2)$$

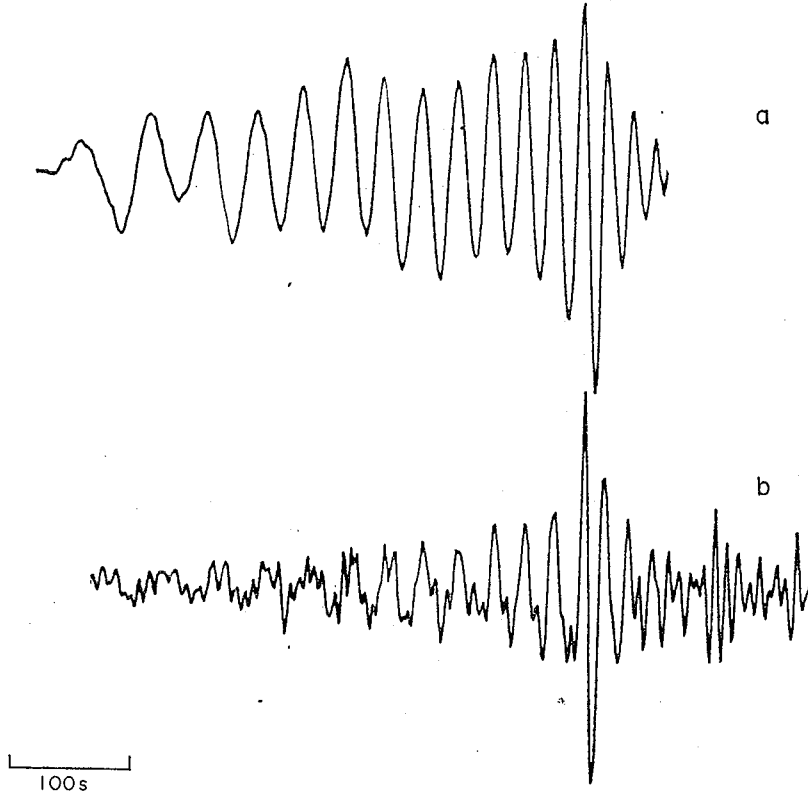


FIG. 1. Recordings at Quetta of (a) Atmospheric and (b) Underground explosions at Novaya Zemlya.

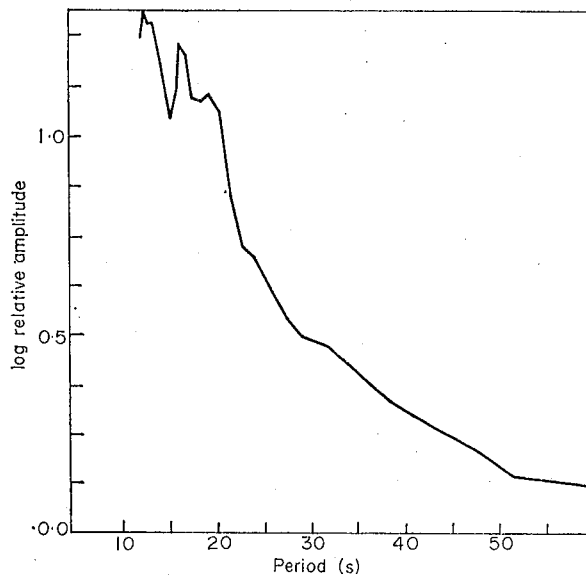


FIG. 2. The log source-layering function of an underground explosion (from the Quetta records).

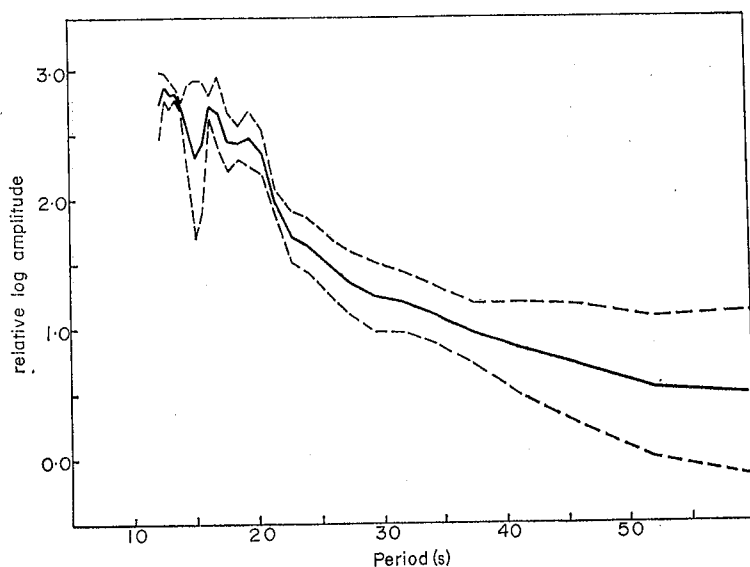


FIG. 3. The mean and one standard deviation variation of the log source-layering function of an underground explosion (from the summation of three sets of records).

The term  $L_A(\omega, 0)$  can be considered as constant because it is a slowly varying function of  $\omega$  in the range of interest (Carpenter & Marshall 1970). Rayleigh waves from two explosions at Novaya Zemlya and recorded at Quetta, Pakistan, were analysed (Fig. 1(a) and (b)) and their Fourier spectra obtained.

Atmospheric explosion:	27.9.62	0803 GMT	$h \approx 0$ km
	74.3° N	52.4° E	
Underground explosion:	27.10.66	0558 GMT	$h \approx 0$ km
	73.4° N	54.9° E.	

The spectral source-layering function (illustrated in Fig. 2) for this underground explosion was calculated for a set of discrete frequency points by substitution into equation (2) at each frequency point. The perturbations at the higher frequencies are probably due to differences in the background noise levels. There is more noise on the underground explosion record than on the atmospheric explosion record (Fig. 1(a) and (b)); ideally the signal-to-noise ratio would be the same for each seismogram.

Perturbations due to noise were reduced by the similar analysis of records from Albuquerque and Istanbul and then summing the individual spectra, the summed spectrum obtained is shown in Fig. 3. This process is valid for explosive sources because they are radially symmetric. The inclusion of one standard deviation from the mean in Fig. 3 illustrates the variation of the spectra which make up the average spectral values. The variation is reasonable although only a few records were analysed.

The 'Common Path' method can be extended to earthquake investigation by using this known source-layering function. The assumption is that  $L_u(\omega, d)$  does not vary significantly over many regions of the world because explosions are shallow events, and  $L_u(\omega, d)$  depends mainly on gross crustal features. The large differences in crustal thickness between Kazakh S.S.R. and Nevada U.S.A. cause observable differences in  $S_u(\omega) * L_u(\omega, d)$  (see Fig. 4, Marshall 1970). However,  $S_u(\omega) * L_u(\omega, d)$  estimated in a region of normal crustal thickness may be applied in a region of similar crustal thickness.

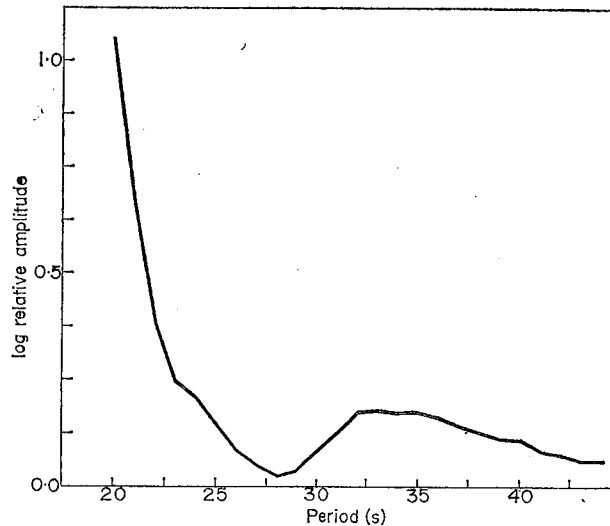


FIG. 4. The log source-layering function of an earthquake (from Milrow records).

The Rayleigh waves from an underground explosion and an earthquake which occurred in the same epicentral region were used to calculate the earthquake source-layering function:

$$S_E(\omega) * L_E(\omega, d) = \frac{S_u(\omega) * L_u(\omega, d) * R_E(\omega)}{R_u(\omega)} = R_E(\omega) * \alpha^1(\omega).$$

The events selected were:

Underground explosion:	2.10.69	2206 GMT	$h \approx 0$ km
(MILROW)	57.4° N	179.2° E	
Earthquake:	18.9.69	0844 GMT	$h \approx 24$ km
	52.5° N	173.5° E.	

and the resultant spectrum of the earthquake is shown in Fig. 4. The summation of several spectra cannot be applied to earthquakes because the source is radially asymmetric. This necessarily implies a study of the variation with azimuth.

As anticipated by other studies (SIPRI 1968; Marshall 1970) the source layering functions for the earthquake and explosion are significantly different, particularly at the longer periods. No further interpretation of the earthquake spectrum is attempted here except to say that the minimum at  $T \approx 28$  s in the earthquake spectrum is associated with the depth of the source (Douglas, Hudson & Kembhavi 1970).

To proceed further with the present analysis and obtain  $S_u(\omega)$  we must eliminate  $L_u(\omega, d)$ . This can be done when the crustal structure is known in the region of Novaya Zemlya.

U.K.A.E.A.,  
Blacknest,  
Brimpton,  
Reading RG7 4RS

Department of Geology,  
University of Durham,  
Durham City,  
Durham.

## References

- Toksöz, M. N., Ben-Menahem, A. & Harkrider, D. G., 1964. Determination of source parameters by amplitude equilisation of seismic surface waves 1. Underground nuclear explosions, *J. geophys. Res.*, **69**, 4355-4366.
- Carpenter, E. W. & Marshall, P. D., 1970. A.W.R.E. Report 0-88/70, H.M.S.O. *Surface waves generated by atmospheric nuclear explosions.*
- SIPRI 1968. *Seismic methods for monitoring underground explosions*, Stockholm 1968, Rapporteur Dr. D. Davies.
- Marshall, P. D., 1970. Aspects of the spectral differences between earthquakes and underground explosions, *Geophys. J. R. astr. Soc.*, **20**, 397-416.
- Douglas, A., Hudson, J. A. & Kembhavi, V. K., 1970. The analysis of surface wave spectra using a reciprocity theorem for surface waves, *Geophys. J. R. astr. Soc.*, **23**, 207.



## Upper Mantle Zone of Low $Q$

SEISMOLOGISTS have great interest at present in delineating laterally varying properties of the upper mantle<sup>1</sup>. A quantity which is of great significance in this respect is the quality factor,  $Q$ , and the contrasting  $Q$  across the Benioff zones<sup>2</sup> and its many tectonic implications<sup>3</sup> have been discussed.  $Q$  is difficult to measure with reasonable accuracy, and even when this has been accomplished the inversion of  $Q$  obtained from surface waves into a depth distribution is difficult. However, the "Hedgehog" inversion technique<sup>4,5</sup> has greatly helped us to interpret some data of this type.

The specific attenuation factors,  $Q_p^{-1}$ , were estimated as functions of frequency by one of us (P. W. B.), for teleseismic Rayleigh waves from a large nuclear explosion<sup>6</sup>. With the help of Hedgehog we show that these data are consistent with a region of low  $Q$  at the depth, about 120 km, of the Gutenberg low velocity zone.

**Table 1** World Wide Standard Seismograph Network Recordings of the Event at Novaya Zemlya (73.6° N, 57.5° E) on December 24, 1962 (GMT: 11-11-42.0)

Addis Ababa	AAE	Godhavn	GOH	Madison	MDS
Albuquerque	ALQ	Golden	GOL	Quetta	QUE
Bermuda	BEC	Istanbul	IST	Toledo	TOL
Balboa Heights	BHP	Kongsberg	KON	Trinidad	TRN
Berkeley	BKS	Lahore	LAH	Valencia	VAL
Blacksburg	BLA	Longmire	LON	Windhoek	WIN
Caracas	CAR	La Palma	LPS		
Copenhagen	COP	Malaga	MAL		

The explosion used was the atmospheric nuclear test of about 20 Mtons<sup>7</sup> conducted at Novaya Zemlya on December 24, 1962. A spectral and dispersive analysis of the Rayleigh surface waves it generated was performed for the station recordings listed in Table 1. The records were digitized, Fourier analysed<sup>8</sup> and corrected for instrumental effects to yield spectral amplitude content. Group velocities were determined by using a multiple filtering technique similar to the method of Dziewonski *et al.*<sup>9</sup>. The radiation pattern from such an event was assumed to be circular for all frequencies of interest.

- <sup>10</sup> Anderson, D. L., Ben-Menahem, A., and Archambeau, C. B., *J. Geophys. Res.*, **70**, 6, 1441 (1965).  
<sup>11</sup> Anderson, D. L., and Archambeau, C. B., *J. Geophys. Res.*, **69**, 10, 2071 (1964).  
<sup>12</sup> Tsai, Y., and Aki, K., *BSSA*, **59**, 1275 (1969).  
<sup>13</sup> Backus, and Gilbert, *Phil. Trans.*, **266**, 123 (1970).  
<sup>14</sup> Solomon, S. C., Ward, R. W., and Toksoz, M. N., MIT, *Woods Hole Conference on Seismic Discrimination*, Mass. Inst. Tech., **1**, 71 (1971).

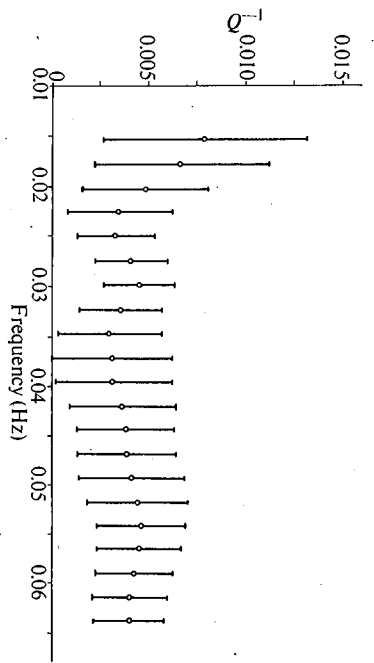


Fig. 1 Observational  $Q_p^{-1}$  data for Rayleigh waves.

Values of  $Q_p^{-1}$  were then obtained from the logarithmic form of the amplitude equation for a recording site

$$A = C(E \sin \Delta)^{-1/2} e^{-\left(\frac{\pi E \Delta f}{Q_p U}\right)}$$

$A$  = spectral amplitude ( $\mu\text{s}$ ) at frequency  $f$  (Hz)

$U$  = group velocity (km/s)

$E$  = radius of the Earth

$\Delta$  = angular distance between epicentre and recording site

$C$  = a constant.

Least squares values of  $Q_p^{-1}$  for the frequency range 0.015–0.065 Hz (periods 65–15 s) and their 95% confidence limits are shown in Fig. 1.

Table 2 Velocity-Depth Model Assumed

P-wave velocity km s <sup>-1</sup>	S-wave velocity km s <sup>-1</sup>	Density g cm <sup>-3</sup>	Thickness of layer km	$Q_\alpha/Q_\beta$
6.10	3.5	2.7	14.0	2.29
6.50	3.72	2.9	22.0	2.29
8.06	4.40	3.33	22.0	2.51
8.08	4.46	3.345	10.0	2.51
8.121	4.45	3.375	55.0	2.51
8.50	4.96	3.64	—	2.19

A velocity-depth model must be assumed to invert the Rayleigh wave  $Q_p(f)$  data into a variation with depth of  $Q_\alpha$ , the  $Q$  for compressional waves, and  $Q_\beta$ , the  $Q$  for shear waves. Most of the propagation paths specified by Table 1 are of continental type, so that the simple, six layer, continental type, velocity-

the other for high frequencies. Our data do not show such a peak (although this does not exclude its possible existence within the 95% confidence limits). So we have been able to interpret our data with a frequency independent  $Q$  model, and have no reason to resort to any frequency dependence in our frequency interval.

Models of type II (Fig. 3), that is, moderate  $Q$  throughout the crust and uppermost mantle, do not seem to have been proposed before, but certainly cannot be eliminated by the present data. The difference between our interpretation and that of other authors is probably due to lateral variations of  $Q$  within the upper mantle for the different epicentral regions and propagation paths investigated. In using our data we did not assume the presence of a low velocity layer, yet all of our types of models show a low  $Q$  zone at depths below 70 kms, in an otherwise higher  $Q$  environment. This is in good agreement with Tsai and Aki, who assumed a Gutenberg-type continental Earth, and is further evidence for a zone of low  $Q$ , coinciding with this low velocity zone.

We thank V. P. Valus, Institute of Physics of the Earth, Moscow, for explaining the "Hedgehog" inversion technique and for the special programmes which he developed. The NERC provided the grant for Dr Valus's visit to Cambridge. B. L. N. K. thanks the British Petroleum Company for a research studentship.

P. W. BURTON

UKAEA,  
Blacknest, Brimpton,  
Reading RG7 4RS,  
and Department of Geology,  
University of Durham

B. L. N. KENNETT

Department of Applied Mathematics  
and Theoretical Physics,  
University of Cambridge,  
Silver Street, Cambridge

Received June 29, 1972.

- Nature*, **236**, 259 (1972).
- Barzangi, M., Isacks, B., and Oliver, J., *J. Geophys. Res.*, **77**, 5, 952 (1972).
- Utsu, T., *Rev. Geophys. Space Phys.*, **9**, 4, 839 (1971).
- Valus, V. P., *Vichslietnaya Seismologiya*, **4**, 1 (1968).
- Kellis-Borok, V. I., in *Proc. Fifthth Enrico Fermi Summer School*, Varenna, 1969 (Academic Press, London, 1972).
- Burton, P. W., thesis (University of Durham).
- Vela Uniform Periodic Information Digest Invert.*, **3**, 1 (1963).
- McCowan, D. W., *Earth Sci. Divis.*, Teledyne Industries Inc., Alexandria, Virginia, Memorandum No. 8-66 (1966).
- Dziwonski, A., Bloch, S., and Landsman, M., *BSSA*, **59**, 427 (1969).

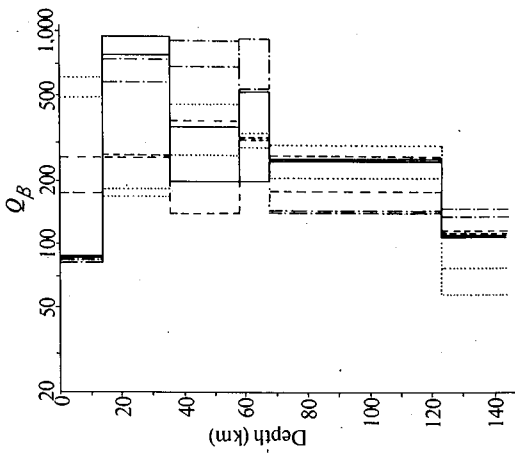


Fig. 3 Four types of inversion models. Model I, — : model II, - - - ; model III, ·····; model IV, - · - · - .

indicative of lateral variations of  $Q$  between regions in the upper mantle<sup>14</sup>.

The Rayleigh wave  $Q$  observed by Tsai and Aki shows a prominent peak at about 25 s period. To interpret this feature they required a  $Q$  model with a simple frequency dependence; they effectively combined two depth models, one for low and

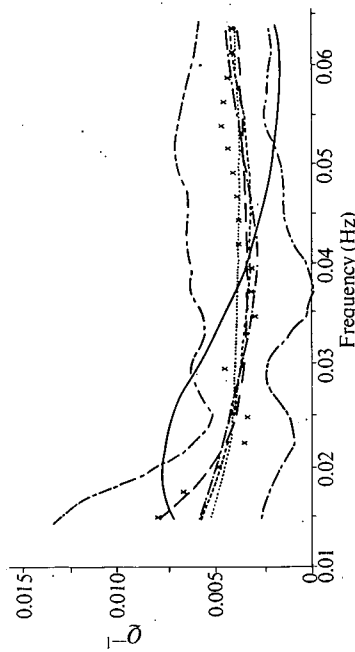


Fig. 4 Comparison between models and observations. —, Anderson model; - - -, model 1; ·····, model 2; - · - · -, model 3; - - - - -, model 4; XXXX, observed data with confidence limits.

depth model of Table 2 was chosen.

The Hedgehog inversion technique<sup>4,5</sup> was used to search for  $Q$  models consistent with the experimental data. Any  $N$ -layered model of the Earth's anelasticity may be specified by  $2N$  parameters  $Q_j$  corresponding to the  $Q_s$  in the individual layers  $Q_{\alpha 1} \dots Q_{\alpha N}$  and  $Q_{\beta 1} \dots Q_{\beta N}$ . We define a region of search in the parameter space by requiring the  $Q_j$  to be positive and also imposing reasonable upper limits on their values. This search region is divided into a  $2N$ -dimensional network, with mesh lengths  $\delta Q_j^*$  between the nodal parameter values.

To start our search for suitable models we use the Monte-Carlo technique to generate a set  $\{Q_j\}$  of values of the parameters. For each  $\{Q_j\}$  a function  $Q_\gamma(f)$  is calculated and compared with the observed value  $Q_{\gamma 0}(f)$ . The theoretical values for Rayleigh wave  $Q_\gamma$  are determined using Anderson's formula<sup>10</sup>. The observed values  $Q_{\gamma 0}$  are obtained as a discrete function of frequency,  $Q_{\gamma 0}(f)$  for  $M$  frequencies  $f_1 \dots f_m$ .

We search for those regions where the match between  $Q_\gamma(f)$  and  $Q_{\gamma 0}(f)$  is good; that is, we require for the  $M$  frequencies considered, setting  $Q_{\gamma i} = Q_\gamma(f_i)$ ,  $Q_{\gamma 0 i} = Q_{\gamma 0}(f_i)$

$$\left| \frac{Q_{\gamma i} - Q_{\gamma 0 i}}{\Delta Q_{\gamma 0 i}} \right| < a \quad i = 1, \dots, M \quad (1)$$

$$\left[ \frac{1}{M} \sum_{i=1}^M \left( \frac{Q_{\gamma i} - Q_{\gamma 0 i}}{\Delta Q_{\gamma 0 i}} \right)^2 \right]^{1/2} < \sigma$$

where  $\Delta Q_{\gamma 0 i}$  is a measure of the error in the observed measurement  $Q_{\gamma 0 i}$ , and  $a$ ,  $\sigma$  are precision measures on the fit.

Once we have found a good set of values  $\{Q_j\}$  we move to the nearest node  $\{Q_j^*\}$  on the network spanning the search region and test this against inequality (1). If these equations are satisfied we test the adjacent nodes  $\{Q_j^* + \delta Q_j^*\}$  and continue until we have determined a connected region of acceptable  $Q$  models in the parameter space surrounded by nodes for which inequality (1) is no longer satisfied. Otherwise we return to the Monte-Carlo technique. Once a good region has been found we again invoke the Monte-Carlo technique and try to find another solution of inequality (1) outside this initial region. Thereafter the process is repeated until the region of search has been exhausted.

If independent values of  $Q_\alpha$  and  $Q_\beta$  were attributed to each layer then we would be searching in a twelve-dimensional space. To reduce the region of search we made the assumption that there are no losses attributable to a bulk modulus<sup>10</sup>, which leads to

$$Q_{\alpha j} = 3/4 \left( \frac{\alpha_j}{\beta_j} \right)^2 Q_{\beta j} \quad j = 1 \dots 6$$



reducing the Hedgehog regional search to a six-dimensional parameter space. For a Poisson solid ( $\alpha = \sqrt{3}\beta$ )  $Q_a = 2.25 Q_b$ , but for our velocity depth model the ratio  $Q_a/Q_b$  varies and is given in Table 2.

Postulated models were accepted if they fitted within the 75% confidence limits at all periods. Consistency was confirmed by repeating the search, but varying the mesh. The chosen region of search is shown in Fig. 2; Hedgehog yields two adequate solutions to the observed data—indicated by shading—but makes no geophysical distinction between them. Also shown are further good points but not connected regions found by the

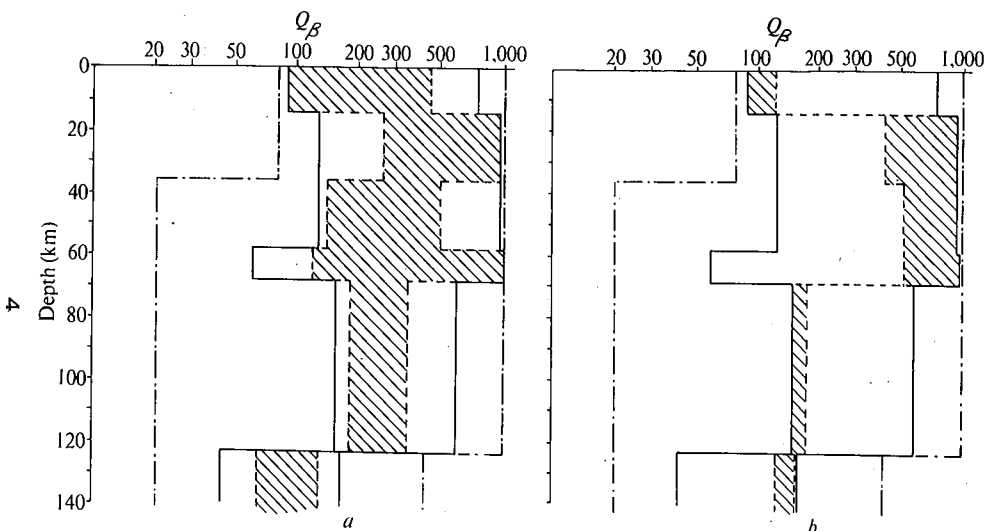


Fig. 2 a and b, Alternative Hedgehog solutions for attenuation data. ---, Region of search; //, Monte-Carlo solutions; //, Hedgehog solutions.

Monte-Carlo solutions; //, Hedgehog solutions.

Monte-Carlo technique.

The models fitting the data fall into four broad classes and examples of these are illustrated in Fig. 3. All the models obtained show a low  $Q$  zone in the upper mantle. In most cases this lies around and below a depth of 120 km. This low  $Q$  zone corresponds to the Gutenberg low velocity zone, but note that the Gutenberg low velocity zone was not assumed to exist during model fitting. The remaining models show low  $Q$  below about 70 km which tends to decrease slightly further below 120 km. This low  $Q$  zone is at a depth corresponding to the low velocity zone in tectonic regions of the continents. The range of models found probably reflects lateral variations in  $Q$  on the paths to the recording stations as well as the non-uniqueness of the inversion process.

Table 3 A Few  $Q$ -Depth Models

Layer	Anderson type model	Model 1	Model 2	Model 3	Model 4
1	1,000	440	90	180	610
2	1,600	700	790	260	180
3	1,400	560	500	260	260
4	180	70	220	120	340
5	180	70	180	260	290
6	400	180	115	115	55

The Anderson type model has a low  $Q$  zone at about 50 km, and  $Q_a, Q_b$  are listed. Our models only list  $Q_b$  because this determines  $Q_a$ .

Table 3 lists four models representative of the classes found and an Anderson type  $Q$  model with a low  $Q$  zone at about 50 km. Theoretical values of Rayleigh wave  $Q$  for these models are shown in Fig. 4 along with the original observational data. Note that none of our models shows the low  $Q$  zone in the depth region 50–120 km with increasing  $Q$  below 120 km, found by Anderson<sup>10,11</sup>. Using short period Rayleigh waves, as in this report (1.5–6.5 s), Tsai and Aki found the Anderson model MM8 (ref. 10) to be unsatisfactory because it did not agree with their observed frequency dependence for  $Q^{12}$ . More recently Backus and Gilbert found that their results did not establish a low  $Q$  zone in the upper mantle<sup>13</sup>. However, Anderson *et al.*<sup>10</sup> used two earthquakes, in Chile and Iran respectively, as their data source. Tsai and Aki used one earthquake in California while Backus and Gilbert used free oscillation studies. This study uses a source in Novaya Zemlya and continental paths—"a continental  $Q$ ". These differences in the type, and more importantly the region, of the data source may lead to variations between the models. Such differences are observed and this is